University of Southampton

Faculty of Medicine

School of Cancer Sciences

The clinical utility of (epi)genomic biomarkers in chronic lymphocytic leukaemia

by

Louise Jane Carr

ORCID ID 0000-0002-0653-7250

Thesis for the degree of Doctor of Philosophy

February 2025

University of Southampton

Abstract

Faculty of Medicine

School of Cancer Sciences

Doctor of Philosophy

The clinical utility of (epi)genomic biomarkers in chronic lymphocytic leukaemia

by

Louise Jane Carr

Chronic lymphocytic leukaemia (CLL) presents as a biological and clinically heterogenous disease, with some patients requiring immediate intervention whilst other have a more benign disease. In this thesis, a large cohort of patients enrolled in chemo(immuno-) therapy clinical trials, CLL4, ARCTIC or ADMIRE, with extensive molecular characterisation is used to examine the clinical power of three novel CLL biomarkers, methylation based epitype, telomere length (TL) and genomic complexity (GC). Published work have reported that these biomarkers are clinically relevant. However, they have not been analysed together within a single clinical trial cohort. Also, a description of the biological context of these biomarkers is an additional aim.

A systematic review with narrative synthesis was completed. Various experimental work and bioinformatic analysis, undertaken by myself, generated new copy number aberration (CNA) (n=153), TL (n=83) and variant (n=42) data using shallow whole genome sequencing, monochrome multiplex QPCR and HS2 target enrichment techniques, respectively. Extensive statistical and survival analysis was completed. Data classifying CLL patients into three epitype subgroups: naïve-like (n-CLL), intermediate (i-CLL), and memory-like CLL (m-CLL) was utilised. GC was defined as low (0-2 CNAs), intermediate (3-4 CNAs) and high (≥5 CNAs) GC. Published TL cut-offs (TL-Short <2.92kb, TL-Intermediate 2.92–3.57kb, TL-Long >3.57kb) was also used.

Results found the n-CLL epitype, TL-S and high GC variables were associated with many other poor risk features and were predictive of a poor survival. A strong relationship between TL and epitype was also found. As well as confirming previously reported results, the key results of this project include: 1) a significant enrichment of i-CLL epitype in intermediate GC patients was found; 2) greater GC was correlated with shortening TL (TL-S) and an increased prevalence of the n-CLL epitype; 3) survival analysis showed that the i-CLL subgroup can be further stratified by TL, with TL-L predicting a prolonged survival; 4) Both TL and epitype have prognostic utility in identifying patients destined to have poor survival; 5) high GC, but not intermediate GC, was an predictor of a dismal overall survival independently of *TP53* aberration or unmutated *IGHV* status.

In conclusion, for the first time the clinical significance of TL, epitype and GC was examined together within a clinical trial cohort. Results suggest that the combination of TL and epitype can further stratify the mutated *IGHV* group. Additionally, the biological composition and clinical significance of three GC subgroups was described. This work supports the use of GC as a prognostic biomarker in the clinical setting. However, as reported in the systematic review, a consensus within the CLL community about the metric used to define GC and what technology should be used to detect GC needs to be reached before this biomarker can be fully validated.

Table of Contents

Table of Tables

Table of Figures

Table of Figures

Table of Figures

List of Accompanying Materials

Supplementary Tables

Supplementary Table 1- Overview of the 25 studies that meet the eligibility requirements and therefore will be used within downstream analysis.

Supplementary Table 2- The 72 probe targets that were designed as part of the SureSelect XT HS2 DNA target enrichment system for the identification of variants within these panel of genes.

Supplementary Table 3- Basic clinico-biological features of the ARCTIC and ADMIRE cohort used within this study compared to the total clinical trial cohort.

Supplementary Table 4- Basic clinico-biological features of the CLL4 cohort used within this study compared to the total clinical trial cohort.

Supplementary Table 5- Univariate survival analysis of the CLL4 cohort examining progression free survival (PFS).

Supplementary Table 6- Univariate survival analysis of the CLL4 cohort examining overall survival (OS).

Supplementary Table 7- Univariate survival analysis of the ARCTIC and ADMIRE cohort examining progression free survival (PFS).

Supplementary Table 8- Univariate survival analysis of the ARCTIC and ADMIRE cohort examining overall survival (OS).

Supplementary Table 9- CLL4 multivariate PFS final model after backward elimination after starting with 8 covariates

Supplementary Table 10- CLL4 multivariate OS final model after backward elimination after starting with 8 covariates.

Supplementary Table 11- ARCTIC/ADMIRE multivariate PFS final model after backward elimination after starting with 8 covariates.

Supplementary Table 12- ARCTIC/ADMIRE multivariate OS final model after backward elimination after starting with 8 covariates.

Supplementary Table 13- List of available FISH data across the four genomic technology cohorts.

Supplementary Table 14- Univariate survival analysis of the CLL4 cohort examining progression free survival (PFS) in a cohort of 251 clinical trial patients.

Supplementary Figures

Accompanying Data

Accompanying data for this thesis is available here; https://doi.org/10.5258/SOTON/D3336.

Research Thesis: Declaration of Authorship

Print name: Louise Jane Carr

Title of thesis: The clinical utility of (epi)genomic biomarkers in chronic lymphocytic leukaemia.

I declare that this thesis and the work presented in it are my own and has been generated by me as the result of my own original research.

I confirm that:

1. This work was done wholly or mainly while in candidature for a research degree at this University;
2. Where any part of this thesis has previously been submitted for a degree or any other qualification at this University or any other institution, this has been clearly stated;
3. Where I have consulted the published work of others, this is always clearly attributed;
4. Where I have quoted from the work of others, the source is always given. With the exception of such quotations, this thesis is entirely my own work;
5. I have acknowledged all main sources of help;
6. Where the thesis is based on work done by myself jointly with others, I have made clear exactly what was done by others and what I have contributed myself;
7. Parts of this work have been published as:

Carr, L. J., Norris, K., Parker, H., Nilsson-Takeuchi, A., Bryant, D. J., Amarasinghe, H. E., Kadalayil, L., Else, M., Wojdacz, T., Pettitt, A., Hillmen, P., Schuh, A., Walewska, R., Baird, D. M., Oscier, D. G., Oakes, C. C., Gibson, J., Pepper, C., & Strefford, J. C. (2023). Telomere Length and DNA Methylation Epitype Both Provide Independent Prognostic Information in CLL Patients; Data from the UK CLL4, Arctic and Admire Clinical Trials. Blood, 142(Supplement 1), 6514. https://doi.org/10.1182/BLOOD-2023-177575

Signature: .....Date: 08/02/2025.....

Acknowledgements

Firstly, I would like to thank my supervisors Professor Jon Strefford, Doctor Helen Parker and Doctor Jane Gibson for their continuous support, invaluable advice and guidance given to me during my PhD program. I would not have gotten to this point without your time, encouragement and kindness you have given me during the past five years, but also during my placement year in the Cancer Genomics research group 7 years ago. Under your mentorship, I gained a great deal of knowledge, skill and confidence and could not have asked for a better supervisory team. I would also like to thank the wider Cancer Genomics research group for being a wealth of knowledge and always being happy to share their expertise. In addition, for their day to day help and endless words of encouragement given to me when I needed it.

I would like to acknowledge my funders, Cancer Research UK and the Medical Research Council, who without their support this research and thesis would not have been possible. Also, I would like to thank the patients and clinicians who have contributed clinical material and data that has been used in this thesis.

To my mum and dad, Clive, Karen and brother James, I would like to thank you for your encouragement and tireless support in this endeavour, as you do in all my endeavours. Mum, you gave the greatest advice when I was feeling overwhelmed. When stressed, you always knew which activities or hobbies, usually involving gardening, would relax me and ensure I was working productively. Dad, it is safe to say you kicked off my love of science and it has been wonderful to be able to share, one scientist to another, this passion and interest. James, moving nearer to you in Southampton and having more time and fun together, either in person or online gaming along with David, has been a great part of my PhD experience.

To my pet cats, Pippin, who was with me from the start, and Henry who joined me nearer the end of my PhD. They have been a source of great company during the work from home and write up periods of my thesis and were a much-needed calming presence during the more difficult times of my PhD.

Finally, I have been very lucky to be championed by many friends and family, based inside and outside Southampton. I want to thank them all for supporting me and providing lots of fun and laughs during my much-needed downtime over the past five years.

Definitions and Abbreviations

Abbreviation	Definition
aCGH	Array Comparative Genomic Hybridisation
AID	Activation-Induced Cytidine Deaminase
ARC/ADM	ARCTIC and ADMIRE
ATM	Ataxia Telangiectasia Mutated
ATR	Ataxia-Telangiectasia and Rad3-related kinase
BCR	B cell Receptor
BR	Bendamustine and Rituximab
BTK	Bruton Tyrosine Kinase
CBA	Chromosome Banding Analysis
CIT	Chemo-immunotherapy
CK	Complex Karyotype
CLL	Chronic Lymphocytic Leukaemia
CNA	Copy Number Aberration
cnLOH	Copy Number neutral Loss of Heterozygosity
CNV	Copy Number Variation
CpG	Cytosine Guanine Dinucleotide
CR	Complete Remission
C_t	Cycle Threshold
DLBCL	Diffuse Large B Cell Lymphoma
DME	DNA Methylation based Epitype
DNA-PK	DNA-dependent Protein Kinase
DOC	Depth of Coverage
DOR	Duration of Response
DSB	Double Strand Breaks
ERIC	European Research Initiative on CLL
FCR	Fludarabine, Cyclophosphamide, and Rituximab
FCMR	FCR and Mitoxantrone
FCMminiR	FCMR with low-dose Rituximab
FCMminiR/FCR	FCMminiR treatment cross over to FCR treatment
FISH	Fluorescence in situ Hybridisation
FPK-PCR	Full Process Kinetics-PCR
GC	Genomic Complexity

HR	Hazard Ratio
i-CLL	Intermediate CLL
IGHV	Immunoglobulin Heavy Chain Variable
IGV	Integrative Genomics Viewer
iwCLL	Internation Workshop on Chronic Lymphocytic Leukaemia
KM	Kaplan Meier
LOH	Loss of Heterozygosity
LRR	Log R Ratio
mAb	Monoclonal Antibody
Mb	Megabase
MBL	Monoclonal B cell Lymphocytosis
m-CLL	memory B-cell-like CLL
M-CLL	*IGHV* Mutated CLL
MDR	Minimally Deleted Regions
MMQPCR	Monochrome Multiplex Quantitative PCR
MVA	Multivariate Analysis
n-CLL	Naïve B-cell-like CLL
NHL	Non-Hodgkin's Lymphoma
NGS	Next Generation Sequencing
OR	Odds Ratio
OS	Overall Survival
PFS	Progression Free Survival
PI3K	Phosphatidylinositol 3-Kinase
PI3KKs	Phosphoinositide 3-Kinase-related protein Kinases
RFU	Relative Fluorescence Unit
R/R	Relapsed/Refractory
RS	Richter Syndrome
S	Single copy gene signal
SLL	Small Lymphocytic Lymphoma
SNP	Single Nucleotide Polymorphism
STELA	Single Telomere Length Analysis
sWGS	Shallow Whole Genome Sequencing
T	Telomere Signal
TFS	Treatment Free Survival
TL	Telomere Length
TL-I	Intermediate Telomere Length

TL-L	Long Telomere Length
TL-S	Short Telomere Length
T_m	Melting Tempterature
TMB	Tumour Mutational Burden
TS	Targeted Sequencing
TTT	Time to Treatment
TTFT	Time to First Treatment
TTST	Time to Subsequent Treatment
U-CLL	*IGHV* Unmutated CLL
VAF	Variant Allele Frequency
WES	Whole Exome Sequencing
WGS	Whole Genome Sequencing
WHO	World Health Organisation
95% CI	95% Confidence Interval

Chapter 1 Introduction

1.1 Cellular and molecular biology of cancer

1.1.1 Cancer development

As cancer can arise from any cell type, there are over 200 distinct types each with distinctive clinical behaviour and pathobiology (1). In the UK, the top four most common cancers; breast, prostate, lung and bowel, account for more than half of the new incidences. Cancer Research UK has reported that in the last 50 years the 10-year survival rate of cancer has greatly improved from 24% to 50%. However, in 2020 1 in 4 deaths recorded in the UK were attributed to cancer and coupled with the growing incidence, it is clear that cancer remains a defining health burden in the UK and globally (2).

A tumour is an abnormal mass of cells that proliferate abnormally due to deregulated cell division, and it can be defined either as benign or malignant. Benign tumours have abnormal and uncontrolled proliferation but remain in the original anatomical location. Malignant tumours have the ability to metastasize by invading surrounding normal tissue and moving to a secondary location using the lymphatic or circulatory system. It is these types of tumours that are referred to as cancer, with their ability to metastasize making them much more threatening to human health (3). Eukaryotes cells undergo two types of cell division which both have distinct functions, namely mitosis and meiosis. The latter is important in sexual reproduction as it produces gametes, a type of haploid cell which contain only half the genetic material as the parent cell. The former produces two identical diploid daughter cells from a parent cell and is required for growth and cell regeneration, and in some unicellular eukaryotic cells is used for asexual reproduction.

The mitosis process can be divided into two phases; interphase and M phase, whereby a mother cell divides into two identical daughter cells. Within S phase of interphase, DNA replication must occur to duplicate the cellular content of the mother cell so that when cellular separation occurs at the end of M phase (comprised of prophase, metaphase, anaphase, and cytokinesis) there is sufficient DNA present for the two daughter progenies. This process is highly controlled with many checkpoints being present throughout the mitotic cell cycle to prevent the accumulation of genetic errors that would then be passed on to descendants (4). One example is the DNA damage checkpoint which, during interphase, can be triggered by DNA double-strand breaks (DSB) causing a rapid response that is dependent on a checkpoint protein kinase; ataxia telangiectasia mutated (ATM). The ATM protein acts to orchestrate the response, repairing the damage through the

recruitment of sensor and effector proteins. DSB can be repaired in two ways; non homologous end joining and homologous recombination, with the prior being able to occur throughout the cell cycle whilst the latter is favoured after DNA replication in the S and G2 phases of the cell cycle when a template strand is present (5). However, if a DSB cannot be adequately repaired, due to the severity of the damage or inability of the DNA damage repair machinery, the cell will permanently exit the cell cycle either by entering senescence or by undergoing apoptosis, all of which are orchestrated by cell cycle mechanisms (4). Many proteins involved in the cell cycle-control signalling pathways are altered in cancer which gives rise to continued cell cycle progression (6). These signalling pathways can be defined into four groups which have different mechanisms of action, impact at different stages, and involve different proteins (**Figure 1**)(7). Research has reported that the continuous abnormal cell accumulation is typically driven by insufficiencies in the apoptosis pathway and issues with exiting the cell cycle rather than through uncontrollable cell cycle progression (8). In cancer, mutations in proteins involved in initiating cell cycle exit or that promote S phase entry are common (9). However, proteins involved in mitotic entry or exit are more rarely altered, are typically involved in the DNA replication stress or spindle assembly checkpoints and are seemly vital for cancer cells (7). For example, loss of function mutations in spindle assembly checkpoint proteins are rare as typically the loss of these proteins would result in a high level of aneuploidy that would not be viable for the cell (10). However, an overexpression of spindle assembly checkpoint proteins, such as MAD2, BUBR1 and CDC20, have also been reported in various cancers but its impact on tumour development is not clear (11,12). Evidence in cancer research has shown that faults in certain areas of the cell cycle, necessary to allow for continued cell division, then cause a significant dependency on the remaining cell cycle pathways to prevent excessive accumulation of genomic instability that would become lethal to the cancer cell (13). This dependency is a possible therapeutic target, as healthy cells are not as reliant on certain cell cycle pathways, making the cell cycle an important aspect of cancer research (7).

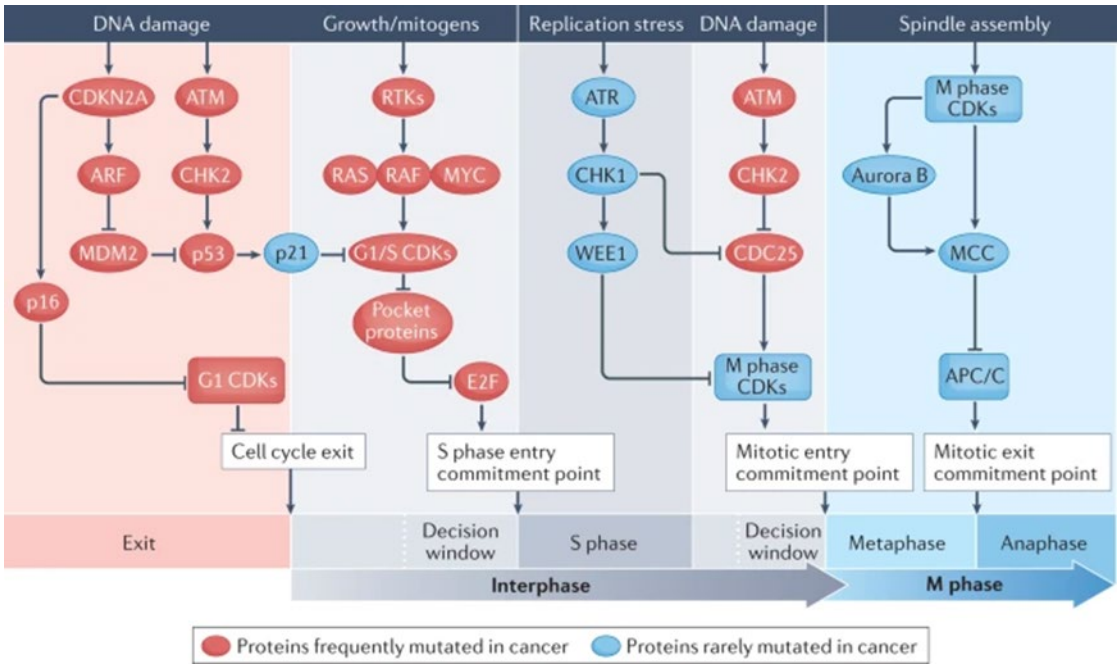

Figure 1- The key cell cycle signalling pathways involved in cancer: DNA damage, growth/mitogens, replication stress, and spindle assembly. Mutations in proteins involved in each of the cell cycle control signalling pathways are shown, with red indicating proteins commonly mutated in cancers and blue showing the rarely mutated proteins. These mutations are also associated more with specific cell cycle control pathways: cell cycle exit, S phase entry, mitotic entry, and mitotic exit. From (7)

A further important principle of cancer research is tumour clonality. Tumour clonality is the development of a tumour from a single normal healthy cell that begins to proliferate uncontrollably and abnormally due to alterations within the genetic sequence and in gene expression (14). These genetic changes typically impact mechanisms that function to regulate cell differentiation, proliferation, and survival. However, tumour clonality does not mean a cancer cell acquires all its characteristics in a single event from the original progenitor cell. And in fact, tumour development is a dynamic multistep process in which the cell undergoes a progressive series of alterations at the cellular, molecular, genetic and epigenetic level (3). Tumour development, also referred to as tumorigenesis, can be divided into three stages: initiation, progression, and metastasis (15). The multi-hit theory of tumorigenesis states that cancer is derived from a single somatic cell that has accumulated many mutations which give the cell a growth advantage, allowing it to multiply unchecked and at a rapid pace (16). This quick cell division allows additional alterations to readily occur, with selection for cells with greater capacity for proliferation, survival, invasion, and metastasis occurring within the expanding tumour population. This selection for properties which confer a selective advantage is continuous during tumour development and similar to Darwinian natural selection (17). Evolutionary clonal expansion of a cancer cell gives rise to intra-tumour heterogeneity. This happens as a result of

tumour cells having different levels of genetic instability and being exposed to a range of selection pressures. Therefore, these tumour subpopulations can acquire different driver and passenger mutations (18). Driver mutations are alterations that drive clonal expansion as they confer growth advantages for the cell in their current microenvironment, while the passenger mutations do not alter the fitness of the cell but could do if the selective pressures change, see **Figure 2**.

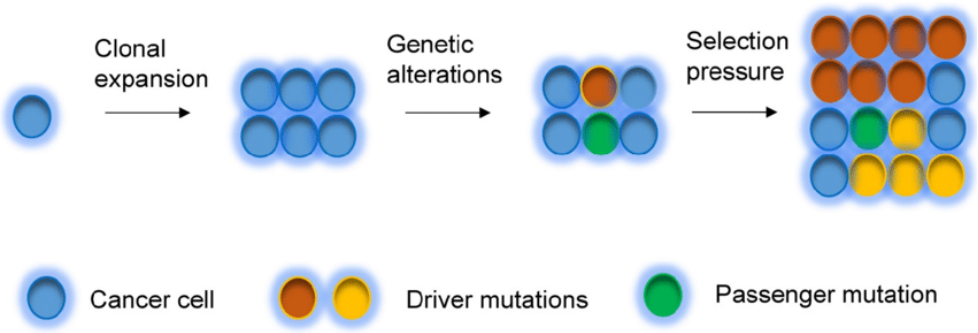

Figure 2- Clonal evolution model. Clonal expansion of the cancer cell (blue colour) through the acquisition of early (red colour) and new (yellow colour) driver mutations resulting in evolution and growth of the tumour. Passenger mutations (green colour) do not confer a growth advantage to the cell under the current selection pressures within the tumour microenvironment, from (18).

Understanding the order of genetic lesion acquisition during cancer development has been an important goal in cancer research as it can provide an insight into the cellular mechanisms in tumorigenesis thereby identifying better ways to detect and treat tumours early (19).

1.1.2 Hallmarks of cancer

The characteristics granted by the driver alteration accrued during tumour development have been extensively researched in the hope that the unifying features, present in all cancer types, can be defined. This was revealed by Hanahan and Weinberg who designated them as the hallmarks of cancer (1). These biological features of tumour cells function to promote growth, migration and survival and are acquired during the multistep tumorigenesis process. In the original publication, six hallmarks of cancer were described but subsequent work on this concept identified two further traits that were deemed emerging hallmarks, but now with additional evidence have been accepted along with the six core hallmarks (1,20). Further reflection upon this concept suggested that these hallmarks failed to address the complexities of tumorigenesis and did not answer the question of how these phenotypic capabilities were acquired (21). Therefore, the idea of enabling characteristics were included along with the eight hallmarks of cancer, see **Figure 3**.

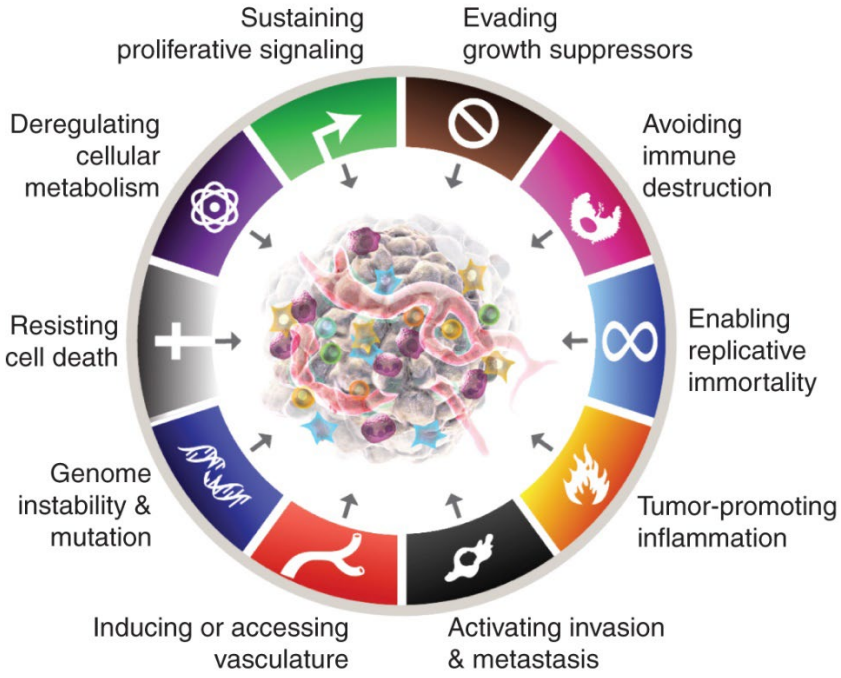

Figure 3- The hallmarks of cancer reported and developed by Hanahan and Weinberg, including the original six hallmarks and the two emerging hallmarks that have recently been validated and accepted. Two enabling characteristic that are vital in allowing the hallmark abilities to be acquired are also shown, from (21)

The eight validated hallmarks of cancer, as well as two enabling characteristics, reported in Hanahan and Weinberg's seminal review are as follows (1,20).

Sustaining proliferative signalling

This is an essential first step in the tumorigenesis process as it grants the tumour an ability for chronic proliferation. This ability is caused by deregulation of growth-promoting signals that both triggers the cell to enter and progress through the cell cycle. Cancer cells can acquire this ability many ways including through producing growth factor ligands or by stimulating normal cells within the microenvironment to produce growth factors which act to stimulate the cancer cells (22). Additionally, cancer cells can also have increased levels of receptor protein on the cell surface, leading to a hyperresponsiveness to normal levels of growth factor ligands (23,24).

Evading growth suppressors

As well as increasing the proliferation signals, cancer cells also must avoid the negative regulatory cell proliferation signals which inhibit cell division. Various tumour suppressor genes have been validated through gain- or loss-of-function mice experiments. For example, the *TP53* gene which has a multifaceted function as a cell cycle checkpoint protein, deciding when a cell can progress

through the cell cycle and proliferate or whether cell senescence and apoptosis programs should be activated (25).

Activating invasion and metastasis

Within the tumour microenvironment, cancer associated cells can change their shape and attachment to other cells and the extracellular matrix which allows for local invasion and then metastasis. An example of this is many cancers have a downregulation and/or mutational inactivation of E-cadherin, which functions normally to provide cell-to-cell adhesion that is required in the formation of epithelial cell sheets which inhibits tumour cell invasion by stopping cells from dissociating from each other (26).

Enabling replicative immortality

Most normal cell lineages only have a limited number of cell cycle divisions. This is due to two problems that can arise during cell growth: cellular senescence and cellular crisis leading to apoptosis. Immortalization is characterised by the ability of a cell to proliferate without evidence of crisis or senescence. Cancer cells acquiring immortality has been attributed to the cells ability to maintain a sufficient length of telomeric DNA (20). Telomere shortening is viewed as a biological clock indicating the proliferative potential of a cell and therefore cancer cells must counter the progressive telomeric shortening which would normally lead to cellular crisis, halting proliferation (27).

Inducing angiogenesis

Both normal and cancer cells require a constant supply of nutrients and oxygen in addition to the ability to remove waste and carbon dioxide. An early event in the development of an invasive and metastasising cancer is the angiogenesis process, whereby new blood vessels are formed (28). Angiogenesis is continuously activated in cancer so blood vessel branching, and formation of capillaries is occurring to help provide for the expanding tumour tissue (29).

Resisting cell death

Programmed cell death is an essential part of the normal cell cycle that protects the cell from passing down DNA errors to the resulting daughter cells thus inhibiting the development of cancer. Whilst the elements that complete apoptosis remain intact in cancer cells, it is the sensors that trigger apoptosis in response to the detection of errors that are abnormal (20). A cancer cell can use many strategies to avoid apoptosis, including the loss of TP53 tumour suppressor function, which typically triggers apoptosis after sensing substantial DNA damage (30). Furthermore, tumours may also overexpress antiapoptotic regulators, downregulate proapoptotic

factors or can avoid the death receptor pathway where death ligands bind to tumour necrosis factor (TNF) death receptors to trigger extrinsic apoptosis (31).

Avoiding immune destruction

An emerging hallmark that has since been validated and accepted along with the original six hallmarks of cancer. The immune system has a significant role in inhibiting the development and progression of tumours, but cancers can develop the ability to avoid detection and elimination by this system (20). Various reports and observations have indicated that immune surveillance and therefore tumour eradication is a significant barrier in tumorigenesis (32). One such observation is deficiencies of certain immune cells such as T and natural killer cells in mice resulted in increased tumour incidences (33). One-way tumours avoid immune destruction is by losing the major histocompatibility complex class I and II antigens, produced in an immune selection process, thus generating a tumour clone that can avoid immune destruction and therefore undergo clonal expansion (34).

Deregulating cell metabolism

A further validated emerging hallmark involves the adjustment to the cellular energy metabolism which is required to sustain the uncontrolled proliferation of a cancer cell. The phenomenon called “the Warburg effect” was characterized as the majority of glucose metabolism in cancer cells was completed under anaerobic condition via the glycolysis process, whereas normal cells primarily rely on mitochondrial dependent energy production (35). Whilst this process has a much lower efficiency of ATP production, cancer cells favour this glucose metabolism even under aerobic conditions. Whilst the complete rationale for this metabolic reprogramming is unclear, many hypothesises have been suggested such as the glycolytic intermediate products are utilized in many biosynthetic pathways to generate many elements required for the assembly of new cells (36).

Enabling characteristic of tumour-promoting inflammation

For many years it has been known that tumours have significant immune system infiltration and therefore have substantial inflammation (37). This infiltration can range from a small presence of innate and adaptive immune cells to considerable immune presence with a substantial inflammation (38). Whilst immune cells typically would function to target and remove these tumour cells and therefore the presence of such an immune response would be considered a negative factor in tumorigenesis, this is not the response that occurs (39). Instead, tumour-associated inflammation aids tumour cells in acquiring hallmarks of cancer in several ways such as supplying growth factors, survival factors and proangiogenic factors to the tumour

microenvironment (40). Furthermore, during inflammation immune cells release many chemicals which can act on the surrounding tumour cells that has a mutagenic effect, furthering the quick acquisition of genetic alterations and thus the hallmark capabilities (41).

Enabling characteristic of genome instability and mutation

During the tumorigenesis process, many hallmarks described above require the presence of multiple genomic alterations for the trait to develop (20). Once a mutation has been acquired that has a selective advantage within a subclone of a tumour, clonal expansion occurs with this mutant being passed down to successional tumour cell progeny. This accumulation of genomic mutations can be aided by the cancer cell either through weakening the DNA surveillance systems or dismembering the genome maintenance machinery, both of which normally function to ensure genome stability (42). For example, many caretaker genes that are involved in the DNA-maintenance machinery, in a tumour suppressor like function, are commonly lost during tumorigenesis either through inactivation mutations or epigenetic repression (43). Across many cancers there is substantial evidence of widespread disruption in nucleotide sequences and gene copy number, suggesting that genome instability is an important factor in tumorigenesis and in the acquisition of the hallmarks of cancer (44).

1.1.3 Drivers of cancer and genomic variation in cancer cells

Across all humans there is genomic variation with around 0.1% of the genome differ between two humans (45). Genomic variation in can broadly be divided into two groups; small alterations, including single nucleotide polymorphisms (SNPs), short tandem repeats and small insertions and deletions (indels) and large-scale alterations such as structural variation (46). Structural variation encompasses rearrangement of large DNA segments and the deletion or duplication of large DNA segments, which alters the number of copies of a DNA sequence i.e., copy number variations (CNVs) or copy number alterations (CNAs) when occurring in germline or somatic tissue, respectively. Whilst there is no definitive rule that distinguishes alterations between the small and large category, a widely used cutoff criteria of 50 bp is used, for example to classify indels and CNAs (47). SNPs are the most common cause of genetic variation across humans, accounting for ~90% of all genetic variation, however not all occur in coding regions or result in an altered protein expression that then contributes to a disease (48). CNAs and SNP arise from different mechanisms, SNPs are typically due to lesions or repair mistakes in single stranded DNA. Whereas CNAs occur due to double stand DNA breaks, incomplete double-stand DNA repair, DNA replication or cell division insufficiencies. One such event that results in substantial structural variation that can co-occur with a deleted copy number state is chromothripsis (49). It is

suggested that a single catastrophic hit shatters one or a few chromosomal arms into >100 of fragments. Whilst the DNA repair pathway attempts to repair the damage, this repair results in a chromosome reassembled in the wrong order and/or orientation. Furthermore, many of the broken fragment are not rejoined during repair and therefore chromothripsis results in deletions (50). Two theories have been suggested to explain how these chromothripsis events occur. One theory is that when cells enter into telomere crisis due to excessive telomere shortening, end-to-end chromosomal fusion and the formation of a chromatin bridge can occur. This chromatin bridge then can break and fragment the DNA strand, which is then errantly repaired (51). An alternative theory is the formation of micronuclei after incomplete mitosis, which are highly error prone and therefore DNA can be readily fragmented and reassembled (51).

Cancer research has identified certain SNPs that target cancer either by influencing susceptibility or outcome. For example, in breast cancer, nonsense, frame shift and splicing SNP are the most common cancer-causing *BRCA1* and *BRCA2* mutations as they in a truncated protein which is unable to complete it function in homologous recombination DNA repair (52). Insufficient DNA repair results in genomic instability and an increased DNA-damaging agent sensitivity, allowing for the further accumulation of genetic alterations (53). Breast cancer patients with a *BRCA* gene mutation have a greater structural variant burden across the genome compared to wild type patients. Clinical research has found that having a *BRCA* mutant increases a person's risk of developing breast cancer to 45-85% compared to only an 8% chance in individuals with wild type *BRCA* (54). Furthermore, patients with a *BRCA1* mutation are more likely to have triple-negative breast cancer, earlier onset, aggressive disease and greater risk of relapse (55).

Broadly these genomic alterations can be separated into germline and somatic changes, with the former occurring parental germ line cells that are then inherited by the offspring. The latter is instead acquired during the life cycle of the cell, either from environmental extrinsic factors or due to errors in intrinsic processes such as the DNA repair and DNA replication machinery (56). Extrinsic factors include tobacco, hormones, the tissue microenvironment, inflammation, and exposure to certain viral infections such as the human papillomavirus (HPV) (57). To examine if intrinsic or extrinsic factors have contributed to the tumorigenesis process, an analysis of the mutational signatures can be completed. Different external or internal stressors acting on a specific cell type will leave a specific imprint or mutational pattern on the human genome (58). Examining the mutational signature will indicate if, for example, UV radiation exposure has contributed to the development of cancer as the highly specific signature known as COSMIC signature 7 will be present (58). It has been reported that 70-90% of lifetime cancer incidences can be attributed to environmental factors (59), however the contribution has been argued to be a much lower value at around 30% (60). It is important to note that typically multiple driver

mutations, with both intrinsic and extrinsic origins, are required as a single mutation will not be sufficient in triggering the transformation of a normal cell to a cancerous one (57).

As mentioned before, acquired changes can either be passenger or driver mutations, the latter of which confer the cancer cell a selective advantage. The discovery and understanding of these driver mutations has long been a significant aim in cancer research. Many of these drivers are tumour suppressor genes and oncogenes. Tumour suppressor genes, as the name indicates, function to maintain normal and controlled cell growth and development, stopping the formation of tumours. The tumour suppressor gene *TP53* is known as the guardian of the genome due to its vital role in cell cycle control, specifically during the G1/S checkpoint, and in orchestrating apoptosis in response to DNA damage being detected (61). *TP53* is commonly altered in many cancers, including haematological malignancies, whereby the activity of the p53 transcription factor is disrupted which allows for cancer development to occur (62). Further examples of tumour suppressor genes are *BRCA1* and *BRCA2*, which are important in breast and ovarian cancer (63). Alternatively, driver mutations can occur in oncogenes, which is a mutated version of a proto-oncogene that normally functions in signal transduction pathways to control cell proliferation and differentiation. These modified oncogenes instead drive cell division and thus tumorigenesis (64). Oncogene modification can either alter the structure of the protein or cause an overexpression. For example, mutations in the oncogene *Ras* results in a protein with an altered binding site which causes continuous Ras activation, leading to aberrant proliferation and cell survival signals (65). It is hoped that the characterisation of these driver mutations that contribute to tumorigenesis will allow new preventative measures and novel therapeutic options to be developed.

Within cancer research, understanding the biology of normal cells can help uncover critical aspects of how the cancerous version of the cell develops and progresses. As the focus of this thesis in a B cell malignancy, insight into normal B cell biology is communicated below.

1.2 B-cell biology

1.2.1 B-cell and B-cell development

The main stages of B cell development are progenitor B cell, pre-B cell, immature B cell and mature B cell. B cell development starts in the bone marrow where VDJ recombination occurs whereby the immunoglobulin (Ig) heavy (H) chain gene loci (V, D, J) are rearranged to create highly diverse Ig molecules as this process is error prone (66). Pro-B cells undergo this VDJ recombination to become differentiated into pre-B cells, which contain IgM heavy chain

molecules that cannot be expressed on the membrane as they do not have an Ig L chain rearrangement. To allow the pre-B cell to develop further a surrogate B cell receptor (BCR) complex is formed using a surrogate L chain. At this point, as a complete BCR is not present the B cell cannot function as an immune cell. During the immature B cell stage, rearrangement of the Ig light chain V and J gene loci occurs, allowing a complete BCR to be expressed on the membrane surface, see **Figure 4**. The two variable heavy chain and two variable light chain are involved in antigen binding whereas the two constant heavy and two constant light chains are required for effector functions (67). Further development occurs to transform into a mature B cell which then can leave the bone marrow and express IgM and IgD class on the surface of the B cell.

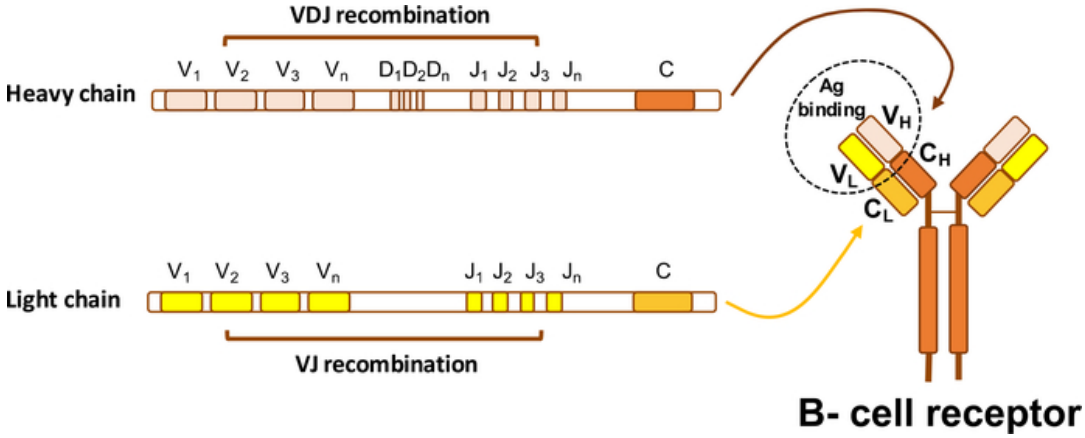

Figure 4- The recombination process as part of B cell development. Recombination of the heavy and light chain genetic regions that form the B cell receptor are necessary to increase antibody diversity, from (67)

Further B cell development occurs within the secondary lymphoid organs once a B cell has recognized an antigen via its BCR. This activates the B cell to differentiate into plasma cells, become germinal center precursor cells or undergo class switch recombination (68). Germinal centers are specialized microstructures that are located within the secondary lymphoid organs and are constituted of a light and dark zone (69). The B cell development within the germinal center is initiated in the dark zone where the B cell rapidly proliferates and undergoes somatic hypermutation. Somatic hypermutation in B cells allows for affinity maturation of antibodies produced by the B cell and thus have a key function in optimizing antibody dependent immune responses (66). The process is initiated by Activation-Induced Cytidine Deaminase (AID) which allows V(D)J rearrangement as well as having a role in class switch recombination (70). AID activity deaminates cytosines within the DNA to deoxy-uracil. Further AID activity and error prone processing of this replacement uracil results in an increased mutation rate in the *Ig* genes that gives rise to a repertoire of antibodies with a greater range in affinity (71). Within the light zone clonal selection occurs in an antigen and T cell-dependent manner. Present in the light zone is a population of T follicular helper cells which function in the positive selection of higher-affinity B

cells by stimulating their proliferation and differentiation (72). A further outcome from the random somatic hypermutation is the introduction of mutations that generate B-cells that recognize self-antigens and thus produce autoreactive antibodies (73). Therefore, whilst a positive selection occurs for cells with high affinity BCR there is also the removal of self-reactive B cells through negative selection within the germinal center (74). As mentioned above AID also induced class switch recombination, a process in which deletion rearrangement within the Ig heavy constant regions occurs. This process allows B cells to switch Ig isotype from IgM and IgD into IgG, IgE, or IgA. Thus, adapting its effector function and tissue distribution to be more specific to the antigen triggering the immune response (71). After antigenic stimulation, a proportion of B cells can transform into small lymphocytes that stop proliferating and have a much greater life expectancy, known as memory B cells. The function of these cells is to be able to quickly differentiate into plasma cells to produce the same antibody if they come into contact with the same antigen again, which is an essential part of the secondary immune response.

1.2.2 B-cell receptor

BCR signaling is essential for B-cell development and survival and can occur either spontaneously or through interactions with ligands present in the environment (75). A unique aspect of BCR is that they, unlike other receptors, can be activated by a range of structurally different ligands. The BCR is also the most prevalent surface receptor on the B cell with around 100,000 to 200,000 per cell (76).

As a monomeric form, the BCR is comprised of an IgM molecule and the Igα (CD79a) and Igβ (CD79b) heterodimer via a non-covalent link (77). IgM is constructed of two heavy and two light chains linked by a disulfide bond. Igα and Igβ are also covalently joined by a disulfide bond and both are compiled of an Ig domain, TM region, and a cytoplasmic tail that contains a ITAM motif (78). Research has found that most membrane BCR occur as oligomers instead of as monomeric receptors and B cell activation and signaling is linked to BCR oligomer opening and binding of regulatory molecules (79).

The function of Igα and Igβ is to act during antigen binding as the main signal transduction molecules and to aid in the expression and transposition of membrane bound Ig. At rest B cells have self-inhibiting BCR oligomers but after antigen binding to BCR, these oligomers open and expose the ITAM domain (80). Once exposed the two tyrosines of the ITAM can be phosphorylated by the Src-family kinases which creates sites for recruitment and activation of Syk. Once recruited, a BCR/Syk complex is formed which activates various downstream signaling pathways, including BTK, which results in NF-kB activation leading to B cell differentiation and

survival (79). For the activation of the PI3K-AKT pathway the co-stimulatory molecule CD19 must also be phosphorylated in addition to BCR activation (81). BCR have an essential function in normal healthy B cell but also are heavily involved in B cell malignancy and B-cell dependent autoimmune diseases and therefore have been extensively studied.

1.2.3 B-cell Malignancy

There are many different types of B cell malignancies which can be defined as leukaemias or lymphomas with the former relating to malignancy that arises in the bone marrow that move into the bloodstream, while the latter originates in the secondary lymphatic organs such as the lymph nodes and spleen. B cell leukaemias are diagnosed as either acute or chronic, depending on the growth speed of the malignant cells, with acute leukaemias being associated with a more aggressive disease (82). Lymphomas can also be broadly split into two groups that have distinct growth rate, different effected lymphocyte and varied treatment response, namely Hodgkin's lymphoma and non-Hodgkin's lymphoma (NHL). (83). Further B cell malignancies such as follicular lymphoma and Burkitt lymphoma were given the classification of NHL. Additionally, within the NHL group are diffuse large B cell lymphoma (DLBCL), mantle cell lymphoma, splenic marginal zone lymphoma, small lymphocytic lymphoma (SLL) and chronic lymphocytic leukemia (CLL), see **Figure 5**. SLL and CLL have identical phenotypic and immunophenotypic characteristics but the former is mainly found in the lymph nodes whereas the latter occurs in the bone marrow and blood. The international workshop on chronic lymphocytic leukemia (iwCLL) guidelines have an arbitrary cut off of $\geq 5x10^9$/L clonal cells to classify SLL from CLL. Due to the biological similarities SLL patients, in most guidelines, are given the same treatment as CLL patients (84). NHL is a common type of cancer with over 500,000 new cases being diagnosed each year worldwide (85). This group of B cell malignancies are highly diverse with each arising from a different stage of B cell development. The stage at which the cancer began is indicated on the malignant B cell by the stage-specific cell surface markers and a distinct molecular profile, which is used in the WHO NHL classification system (85). Whilst there are many types of NHL, each with unique biology and clinical presentation, CLL is the focus of this thesis and further detail on its biological characteristics and clinical presentation is given below.

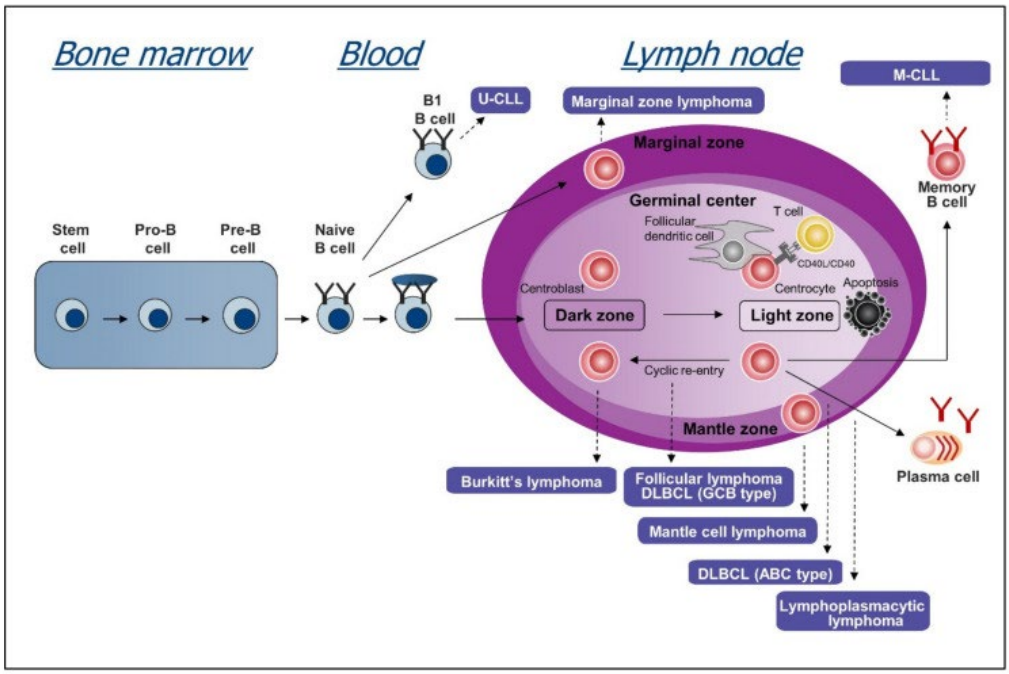

Figure 5- Schematic representation of B cell development, highlighting the cell of origin for various B cell malignancies, from (86). U-CLL: Unmutated *IGHV* CLL, DLBCL: Diffuse large b cell lymphoma, M-CLL: Mutated *IGHV* CLL.

1.3 Chronic lymphocytic leukaemia

1.3.1 Clinical phenotype of chronic lymphocytic leukaemia

CLL is a B-cell malignancy characterized by the accumulation of CD5, CD19, CD23 and CD20 expressing B-cells in the bone marrow, lymph nodes, spleen and peripheral blood (87). Diagnosis of CLL requires the detection of ≥5x10^3/µl B cells in blood for at least three consecutive months (87). Tumour cells cannot sufficiently complete their immunological function and crowd out normal immune cells, inducing many of the symptoms observed in patients. Formerly it was stipulated that CLL was the result of the accumulation of long-lived resting B cells with the build-up being attributed to a defective cell death rather than excessive cell division. However, research has discovered the presence of a reservoir of active and proliferating CLL cells (88). CLL patients are, on average, 70 years old at diagnosis and follow a highly heterogenous disease course with some requiring immediate intensive treatment, whilst others can be on a 'watch and wait' intervention course for many years. If patients present with a clonal B cell expansion of <5x10^3/µl B cells in peripheral blood and no symptoms of lymphoproliferative disorders, they are then classified as having monoclonal B cell lymphocytosis (MBL) (89). Clinically MBL has overlapping entities with CLL and the majority of cases have the same immunophenotype of CLL. MBL is considered a pre-neoplastic condition to CLL with nearly all CLL cases preceded by MBL (90). MBL

can be divided into low-count and high-count MBL, with the latter progressing to CLL at a rate of 1-2% per year (90). Additionally, 2-10% of CLL patients will progress and transform into Richter syndrome (RS) which is a type of aggressive lymphoma, most commonly being DLBCL (91).

1.3.2 Treatment of chronic lymphocytic leukaemia

CLL is currently incurable without an allogeneic stem cell transplantation and the efficacy and response to various treatments differs across the CLL patient population. Patient outcomes have improved significantly in recent years predominantly due to the development of new treatment regimes (92). In the past only chemo-immunotherapy (CIT) was available, such as a fludarabine, cyclophosphamide, and rituximab (FCR) or a bendamustine, rituximab (BR) regime. Fludarabine, cyclophosphamide and bendamustine are all chemotherapy drugs that function to kill cells that are rapidly dividing, including both tumour and normal cells. Fludarabine is a type of purine analogue which inhibits cell division by becoming incorporated into the newly synthesized DNA as has a similar structure to normal nucleotides present in the nucleus. Once erroneously incorporated into the DNA, apoptosis is triggered typically due to DNA breakages (93). Whereas cyclophosphamide and bendamustine are alkylating agents that cause apoptosis by cross-linking DNA strands which results in strand breaks, abnormal base pairing, and inhibition of cell cycle progression as DNA replication is incomplete (94). The addition of anti-CD20 monoclonal antibody (mAb), rituximab, to many chemotherapy treatments has significantly improved CLL patient response. For example, in one clinical trial, patients given FCR treatment as an initial treatment compared to just FC chemotherapy had a complete remission (CR) rate of 70% compared to just 38% (95,96). The mAb rituximab binds to CD20, a B-cell specific transmembrane protein present on nearly all normal and malignant B-cell (97). Once bound apoptosis is triggered via a range of mechanisms including antibody-dependent cellular cytotoxicity, complement-dependent cytolysis, and direct apoptosis induction through intercellular signalling and downregulation of antiapoptotic factors (98). This evidence resulted in FCR being the gold standard for frontline treatment of CLL patients and for relapse patients.

However, in recent years the treatment landscape for CLL patients has changed due to the emergence of novel oral targeted therapies and next-generation anti-CD20 mAb. The development of targeted agents has improved the treatment response, especially in patients with high-risk biomarkers such as *TP53* aberrations or unmutated immunoglobulin heavy-chain variable (*IGHV*) region gene status (99). Patients with these biomarkers typically have a high relapse rate after CIT with a reported 35-50% of patients relapsing with a progressive disease within three years of treatment (100). Current guidelines state that FCR should no longer be used as frontline management of CLL and CIT should only be used in patients with low-risk features,

such as being young of age, but also whilst considering any additional patient comorbidities (101). The decision about when to treat and with what, are regularly reviewed at the iwCLL meeting. The iwCLL current decision tree for the management and treatment of newly diagnosed CLL patients is shown below in **Figure 6**, which clearly highlights the preferential use of targeted therapies for high and low risk untreated CLL patients.

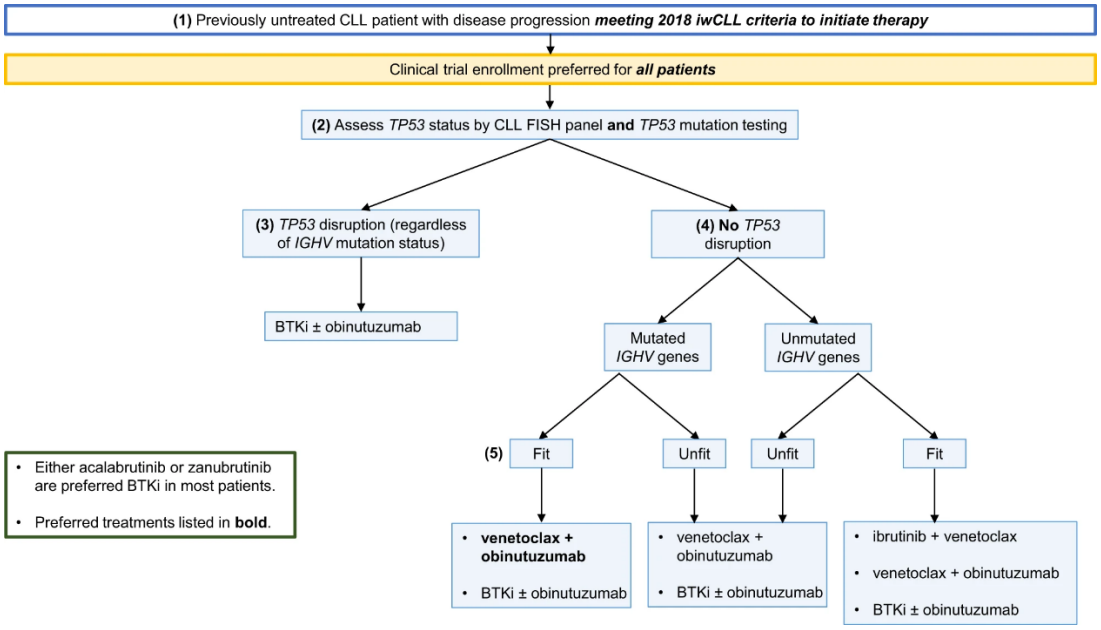

Figure 6- Chronic Lymphocytic Leukemia treatment algorithm from the 2018 iwCLL meeting. Abbreviations- BTKi- Bruton tyrosine kinase inhibitors, IGHV- immunoglobulin heavy chain gene, from (102).

Currently there are a range of oral targeted agents that have been approved for use in treating CLL patients, either as first line treatment or for people that have relapsed. Not only have these targeted treatments been recorded to have a greater efficacy, as shown by improved progression free survival (PFS) and overall survival (OS) rates but are also more tolerable than chemotherapy and therefore are more appropriate for the elderly CLL population. Nevertheless, these targeted agents are expensive, and the patient can experience a relapse and refractory disease after treatment initiation. Therefore, greater accuracy of risk-adapted patient stratification is needed to ensure each patient is enrolled on a treatment regime that will have the greatest clinical outcome based on the genotype of the patient (103).

These oral agents function by acting on a specific target that is present within a CLL cell. For example, by targeting and inhibiting phosphatidylinositol 3-kinase (PI3K), Bruton tyrosine kinase (BTK), or Bcl-2 regulatory proteins. Additionally, a next generation of anti-CD20 mAb has been developed and evaluated for use in CLL. A phase three study found that the anti-CD20 mAb obinutuzumab in combination with chlorambucil compared to rituximab with chloramucil or chlorambucil alone had a significantly greater PFS of 26.7 months, 15.2, or 10.7, respectively (p-

value<0.001) (104). Due to this evidence of obinutuzumab improving outcomes of CLL patients this anti-CD20 mAb, in combination with chlorambucil, has been approved for the frontline treatment of CLL.

An appealing target for these oral agents is the BCR, which has led to the development and approvals of two main groups of drugs in CLL that target BCR signalling pathways; PI3K inhibitors and BTK inhibitors. There are three classes of PI3K, each contains a range of different isoforms of the kinase (105). PI3K are key signalling molecules that are involved in cellular proliferation, development, and survival. Isoform PI3Kδ is primarily expressed in B cells and involved with the BCR whereas PI3Kγ is mainly expressed on other haematopoietic cells, such as T cells (106). Idelalisib and duvelisib are both PI3K inhibitors which function to trigger cell death by competitively binding to various PI3K isoforms, stopping their action. Idelalisib is a selective PI3Kδ inhibitor which causes cell death by inducing caspase-dependent apoptosis (105). Duvelisib is a dual inhibitor that stops the activation of both PI3Kδ and PI3Kγ isoforms (106). Inhibition of PI3Kγ aims to reduce cytokine production from T cells which promotes CLL-m, cell survival, cell cycle, metabolism and migration (107). Whilst these two treatments are associated with significant toxicities and have a high rate of relapse, the incurable nature of CLL still makes them a useful therapeutic option with good efficacy reported in patients with high-risk features (106). In 2018, duvelisib was approved for the treatment of CLL patients who have relapsed at least twice before; this decision was based on evidence from therapeutic trials. One such trial aimed to assess the efficacy of duvelisib as a monotherapy in patients with relapsed or refractory (R/R) disease compared to the current standard ofatumumab dose, a type of anti-CD20 mAb. The Duvelisib treatment group were found to have significantly improved PFS (median 13.3 vs 9.9 months, p-value<0.001) and overall response rate (74% vs 45%, p-value<0.001) compared to the control group of ofatumumab-treated patients, even in high-risk patients with deletions of chromosome 17p (106).

BTK inhibitors, such as ibrutinib and acalabrutinib, are much more tolerated by CLL patients and, therefore, are more widely prescribed at any treatment line for patients with and without *TP53* dysfunction. Many clinical trials have found this treatment is superior to traditional CIT; for example, a significantly improved PFS and OS were identified in the ibrutinib-rituximab regime compared to FCR within untreated patients (PFS HR:0.27, p-value<0.001 and OS HR:0.47, p-value<0.018) (108). This superior efficacy is also recorded in cohorts of R/R CLL patients. For example, a greater PFS, OS and response rate was found when ibrutinib was given compared to anti-CD20 mAb, ofatumumab. The overall response rate for the ibrutinib-treated group compared to ofatumumab was 43% vs 4.1%, p-value<0.001, with a greater OS rate also being found in the ibrutinib group (HR:0.43, p-value<0.005) (109). The mechanism of action of BTK inhibitors, such as

ibrutinib, is stopping BTK downstream signalling, such as NF-kB transcription factor activation, leading to reduced cell proliferation, migration, and survival (110).

An additional target, outside of the BCR, is the family of B-cell lymphoma 2 (Bcl-2) proteins comprising of proapoptotic and antiapoptotic/prosurvival proteins that regulate apoptosis. Bcl-2 is an antiapoptotic protein that is overexpressed in cancer cells as it inhibits the release of mitochondrial proapoptotic factors into the cytoplasm, which would lead to cell death (111). Currently, venetoclax is the only approved Bcl-2 inhibitor available for treating CLL. Inhibition of Bcl-2 occurs through the highly selective and competitive binding of venetoclax, displacing pro-apoptotic proteins that have been bound and blocked by Bcl-2. Once released, these pro-apoptotic proteins can trigger and restore the intrinsic apoptosis pathway in CLL cells (112). This targeted therapeutic was initially approved for use in patients with *TP53* aberrations but has since been prescribed for all patients after evidence found no difference in response rates for patients without *TP53* disruptions. A clinical trial with untreated CLL patients found that a venetoclax and obinutuzumab regime had a more significant PFS than a CIT-based chlorambucil and obinutuzumab regime. Additionally, the venetoclax treatment group had a significantly greater percentage of patients with PFS at 24 months than the CIT group (88% vs. 64%) (113). Furthermore, a clinical trial using a cohort of del17p CLL patients found that an overall response rate for patients on venetoclax monotherapy was 77%, with a complete response of 20%. At 24 months, the 122 patients with a response had a median duration of response (DOR) 33.2 months and this translated into a median PFS of 27.2 months (114). They concluded that venetoclax monotherapy was well tolerated by patients and produced a durable response in high-risk patients, who typically have limited treatment options.

Whilst targeted therapies as a monotherapy or as a combination therapy have shown to improve response and survival in treated and relapsed patients, a 2015 study found that BTK inhibitors were the most prescribed treatment for R/R CLL. However, CIT was still the most prescribed from treatment naive patients (115). Although improved efficacy and greater tolerance have been shown in patients given targeted agents compared to CIT, relapse is still a prevalent problem in the target agent treatment landscape and CIT is still heavily utilized. A further important conclusion from this research was that of the patients with unknown risk status, 25% of them received CIT which was potentially not the most appropriate treatment. Therefore, by validating additional prognostic and predictive biomarkers a more accurate risk stratification of these unknown risk patients can occur. Ultimately so a more appropriate treatment regimen can be chosen, which would positively impact patient outcome.

1.4 Prognostic and predictive biomarkers in CLL

Various patient features, from serological to specific genomic characteristics, have been found to indicate patient prognosis or treatment response and, therefore, have clinical utility as prognostic and predictive biomarkers. Prognostic biomarkers include, but are not limited to, numerous host factors such as age, gender and ethnicity, serological markers such as beta-2microglobulin (B2M) and thymidine kinase levels, antigen expression such as CD38 and ZAP70 and genetic features such as *TP53* gene disruption and *IGHV* gene mutation status (116). Predictive biomarkers include genetic characteristics such as *IGHV* mutation status, *NOTCH1* mutations in the CIT setting, and *TP53* disruption in the context of both CIT and oral agents (117,118). The first biomarkers used for risk stratification were the Binet and Rai staging systems, which are still used today (119). To understand the heterogeneity underpinning the pathogenesis of CLL, the genomic landscape has been extensively examined using a range of genomics techniques (120). These evaluations have shown the CLL genome to be complex, with many different combinations of genetic alterations occurring within the CLL population but also within a single tumour, demonstrating both intra- and inter-tumour diversity (121).

1.4.1 *IGHV* mutation status

The mutation status of *IGHV* genes approximately divides the CLL population into two groups named unmutated (U-CLL) and mutated (M-CLL) CLL. These two CLL subgroups arise during the normal multistep B-cell development process. If CLL arises from a B-cell pre or post-germinal centre reaction, where somatic hypermutation occurs, it is classified as U-CLL or M-CLL, respectively (122). A cutoff of ≥98% sequence homology with germline variable Ig gene has been used to classify patients with unmutated *IGHV* genes and <98% sequence homology with germline variable *Ig* gene for patients with mutated *IGHV* genes (123). The BCR present in U-CLL and M-CLL cases have distinct signaling responsiveness, with the former having high responsiveness whilst the latter has low anergic BCRs (124). Two landmark studies discovered the prognostic importance of identifying whether the B-cell of origin had undergone somatic mutation or not, with both studies finding that M-CLL correlated with greater PFS and OS (89,123). *IGHV* mutational status has also found be able to predict the durability of response to CIT with a PFS of 53.9% of patients with M-CLL compared to just 8.7% in U-CLL patients after a follow up of 12 years (125). However, this greater response in M-CLL patients does not seem to be present when patients are treated with novel agents that impact the BCR, for example ibrutinib. In fact, it is the U-CLL patient that have a more rapid response. A three year follow up study that used ibrutinib as a frontline treatment recorded a complete response rate of U-CLL and M-CLL patients as 40% and 6%, respectively (126). This is possibly due to an increased reliance of U-CLL cells in tonic BCR

signaling but this does not necessarily mean ibrutinib has a greater efficacy for U-CLL patients as a complete response is classed as a complete clearance of lymphocytosis, which is typically delayed in M-CLL even when patients are responding well to treatment (122). Unlike the PFS reported after CIT, the five-year PFS of patients treated with ibrutinib was equivalent for both U-CLL and M-CLL (127).

1.4.2 IGLV and BCR stereotype

Whilst somatic hypermutation in B cell development is a random process, within CLL a recurrent or "stereotyped" amino acid changes of the BCR has been identified. The CLL Ig repertoire includes an overrepresentation of selected *IGHV* genes, with somatic hypermutation not occurring uniformly across the *IGHV* genes (128). Specifically, by examining the variable heavy complementarity determining region 3 (VH-CDR3) sequences for mutations, around 30% of CLL patients can be grouped into common subsets based on highly similar or identical sequences (129). Additional work using over 7,000 IGHV sequences identified 19 subsets that were the identified in 12% of CLL patients. Interestingly the expression of certain stereotyped BCRs is reported significantly more frequently in U-CLL or M-CLL patients with this 'CLL-biased' not being found in normal B cells. Furthermore, CLL cases that express the same stereotyped BCR can also share similar clinical and molecular features (128). For example, subset #4 (*IGHV4-34*) was associated with an indolent disease, high number of mutations, and with M-CLL status. Whereas subset 1# (*IGHV1-5-7*) is common in U-CLL and is associated with a poor prognosis. Further stereotypes that have been shown to be associated with poorer prognosis, independently of *IGHV* mutation status, include *IGHV3-21*, *IGHV3-48* and *IGHV3-53* (130). A bias in the immunoglobulin light chain (IGLV) repertoire has also been reported in CLL with IGLV3-21 being a frequency used IGLV stereotype. B cells expressing this IGLV3-21 stereotype can acquire a single point mutation (R110) which causes autonomous BCR signalling and aggressive disease presentation (131). Additionally, IGLV3-21^{R110} patients have an overexpression of the *WNT5A/B* gene, which regulates proliferation and apoptosis.

The existence of these quasi-identical BCR may suggest the presence of a common antigen or classes of epitopes with similar structures, that interacts with specific BCRs to stimulate their proliferation and clonal expansion. This antigenic pressure on the cell of origin suggests that the reactivity of a CLL clone is linked with the BCR stereotype which influences the disease progression and outcome (132). Research into characterising these antigens have found specific binding of various microbes and motifs present on apoptotic cells with specific stereotypes, for example *IGHV3-21* showed binding to cofilin-1 protein, which is present on the membrane of apoptotic cells. It was concluded that the presence of infections and self-antigens can

continuously trigger BCR signaling causing an increased chance of a tumour-transforming event through the rise in B cell proliferation and survival, however the full mechanism of BCR stereotype in CLL is not currently known (133).

1.4.3 Döhner fluorescence *in situ* hybridization prognostic classification

During thirty years of CLL genome research, numerous recurrent chromosomal lesions and gene mutations have been identified and shown to have clinical relevance. The fluorescent in situ hybridization (FISH) technique was developed in the 1980s. The technique utilizes single stranded fluorescent labelled DNA probes to examine chromosomes and allows the detection, quantification, and localization of specific target sequences (134). FISH can detect chromosomal structural changes, but due to a greater resolution than chromosome banding analysis (CBA), it can also examine small segments of chromosomal abnormalities, such as microdeletions and small translocations. In 1999, FISH technology was used to detect recurrent chromosomal abnormalities in CLL patients, which enabled their clinical significance to be described in a hierarchical prognostic model for CLL (135). This Dohner hierarchical model, groups CLL patients into five clinically relevant subgroups depending on the presence of four recurrent chromosomal abnormalities; 17p, 11q, and 13q deletions, and trisomy 12.

The presence of a del17p is associated with the poorest patient survival, shorter time to treatment (TTT) and resistance to chemotherapy (136). This chromosome aberration results in the loss of *TP53* and is the least common chromosomal abnormality with a prevalence of <5% of the newly diagnosed CLL population (137). As mentioned above, the gene *TP53* synthesises the tumour suppressor protein p53, which has a function in responding to cellular stress and in maintaining genomic integrity through its involvement in the DDR pathway (138). The p53 protein can be activated in response to DNA damage, hypoxia or activation of oncogenes. P53 largely functions as a transcription factor that orchestrates a variety of antiproliferative pathways by activating or inhibiting the transcription of numerous effector genes (139). These pathways result in numerous biological outcomes including cell-cycle arrest, cell senescence, apoptosis or modulation of autophagy (140). Although p53 is an extensively studied protein in cancer research its biological function is not truly understood currently. This is in part due to the function of the protein being highly context-dependent with factors such as cell type and the oncogenic events acquired during tumour evolution, influencing its function (139).

Deletions of the 11q chromosomal arm impacts the *ATM* locus, is present in around 20% of patients and predicts a dismal survival, however not as poor as del17p events. Around 80% of del11q patients also are U-CLL. Additional mutations of the *ATM* gene have been reported at

various frequencies (30-40%) and has been found to be associated with a poorer survival than sole del11q patients (141).

Trisomy 12 is present in around 15-18% of CLL cases however much is unknow about its pathophysiology. These cases typically co-occur with a mutation in the *NOTCH1* gene (~50%), are associated with U-CLL and have higher incidence of progressing to RS (142). Patients with a trisomy 12 have an intermediate survival, greater than patients with del17p or del11q but worse than patients with a normal karyotype (135).

The most common, clinically relevant chromosomal abnormality is the deletion the long arm of chromosome 13 (del13q) which has a prevalence of 60-80%, based on the screen tool that is employed (137). When del13q occurs as the sole abnormality it indicates a good patient outcome and was ranked at the top of Döhner hierarchical model with the greatest median survival of 133 months (135). The 13q minimally deleted region (MDR) includes DLEU1 and part of *DLEU2* gene that encompasses the microRNA (miRNA) 15a/16-1 cluster. Both miRNAs function as tumour suppressors by targeting the oncogene *BCL2*, as well as others, as this gene is typically overexpressed in CLL meaning a greater threshold of proapoptotic signalling is required for apoptosis to be triggered (143). However, 13q deletions are highly variable in both size and gene content (144), with larger deletions being associated with a more aggressive phenotype and inferior survival in patients. In addition, these large deletions have been found to co-exist with elevated levels of chromosomal complexity (144). Various candidate genes have emerged to explain these characteristics of these large deletions, these include *RB1* and *RNASEH2B*. *RB1* is considered as a tumour suppressor gene that encodes the retinoblastoma protein, a critical regulator of the cell cycle (145). Whereas *RNASEH2B* functions in ribonucleotide excision repair, an important DDR pathway which removes ribonucleotides which are mistakenly added into DNA via DNA repair polymerase (146). Additionally, these deletions can be heterozygous (monoallelic) or homozygous (biallelic). Biallelic loss of 13q occurs in 30% of patients with del13 events, are typically smaller in size, do not involve *RB1* and are associated with a more aggressive disease (145).

Although the Döhner model was develop over 20 years ago it has been amended to include gene mutational data that has clinical relevance and therefore has remained the most accepted and utilized genomic prognostic model for CLL patients within the clinical environment (147).

1.4.4 Genetic mutations

More recently, the development of next generation sequencing (NGS) has allowed the CLL genome to be investigated at a base-pair resolution through whole-exome (WES) and whole genome sequencing (WGS) studies (147). These studies have allowed the mapping of the

mutational landscape of CLL and have identified numerous recurrent genetic mutations that disrupt many cellular processes. The average mutational burden of CLL is comparatively lower than the mutational burden of solid tumours with an average of 0.6-0.87 mutations per megabase (Mb) of genomic DNA in a CLL patient (148). Currently there has not been the identification of a unifying mutation that all CLL patients possess. Nevertheless, four genes, *TP53, ATM, NOTCH1* and *SF3B1,* have been identified in numerous studies to be recurrently mutated at relatively high prevalence in the CLL population.

Both del17p and the deletion of chromosome 11q (del11q), as previously discussed, are frequently observed in tandem with deficiency mutations of *TP53* and *ATM* genes, respectively resulting in a biallelic loss of function of that gene (149). *TP53* aberrations*,* including either del17p events or *TP53* mutations, are a marker of an aggressive disease and resistance to chemotherapy. Therefore, it is among the strongest predicative markers that guide treatment decisions with all newly diagnosed patients screened for *TP53* aberrations (136). The gene *ATM,* located on chromosome 11q, is vital for the repair of DSB which can occur after oxidative stress or during normal biological events such as the rearrangement of *IGHV* genes during B-cell maturation (150). The ATM protein is one of the three phosphoinositide 3 kinase-related protein kinases (PI3KKs). The primary sensor of DSB is the MRN complex which forms a physical bridge across the DSB and retains ATM at the site (151). Subsequently, ATM can phosphorylate many downstream effectors involved in DNA repair, cell cycle checkpoints and transcription, which then can in turn activate their own targets **Figure 7**. A prime example of this is the activation of p53 by ATM directly, by the phosphorylation of p53 on serine 15. Or indirectly by ATM, through the phosphorylation of MDM2 which inhibits its ability to ubiquitinate p53 thus triggering checkpoint arrest to either allow for DNA repair to occur or cell apoptosis (152). Various DSB response proteins are also phosphorylated by ATM including MDC1 and histone H2AX, which generates y-H2AX. The activation of MDC1 by ATM also aids in the continued local phosphorylation of H2AX which form mega-base-size foci along the DSB (153). These foci are involved in the recruitment of many downstream repair factors including BRCA1 and 53BP1 (154). y-H2AX functions by sending an epigenetic signal to downstream DDR proteins, anchoring the broken ends of the DSB by repositioning the nucleosome and reduces the chromatin density to helps facilitate the re-joining of DSBs (155). It has also been found that H2AX can be phosphorylated by another member of the PI3KK family, DNA-dependent protein kinase (DNA-PK) and potentially by ataxia-telangiectasia and Rad3-related kinase (ATR), suggesting an ATM independent function for H2AX (156). *ATM* has been identified as the key target of chromosome 11q deletion which occurs in ~20% of CLL patients. Within CLL, del11q are associated with a shorter time to first treatment (TTFT) and poorer OS (135). Furthermore within 30-40% of patients with a del11q event an additional

mutation of the *ATM* gene is also found. Patients with this biallelic loss of *ATM* have inferior PFS and OS, comparable to the survival of patients with *TP53* dysfunction (141).

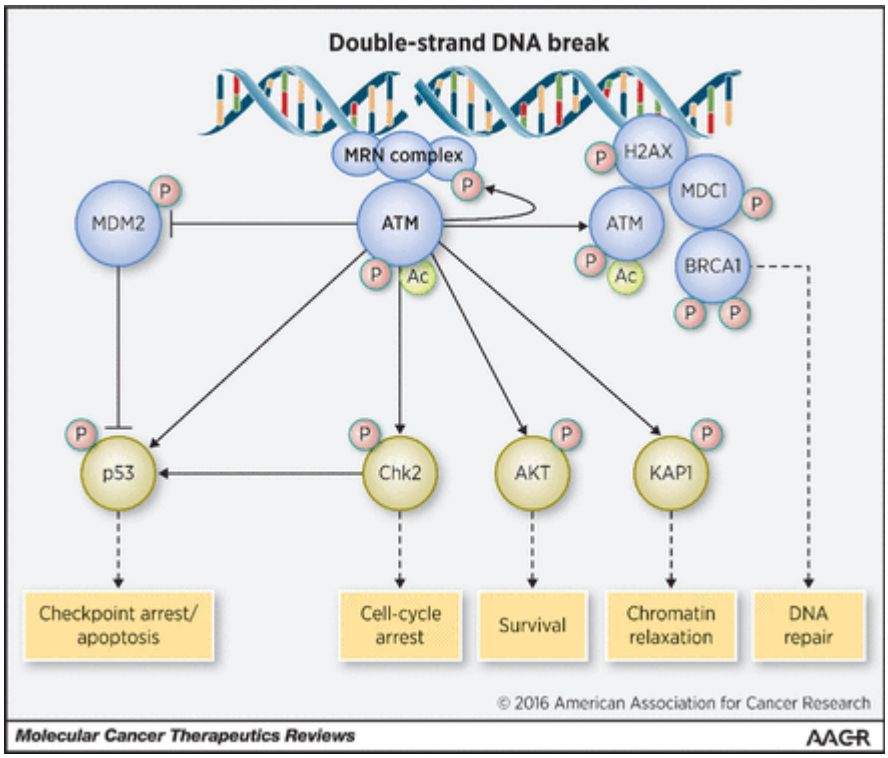

Figure 7- The biological function of ATM in repairing double-stranded DNA breaks. The MRN senses that a DDB has occurred and recruits ATM. ATM phosphorylates other sensor proteins, such as MDC1which also function in DNA repair. ATM also activates checkpoint kinase 2 (CHK2) which results in cell cycle arrest. ATM activates p53 directly and indirectly to cause checkpoint arrest and apoptosis of damaged cell. Chromatin relaxation to aid DNA repair is achieved through activation of KAP1. Furthermore, ATM activates pro-survival signals through phosphorylation of AKT and activation of NF-kB, which regulates cell proliferation (not shown). From (151)

Additional mutations have been identified that occur at lower frequencies, around ~5%, within the CLL genome such as *BIRC3, CHD2* and *SETD2* (157,158). Whilst *BIRC3* mutations are not common in the general CLL population, *BIRC3* has been found to be monoallelically deleted in ~80% of patients with a del11q (141). Within ~10% of CLL patients who have lost *BIRC3* through a del11q event an additional mutation of *BIRC3* can occur resulting in a biallelic loss of the gene which has been found to be an independent prognostic marker for a dismal TTFT and OS (159). Both the recurrent and less prevalent gene mutations have been found to impact eight key cellular pathways including cell cycle, chromatin remodeling and BCR signaling (147), see **Figure 8**.

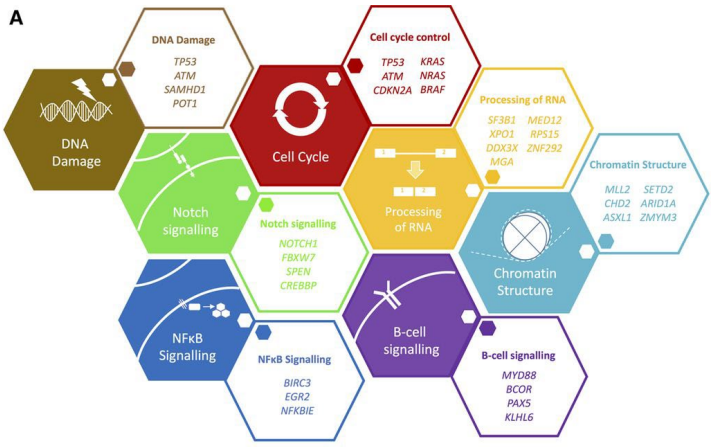

Figure 8- The key biological relevant genes recurrently mutated in CLL and the pathways to which they disrupt. These include cell cycle regulation, DNA damage response, apoptosis, Notch signalling, RNA metabolism, NF-Kβ signalling, chromatin remodelling and BCR signalling, from (147)

1.4.5 Telomeres

A further genomic characteristic that has been identified to play a pivotal role in the progression and patient outcome of CLL is the length of telomeres. Telomeres are complex nucleoprotein structures composed of hexanucleotide tandem repeats ((TTAGGG)*n*) of up to 25kb (160), and a number of proteins with regulatory and structural functions (161). They function to protect the chromosomal ends from replicative damage and prevent the ends from being recognized as DNA double-stand breaks, thus conferring genomic stability (162). Telomeres shorten with each cellular division, due to the end-replication problem, until reaching a critical length. At this point apoptosis/senescence or repair is triggered by mechanisms regulated by *TP53* and/or *ATM* which is part of their vital tumour suppressor function (163). Due to this progressive shortening as the cell ages, telomeres act as a mitotic clock (164). The repeated DNA sequence is organized into a looped structure known as a T-loop, using the 3' telomere overhang by strand invasion. They are also associated with a number of proteins with regulatory and structural functions that, among others, form the Shelterin complex (165). In stem/progenitor cells, germ cells and in a range of cancers, including CLL, telomere length (TL) is maintained. TL is maintained by telomerase, a ribonucleotide complex that compensates for this continual loss by adding TTAGGG repeats to chromosome ends (166). Telomerase is composed of; hTERT (a catalytic human telomerase reverse transcriptase), hTR (a RNA) and DYSTERIN subunits, which regulate elongation; the shelterin complex (TRF1, TRF2, TIN2, hRAP1, TPP1, POT1) that controls length and prevents degradation and fusion; and additional multifunctional factors (RPA1, hEST1A, KU70/KU80, RAD-MRE11-NBS1 complex) (167). Increased telomerase activity and overexpression of the hTERT subunit is observed in the germinal centers of proliferative lymphoid cells (166,168,169). This

facilitates long term proliferation by providing germinal centre-derived memory B-cells with an extended telomere reservoir for future cell divisions (166).

However, dysfunctional telomeres are frequent observations in many human malignancies (170–173) and play a complex role in the pathology of CLL. For example, cells with deregulation of the *TP53* and *ATM* gene have compromised DNA damage checkpoints and can bypass the replicative senescence or apoptosis usually triggered by erosion and uncapping of telomeres. Consequently, cells enter replicative crisis, resulting in extensive telomeric fusions and dicentric chromosome formation, breakage-fusion-bridge cycles, genomic instability, and cell death. However, this telomere driven crisis can offer a proliferative advantage, generating the genomic rearrangements that drive clonal evolution and disease progression (174–177). Increased hTERT expression and telomerase activity is also observed in CLL cells compared to normal B-cell counterparts, and the consequent stabilization of shortened telomeres is one mechanism responsible for the unlimited proliferation of malignant cells (178–181). This activity is lower at diagnosis and increases with disease progression (182), and in poor prognosis groups including unmutated *IGVH* (183) and *TP53* dysregulation (184). Although CLL is typically a disease of the elderly, the shortened telomeres observed at diagnosis are not just a function of aging, as the telomeres of aberrant cells are significantly shorter than their normal counterpart (169,170,176).

Research within CLL have found that TL was significantly associated with *IGHV* mutation status, *TP53* abnormalities (including *TP53* mutation and/or del17p), *ATM* and *SF3B1* mutations and genomic complexity (GC), defined as ≥3 CNAs (185). Survival analysis using TL as a continuous variable found that increased TL was associated with a significant (p-value<0.001) increase in PFS (Hazard ratio (HR)=0.89, 95% Confidence interval (95%CI): 0.85-0.93) and OS (HR=0.84, 95%CI:0.8-0.89). TL was also assessed as a categorical variable using the cut offs of; short (TL-S) <2.92 kb, intermediate (TL-I) 2.92 kb≤ and ≥3.57 kb, and long (TL-L) >3.57 kb. Within a multivariate cox regression model, TL-S were found to be an independent marker poorer PFS and shorter OS (185). Additional research has shown that short telomeres are associated with GC, defined as having two or more genomic aberrations (186). This is biologically relevant as the progressive loss of the telomeric caps results in telomere crisis where extensive genome instability results in the subsequent rapid accumulation of genetic abnormalities (187). They also found that these losses and gains were concentrated at the chromosomal ends and therefore are typical of aberrations that occur through telomere fusion.

Additional CLL research investigated TL using different definitions; the fusogenic mean and median. Previous work had found telomere end-end fusion events can be detected in CLL patients with short telomeres (177). This research was furthered, by using the ‘single telomere length

analysis' (STELA) technique, which allows an absolute TL measurement, to identify the range of TL in which a fusion event is detected. The range was 0.44-3.81kb and the mean of this range was 2.26kb which is known as the fusogenic mean. The upper threshold for telomere dysfunction was >3.81kb which was used to define the fusogenic median. The authors then examined the fusogenic mean as a prognostic marker and found that patients with TL below the fusogenic mean (≤FusoMean) had significantly (p-value<0.0001) poorer TTFT (HR=15.9, 95%CI:8-31.8), PFS (HR=14.1, 95%CI:6.5-30.3) and OS (HR=13.2, 95%CI:11.6-106.4). This was found even in a cohort of Binet stage A CLL patients and thus can stratify early-stage patients. A comparison of the fusogenic mean and median was completed to identify which threshold was the most prognostic for survival. Whilst both cut offs were found to highly prognostic compared to established markers such as CD38 expression, Binet stage and *IGHV* status, the fusogenic mean had the highest HR for progression and death and was found to be independent of all other biomarkers included in the multivariate analysis (MVA) (188). A further study used the fusogenic mean as a cut off to analyze TL as a categorical variable and found a significantly (p-value<0.001) shorter PFS and OS survival in the ≤FusoMean CLL group (189). Overall, many studies have shown the prognostic and predictive power of TL in CLL.

1.4.6 Epigenome

A more recent development is the investigation of the CLL epigenome which has been found to have disease-defining features. Epigenetics is an additional layer of complexity that guides the genomic function and activity of genes. Epigenetics can function in two ways; either through the modifications to chromosomal proteins to alter the genome and/or the protein-DNA interaction or through a chemical modification to the stranded DNA (190).

One aspect of epigenetics that has been found to have clinical significance across many cancers is the changes in DNA methylation. DNA methylation is a type of epigenetic modification which is stable over time but also reversible. It is characterized by the addition of a methyl group to the 5' carbon of any cytosine across the genome, however more than 98% occurs within the cytosine guanine dinucleotide (CpG) sites (191). This addition of a methyl group is orchestrated by DNA methyltransferases. In normal healthy cells DNA methylation functions to regulate gene expression and assures stable gene silencing (192). Alterations in DNA methylation patterns is one of the molecular hallmarks of cancer cells. These epigenetic hallmarks include global DNA hypomethylation and locus-specific hypermethylation (191). The first, hypomethylation, occurs due to a loss of methylation at sites of repeat elements, such as retrotransposons, that are normally heavily methylated. This can promote genomic instability and result in oncogene activation. The latter, occurs at promoter CpG islands of tumour suppressor genes which cause a

heritable transcriptional silencing (191). Therefore, DNA methylation functions in causing cancer by physically stopping the binding of transcriptional regulators to the gene and through the formation of chromatin via interactions with other epigenetic modifications including nucleosome positioning or the histone code. Many associations between cancer and DNA methylation have been identified with many of these epigenetic changes occurring early on in tumorigenesis (190). DNA methylation is functionally equivalent to genomic lesions such as deletions or mutations (192). Additionally, DNA methylation has been shown to be associated with cellular identity and memory of activity states and thus can be applied to investigate the cell of origin (193).

Research using whole genome DNA methylation analysis, three clinicobiological CLL subgroups defined based on distinct epigenetic signatures develop from five epigenetic markers have been identified. These three novel subgroups named naïve B-cell-like CLL (n-CLL), intermediate CLL (i-CLL) and memory B-cell-like CLL (m-CLL) were found, to some degree, to reflect the stage of B-cell maturation the tumour arises from (194). The original publication identified that this novel epigenetic classification was the strongest predictor of TTT in a multivariate cox model, with the m-CLL group being clinically favorable. Additional work completed by Wojdacz et al applied these epigenetic subgroups to a clinical trial cohort of 605 CLL patients (195). Similar to the original publication, the m-CLL epitype was an independent marker of prolonged PFS and OS in multivariate models (195). Therefore, research has found that these novel epigenetic subgroups have potential clinical use within CLL by identifying patients that are destined for prolonged survival after being given CIT.

1.4.7 Deficiencies in current biomarkers

As described above, numerous predictive and prognostic biomarkers have been identified in CLL. The most important being *TP53* aberrations and *IGHV* mutation status due to their usage in the clinical environment. Nevertheless, there is currently a migration away from investigating the impact of a singular biomarker and instead a more global approach is being considered within many types of cancers but is championed in CLL research. Although these single markers do have utility in CLL, reality is far more complex as patients typically do not have just one of these biomarkers present (196). One inconsistency is that single biomarkers do not always accurately portray or predict disease pathogenesis, for example there is a subset of CLL patients with *TP53* aberrations that present with an indolent disease course which is not captured within current biomarkers (197). Moreover, clinical staging systems typically fall short in truly capturing the disease course for patients that are classified in the low stages, i.e. Binet A and Rai 0, which accounts for the majority of newly diagnosed patients (196,198).

In terms of predictive markers, the need for treatment algorithms to be updated has been driven by the recent development of targeted agents that have the possibility to replace traditional CIT as the golden standard for treatment (199). Current treatment guidelines state that patients with *TP53* aberrations are only to be given targeted agents such as ibrutinib and venetoclax as frontline treatments (200). Additionally, frontline treatment options for patients without *TP53* aberrations have been changed to also include targeted agents as older patients can struggle with traditional CIT treatment (116). The identification of reliable and accurate predictive markers has benefits in terms of guiding clinical decision-making to select specific regimes that will have the greatest efficacy and therefore result in the best patient outcome, thereby shifting towards personalized medicine (119). Conversely treatment selection also has economic considerations, especially as targeted agents are relatively expensive and therefore should only be given to patients who will have the greatest response (201). Although there is clear evidence that patients with *TP53* aberration respond poorly to CIT and therefore should not receive this treatment (202), the evidence for patients with *TP53* aberrations responding well towards novel agents is lacking in long-term survival data with many of these studies still maturing (116). Additionally, it is not clear what other biomarkers may be present in this subpopulation of CLL patients that can further predict response to these targeted agents.

The need for reliable and accurate prognostic and predictive biomarkers in CLL is clear, however current biomarkers seemly fall short of this endeavor. Therefore, there is a need for further work to identify a biomarker that not only captures the true complexities of a patient's disease biology but also consolidate this into a reliable biomarker that can be used across the clinically heterogenous CLL population and within the emerging era of targeted therapies.

1.4.8 Genomic Complexity

One such novel biomarker that is the topic of much discussion within the CLL research community is GC. GC incorporates multiple established markers to create a useful and robust prognostic and predictive biomarker that can be used within CLL. Current published research shows that GC can accurately predict poor outcome in CLL patients, even within the high-risk subsets of the CLL population such as del17p patients (103,203,204). A seminal paper completed by the European Research Initiative on CLL (ERIC) found that cytogenetic complexity, defined by the presence of ≥5 CNAs, was an independent prognostic factor with adverse outcome in CLL within a retrospective study that included over 5,000 patients. Additional evidence has shown GC to be a predictive marker not only for refractoriness in chemotherapy (205), but also within targeted agent regimes such as ibrutinib and venetoclax (206,207). This illustrates that GC can feasibly be used to guide treatment regime decisions around when to treat and with which specific treatment to allow for

best patient outcome, even in high-risk individuals (208). However, many obstacles are limiting its application, such as the need for a universal GC classification with an optimized and reliable detection technique which can be easily replicated within various international research groups studying CLL.

1.4.9 Genomic detection technologies

The various genomic biomarkers that have been reported to have prognostic and/or predictive abilities within CLL incorporate various detection technologies used to measure specific genomic characteristics. For example, biomarkers including CNA, such as Dohner prognostic hierarchy and GC, have been detected using CBA, FISH, microarrays and shallow whole genome sequencing (sWGS). Whereas the presence of genetic variants has been detected using Sanger sequencing and more recently NGS techniques, such as targeted sequencing (TS), WGS and WES.

CBA or karyotyping is a type of cytogenetic technique in which a cells chromosomes are isolated and stained. This staining creates the characteristic light and dark bands which allows the detection of large structural changes including deletions, insertions, translocation and aneuploidies. (209). The resolution of this technique is 2-3 Mb at best, with resolution being highly dependent on the cell of origin and the quality of the metaphase spread (209). In the 1980s, FISH technique was developed and allows the detection, quantification, and localization of specific target sequences (134). Like karyotyping, FISH can detect chromosomal structural changes, but due to the greater resolution can also examine small segments of chromosomal abnormalities, such as microdeletions and small translocations. More recent developments in probe-labelling techniques and probe design have improved the sensitivity of FISH. FISH has a resolution of around 200 Kb-2 Mb but is limited by its genomic coverage as it uses targeted probes instead of examining the whole genome (210). Microarray techniques utilise probes that are designed to bind to complementary sample DNA sequences. Unlike FISH and karyotyping, microarrays, assess the entire genome for imbalances, at a greater resolution and does not require cells to be in metaphase. Whilst microarrays can assess CNAs at a higher resolution (~5-50 kb), this is heavily influenced by the size of probes and the genomic distance between the probes.

Sanger sequencing, also known as the chain termination method, was developed in 1977. Sanger sequencing is a first-generation DNA sequencing method for determining the nucleotide sequences of DNA and is used for variant calling (211). Whilst sanger sequencing has been the gold standard for mutation screening for many years due to its over 99% accuracy. It has been gradually replaced by high throughput and massively parallel NGS techniques, also known as “second” generation sequencing. The ability of NGS technologies to be high throughput has

greatly reduced the cost of sequencing a genome. Furthermore, the technique has a sequencing depth of coverage (DOC) of 1000x or higher, which is greater than Sanger sequencing and other non NGS base techniques. As TS examines only a specific panel of genes and/or coding regions, it can detect variants at a variant allele frequency (VAF) of around 0.1-0.2% (212). Whereas WGS and WES, which examined the whole genome or exome, respectively, can be employed in the discovery of new genomic variants as it has a more comprehensive coverage that is not limited to a panel of genes. The trade-off between a greater breadth of profiling is a poorer depth of sequencing as WGS and WES has a sequencing depth of 30-60x and 100-200x, respectively (212). Finally, sWGS can infer CNA data from WGS data at a ~0.1x coverage, which can be altered to adjust resolution. However, unlike SNP microarrays, copy number neutral loss-of-heterozygosity (cnLOH) events are not able to be detected using sWGS (213).

1.4.10 Importance of genomic technology choice

The use of certain genomic technologies for the detection of clinical biomarkers must be considered during biomarker validation. As highlighted above, this is because different detection techniques can introduce bias due the varying technical resolution and the limited genomic coverage that is offered by certain techniques. The advantages and disadvantage of the technologies used to detect certain genomic characteristics must be considered. The use of similar technologies, such as two types of microarrays which may have comparable outcome, may differ across different institutions or cohorts due to numerous reasons, such as technical expertise at an institution or budgetary reasons. However, understanding and evaluating these detection techniques is important when trying to develop and validate a novel biomarker for use in the clinical setting. In 2008, Cancer Research UK published the ‘strategic review in biomarkers’ that included many biomarker roadmaps which describes the process and steps required for biomarker validation. They stated that an essential part of biomarker validation is the development of an accurate and reproducible assay to measure the biomarker (214). Therefore, before a biomarker can proceed to being assessed in the context of clinical outcome, a single assay or genomic technology used to measure the biomarker must be chosen. Currently this a limiting step in the validation and application of GC as a prognostic and predictive biomarker in CLL.

1.5 Rationale and Aims

Currently only two biomarkers are clinically utilized in the assessment and treatment of CLL patients. Therefore, there is a real need for further development and validation of prognostic and

predictive biomarkers in CLL that will improve risk stratification of patients and allow a more personalized treatment regime to be chosen.

Based on publicized evidence, GC is now a widely accepted biomarker in CLL. Regardless, these conclusions are predicated on limited experimental evidence and research that used cohorts that did not represent the whole patient population. Moreover, research that has shown GC to be an important biomarker have used a wide variety of definitions, as well as a range of technologies and cutoffs used for its detection (103). Furthermore, the discordance in the prognostic significance of different GC metrics that has been reported in CLL, suggests than an underlying biological heterogeneity may influence the clinical relevance of GC which has not been fully assessed in current published research. This is the principal concern within my PhD as the community is fully behind a biomarker that has yet to be thoroughly validated and optimised. Therefore, the first aim of this PhD research was to understand and assess the current 'state of play' of GC research in CLL, by completing a systematic review of published research with a narrative synthesis approach to analysis. Additionally, an aim was to increase the data available for patients enrolled in three clinical trials, CLL4, ARCTIC and ADMIRE, through the completion of extensive laboratory and computational work. Using this newly developed, data-rich CIT clinical trial cohort with extensive molecular characterization, I aimed to assess GC as a prognostic and predictive biomarker. Furthermore, I aimed to describe the biological heterogeneity of CLL patients in the context of GC, by analyzing the distinct genomic profile of each GC group.

Two biomarkers, TL and DNA methylation based epitype (DME), have also been shown to be important in CLL pathogenesis and clinical presentation. However, due to a well-documented relationship between TL and DME, it is currently unknown which of these biomarkers contributes the most to clinical outcomes. Additionally, at present, these biomarkers have not been studied together within a singular clinical trial cohort. Therefore, an aim of this research was to establish the relative prognostic impact of TL and DME in a clinical trial cohort with extensive follow-up data, using pre-existing data augmented with a cohort of newly generated data. Furthermore, this project aims to establish the relationship between TL and DME subgroups and their association with many established biomarkers, using a large cohort that has extensive molecular characterisation.

Chapter 2 Systematic review of the clinco-biological importance of genomic complexity in chronic lymphocytic leukaemia

2.1 Synopsis

This chapter examines the published literature to create a systematic review, evaluating GC's current 'state of play' within CLL. Eligible studies are collated to explore and compare various features recorded in the publications, such as the definition used to describe GC. This chapter takes a comprehensive look at how GC has been reported in CLL previously, including a substantial discussion on the strengths and weaknesses of the current published literature and comments on how any insufficiency present in current research can be solved.

Louise Carr performed the systematic review, including the literature search, manuscript selection, data extraction, and analysis of the results. Doctor Helen Parker was the second investigator to perform the search and study selection. Professor Jon Strefford, Doctor Helen Parker and Doctor Jane Gibson supervised the review and gave guidance on the analysis and interpretation of the data.

2.2 Introduction

A systematic review titled 'A Systematic Review of the Clinico-Biological Importance of Genomic Complexity in Chronic Lymphocytic Leukaemia' was employed. Systematic reviews are a type of research that allows the collation of empirical evidence from many studies that meet certain eligibility criteria intending to answer specific research questions. This type of analysis is used to present an unbiased report of up-to-date findings, to identify gaps in knowledge and evaluate the benefits or risk associated with interventions or policies. This information can also be used to identify any flaws within the evidence, all of which are important to feedback to researchers, clinicians, policymakers, and patients (215). When completing a systematic review, the principles of PRISMA-P must be followed, Preferred Reporting Items for Systematic Review and Meta-analysis Protocols, to ensure transparent and unbiased reporting (216). Within this systematic review, three research questions were addressed;

1. Does the patient composition of current published studies recapitulate the natural history of the disease?
2. What techniques and metrics have been utilised to establish levels of GC in CLL?

3. Will CLL patients identified as having high GC compared to patients with low GC have poorer survival outcomes, irrespective of the metric used?

An additional list of aims also included, focusing on the assessment of the published literature for a) the patient cohorts studied, b) the technological platform used for the detection of GC, c) the various definitions and cut-offs utilised for measuring GC, and d) the prognostic significance of GC.

Numerous papers on CLL have identified GC as an important biomarker with potential use in patient risk stratification. However, these conclusions are based on evidence representing only part of the CLL population, as cohorts do not span the complete disease history. For example, GC must be examined in cohorts of treated, untreated, relapsed and refractory patients. With the former, there is currently a lack of evidence showing the utility of GC within patients treated with oral targeted agents, which are quickly becoming standard practice in CLL treatment regimes. Additionally, there is little to no representation of patients that have progressed to a clonal Richter transformation, an aggressive B-cell lymphoma that will be part of the natural history of the disease in 2-10% of CLL patients and which is associated with a dismal survival (217). A further factor limiting the application of GC is the lack of a universal metric to describe it, which is then compounded further by the issue of there not being a consistent technique used to detect it. The range of techniques used for its detection in current research influences the metric and the cut-off that can be applied. This is because different techniques can examine different genetic features, i.e., CNA or mutations, and can have distinct resolutions, i.e., 5-10 Mb for karyotyping techniques, all of which influence what data can be included in the GC metrics (218). Therefore, a singular definition, detection technique, and cut-offs must be agreed upon within the CLL community before GC can be fully validated as a clinical biomarker. It is these limitations, as well as others, present in current CLL research that I wish to address in my PhD and something I aim to overcome within my research. A good starting point for this endeavour is to complete a systematic review to gain a comprehensive overview of published research to understand the current 'state of play' of GC in the context of the disease, CLL.

2.3 Methodology

2.3.1 Search strategies

This project followed the principles of PRISMA-P, which aims to help researcher with transparent reporting within a systematic review (216). Relevant published literature was searched for using two independent search engines, PubMed (since 1966) and Ovid MEDLINE(R) ALL (since 1946), in September of 2023. Combinations of four keywords, either "Chronic Lymphocytic Leukemia" or

"CLL" with either "Genomic Complexity" or "Complexity," were inputted into both search engines. The manuscripts identified from the eight searches combined resulted in 633 entries (n=345 in PubMed, n=288 in Ovid). 472 duplicate entries were removed, resulting in 161 unique manuscripts. The complete filtering stages, as well as the inclusion and exclusion criteria utilized, are given in **Figure 9**.

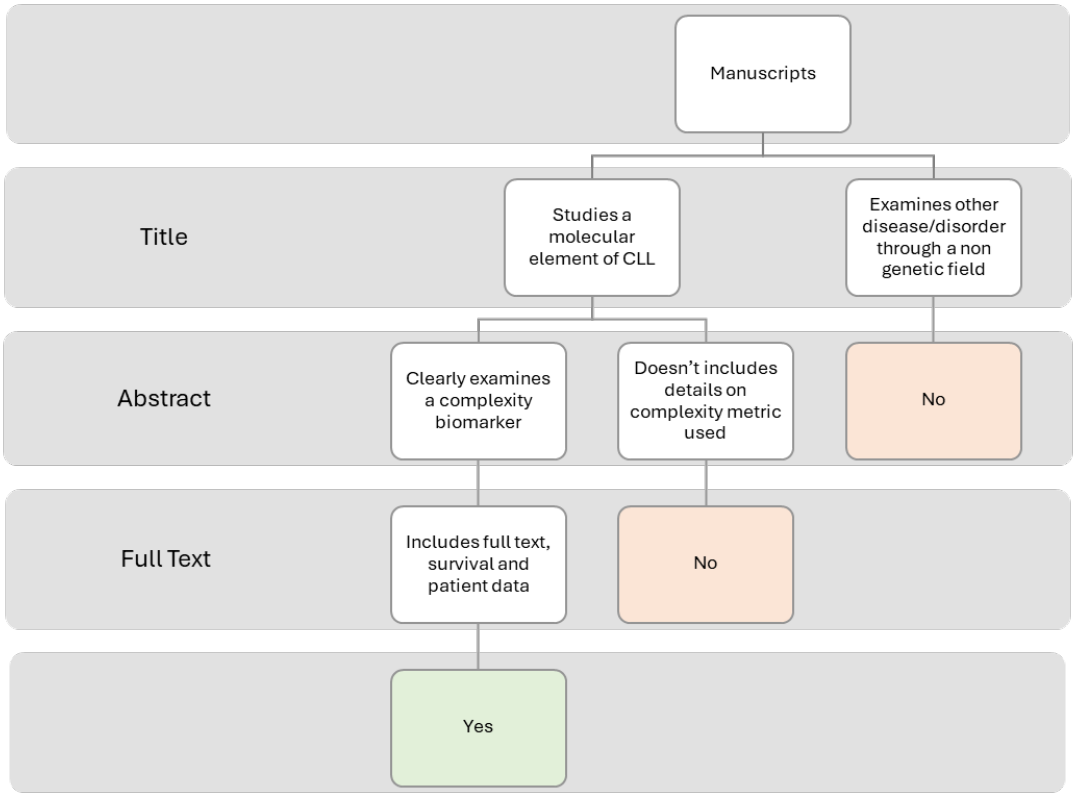

Figure 9- Decision tree used for the manuscript selection. The main steps of manuscript selection were as follows, assessment of the title, the abstract and then the full text and any supplementary material. The inclusion and exclusion criteria used in the three main steps are stated. If either reviewer needed clarification about any action, the manuscript passed to the next filtering stage to be further reviewed.

2.3.2 Manuscript selection and data extraction

Two independent reviewers (LC and HP) assessed the unique papers to determine study eligibility. Inclusion and exclusion criteria were first applied to the title, then the abstract and then the full text. If the title was ambiguous, the reviewer read further into the abstract and full text until this uncertainty was resolved. Inclusion criteria were as follows: (1) the title mentions CLL and a genomic characteristic(s); (2) the abstract specifies a GC metric; (3) full text or supplementary material reports survival analysis data including GC as a factor; hazard ratios (HRs) and corresponding 95% confidence intervals (95% CIs) or mean/median survival and p-values when comparing survival across different groups. Manuscripts that failed to meet these criteria or

lacked full text were excluded from future analysis. Review articles and editorial letters were omitted. The search was limited to papers written in English.

Once a list of studies that met inclusion requirements was created, the following data was extracted from the papers: first author, year of publication, description of the cohort, GC metric, detection method and survival data. The survival data extracted was either HRs and 95%CIs or mean/median survival and p-values, or some studies reported on both. Data was extracted by reading the full text of all eligible studies and any additional supplementary material available.

2.3.3 Data visualisation and analysis

Descriptive statistics, such as percentages and ratios, were employed to assess patient composition and features that influence CLL prognosis. Graphical summaries were created using R (version 4.1.2) within the Rstudio environment (version 2021.09.1) and using various packages such as 'ggplot2' (version 3.3.5). Graphs were used to compare the different technologies, metrics and cutoffs used in the eligible publications to measure GC. The impact of GC on survival was considered statistically significant if the CI did not overlap with 1, and an HR>1 would indicate a poorer prognosis for that GC group compared to the control group, i.e., patients with GC compared to patients without GC (219). Survival was evaluated using many outcomes, for example, OS or TTFT. OS was measured from the study enrollment until death; however, some publications used time at diagnosis as a starting point. Also measured was TTFT, which was defined as the time of enrollment until the first treatment. In contrast, time to subsequent therapy (TTST) was measured between completion of chemotherapy before registration and the start date of the subsequent treatment. Both PFS and DOR used the end point of the detection of a progressive disease, whereas diagnosis date and first response to therapy were used as starting points, respectively.

2.4 Results

2.4.1 Study Selection

The results from the manuscript selection are shown in **Figure 10** below, with each step of study selection clearly shown. The reported values represent the number of papers included and excluded at each step. The concordance between the two independent reviewers used to control for selection bias was 100% on the final accepted manuscripts. **Supplementary Table 1** gives an overview of the 25 eligible papers, identified during manuscript selection, that are used in this systematic review.

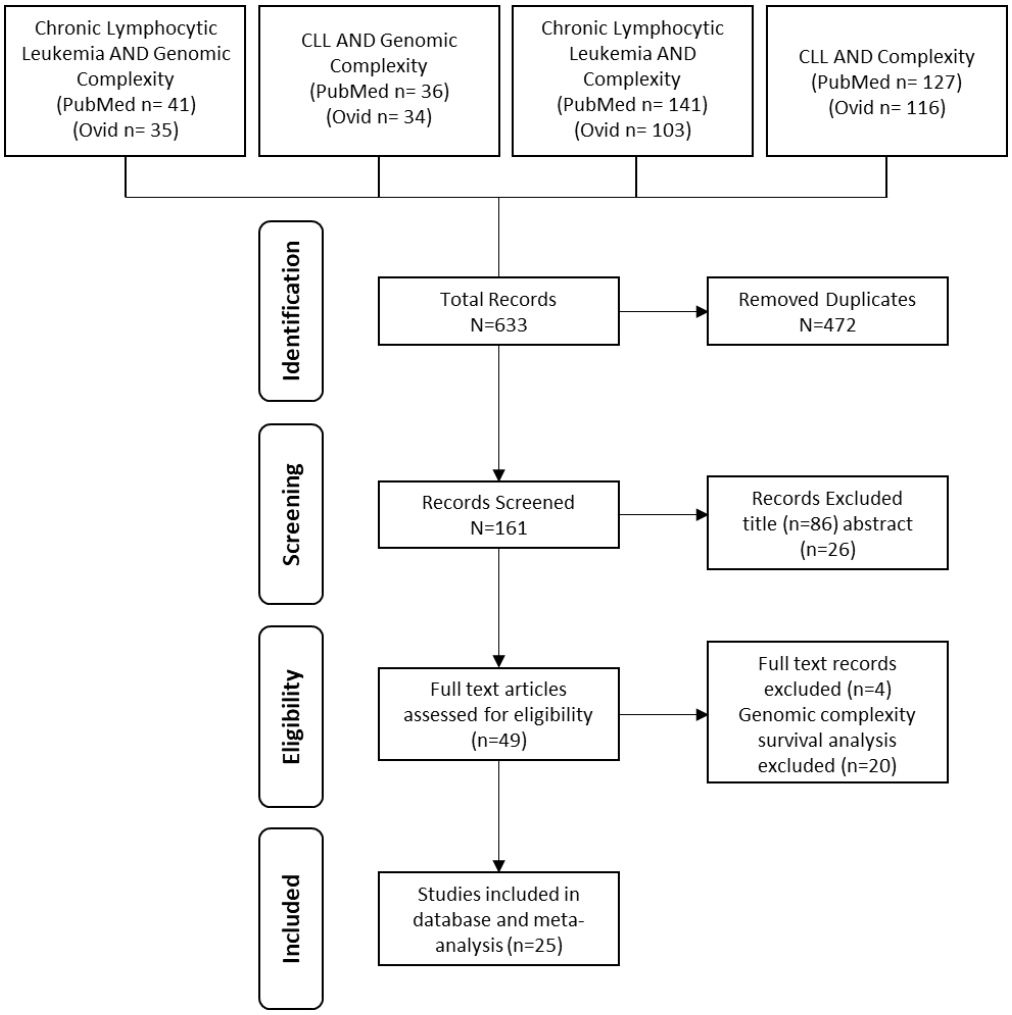

Figure 10- Flowchart showing an overview of manuscript selection. The flowchart starts with the keywords and search engines used to compile manuscripts into a single list for further assessment. Duplicate entries were removed. The remaining papers had the eligibility of their titles and abstracts assessed, papers not meeting inclusion criteria were removed. Papers were also removed if full text was not available. Papers were excluded if genomic complexity was not a factor assessed within the survival analysis. Numbers denote the number of manuscripts excluded and included after each step.

2.4.2 The composition of cohorts within the eligible studies

Assessment of the composition of the cohort used within the 25 eligible studies identified that many of the publications used a cohort of only treatment naive (n=12) (121,220–230) or treated patients (n=3) (231–233). Whereas others included both treated and untreated patients in their cohorts (n=9) (103,198,203,204,234–238). Interestingly, only one paper included a cohort of relapsed and treated patients (239). Furthermore, none of the eligible papers had patients that had progressed to an advanced disease such as RS, which is part of the pathogenesis of CLL for 2-10% of patients (91). A schematic timeline spanning the whole natural history of the disease is shown in **Figure 11**, with details about the cohorts used within the 25 eligible studies annotated to

the timeline. Across the papers inspected, at the time of GC assessment, 11052 patients were treatment naïve, 2774 were treated, 59 were relapsed patients, 48 were sequential samples, and 228 had unclear status. Of the 12 publications that included treated patients above, 42% included the application of oral agent treatment regimens (n=5), such as BTK, Bcl2 or PI3K inhibitors (231–233,236,238). Most treated CLL patients examined within the eligible studies were enrolled on CIT, see **Figure 11**.

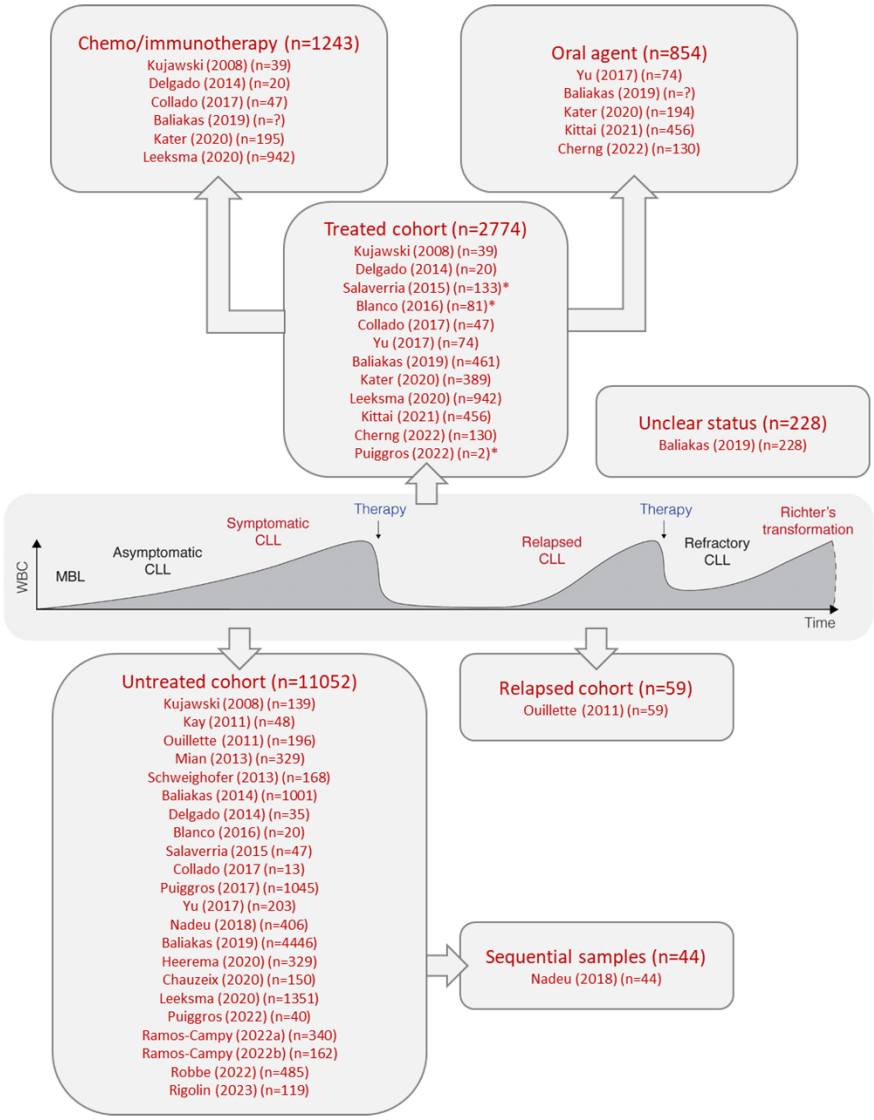

Figure 11- Schematic presentation of the different stages of the natural history of the CLL disease. From the precursor disease, to treated, to relapsed and finally, for some, Ritcher's transformation. A detailed breakdown of the different cohorts used in each of the 25 eligible studies are clearly annotated to different stages of the timeline, relevant to the patient's status at time of GC testing. The values show the total number of patients analysed at that stage in the natural history and how many came from each publication, i.e. 2774 patients were treated with 130 of these individuals were part of the Cherng et al 2022 paper. For treated patients, further information is provided to show the number of each cohort that were treated with either

chemo/immunotherapies or oral agents. For 228 patients their status at time of GC was unclear and therefore has been shown in a separate grouping. * signifies this cohort was treated but it was not clear which treatment option they were given. ? signifies that the exact number of patients in this treatment arm was not clear in the publication. Adapted from (240)

The sample size of these cohorts was another highly variable feature, with a range of 42-5290 patients and a mean of 572 patients. Five studies used a cohort of less than 100 patients (203,204,224,234,237) in their research. Of these five publications with a small sample size, three have focused on a subset of the CLL population, for example, including only CLL patients with *TP53* aberrations (203,204,234). The prevalence of *TP53* aberrations in untreated CLL patients is only 5-10%, which could explain the limited cohort that could be collected (241).

2.4.3 Inspection of the metrics and technologies used for the assessment of genomic complexity

Within the eligible publications, a broad series of metrics were used to measure GC (n=11). Metrics ranged from being a continuous or categorical variable, including CNAs and/or mutations and using a variety of cut-offs to categorise patients into having high, low or no GC. In certain publications, only specified CNA signatures were included in the GC variable, for example, only including chromosomal gains or losses into copy number count or only including CNAs of a specific size. The variety of GC metrics used within the eligible studies is displayed in **Figure 12** where complex karyotype (CK), defined as ≥3 CNA, was shown to be most popular metric for GC and used in 44% of publications (n=11) (203,222,223,225,227,229,231,232,234,236,238). However, this GC metric varied across the 11 publications with some publication apply different inclusion criteria for defining CNA, for example including a size cut-off where CNA ≥5MB in size are included (223). The second most popular metric used were copy number count, either as a categorical or continuous variable, as both accounted for 17% of the different metrics used across the eligible studies. Copy number count as a categorical variable, referred to as copy number groups, had different grouping across the publications; for example, Ouillette et al., 2011 had groups of 0, >1, >2, >3 and >4 CNAs, whereas Puiggros et al., 2022 used a cut off of >10 CNA to define GC (237,239). The categorical variable, named high complexity, described GC as ≥5 CNAs and accounted for 14% of GC metrics used across the publications (n=6) (103,223,229,231,232,238).

Mutation data was also included to define GC, albeit less frequently and with various inclusions criteria and cut offs. Similarly to CNA count, mutation count can be defined as a continuous or categorical variable. The mutation count as a categorical variable, referred to as mutation count groups, was used in two publications and accounted for 5% of metrics used. Patients were classified as having GC if ≥21 mutations or ≥1 of the eight estimator genes, including *ATM, SF3B1*

and *TP53*, were detected (230,236). Remarkably, over half (52%, n=13) of the eligible publications reported using more than one metric to investigate GC, alluding to the discrepancy within the CLL community regarding how GC should be assessed.

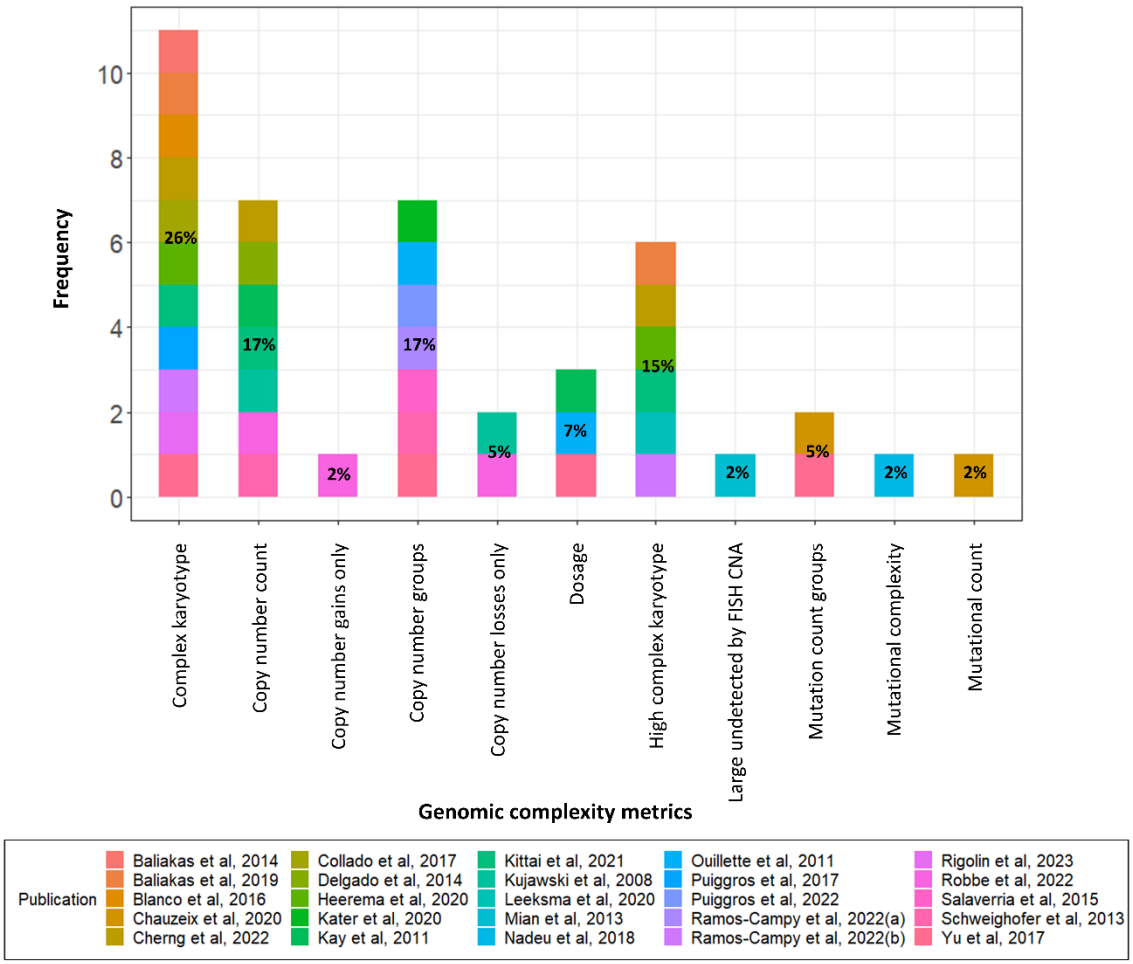

Figure 12- A bar chart showing the 11 different GC metrics used across the 25 eligible studies. Metrics including CNA were frequently used via many different cut-offs and definitions. CNA was studied as a continuous variable in copy number count but also as a categorical variable, for example, in complex karyotype, using a ≥3 CNA cut-off, high complexity, using a ≥5 CNA cut-off and copy number count groups where various cut-offs were applied (>1, >2, >4, >6 and >10 CNA). Dosage is calculated by the total length (Mb) of sub chromosomal losses and gains. The large undetected CNA metric was defined by the presence of a CNA greater than 5Mb in size, previously undetected by FISH. Mutation count, a continuous variable, included the number of mutations detected. As a categorical variable (mutation count group), various cut-offs was used, including ≥21 mutations and the presence of ≥1 of eight gene estimators. Mutational complexity refers to the sum of driver alterations, including both CNA and mutations. Percentages shown are calculated from the frequency of each metric out of the total number of metrics used across the 25 publications, i.e. Complex karyotype (11/42)*100= 27%.

Across the 25 eligible studies, various detection techniques have been used to assess GC within CLL; a graphical display of the variation and their prevalence is shown in **Figure 13**. The nine different techniques can be divided into three main groups; cytogenetics, microarrays and NGS. Examining these three distinct groups, found that microarrays, including Array comparative genomic hybridisation (aCGH), SNP array and optical genome mapping, were the most common technique (64%, n=16). Conversely, cytogenetic techniques were used in nine publications (36%), whereas NGS techniques were only used in six eligible publications (24%). These various techniques have varying resolutions, coverages, and types of detail recorded in the data. Therefore, the type of technique used to detect GC can have a profound impact on biomarker measurement and therefore its usefulness. The two most frequently used techniques were SNP arrays and CBA, both present in 8 of publications and account for 23% of technologies used, see **Figure 13**. aCGH was the subsequent most frequently used detection technique, present in 24% of eligible publications (n=6) (103,204,224,233–235). For the application of GC metrics involving mutation data both targeted NGS and WES have each been used in two publications to detect mutation variants (121,230,233,236). **Figure 13** also highlights Leeksma et al., 2020 as having greatest number of technologies used within a single publication with three techniques employed (103). Further inspection of this paper identified that the wide range of technologies used was due to it being a retrospective study collating data from 13 different research centres. This emphasises the lack of agreement across research groups regarding how GC should be studied.

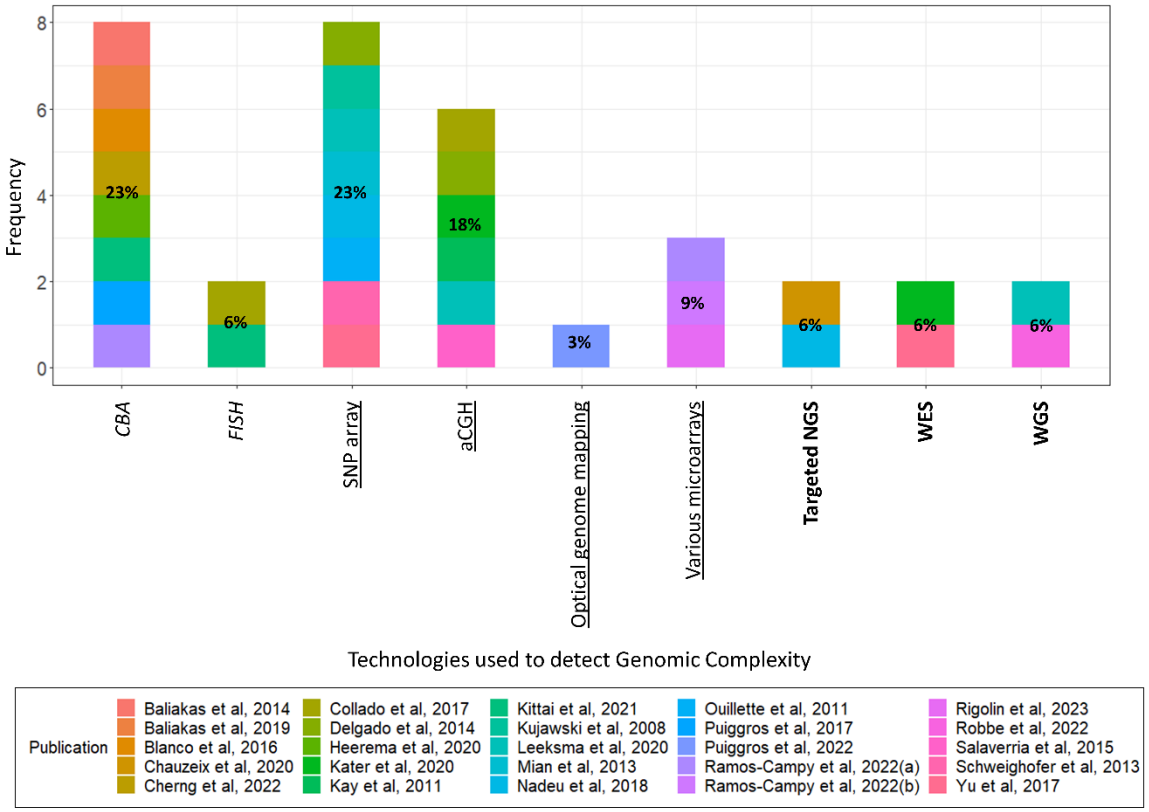

Figure 13- A bar chart showing the nine different technologies for detecting GC across the 25 eligible studies. The frequency of use of a technique is shown along the y-axis. Percentages indicate the frequency of use each technology has compared to all the technologies used, i.e. aCGH (6/34)*100=18%. Colours correspond to publications, with numerous papers using multiple technologies for GC detection. The three broader technology groups of cytogenetics, microarrays and NGS are shown in italics, underlined and bold, respectively. SNP array group includes 250k SNP, 50kXbaI SNP and SNP 6.0 arrays. aCGH- Array Comparative Genomic Hybridisation, CBA- Chromosomal banding analysis, FISH- Fluorescent in situ Hybridisation, NGS-Next Generation Sequencing, WES-Whole Exome Sequencing, WGS- Whole Genome Sequencing.

2.4.4 Associations between genomic complexity and survival outcomes

To investigate the final research question of this systematic review, the reported survival data from the 25 published papers were compared and assessed. Within 92% (n=23) of the studies, a univariant survival analysis has been completed (103,198,203,204,220–232,234–239) evaluating the impact of GC on a range of survival outcomes such as treatment free survival (TFS), TTFT, TTST, PFS and OS. Within ten publications a HR and 95% CI have been reported, with the remaining 13 only including p-value and median survival time for different GC groups analyses and therefore could not be included in a forest plot. **Figure 14** displays the reported univariate analysis from five publication that have used the survival endpoint of TTFT; each GC metric and

detection technology is also indicated (221,223,230,235,239). The forest plot indicates that the presence of GC, measured and detected in numerous ways, indicates a significantly poorer TTFT. This trend was also found in univariate analysis using survival endpoints of PFS or OS, with Puiggros et al., 2022 recording a significant difference (p-value<0.014) in OS in patients with complexity (>10 CNA median; 2 months) and without complexity (<10 CNA median; 43 months). As highlighted above, many publications have included multiple metrics of GC. One such paper is Ramos-Campoy et al., 2022, which examined high GC (≥5 CNAs), intermediate GC (3-4 CNAs), and no GC (0-2 CNAs) metrics. Univariate analysis using these metrics found high GC group had a significantly shorter TTFT compared to no GC (p-value=0.006, 3 vs 17 months), but the intermediate GC v.s. no GC group did not reach 95% significance (p-value>0.05, 21 vs 17 months).

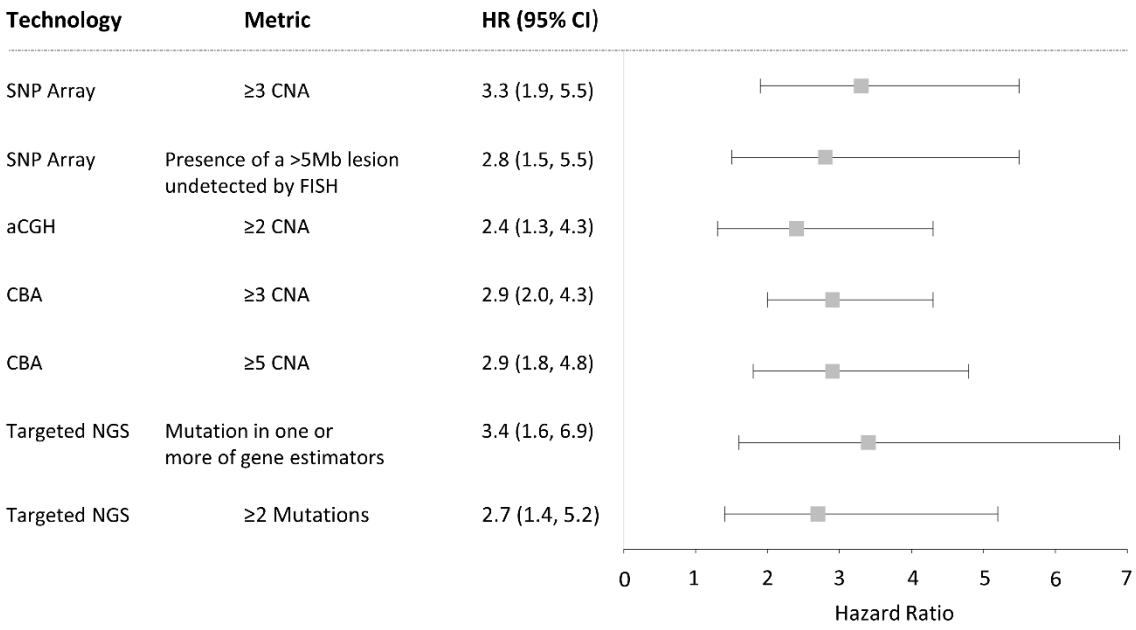

Figure 14- A forest plot of univariate results studying GC metrics using the TTFT survival endpoint. The technology and metrics used to examine GC are recorded. For each metric, however defined, a comparison of patients with GC and patients without GC is completed. Abbreviations: HR- hazard ratio, 95% CI- 95% confidence interval, SNP array- single nucleotide polymorphism microarray, CNA- copy number alteration, aCGH- array comparative genomic hybridisation, Targeted NGS- targeted next generation sequencing using a panel of genes.

Many studies have completed a multivariate Cox regression model analysis including GC as a variant (n=21) (103,121,198,203,204,220–223,225,227–233,235,236,238,239). Within nineteen of these models, a GC metric has been significant and therefore found to be an independent biomarker for poorer survival. For example, Kater et al., 2020 reported in their PFS MVA that low GC (3-4 CNAs) compared to no complexity status (0-2 CNAs) had a shorter PFS (HR:2, 95% CI:1.1-

3.6, p-value=0.025 and HR:1.7, 95% CI:1-2.7, p-value=0.039) in both an oral agent (venetoclax) and chemotherapy (bendamustine) based treatment cohort, respectively (233). Kittai et al. (2021) also found that GC, defined by CNA count as a continuous variable, remained an independent and significant covariate within the model, predicting a shorter PFS (HR:1.07, 95% CI:1.04-1.1, p-value<0.001) in the presence of other covariates such as age, gender, Rai stage, FISH data and *IGHV* mutation status (232). This study also found that CNA count remained significant in the OS multivariate model (HR:1.09, 95% CI:1.05-1.12, p-value<0.001). Yu et al. investigated ten different GC metrics within their study. Seven were reported as independent markers of poor OS within their multivariant model, when adjusted for *IGHV* mutational status and del17p events (236). For example, total number of mutations (≥ 21 vs. <21) had a reported HR of 3.55 (95% CI:1.55-8.16 p-value=0.003) and total number of CNA (≥4 vs <4) had a reported HR of 2.28 (95% CI:1.12-4.66 p-value=0.02) (236). Additionally, the dosage metric was found to be significant only when genomic losses were calculated (HR:3.88, 95% CI:1.74-8.55, p-value<0.001) but not when gains were included (p-value>0.05). Conversely, both Mian et al. and Nadeu et al. reported that GC was insignificant in their OS MVA (121,221). However, both publications, found their GC metrics to be significant in the TTFT MVA. Nadeu et al. reported an HR of 1.44 (95% CI: 1.21-1.72, p-value<0.001) and Mian reported a p-value=0.036 in the complexity groups compared to control, with GC defined as mutational complexity or presence of >1 lesions undetected by FISH respectively. Finally, a MVA using TTST as the survival endpoint found that both the number of copy number losses and the total number of CNAs (losses, gains and loss of heterozygosity (LOH)) remained significant and predicted a shorter TTST (HR:2.58 and 2.82, respectively p-value<0.05) in the final model, which included *IGHV* mutational status, Rai stage, CD38 expression, del11q and del17p events, and (198). The overarching conclusion from the survival data within the 25 eligible studies was that greater GC correlated with poorer survival outcomes, with multiple studies identifying GC as an independent prognostic marker of TTFT, TTST, PFS and OS.

2.5 Discussion

Within the CLL community GC is considered clinically valuable in risk stratification through the identification of patients that possess aggressive tumours. Many obstacles are limiting its application, such as the need for a universal GC classification with an optimized and reliable detection technique that can be easily replicated within various international research groups studying CLL. Currently in CLL, only two biomarkers have been fully validated and used in the clinical setting for patient risk stratification and as a predictive biomarker to guide treatment decisions. The 2008 iwCLL guidelines for the management of CLL highlighted the important

prognostic role of *IGHV* mutational status and the presence of *TP53* alterations and gave the recommendation for screening all patients at point of diagnosis, before treatment initiation (242).

Completion of this systematic review has allowed the current 'state-of-play' to be thoroughly investigated and critiqued with various suggestions on how to rectify any deficiencies within current evidence being discussed. Numerous limitations were identified within the papers studied, as well as limitations within the systematic review itself which hindered the scope of the analysis. Assessing the patient composition of current published studies, one of the aims of this systematic review highlighted limitations within the current literature. For example, four papers used a small sample size of less than 100 CLL patients, which suggests that these cohorts might be underpowered. Furthermore, none of these small cohort studies included a power analysis to establish if the sample size was adequate to investigate the survival trends within their specific CLL population. Therefore, insights into survival could have been missed, and the work could be statistically inconclusive (243). A further limitation within the literature examined is publication bias and selective reporting, with two studies omitting results from the MVA as it did not find GC to be an independent marker (121,235). Publication bias is the increased tendency of researchers to publish only positive results which then artificially increases the belief of the relationship that is being investigated (244). Therefore, research studying GC could have found it insignificant in their own MVA but chose not to include that work when it was published due to the desire of researchers to only report on positive results and therefore this unpublished data would not be included in the systematic review.

This work has been limited by its research design of a systematic review with a narrative approach for data synthesis. Limitations that typically occur in systematic reviews, and that apply to this research, include variations in experimental designs hindering comparisons and a lack of detail within methodologies and the analysis reported in published work (245). I had difficulty in combining results, the first required step in a meta-analysis, as I was uncertain of the similarity of many aspects of the publications. For example, several manuscripts included a description of the technology they used to measure GC within their methodology that was detailed enough to replicate the experiment and analyse the raw data generated, whilst others were much less meticulous in their description, see **Supplementary Table 1**. Typically, the publications that included very basic information about how GC was detected were multi centre studies that had pulled data from many institutions over many years. This hindered my analysis into how different technologies influence the clinical utility of GC as I had to cluster the technologies into much broader groups of cytogenetics, arrays, and NGS. Furthermore, I was unable to include a meta-analysis as part of the systematic review due to this varied reporting within the publications.

Despite these limitations, many important insights with valuable applications for CLL have been gained. As mentioned above, there were inconsistencies across the studies on how to define GC as a metrics and what technology were used to detect it. Using different technologies to detect GC can introduce a technical bias due the varying resolution and the limited genomic coverage that is offered by certain techniques. For example, CBA allows chromosomal deletions or duplications to be identified at a resolution of >10MB in size. This resolution is dictated by the resolution of the light microscope and the quality of the metaphase chromosomes that are being used. Whereas FISH has a better resolution of 200Kb-2Mb, but is limited by its genomic coverage as it uses targeted probes (210). Microarray resolution is heavily governed by its probe size and the genomic spacing which determines the density of the probes (246). For instance, SNP array uses ~2 million probes spanning across the genome resulting in a greater probe density and therefore greater resolution than FISH (246). Finally WGS, a type of NGS technology, that was used within one of the eligible studies and allows single-nucleotide resolution (247). This range of resolution abilities of different technologies has resulted in a bias for the detection of larger CNA, with smaller CNA going undetected by most of the techniques. Additionally, techniques that have limited genomic coverage incur a bias for regions that have probes designed for and therefore will have less validity than techniques that study the genome as a whole. This technical variation introduced within the studies highlights the need for a singular detection method to be selected, until then the validation of GC as a clinical biomarker within CLL cannot occur.

The prevailing conclusion from the eligible studies is that increasing GC, measured and detected in numerous ways, is a prognostic biomarker indicating poorer survival. Numerous studies have also shown GC as a biomarker of progression independently of various factors that have a known survival impact, such as *TP53* aberrations, *IGHV* status and *ATM* mutations. This indicates a potential application within patient risk stratification, allowing patients with an aggressive disease to be identified and treated accordingly. One exciting finding was the presence of high GC, detected using aCGH, within patients that had previously been classified as low risk based of FISH results, for example patients with a sole del13q events (224). Patients with high GC, defined by the presence of ≥15 CNA, had a significantly worse (p-value<0.01) PFS than patients with <15 CNA. Whilst this high GC group included, as expected, patients with del17 events it also included patients with trisomy 12 and del13q events. Even patients identified as low risk can exhibit an aggressive disease course which is not truly captured using current prognostic markers. Therefore, further research is warranted to investigate GC within 'low risk' CLL patients in the hope that this clinically heterogenous group can be further risk stratified and thus lead to improved patient outcome. When assessing the various metrics used to describe GC it was found that increasing CNAs was a greater predictor of survival than increasing number of mutations (197). This

highlights the need to include CNA within the universal measurement of GC as it seemingly gives greater clinical insights. However, the aspect of CNAs to measure, i.e. dosage or CNA count, and the specific cut-offs, i.e. only include CNAs >5Mb in size, remains unclear. Within certain publications, GC has been shown to have utility as a predictive marker for refractoriness or short remission after initiation of a chemo/immunotherapy regime. Less evidence is available showing the clinical utility of GC in patients treated with targeted agents, which are becoming important in the frontline treatment of CLL. Notably, the first publication to include a cohort of patients treated with oral agents was published in 2017 (236). Since then, four additional publications included in this systematic review have included a cohort of oral agent treated patients see **Figure 11**. Kittai et al., 2021 found that increasing karyotypic complexity (increasing 1 CNAs) was an independent predictor of shorter PFS (HR:1.07, p-value<0.0001) and OS (HR:1.09, p-value<0.0001) in a MVA using relapsed/refractory and treatment naïve patients treated with ibrutinib. This suggested that karyotypic complexity is an important prognostic and predictive marker in patients treated with oral agents as frontline and second line therapies. However, validation of this application is currently halted as the evidence showing GC utility as a predictive biomarker is based on small samples sizes or without extensive follow up data (236).

This chapter had four main aims, all of which have been addressed. Firstly, the composition of the patient cohorts used in the current published literature was assessed, and various deficiencies were identified due to small sample sizes or not including patients that represent the whole natural history of the disease. The systematic review examined and reported not only the different technological platforms used for the detection of GC but also the various definitions and cut-offs used. Across the 25 studies employed in this systematic review, the most frequently used metric is complex karyotype defined as ≥3 CNAs, and the most used detection method is CBA and SNP arrays. The final aim of investigating the prognostic significance of GC was addressed and found that increasing GC, no matter how defined, was prognostically important in various institutional and clinical trials.

Whilst GC is newly being investigated in the era of oral targeted therapies, recent published work is still using cohorts of patients enrolled in CIT regimes. These cohorts used historical clinical trials which included patients treated with CIT regimes, as CIT was the gold standard of treatment at the time of enrolment. The benefit of still using these historic CIT clinical trial cohorts is that these are typically larger cohorts, with rich molecular data and extensive survival data available. Furthermore, these oral agents, whilst they have a good response in many patients, they are expensive and thus their affordability and economic impact on a society must be considered. A simulation modelling the economic burden of CLL treatment in the era of oral agents in the United States reported a 590% increase in the annual cost, with an out-of-pocket cost to the

patient increasing by 520% compared to CIT (248). Therefore, oral agents may not be suitable for patients from all social-economic backgrounds and thus an evaluation of GC within a CIT treated cohorts is still vital and relevant research.

In conclusion, current CLL research investigating GC is drawn from highly disparate cohorts, methodologies, and definitions for defining GC. Nevertheless, this research has consistency found GC to have importance within CLL as a prognostic and predictive marker. Presently, no definitive metric or detection technique can be stated from this systematic review although many have been mentioned with the advantages and disadvantages being debated above. Further work is required to expand the size and breadth of cohorts that have been used to study GC. Additionally, a singular detection method and definition of GC must be decided upon before GC can be fully validated as an important biomarker within CLL. Pending this research, GC cannot be used within the clinical environment to risk stratify patients and direct treatment regimens which would result in better patient outcomes.

Chapter 3 Methodology

3.1 Synopsis

This chapter presents the methods and techniques used within this thesis. Prior to my PhD, CNA, somatic variant, and TL data had been generated and used in published projects by other researchers based in Southampton and across other universities and institutions. During this PhD, new datasets were produced by completing laboratory work and bioinformatic analysis of the raw data generated. I produced the DNA libraries for the SureSelect sWGS and Agilent HS2 sequencing myself. Once sequenced, I processed the raw sWGS and HS2 sequencing data and manually curated the analysis output. Additionally, I completed the laboratory work to generate TL data using the MMQPCR technique and the analytical work required to quantify and convert the output to an absolute TL value. Infinium HumanMethylation450 (450k) array data was available as it had been generated for a sub-cohort of ARCTIC and ADMIRE patients beforehand for a previous project. I completed the analytical work to analyse this raw microarray data to extract CNA profiles for certain ARCTIC and ADMIRE patients. This preexisting data was integrated with newly generated data I created to form a large cohort of clinical trial patients. This cohort was then used in statistical and survival analysis. Finally, the methodology utilised to complete a systematic review is also illustrated in this chapter.

3.2 Systematic Review

3.2.1 Search Strategies

The work presented in Chapter 2 followed the principles of PRISMA-P Preferred Reporting Items for Systematic Review and Meta-analysis Protocol which aims to aid transparent reporting within a systematic review (216). Relevant published literature was searched for using two independent search engines, PubMed and Ovid (MEDLINE) during September of 2023. Combinations of four keywords were inputted into both search engines: either “Chronic Lymphocytic Leukemia” or “CLL” with either “Genomic Complexity” or “Complexity”. The manuscripts identified from the eight searches were combined. Duplicate entries were removed resulting in a list of unique manuscripts.

3.2.2 Manuscript Selection

Two independent reviewers (Miss Louise Carr and Doctor Helen Parker) assessed the unique papers to determine study eligibility. Inclusion and exclusion criteria were first applied to the title, then the abstract and full text. If the title was ambiguous the reviewer read further into the abstract and full text until this problem was resolved. Inclusion criteria was as follows: (1) title mentions CLL and a genomic characteristic(s), (2) abstract specifies a GC metric, (3) full text and/or supplementary material reports survival analysis data including GC as a factor; HRs and corresponding 95%CIs or mean/median survival and p-value when comparing survival across different groups. Manuscripts that failed to meet these criteria or that lacked full text were excluded from future analysis. Review articles and editorial letters were not included. The search was limited to papers written in English.

3.2.3 Data Extraction

Once a list of studies that meet inclusion requirement was created the following data was extracted from the papers; first author, year of publication, cohort details, GC metric, detection method and survival data. Survival data extracted was either HRs and 95%CIs or mean/median survival and p-values or some studies reported on both. Data was extracted by reading the full text of all eligible studies and any additional supplementary material that was available.

3.2.4 Statistical Analysis

To assess patient composition and features that are known to influence CLL prognosis basic descriptive statistics were employed, such as percentages and ratios. For the comparison of the difference technologies and cutoffs used to measure GC, graphical summaries were created using R studio. When assessing survival, reported HRs and CIs were studied across various GC metrics and detections techniques. The impact of GC on survival was considered statistically significant if the 95%CI did not overlap with 1 and a HR>1 would indicate a poorer prognosis for the specific GC group (219). Survival was evaluated using many outcomes for example OS or TTFT. OS was measured from time of study enrollment until death however some publications time at diagnosis was used as a starting point instead. Also measured was TTFT which was defined as time of enrollment until first treatment whereas TTST measured between completion of chemotherapy before enrollment to the start date of the next therapy. Both PFS and DOR used the end point of progressive disease detection but used diagnosis date and first response to therapy as starting points, respectively.

3.3 Data consolidation

The complied dataset generated and analyzed in Chapter 4 and Chapter 6 were curated from three clinical trials; CLL4, ARCTIC and ADMIRE, which contained treatment naïve CLL patients. The UK LRF CLL4 (NCT00004218) clinical trial randomly assigned 777 patients into two chemotherapy treatment groups. ARCTIC and ADMIRE clinical trials (NCT02352948 and CRUKE/09/016) recruited 216 and 196 patients, respectively, and assigned patients to several CIT regimes.

3.3.1 CLL4 cohort

The patients that were part of the CLL4 clinical trial were enrolled into either a Fludarabine plus Cyclophosphamide (FC), Chlorambucil (Chl) or Fludarabine (FDR) treatment regimes. This clinical trial has been used in a lot of published research and therefore many datasets have been generated for subsets of the cohort. Variant data has been previously generated for a cohort of 499 patients, using the Illumina TruSeq custom amplicon targeted sequencing technology (159). CNA data has been previously generated for a cohort of 133 patients, using the Affymetrix SNP 6.0 platform (141). TL data was generated for 384 patients using the monochrome multiplex QPCR (MMQPCR) technique (185).

3.3.2 ARCTIC and ADMIRE cohort

ARC/ADM patient were split into the following treatment arms; fludarabine, cyclophosphamide and rituximab (FCR), the addition of mitoxantrone to FCR (FCMR) or mitoxantrone with low-dose rituximab (FCMminiR). A final cohort of patients that started a FCMminiR regime but were recommended to cross over the FCR (FCMminiR/FCR), due to significant toxicities they experience with FCMminiR. Similarly to the CLL4 clinical trial, the ARC/ADM trials have been used extensively in previous projects and therefore a wealth of data is available for different subsets of patients. Previous work has generated variant and CNA data for a cohort of 250 ARC/ADM patients using a Illumina TruSeq custom amplicon panel and HumanOmni2.5-8 SNP array, respectively (249). Additionally, 260 patients had TL data generated using the STELA technique (189).

The extensive catalogue of previously generated data for both clinical trial cohorts has been used within the research completed in this PhD, and directed what experimental work was completed. Starting with the previously generated data, experimental work was used to then ‘fill the gaps’ where patients were missing certain data points. This meant a large complete cohort of clinical trial patients with variant, CNA and TL data was created.

3.4 Data Generation

3.4.1 Quality Control Assessment

3.4.1.1 Qubit Fluorometer

The Qubit fluorometer uses a fluorescent dye that once it binds with DNA emits a signal which is then recorded by the machine. The greater the level of fluorescence recorded by the fluorometer represents a greater concentration of DNA in the sample with the concentration given in ng/µl (250). A calibration curve is produced from measuring the fluorescence levels of two standard samples with a known concentration. Next the relative fluorescence units (RFUs) of the unknown sample are compared to the RFU of the standards to calculate the concentration of the DNA sample.

3.4.1.2 NanoDrop Spectrophotometer

The NanoDrop is a spectrophotometer instrument that allows the quantification of a DNA concentration and assessment of purity based on the absorbance measures of the sample. It works on the principle of ultraviolet-visible spectrum absorbance and Beer-Lambert law which states that the amount of light absorbed at 260nm is proportional to the concentration of nucleic acid in the sample (251). Conversely, purified proteins can be measured by assessing light absorption at 280nm. To calculate the purity and identify any potential contaminants in the sample a ratio of the absorbance values of 260nm vs 280 nm, with an increase or decrease in this ratio indicating a protein or RNA contamination of the sample, respectively. A 260 nm vs 230 nm ratio can examine the presence of other contaminants such as chaotropic salts (252).

3.4.1.3 Fragment Analyzer

The Fragment Analyzer 5200 is a multiplex capillary electrophoresis instrument that allows for the separation and quantification of DNA and RNA. The instrument functions by using conductive gel matrices, which when a high voltage is applied, causes the DNA/RNA to migrate through the gel within the capillary array as a function of size (253). For example, smaller fragments will travel through the gel much faster than larger fragments. Visualization of this size dependent separation is achieved by detecting the fluorescence of an intercalating dye added into the gel matrix. The recording of the RFU intensity over time not only allows the calculation of the size of the fragments but also the concentration of the sample. See **Figure 15** below for an example of a fragment analyzer trace. Both these readings are required for calculating the volumes of each sample that will be added to the pool DNA libraries that will then be sequenced. Measuring the

concentration of these fragments is completed by integrating under the desired peak by adjustment of the peak bars. This step is completed using the ProSize data analysis software (254).

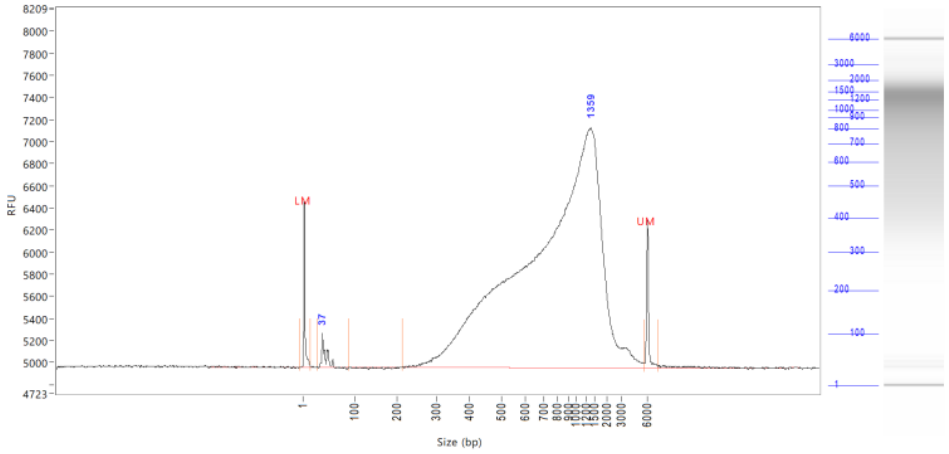

Peak	Size (bp)	Conc. (ng/uL)	From (bp)	To (bp)	Avg. Size (bp)	CV%	RFU	Corr. Peak Area
1	1 (LM)	0.0427	0	15	2	154.27	1521	9.086
2	37	0.2700	29	88	42	15.53	307	4.789
3	1359	19.8970	212	5600	917	62.37	2170	352.899
4	6000 (UM)	0.0273	5600	7247	6048	4.18	1342	5.801
	TIC:	20.1670	ng/uL					
	TIM:	46.2324	nmole/L					
	Total Conc.:	20.1712	ng/uL					

Figure 15- A typical electropherogram produced by the Fragment Analyzer and visualized on ProSize software showing a successful sWGS DNA library with the average fragment size of 917bp (within the desired size range, 600-1000bp).

3.4.2 Mechanical shearing to create DNA fragments

Mechanical shearing of sample DNA was the first step in the SureSelect XT HS2 target enrichment DNA sequencing experimental procedure. A starting concentration of 2ng/µL was used for the DNA library preparation (255), this concentration was measured using the Qubit fluorometer. Next mechanical shearing of each DNA sample to fragment it was completed using the Covaris M220 focused-ultrasonicator. The Covaris fragments DNA by mechanically shearing the phosphodiester backbone using Adaptive Focused Acoustics technology. This technology employs controlled bursts of high-power acoustic energy to a sample in a temperature-controlled water bath. The use of this mechanical shearing in a water-controlled environment allows a high recovery of DNA with unbiased fragmentation (256). The settings used for the mechanical shearing followed the manufacturers advice for the desired fragment size of 180-250bp using the specific M220 model as shown below in **Table 1**.

Table 1- DNA shearing settings for M220 instrument as recommended by the manufacturer (257)

Setting	Covaris M220 instrument
Bath Temperature (°C)	20
Peak Incident Power (W)	75
Duty Factor (%)	20
Cycles Per Burst	200

These settings differed from the HS2 methodology as the setting given in protocol were designed for a different Covaris model and therefore an adjustment to the protocol was required. Furthermore, as an additional quality control step, samples were run on the Fragment Analyzer to ensure the correct fragment size was produced from the Covaris step.

3.4.3 Generation of telomere length data

To generate new TL data for a cohort of 83 cases that lacked this dataset, I undertook laboratory work using the MMQPCR technique. The technique, which is discussed in much greater detail in 5.4.2, calculates a relative TL using fluorescence measurements of a telomere signal (T) and a single copy gene signal (S), which gives a T/S ratio. This T/S ratio is recorded for both the unknown DNA sample and a series of a diluted standard. The TL given for the unknown sample is relative to the standard used (258).

3.4.3.1 Experimental protocol

This protocol was adapted from another the published work of Cawthon et al, 2009 (258). Experimentally, three PCR reaction wells are needed for each DNA sample and each of the five reference 'standard' dilution being examined. This is because each reaction is completed in triplicate and an average of these three replicates is taken during the data analysis stage. A concentration of 10ng/ul is required for each of the test DNA samples and therefore before the PCR reaction was set up all 83 samples included in this analysis underwent a quality control step. The Qubit 3.0 fluorometer was used to quantify the concentration of the experimental samples which was used to calculate the dilution factor of each sample, producing the correct concentration in a volume sufficient for three PCR reactions. Once a 386 well PCR was loaded up with a prepared PCR master mix, and the test DNA and reference DNA is added to the relevant wells, ensuring the replicates are spaced across the plate to account for edging, the plate is run on a Roche LightCycler 480 instrument. The LightCycler 480 instrument is a high-throughput real-time PCR device that runs a specific cycling programme. It records cycle threshold (C_t) values for

the amplification of the telomere at 74^{o}C, when the single copy gene is at baseline, at the next stage the temperature increases to 88^{o}C and the single copy gene template amplification C_t values are recorded. Data generated on the LightCycler 480 machine is exported in a text file format as raw data formatted as fluorescence by cycles for downstream data analysis.

3.4.3.2 Data analysis

The first steps of analysis of this data was completed using RStudio (version 4.3.0) within the R environment and a R packaged called 'minpack.lm' (version 6.4). As part of the QPCR analysis, Ct calculations were completed using the Full Process Kintetics-PCR (FPK-PCR) method, a R-based technique that uses 'minpack.lm' R package. FPK-PCR protocol was included to optimize the data analysis of MMQPCR data, this decision is discussed in detail 5.4.2.2. Then Microsoft Excel was used to finish the analysis and covert the relative TL measurement given from MMQPCR to an absolute value, using a linear regression equation. This absolute TL value could then be integrated with the established TL dataset that were previously generated using MMQPCR and STELA techniques.

3.4.4 Generation of genetic variant data

To generate new variant data for a cohort of 52 cases that lacked this dataset, I undertook laboratory work employing the Agilent SureSelect XT HS2 DNA NGS Target Enrichment system to prepare the DNA libraries before Illumina sequencing. The HS2 DNA workflow is shown in **Figure 16**, and can be broadly divided into probe design, DNA library preparation and target enrichment using hybrid capture. The captured libraries are then pooled, before sequencing using Illumina based technologies.

3.4.4.1 Probe design

Probe design was completed in November of 2021. A final custom panel of 72 target genes or regions was included, for more detail on probe design see 5.4.3.1.1. The complete list of genes or regions that were included in the probe design are shown in **Supplementary Table 2**.

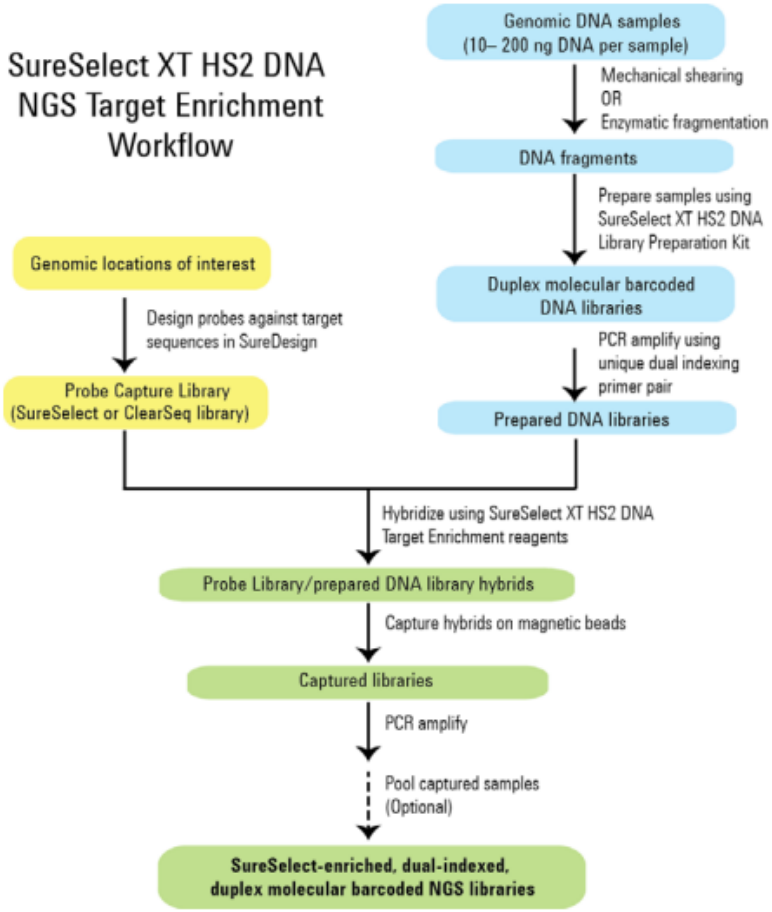

Figure 16- Overview of the SureSelect XT HS2 DNA NGS Target Enrichment workflow, detailing the steps involved to prepare a sample for sequencing, from (255).

3.4.4.2 Library Preparation

A starting concentration of 2ng/µL was used for the DNA library preparation (255), this concentration was measured using the Qubit fluorometer. Next mechanical shearing of each DNA sample to fragment it was completed using the Covaris M220 focused-ultrasonicator. The settings used for the mechanical shearing followed the manufacturers advice for the desired fragment size of 180-250bp using the specific M220 model as described in **Table 1**.

Library preparation involved the addition of both a molecular-barcoded adaptor and a unique dual-index to the fragmented DNA sample. Furthermore, various PCR amplifications and sample purification steps, using AMPure XP beads, are completed. At the end of library of preparation, quality and quantity assessment of the DNA library was completed using the Fragment Analyzer.

3.4.4.3 Hybridization and Capture

The prepared DNA library is then hybridized with the previously designed target-specific probe. Probe hybridization is followed by the capture and amplification of the hybridized library. Capture

occurs through a streptavidin-biotin interaction whereby the streptavidin magnetic beads bind to the biotinylated target probes, allowing these probe bound DNA fragments to be extracted from the sample using a magnetic device.

3.4.4.4 Post-Capture Processing and Pooling

During this step, the captured libraries are amplified through a PCR process and then purified using AMPure XP beads. The quality and quantity of the final prepared DNA library is assessed by running 2ul of the sample on the Fragment Analyzer. The desired fragment size, post capture, is 200 to 450 bp in length, see **Figure 17**. Only 42 of the 52 cases successfully passed the DNA library preparation and therefore only 42 samples were pooled together and sequenced. The minimal sequencing data required for this experiment it was 6.29 Gb of sequencing. To combine the libraries the concentration of each library was converted from ng/ul to nanomole. A concentration of 4nm of each sample was desired, 42 samples were pooled to give a final pool volume of 100 ul. The pooled library was then sequenced on the NovaSeq 6000 Illumina platform using v1.5 chemistry. The generated raw sequencing data, in the form of FASTQ files were then analysed using a bioinformatic pipeline.

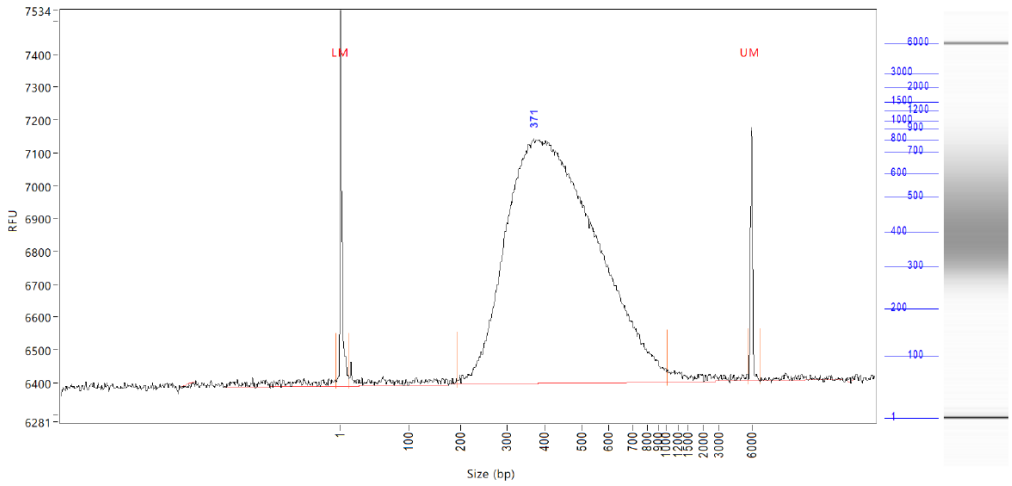

Peak	Size (bp)	Conc. (ng/uL)	From (bp)	To (bp)	Avg. Size (bp)	CV%	RFU	Corr. Peak Area
1	1 (LM)	0.0118	0	14	2	161.36	1822	11.474
2	371	1.9694	193	1010	434	28.62	746	159.708
3	6000 (UM)	0.0030	5712	6788	5993	1.97	772	2.911
	TIC:	1.9694	ng/uL					
	TIM:	7.4662	nmole/L					
	Total Conc.:	2.0409	ng/uL					

Figure 17- Fragment Analyzer result of a post capture PCR quality control check of a successful DNA library with an average fragment size of 434bp.

3.4.4.5 Data analysis

I undertook the analysis of the raw sequencing data, this was started on the University's high-performance computing cluster IRIDIS 5 for preprocessing, alignment and variant calling and then finished with RStudio within the R environment whereby variant filtering was completed. I also used the Integrative Genomics Viewer (IGV) software to manually curate the final filtered list of variants.

3.4.4.5.1 Preprocessing, alignment and variant calling

FASTQ files are generated from the sequencing on the Illumina NovaSeq 6000 sequencer. The sequence quality of each FASTQ file is assessed using the FASTQC software (version 0.11.9) with the output of all files being merged to create a report, using the MultiQC tool (version 1.23). Preprocessing and alignment of the raw sequencing files was completed with IRIDIS 5, using various software including BWA (version 0.7.17), samtools (version 1.20), picard (version 2.18.14) and Mosdepth (version 0.3.4). Variant calling steps used GATK (version 4.1.9.0) and the Mutect2 (version 4.1.4.1) software.

Once FASTQ files pass the quality control step outlined above, preprocessing of the data is completed. The first step of preprocessing the data is the identification and removal of adaptor sequences using the trimmer tool (version 3.0.5) of Agilent's AGeNT software (version 3.0.6). These trimmed FASTQ files were run through BWA-mem and aligned to the GRCh38 genome reference consortium human build 38, reference genome. The SAM file created during alignment is then converted to a BAM file using samtools. This aligned BAM file was the indexed using samtools index. Next, the trimmer tool is also used to extract the dual MBC that are then processed using the AGeNT CReaK (version 1.0.5) tool, so duplicate reads can be marked, and a consensus read generated. The aligned and indexed BAM file then sorted by coordinate using the SortSam tool from Picard (version 2.18.14). A further indexing of the BAM file is completed using the Picard BuildBamIndex tool. FixMateInformation for Picard is used to verify that all pair information is synced between paired reads. Finally, Mosdepth was used to calculate genome-wide sequencing coverage, again MultiQC was used to merge all output files into a single report of all samples for easier examination.

Variant calling was completed using the GATKs tool, Mutect2, which calls somatic mutation through the assembly of haplotypes. Next filtering of the raw output of Mutect2 was completed with the FilterMutectCalls tool with minimum median mapping quality and median base quality parameters being set to 20. Finally, GATKs Functotator tool was used to analyse the function of the called variants which allows additional annotations from data sources (version 1.7.20200429s), see **Table 2** for a list of data sources used. The final output file from this analysis for each sample was a MAF file, which is a tab-delimited file that contains somatic mutation

annotations. Therefore, these MAF files were consolidated into one MAF file and inputted into RStudio ahead of variant filtering.

Table 2- List of databases used for annotating called variants by GATKs Functotator tool

Database
Achilles
Cancer_gene_census
Clinvar
Clinvar_hgmd
Cosmic
Cosmic_fusion
Cosmic_tissue
dbSNP
Dna_repair_genes
Familial
Gencode
Gencode_xhgnc
Gencode_xrefseq
Hgnc
Oregano
Simple_iniprot

3.4.4.5.2 Variant filtering

The MAF file containing the output of all samples was read into RStudio using the read.maf function from the maftools package (version 2.18.0). An additional clinical data text file containing patient data on certain variables was also included to create a maf object. Variables included were treatment arm, age, sex, *IGHV* mutation status, epitype and TL. Filtering using the gnomAD genome database with an inclusion criterion of <0.001 allele frequency (0.1% allele frequency) was applied. Similarly, the gnomAD exome database with a <0.001 allele frequency cut off was applied. These reference population databases were used to distinguish somatic variants from germline variation, as a matched germline sample not available so this could not be done a per

sample basis. Therefore, likely germline variation was removed during this filtering step. Using the maftools package, graphical summaries of these variants could be made to examine further the final filtered variant list.

3.4.4.5.3 Manual curation

Manual curation of the filtered list of variants, identified in the previous step, began by assessing whether the variant had a COSMIC ID. Any entries or additional references to published research that were linked to the variant in the COSMIC database (version 3.4), were assessed. If a variant did not have a COSMIC ID, an alternative identification was used such as; dbSNP number (NCBI SNP databased build 152), the cDNA change, or the protein change. Using this information, the variant was searched for in published CLL literature and was included if it was reported as somatic or likely pathogenic. For certain gene variants specific criteria was employed for manual curation, these criteria follow the manual curation methodology outlined in Blakemore et al (2020) (159). Firstly, variants were only considered if previously observed as somatically acquired in CLL or annotated in COSMIC (version 84). Variants in the *TP53* gene were only included if they were present in the International Agency for Research on Cancer (IARC) TP53 database (updated in 2018, version R19). Similarly, *ATM* variants were included if they were present in the Leiden open variation database (LOVD) as were observed in AT families as pathogenic. Additionally, *ATM* variants that were reported as an evolutionary rare missense mutation in pooled published data from mutation-screening studies (259) or if they were one of the 36 *ATM* variants reported to be somatically acquired in CLL (260). Finally, *BIRC3* and *NOTCH1* variants were included if they were predicted to result in protein truncation.

The final step in manual curation is visual inspection of the variant and its surroundings using the IGV software. Established criteria for distinguishing true somatic variants were used (261); which included assessing if the change was present on both the positive and negative strand, what percentage of the reads had the change, if the surrounding reads have many changes (noisy reads), if the variant was present at the end of the gene or frequently at an end of a read. More complex cases were discussed with a second reviewer (HP) until a decision was agreed upon. The final list of variants produced by this technique was then integrated with previous generated variant data, for downstream analysis.

3.4.5 Generation of copy number data

3.4.5.1 450k Array Data Analysis

Previously generated raw 450k array data was available for a cohort of 285 ARC/ADM patients. This analysis was completed using R (version 4.1.2) within the Rstudio (version 2021.09.1) environment R with the package 'conumee' (version 1.30.0). This package allows copy number variant analysis in a two-step process using the data generated from the 450K array technique. The first step involves normalizing both the methylation and unmethylated channel at each CpG site. Next the neighboring probes are combined to create the minimal size and number of probes (262). For normalization the MSetEx dataset from the R package 'MinfiData' (version 0.42.0) was used (263). A log R ratio (LRR) is calculated for each DNA segment, with CNA being identified as deviations of the LRR from the baseline level, after correction. 450k array data is considerably noisy and therefore a widely accepted cutoff of +/- 0.1 segment median LRR is used to define aberrant copy numbers in a sample (264). A further parameter used was a p-value<0.001. As data was originally aligned to the hg19 reference genome, a liftover was completed to convert all data to the hg38 reference genome. This was completed so that all data complied together in the final cohort used in the following chapters were all aligned to the same reference genome. Relevant CNAs reported in CLL, were defined using the hg38 human reference genome location of certain genes that are associated with these specific CNAs, see **Figure 18** for further detail. Of the 285 ARC/ADM patients, 31 cases were used cohort described in Chapter 6. Only 31 cases were included as these patients were missing CNA data, therefore analyzing the 450k array sequencing data meant they met inclusion criteria.

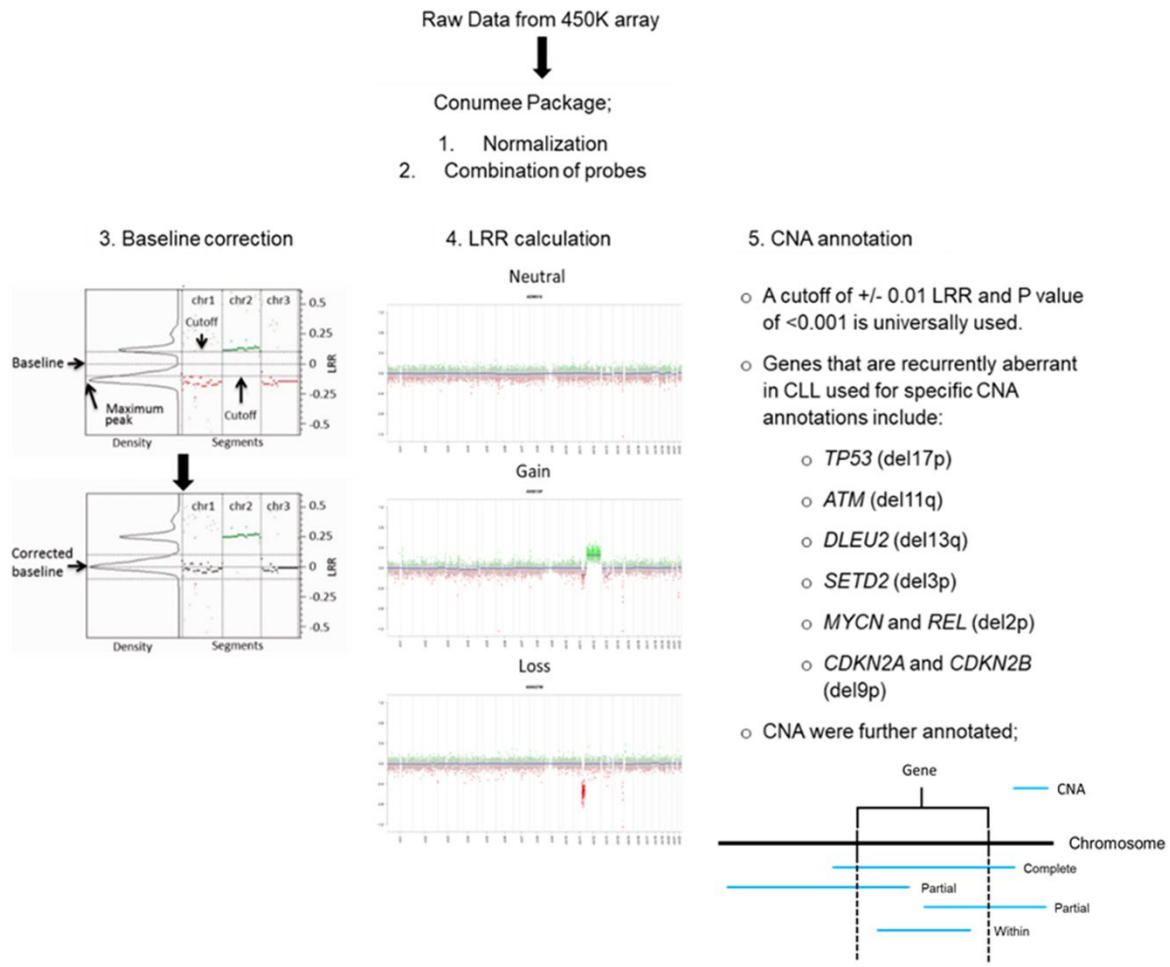

Figure 18- 450k Array Bioinformatic pipeline overview. Steps are shown in numerical order. 3. Baseline correction is required to assess tumour samples as typically they include many large aberrations (shown by the large green segment at chr2) which can cause shifting in the probe intensities and therefore can affect downstream CNA calling. 4. LRR has been plotted for each read as shown by the many dots, with the average LRR for a segment being shown by the vertical line, deviation in the LRR for a segment result in a gain (highlighted in green) or a loss (highlighted in red). Known important CNA in CLL were identified and annotated with either total, partial or within, which depicts if the CNA completely encompasses, partially encompasses, or occurs within a set genomic region, respectively. Adapted from (264).

3.4.5.2 Shallow whole genome sequencing

sWGS describes a methodology developed in 2014 which allows copy number to be inferred from WGS data. The method uses DOC technique to estimate copy number profiles and identify CNAs in tumour samples. sWGS sequences the whole genome at an average coverage of around 0.1x and by assuming a relatively consistent DOC is captured across the genome the deviations from the normalised baseline can be called as CNAs. A total of 177 cases were included in this experiment to generate novel CNA data.

3.4.5.3 Library preparation

SureSelect library preparation encompasses multiple steps that results in fragmented amplified adaptor-tagged and indexed DNA for pooling prior to sequencing. An overview of the experimental pipeline is shown in **Figure 19**. The Agilent SureSelect^{QXT} whole genome library prep for Illumina multiplex sequencing protocol was used.

Assessment of the concentration of DNA sample prior to the library prep was completed using the Qubit dsDNA BR Assay Kit. A starting concentration of 50 ng/ul for each DNA sample was required. Library preparation was completed on two separate occasions with a batch of 70 and 107 CLL4/ARC/ADM clinical trial patients. Firstly, DNA samples were enzymatically fragmented. This fragmented DNA was then tagged with an adaptor and purified using AMPure XP beads. Next, the sample was PCR amplified using a specific thermal cycler program on the SureCycler 8800 thermal cycler. During this step, the DNA library was also indexed using a unique combination of two index primers (P7 and P5 indexing primers). The DNA library was then again purified using AMPure XP beads. Finally, the assessment of quantity and quality of the prepared library was completed using the Agilent Fragment Analyzer 5200. The desired fragment size range of the created whole genome libraries are 600-1000 base pairs (bp). Both readings are required to calculate the volumes of each sample that will be added to the pool of DNA libraries that will then be sequenced using the Illumina NovaSeq 6000 platform.

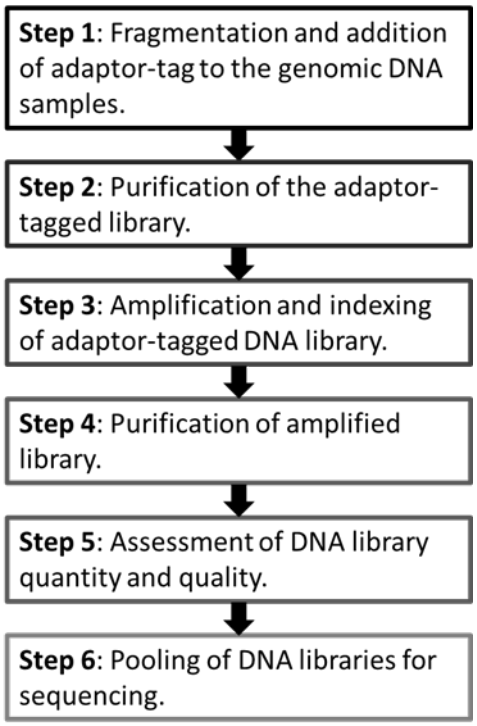

Figure 19- Adapted from the SureSelect^{QXT} whole genome library preparation for Illumina multiplexed sequencing protocol, from (265).

3.4.5.4 Data analysis

Sequencing data generated from sWGS DNA libraries were analysed using an in-house pipeline, with optimizations which will be discussed further below (5.4.4.2). The raw sequencing data generated from the Illumina platform is in the format of FASTQ files. The conversion of bcl files to FASTQ files includes the demultiplexing of data. Therefore, de-multiplexing using the sample specific combination of two 8-base indexes was completed prior to the data being returned to me. Thus, a FASTQ file for each sequencing read per patient assessed was produced and included in the data analysis described below.

Computationally, FASTQ files containing raw sequencing data is aligned to the hg19 human reference genome that was constructed from the 100,000 genome project and an annotated file of all known common human SNPs. The hg19 reference genome was used in alignment as CNA data generated prior to this work was aligned to the hg19 and then was converted, by me, to hg38 by a liftover using the UCSC genome browser application. Therefore, to ensure all CNA that will be merged together for downstream analysis undergoes a similar processing, the sWGS data was first aligned to hg19 and then converted to hg38 via a liftover. An annotated file of know human SNP is used for base quality recalibration and is sourced from NCBI by selecting the dbSNP variation human database.

Alignment and processing of aligned reads is completed using the IRIDIS 5, the high-performance computing facility at the University of Southampton. Multiple programs are required for this analysis including bwa (version 0.7.17) to maps the FASTQ files to reference genome. Next samtools (version 1.9) is used to convert the SAM file, containing aligned reads, to a BAM files which are a smaller, binary version of SAM files. Samtools is also used to sort this newly created BAM file. A further package is picard (version 2.18.14) which is used to remove PCR duplicates. Finally, the program samtools (version 1.9) is used to generate index files for each reference aligned sample BAM file which allows the visualization of the sequencing data downstream using the IGV software.

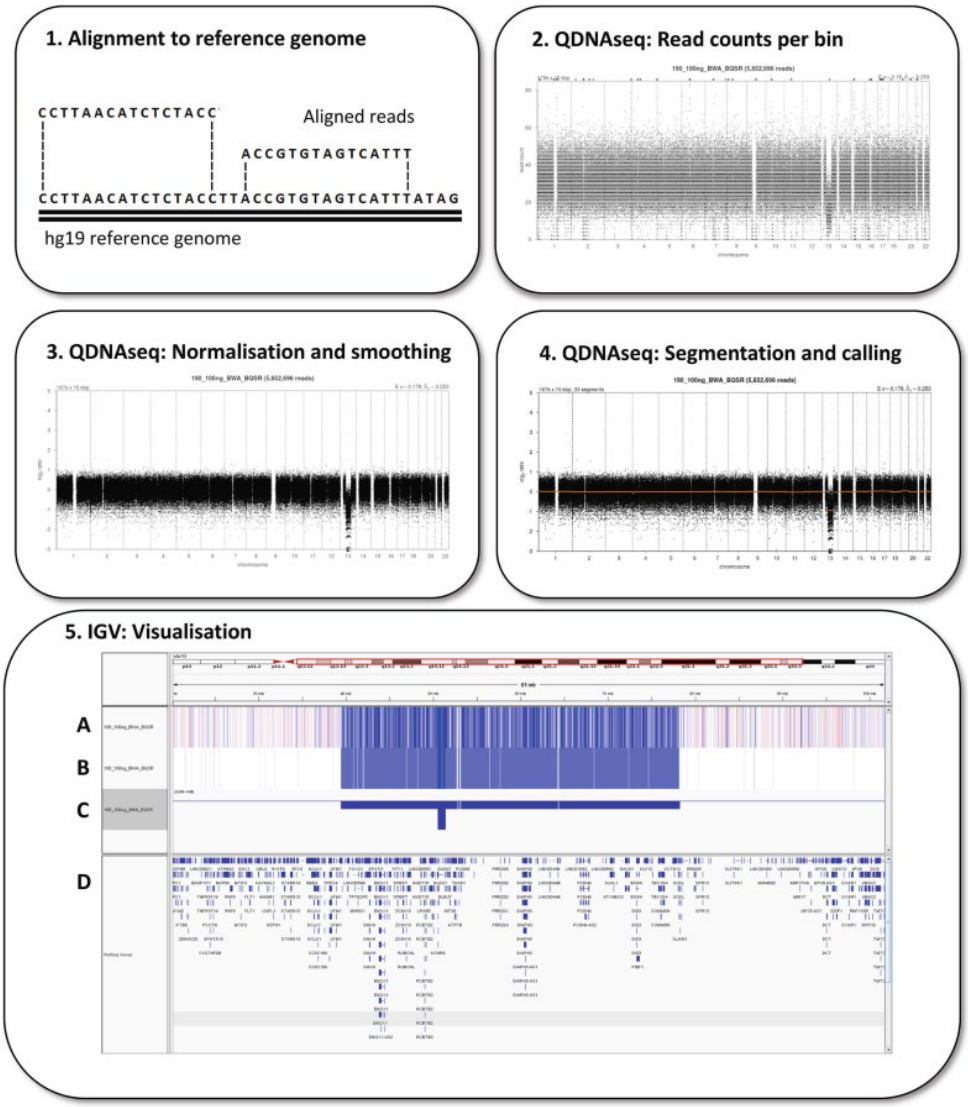

Figure 20- Overview of the shallow whole genome sequencing data analysis workflow, from (266)

Next, analysis using R (version 4.1.2) within the Rstudio (version 2021.09.1) environment and the R package QDNASeq (version 1.26.0) is completed. Once in the R environment data is divided into 30kb bins, normalized and corrected for mappability and GC content, log2-transformed and CNA calls are made from segmented data (266), see **Figure 20** for an overview of the workflow. Using a 30kb bin size was decision was based on the literature and the comparison of other bin sizes using a small cohort of samples, see below for more detail (5.4.4.2). The output of QDNAseq includes a .txt file that gives the whole genome, per sample, segmented into the 30kb bin sizes with the mean log2 ratio for that bin. A positive or negative log2 ratio indicates that that a segment is present more or less than the baseline, respectively. A further output from QDNAseq is CNA count plots, which has a y axis on the left showing the log2 ratio and the y axis on the right is the probability scale. Segments with a bar extending beyond the middle axis, where the probability is 0.5, are then called as CNAs (**Figure 21**). This CNA calling was completed using 'CGHcall' (version 2.58.0), a calling method that was developed for cancer sample sets using a mixture model with

six states to reflect the six biologically important calls of double deletion, single deletion, normal, gain, double gain, and amplification (267).

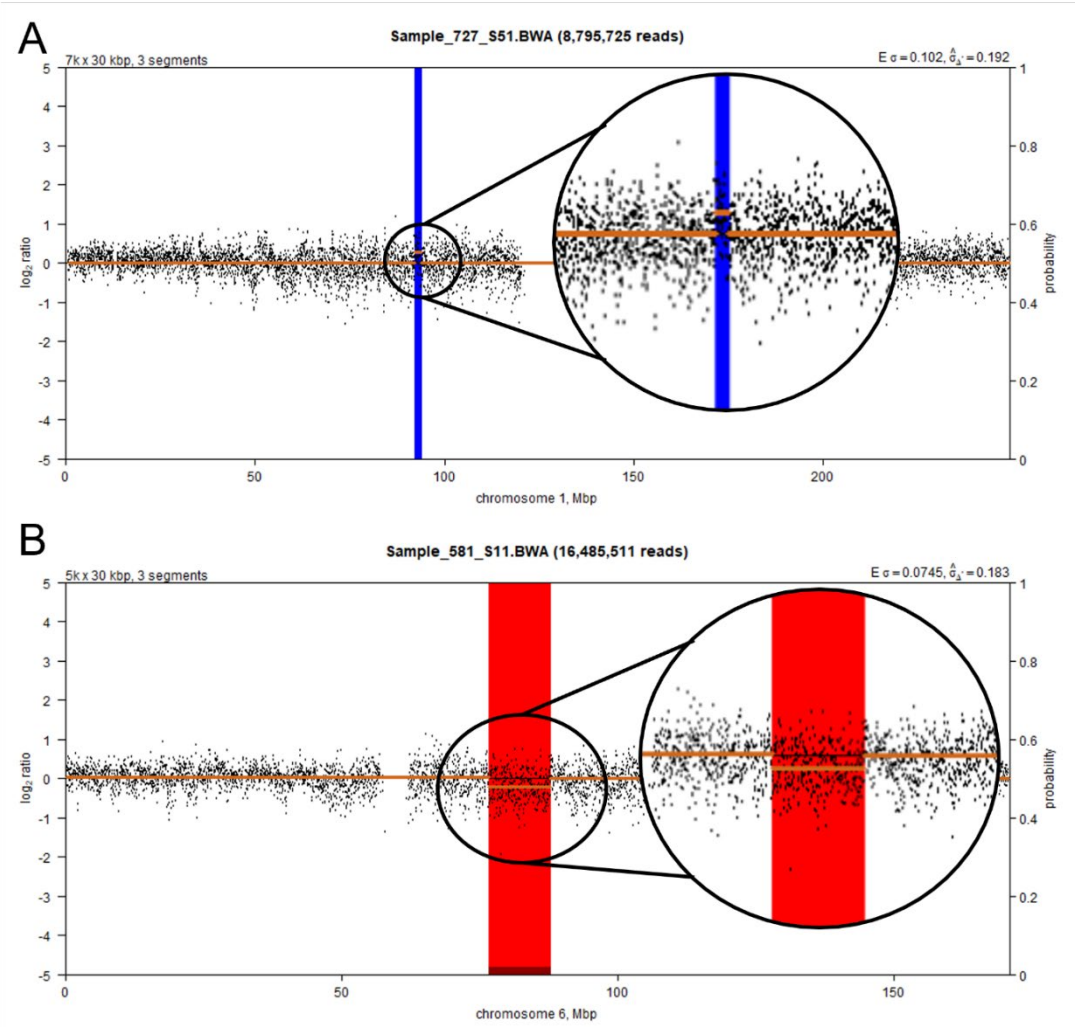

Figure 21- Copy number called plots showing examples of CNA that passed filtering but were then excluded during manual curation. The left y axis shows the log2 ratio and the right axis gives the probability scale: A. This CNA was discounted because there is not a clear gain with main points present at the baseline and below the baseline. B. This CNA was discounted because the distribution of the points in the called CNA, shown in red, is similar to the sections either side of the called CNA and if the orange mean log2 ratio for the section was removed it would look similar to the non-called sections.

To classify CNAs from the data generated by QDNAseq, a cut off of +/-0.2 log2 ratio was applied which is a widely used threshold for the analysis of sWGS data (268–270). Furthermore, a size cut off of ~1Mb was included in the filtering in which 33 consecutive bins (33x30kb=990kb) all with the same log2 ratio were required to be counted as a CNA (103). This filtering, although stringent, was applied as the small CNAs where hard to be confident in, especially in cases that had noisy

data. After each filter had been applied and the list of potential CNAs were constructed for each case, manual curation was completed.

3.4.5.5 Manual curation

Manual curation was completed by two independent reviewers (LC and HP) which had the same inclusion and exclusion criteria. Cases that were not clear or were complicated were discussed and decided upon together. Manual curation started by examining the list of CNAs that passed the filtering requirements as outlined above. These CNA were assessed by looking at the copy number called plots which shows the distribution of the 30kb bins across the whole genome and per chromosome. The profile created by the CGHcall calling method colour codes the calls as such; red indicates the probabilities losses and blue indicates the probabilities of gains. From these figures the noise of the data can be ascertain by the vertical spread of bins. Additionally, the specific CNAs that had been called can be assess by looking at the region being called and see the spread of the data compared to the baseline and the surrounding data. Common reasons to remove a CNA during manual curation include if there were considerable data points across the baseline and therefore not a clear shift up or down if calling a gain or loss, respectively. Also, if there is a similar section next to the CNA called that has not been called then this CNA is disregarded, see **Figure 21** for examples.

Additionally, through the examination of the copy number called plots, CNAs that may have been removed through the filtering can be added back. For example, CNAs that are smaller than 990kb but are very clearly present when looking at the plots. This was especially important in regions of known recurrent CNAs such as del13q, del11q and del17p. Trisomy 12 events were clear to identify from the copy number called plots (see **Figure 22**), however there were cases where the CNA calling parameters called this as multiple different CNAs and therefore during manual curation these were consolidated into one trisomy 12 event. Additionally, biallelic events were also called by visual inspection of the copy number called plots in addition to the log2 ratio, see **Figure 22B**.

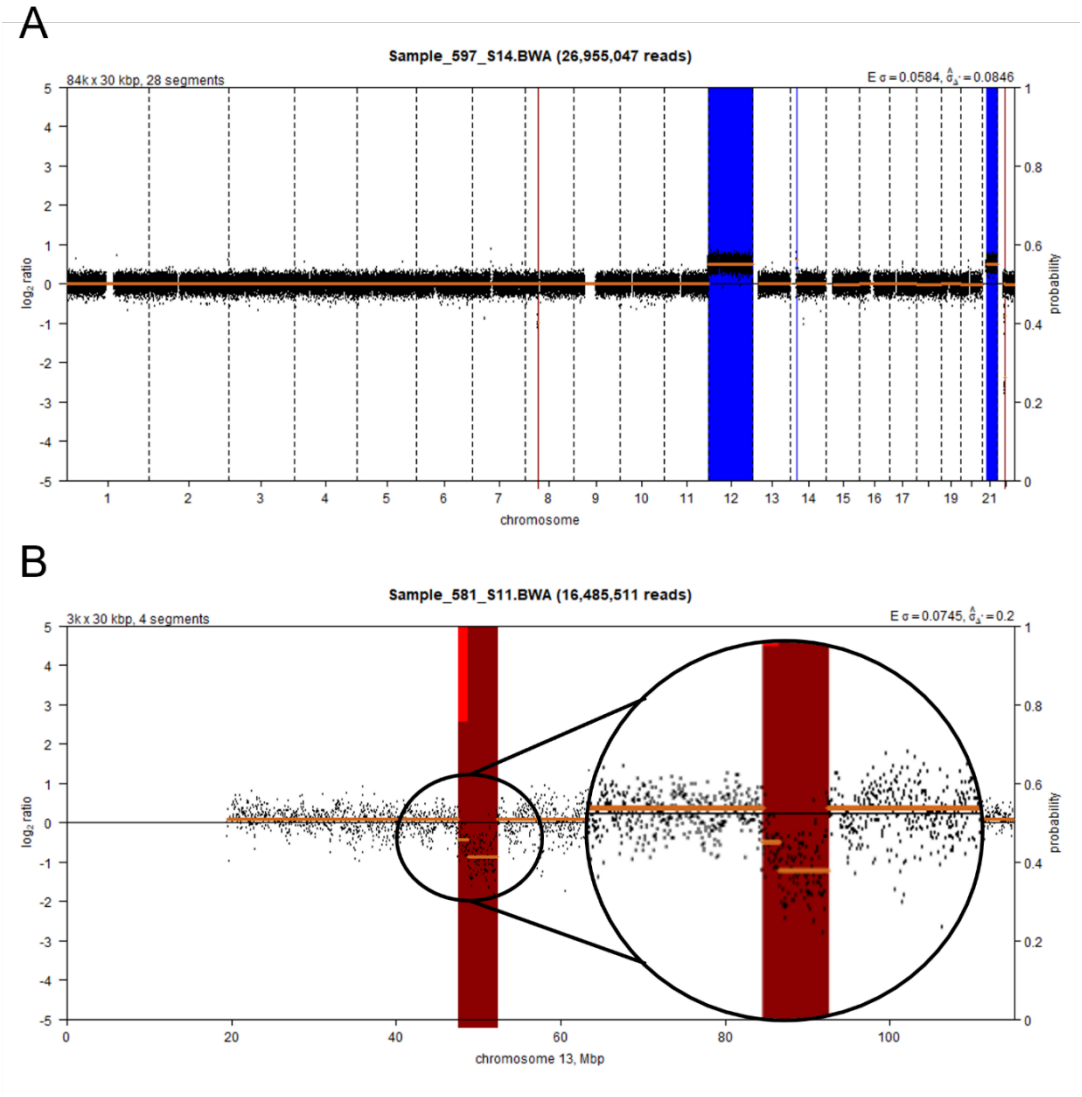

Figure 22- Examples of called CNA that passed manual curation as clearly show a (A) trisomy 12 event and a (B) biallelic and monoallelic loss of 13q.

The 153 sWGS cases that passed all data analysis and manual curation steps were integrated with CNA data previously generated either from SNP 6.0 array, HumanOmni array or 450k array technologies.

3.5 Statistical and Survival Analysis

Statistical analysis was completed using Rstudio in the R environment (version 4.3.0). R packages 'tidyverse' (version 2.0.0), 'table1' (version 1.4.3), 'ggplot2' (version 3.4.4), 'dplyr' (version 1.1.4), 'hrbrthemes' (version 0.8.7), 'viridis' (version 0.6.5) and 'networkD3' (version 0.4) were used in statistical analysis. The statistical cohort used in Chapter 4 was compiled of 519 patients (CLL4: 304 and ARC/ADM: 215) whereas Chapter 6 used a statistical cohort of 495 clinical trial patients (CLL4: 251 and ARC/ADM: 244).

A Wilcoxon rank sum and chi squared test were employed to test for differences between continuous (i.e. Age) and categorical variables (i.e. *IGHV* mutation status), respectively. An odds ratio (OR) was calculated to test associations between variables assessed in Chapter 4 and Chapter 6. An OR is a statistic that quantifies the association between two events, i.e. one epitype group and one TL group. A value of OR >1 or <1 suggests a positive or negative association between two variables, respectively. The Fishers exact test is a non-parametric statistical test used to compare the proportion of categories in two independent categorical variables. These statistical tests were applied in a pairwise comparison of the variables and the output were adjusted using the Benjamini-Hochberg method to account for multiple testing. These values were visualised in an association plot. To test concordance between FISH and each of the four genomic technologies for the detection of copy number events; del17p, de;11q, Trisomy 12 and del13q, a Cohens kappa test was used. This statistical test states the degree of agreement between two raters. A Sankey plot was used to visualise the distribution of certain variables in cohorts of patients, i.e. the prevalence of the three TL groups within each of the three epitype groups, and vice versa. Many graphical displays of the data were used, including bar charts, scatterplot, violin plots and density plots. Descriptive statistics such as mean, median and percentage of cases, was also employed to examine the data.

Survival analysis was also completed using Rstudio in the R environment (version 4.3.0). R packages 'survival' (version 3.5.7), 'survminer' (version 0.4.9) and 'survivalAnalysis' (version 0.3.0). Survival analysis was completed on separate clinical trial cohorts with the CLL4 patients forming the discovery cohort and ARC/ADM patients forming the validation cohort. These clinical trial cohorts were kept separate during survival analysis due to different amounts of follow up data available for each trial. Chapter 4 used a cohort of 304 and 215 CLL4 and ARC/ADM patients, respectively. Chapter 6 used a cohort of 251 and 226 CLL4 and ARC/ADM clinical trial patients, respectively. Kaplan Meier (KM) plots were created, and a log rank test was used to compare differences in survival curves. A cox regression analysis including only one covariate was completed as part of the univariate analysis. MVA was completed using Cox proportional hazard analysis. Covariates that were significant (p-value<0.05) in the univariate analysis were then included in the first multivariate model. A stepwise backwards elimination process was used to reach a final model that included covariates that were all significant in survival. In an iterative process, a covariate with the lowest significance in the model was removed. A comparison of the two models, one with and one without the removed covariate, using a likelihood ratio was completed, to assess if it was appropriate to remove the covariate (likelihood ratio p-value>0.05). This was completed until a final model was reached. For each clinical trial survival cohort two survival endpoints of PFS and OS were used, meaning four multivariate models was produced in

Chapter 4 and Chapter 6. Results from the univariate and MVA were displayed in forest plots created using Rstudio and the 'forestplot' (version 3.1.3) package.

Chapter 4 Investigating telomere length and methylation based epitype as clinical biomarkers within a discovery and validation CLL clinical trial cohort

4.1 Synopsis

This chapter describes the research completed to assess the clinical impact of TL and DME biomarkers together within a singular clinical trial cohort. The analysis completed in the chapter assessed the relationship between the two biomarkers. The novelty of the survival analysis completed in this chapter is the inclusion of both TL and DME into univariate and MVA. Most data utilised in this chapter was generated previously and gifted, for example the epitype data was generated using pyrosequencing within a previous publication (195). The laboratory and data analysis work required to generate TL using either MMQPCR or STELA techniques were completed beforehand by other researchers (185,189). However, I supplemented this work by generating novel data for a sub cohort of patients. I completed the laboratory and analytical work to produce TL data using the MMQPCR technique. Additionally, I carried out all the statistical and survival analysis work that is reported within this chapter.

4.2 Introduction

Patients with CLL exhibit a highly heterogenous clinical course from the requirement of rapid and aggressive treatment to a benign disease with a life expectancy comparable to an age matched control population (116). Despite the discovery of a plethora of molecular and cellular biomarkers, discussed above in 1.4, only two are currently deployed in the clinical setting to aid risk-adapted patient stratification, namely the presence of *TP53* aberrations and/or U-CLL status (84,271). A limitation of many CLL biomarkers lies in their co-existence with other poor-risk confounding indicators, and the consequent inability to provide clinicians with independent prognostic or predictive information over established clinico-biological features. For example, whole exome or genome sequencing projects have identified low frequency mutations such as *SAMHD1* mutations which occur in occur in 3% of untreated CLL patients. Whilst this mutation has been reported to increase risk of chemotherapy relapse, its independent prognostic impact has not been able to be fully validated in a large, data rich clinical trial (272). The independent clinical

significance of any biomarker is most easily established in the context of large Phase II/III clinical trials with long follow-up and extended molecular characterization. As such, in this chapter, a large clinical trial cohort with extensive molecular characterisation has been employed within this publication to examine and validate two novel CLL biomarkers, DME and TL.

Within CLL, patients can be classified into three distinct DME subgroups, defined as n-CLL, i-CLL and m-CLL using DNA methylation comparisons with normal B-cell maturation (194,273). A seminal paper published in 2012 discovered that these three epigenetic groups were associated with different clinico-biological features (p-value<0.05), for example, the majority of i-CLL (84%) and m-CLL (96%) also had mutated *IGHV* genes. The research also identified that this novel epigenetic classification was the strongest predictor of TTT in a multivariate cox model (Relative risk: 6.63, 95%CI: 3.91-11.24, p-value<0.0001), with the m-CLL group being clinically favorable (194). Work completed by Wojdacz et al furthered this research by applying these epigenetic subgroups to a clinical trial cohort of 605 CLL patients. Similarly, to the original publication, a significant association was found between epitype and *IGHV* status with the n-CLL, i-CLL, and m-CLL signature being identified in 80%, 17% and 2%, of the U-CLL group, respectively. Additionally, a strong association (p-value<0.001) was also found between the epitype group and the presence or absence of various recurrent CNAs. For example, 68% of del11q cases and 77% of trisomy 12 cases were in patients with the n-CLL signature. Completion of a MVA found that m-CLL retained independent prognostic significance in PFS (HR: 0.25, 95%CI: 0.1-0.57, p-value<0.01) and OS (HR: 0.46, 95%CI: 0.24-0.87, p-value<0.05) when included in models with various variants such as del11q and del17p events, *IGHV* status, *TP53* mutations, treatment and stage (195). It was concluded that the m-CLL epitype was an independent marker of prolonged PFS and OS using treatment naive clinical trial cohorts (195). Therefore, research has found that these novel epigenetic subgroups have potential clinical use within CLL by identifying patients that are destined for prolonged survival after being given CIT.

As mentioned in 1.4.1.1 and 1.4.1.2 the survival and clonal selection of CLL cells is influenced by the nature of the BCR, which is composed of two heavy and two light chains. The level of somatic hypermutations within the variable region of the IGHV dichotomise CLL patients into two distinct subtypes (U-CLL and M-CLL) (274). Additionally, a bias in the IGLV and IGHV repertoire has been reported, with certain genes being present more in CLL compared to normal B cells. One such common light chain is IGLV3-21. The epigenetic subgroup i-CLL has a borderline *IGHV* mutational load and intermediate survival outcome however has a much higher IGHV3-21/IGLV3-21 usage. B cells expressing IGLV3-21 stereotype can acquire a single point mutation (R110) which causes autonomous BCR signalling and aggressive disease presentation (131). Research has found an enrichment of IGLV3-21^{R110} within the i-CLL epigenetic subgroup, with i-CLL/IGLV3-21^{R110} patients

having methylation patterns similar to n-CLL. Additionally, IGLV3-21^{R110} patients have an overexpression of the *WNT5A/B* gene, which regulates proliferation and apoptosis. A cohort of 584 CLL patients identified that i-CLLs cases with IGLV3-21^{R110} had a shorter TTFT and OS. Whereas i-CLL patients without IGLV3-21^{R110} reported a better prognosis, like that of m-CLL and M-CLL patients (275). The presence of the IGLV3-21^{R110} mutation remained significant in the multivariant model which included epigenetic subgroups and the IGHV3-21 stereotype (131). Therefore, evidence suggests that the i-CLL epitype, which has intermediate survival outcome, can be further classified, with IGLV3-21^{R110} identifying individuals with a poor prognosis, similar to that of n-CLL and U-CLL patients.

Whilst the presence of these DME subgroups have been shown to be associated with clinical survival in institutional and clinical trials cohorts (194,195), they exist in the presence of variable TL and other variable biomarkers, which are heterogeneous in patients and associated with survival in CLL cohorts (195). As explained in detail in 251.4.1.5, TL has been studied using many different metrics including published quartile cutoffs, which is the focus of this chapter, and the fusogenic range (fusogenic mean and median) which captures the threshold at which telomere fusion events occur (185,188). Research has shown that telomere dysfunction can not only precede disease progression but be used also risk stratify CLL patients further (188,189).

Assessing TL using quartile cutoff and as a continuous variable in a CLL4 clinical trial cohort of 384 CLL patients found that TL associated with many biological features and clinical outcomes (185). Firstly, increased TL, as a continuous variable, was found to reduce the risk of a short PFS and predicts a longer OS. Assessment of TL using quartile cutoffs found that the TL-I, and especially the TL-S group, were associated with many poor risk features such as U-CLL, *TP53* aberration and GC. Furthermore, the TL-S emerged as an independent marker of a shorter PFS (HR: 2.1, 95%CI: 1.37 to 3.21, p-value<0.01) and OS (HR:2.21, 95%CI: 1.27 to 3.87, p-value<0.01), in a multivariate cox regression model (185). Therefore, TL has been found to be prognostically important with various classification being used in the literature that captures different aspects of the TL distribution. An association between DME and TL, using published quartiles, has been reported, with 59% of n-CLL patients and 85% of m-CLL patients exhibiting TL-S and TL-L, respectively (195). This suggests that the co-existence of these two biomarkers might have a confounding or interacting effect on the observed clinical outcome. However, their clinical utility and relative power have yet to be fully validated together within a single cohort.

This project will investigate the impact of DME and TL on survival using two endpoints of PFS and OS in three large, well characterised clinical trial cohorts; CLL4, ARCTIC and ADMIRE. The

hypothesis is that 'Patient outcome is more significantly associated with TL than DNA methylation epitype.' Aims of this project are to;

A) Describe the biological associations and features of the TL and DME subgroups and investigate the relationship between the TL and DME biomarkers.
B) Identify the clinical merit and relative power of these two biomarkers within a discovery and validation CLL cohort of patients enrolled in CIT trials.

4.3 Methodology

4.3.1 Cohort selection

Our research included a cohort of 519 CLL patients enrolled in the UK LRF CLL4 chemotherapy trial (NCT00004218, n=304), UKCRN ARCTIC ('ARC', ID7136, n=107), or UKCRN ADMIRE ('ADM', ID6897, n=108) immunochemotherapy trials. Inclusion into our study cohort was dependent on the presence of pre-existing data, augmented with newly generated data on a subset of patients (n=60). All patients were required to have extensive clinical and follow up data, generated from clinical trial involvement, as well as DME and TL data generated subsequently during involvement in publications. DME was investigated using previously generated pyrosequencing data (n=605) (195). Stereotype data for 86 patients enrolled in the ARC/ADM clinical trial was included in this project which was shared from Genomics England. TL was measured using both STELA (n=260) and MMQPCR (n=444) techniques, as previously reported (185,189). Of the 444 patients with MMQPCR measurements, 60 cases were newly generated using the same technique as outlined in Strefford et al (185). For the assessment of TL, established published cut-offs were employed, namely TL-S <2.92kb, TL-I 2.92–3.57kb, TL-L >3.57kb. The cohorts analysed in this project were consistent for the prevalence of an extensive panel of biomarkers compared to each entire clinical cohort, see **Supplementary Table 3 & 4**.

4.3.2 Generation of new data

Generation of TL data for a subgroup of 60 CLL4 patients using the MMQPCR technique as outlined in section 3.4.3 and was transformed into an absolute value from a relative length using a linear regression equation further described in section 5.4.2.2. This new TL data allowed these 60 patients to be included into the study as they then met the inclusion requirements.

4.3.3 Statistical and survival analysis

Statistical and survival tests were completed using Rstudio in the R environment (version 4.3.0). A Wilcoxon rank sum and chi squared test were used to test for differences between continuous (i.e. Age) and categorical variables (i.e. *IGHV* mutation status), respectively. To test associations across 18 variables an odds ratio (OR) was calculated and the Fisher's Exact test was used to evaluate the statistical significance. These statistical tests were applied in a pairwise comparison of 18 variables and the output were adjusted using the Benjamini-Hochberg method to account for multiple testing. Univariant analysis was completed using Cox regression analysis and KM plots. MVA was completed, by myself, using a Cox proportional hazard analysis. Multivariate models were built using a stepwise backward elimination process, starting with the covariates that were found significant in the univariate analysis. In an iterative process, a covariate is individually removed from the model and the two models (with and without the covariate) were compared using a likelihood ratio which assesses whether the significance of the small model is the same as the larger. Two survival endpoints of PFS and OS were used for this survival analysis. A sensitivity and specificity analysis using either a single and combined biomarker as the predictor of PFS or OS was completed. Within this analysis the likelihood ratios, accuracy, sensitivity, and specificity of each predictor was calculated. When the TL and epitype variable was used as a single predictor two of the three subgroups were combined for the analysis, for example n-CLL and i-CLL epitype were compared to the m-CLL patients. When two variables were used as a predictor, the epitype and TL groups were combined to give four unique groups, for example the epitype group n-CLL&i-CLL epitype was combined with either TL-S&TL-I or TL-L to give a group of n-CLL or i-CLL patients with TL-L. These four groups were then compared in a pairwise fashion.

4.4 Results

During statistical analysis, comparing the composition of the TL and epitype variable in the context of many other established biomarkers, the combined ARC/ADM and CLL4 cohort of 519 patients was used. However, for all analysis using survival data the ARC/ADM (n=215) and CLL4 (n=304) cohorts were kept separate as had an incomparable amount of follow up data available, see **Table 3** for the baseline clinico-biological variables of the two cohorts.

Table 3- Baseline clinico-biological variables of the ARCTIC, ADMIRE and CLL4 trials.

Variable	**ARCTIC & ADMIRE** **N (%)**	**CLL4** **N (%)**	**Concordance** **P-value**
Total number of patients	215	304	

Age, median years (range)	62 (36-80)	65 (42-86)	<0.001
Gender			
Male	167 (77.7)	229 (75.3)	0.54
Female	48 (22.3)	75 (24.7)	
Binet Stage			
A	34 (15.8)	81 (26.7)	0.013
B	107 (49.8)	129 (42.4)	
C	74 (34.4)	94 (30.9)	
IGHV Mutational Status			
IGHV-U	116/196 (59.2)	163/267 (61)	0.69
IGHV-M	80/196 (40.8)	104 /267(39)	
ATM Dysfunction			
Absent	120/156 (76.9)	184/234 (78.6)	0.159
Del11q	25/156 (16.0)	43/234 (18.4)	
Biallelic inactivation	11/156 (7.1)	7/234 (3.0)	
TP53 Aberration			
Absent	151/176 (85.8)	223/250 (89.2)	0.291
Present	25/176 (14.2)	27/250 (10.8)	
SF3B1 Mutation			
Absent	138/180 (76.7)	200/264 (75.8)	0.825
Present	42/180 (23.3)	64/264 (24.2)	
NOTCH1 Mutation			
Absent	154/180 (85.6)	226/265 (85.3)	0.936
Present	26/180 (14.4)	39/265 (14.7)	
Epigenetic Subgroup			
n-CLL	102 (47.4)	159 (52.3)	0.0068
i-CLL	61 (28.4)	104 (34.2)	
m-CLL	52 (24.2)	41 (13.5)	
Telomere Length Group			
Short	48 (22.3)	158 (52)	<0.001
Intermediate	59 (27.4)	80 (26.3)	
Long	108 (50.2)	66 (21.7)	

Telomere Length, median length kb (range)	3.66 (1.13-7.68)	2.91 (1.93-10.86)	<0.001

Footnote: Continuous variables were summarised as median and range and categorical variables as proportions. The denominator for the percentages reported represented the number screened for each of the features in the respective cohorts. For example CLL4 cohort had 27 patients with TP53 dysfunction out of 250 patients who were screened for it (10.8%). Concordance across the two cohorts groups was tested using Wilcoxon rank sum and chi squared tests for continuous and catagorical variables respectively. P-value<0.01 indicated a statistically signficant difference between the variable interogated across the two cohort groups.

4.4.1 DME and TL are strongly associated with each other and with established clinical biomarkers

Firstly, associations between the two biomarkers of interest were established with a strong association being found between the two variables. A significant difference in TL was found across all DME groups (p<0.01). For example, 73% of m-CLL patients also had TL-L, whereas only 18% of n-CLL patients had TL-L (**Figure 23**). Conversely when studying the three TL groups there was a significant difference in epitype composition with TL-L and TL-S or TL-I (p-value<0.001). Unlike TL-L, TL-S and TL-I constituted majority of n-CLL epitype, 63% and 60%, respectively. TL-S and TL-I also had few patients with the m-CLL epitype. Whereas the TL-L group included 28%, 33%, and 39% of n-CLL, i-CLL, and m-CLL patients, respectively. Assessing the relationship between epitype and TL as a continuous variable found a significant difference (p-value<0.01) in TL across the three

epitype group. The m-CLL group (median:4.17 kb) had the greatest TL length, followed by i-CLL (median:2.94 kb), and n-CLL having the shortest (median:2.78 kb), see **Supplementary Figure 1**.

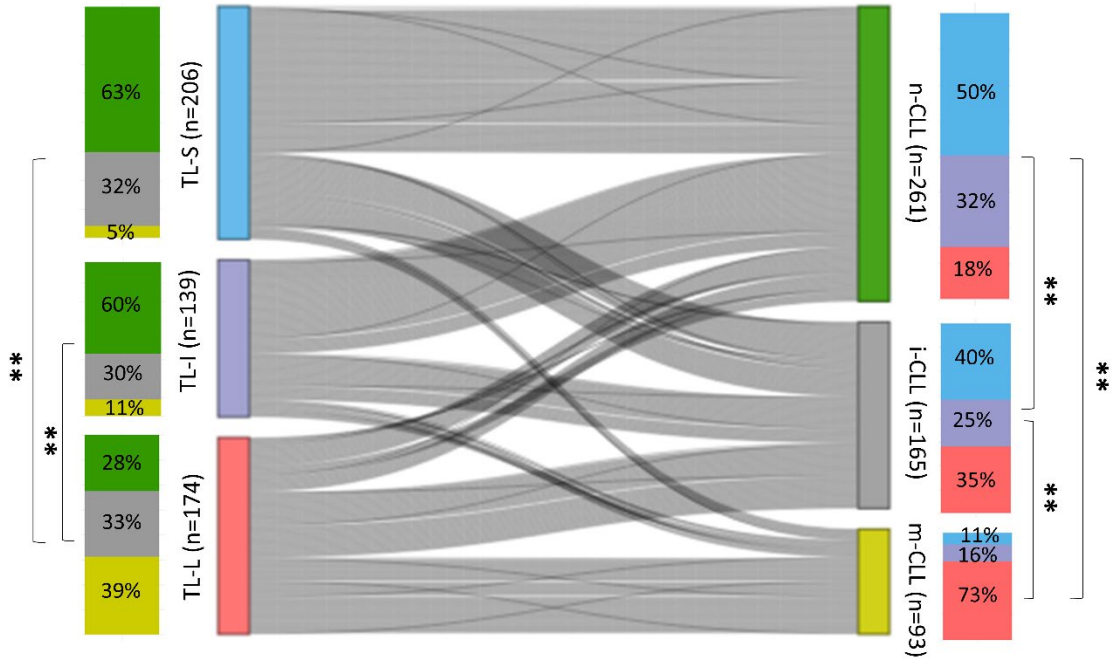

Figure 23- Sankey plot showing the relationship between epitype and TL subgroups surrounded by stacked bar charts showing the percentage of each epitype groups within each telomere length group, and vice versa. The three epitype type groups are shown in green, grey and yellow for n-CLL, i-CLL and m-CLL epitype, respectively. The telomere length groups are shown in blue, purple, and red for short, intermediate, and long, respectively. A chi squared test was employed to examine the difference across the three stacked bar charts, p-value<0.01 is indicated by two asterisks (**).

Next, we assessed these novel biomarkers in the context of established CLL biomarkers using an association plot. Similar to the Sankey plot in **Figure 23**, which showed that 63% of TL-S cases had a n-CLL epitype and 73% of m-CLL patients had TL-L, a significant co-occurrence between n-CLL and TL-S as well as m-CLL and TL-L was found in the association plot (p-value<0.01). Across the three TL and epitype groups a significant difference in *IGHV* mutation status was observed (p-value<0.01). Whilst TL-S, TL-I and the n-CLL group co-occurred with an unmutated *IGHV* status, TL-L, i-CLL and m-CLL patients were associated more with a mutated *IGHV* status (**Figure 24**). Assessing the relationship between *TP53* aberration, a poor risk factor, and TL or epitype, a significant co-occurrence was found with TL-S (p-value<0.01) and n-CLL (p-value<0.05) patients. Specifically, of the 52 *TP53* aberration cases reported, 34 (65%) of them occurred in patients with TL-S and 34 (65%) occurred in n-CLL patients. Furthermore, 23/52 TP53 aberration cases have both TL-S and a n-CLL epitype. Additionally, a significant negative correlation was found between *TP53* aberration and TL-L (p-value<0.01). Further poor risk factors, such as del11q events (p-

value<0.05) and IGLV3-21^{R110} mutations (p-value<0.05) were significantly associated with the TL-S group. However, only del11q events were positively associated with the n-CLL epitype, as the IGLV3-21^{R110} mutation had a significant degree of mutually exclusivity with n-CLL (p-value<0.01) and the m-CLL epitype (p-value<0.05). Instead, this mutation was strongly associated with the i-CLL epitype (p-value<0.01). The presence of a good risk factor, del13q, was associated with the TL-L and m-CLL group and negatively associated with the TL-I and n-CLL groups. Specifically of the 93 m-CLL patients, 47% (44/93) also had a del13q event and 75 of the 174 (43%) TL-L patients had a del13q event.

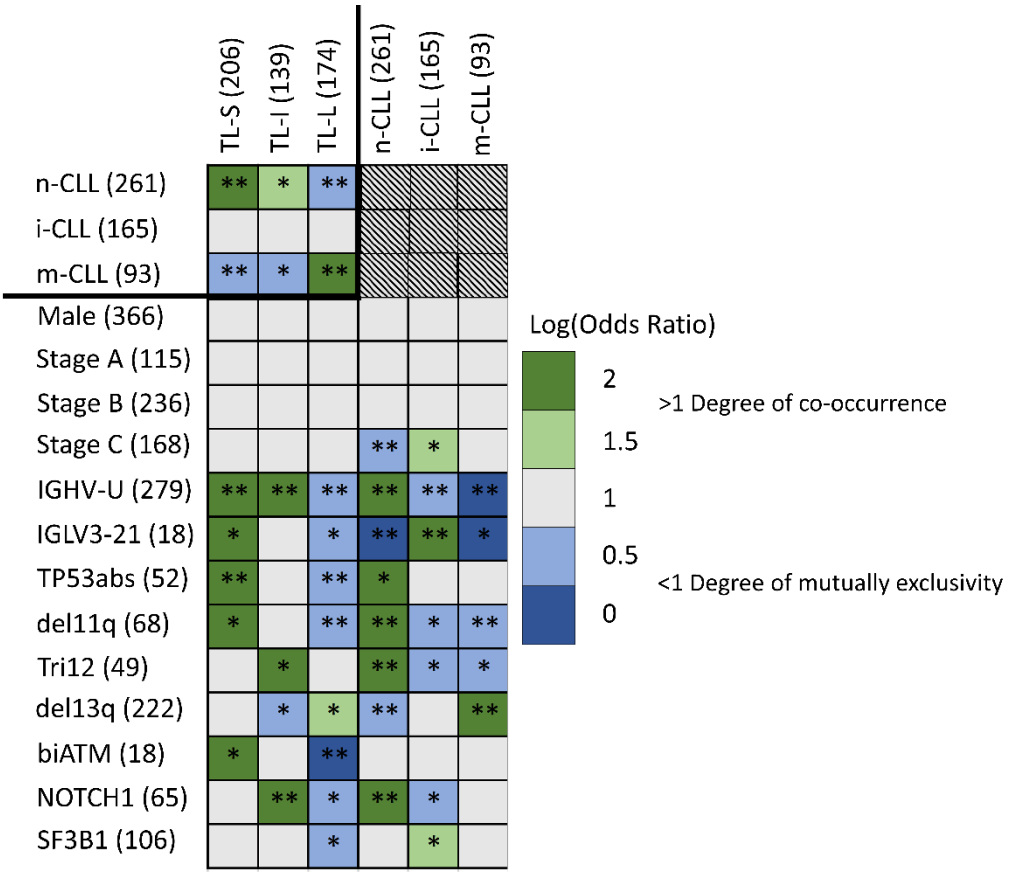

Figure 24- Association plot presenting an odds ratio (OR) that is calculated for each pairwise comparison of 18 variables. An OR with a p<0.05 (Fisher's exact test) is shown by an asterisk (*), an OR with a p<0.01 is shown by two asterisks (**). A blue coloured square indicates an OR<1 and therefore the two variables are negatively associated, whereas a green square indicates an OR>1 and therefore the two variables are positively associated. The hashed-out boxes indicate a pairwise comparison of the epitype variable.

4.4.2 IGLV3-21^{R110} mutation cases are prevalent in i-CLL patients.

The investigation of the sub cohort of 86 cases with stereotype data available identified, as previously reported, an enrichment of IGLV3-21^{R110} mutations in the i-CLL epitype patients (n=13)

which account for 93% of the IGLV3-21^{R110} mutations recorded. A further IGLV3-21^{R110} mutation was identified in a n-CLL patient, however none were found in the m-CLL epitype, see **Supplementary Figure 2**. Due to having a limited stereotype dataset, only a cohort of 14 IGLV3-21^{R110} mutated cases was available. Therefore, downstream analysis was restricted so the survival impact of this variable was not able to be investigated within this project, however the biological context of these cases was able to be examined. When ascertaining where the IGLV3-21^{R110} mutations occurred in the context of TL groups, a significant difference (p-value<0.01) in TL was found across the mutated and wild type group (**Supplementary Figure 3**). Specifically, the IGLV3-21^{R110} mutated cases were mainly composed of TL-S patients (58%) instead of TL-I (21%) and TL-L (21%). Additionally, the median TL in IGLV3-21^{R110} wild type patients was greater (median:3.7kb) than the IGLV3-21^{R110} mutated patients (median:2.8 kb). To further investigate the composition of the IGLV3-21^{R110} mutated patients a heatmap was constructed, containing further variables reported to be associated with this mutation. This highlighted again the enrichment of IGLV3-21^{R110} mutated patients in the i-CLL epitype (see **Figure 25** and **Supplementary Figure 2**). Similarly to published work, the 11 IGLV3-21^{R110} mutated patients included in the heatmap showed varied IGHV status with 3 and 8 cases of U-CLL and M-CLL, respectively. Interestingly, there were no events of *TP53* aberration and IGLV3-21^{R110} mutants, both in the wider cohort of 14 patients with IGLV3-21^{R110} mutation or in the cohort of 66 patients which included 11 cases of IGLV3-21^{R110} mutants. Conversely, 5 of the IGLV3-21^{R110} mutated patients also had an *ATM* mutation, accounting for 35% of the *ATM* mutation identified in this analysis of 66 ARC/ADM patients used in **Figure 25**. Similarly, of the 12 *SF3B1* mutation reported in this cohort, a third were present in a IGLV3-21^{R110} mutated patient (n=4). Conversely of the 14 IGLV3-21^{R110} mutated cases, none were found to also have a *NOTCH1* mutation which does not match current published findings, however this could be a limitation of the cohort size. Expanding the BRC stereotype dataset for this clinical trial cohort would also allow the IGLV3-21^{R110} mutation variable to be included in survival analysis completed below.

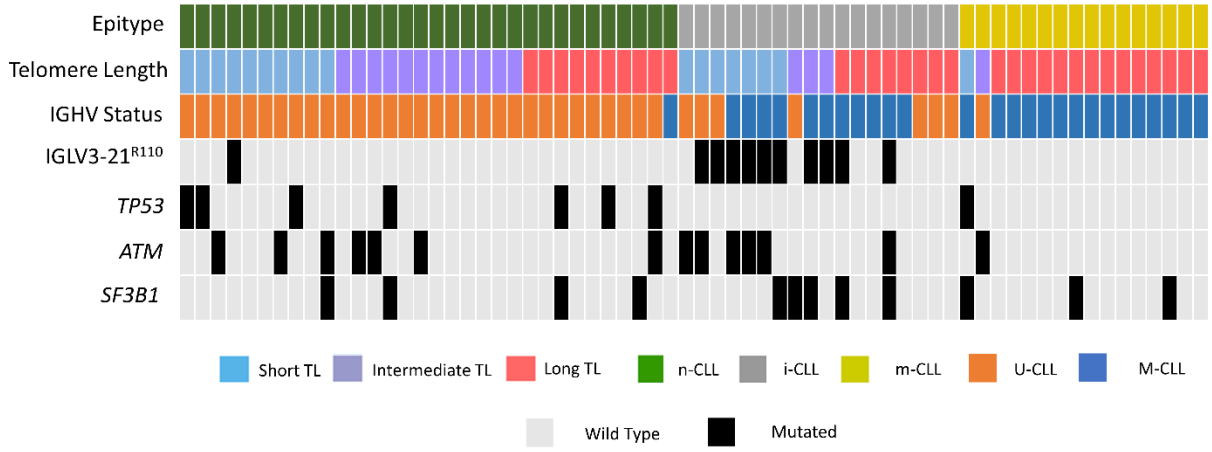

Figure 25- A heatmap describing the prevalence of IGLV3-21^{R110} mutation its association with established biomarkers. Cohort of 66 patients from the ARC/ADM clinical trial that had data for all 7 variables was used. The three epitype and TL groups are included. *IGHV* mutation status, *TP53* aberration, *ATM* and *SF3B1* mutations are also shown.

4.4.3 Both TL and DME have a significant impact on PFS and OS in a univariate analysis

To verify the impact of each clinico-biological variable, including DME and TL, on PFS and OS we first completed a univariate analysis on a separate CLL4 (n=304) and ARC/ADM (n=215) cohort. A total of 11 variables were examined in the univariate analysis in both cohorts, these variables were chosen to be included in the univariate analysis based on current published CLL literature. An additional variable of IGLV3-21^{R110} mutation was also included in the ARC/ADM univariate analysis, using the cohort of 86 patients that had this data available. The variable *ATM* dysfunction was coded to include biallelic (Bi*ATM*), which are patients with both a deletion and mutation of the *ATM* gene, del11q and wild type patients. *TP53* aberration (*TP53*ab) was classified as the presence of mutation of *TP53* and/or del17p event. The treatment arm patients were enrolled onto was also included in the analysis as a covariate. The median PFS and OS for the CLL4 cohort is 2.3 years (Range: 0-10.1 years) and 6.05 years (Range: 0.1-17.4 years), respectively. Whereas the median PFS and OS for the ARC/ADM cohort is 4.8 years (Range: 0.02-9 years) and 6.5 years (Range: 0.02-9.1 years), respectively.

4.4.3.1 Discovery survival cohort of 304 CLL4 clinical trial patients

Both covariates, TL and epitype, were significant in the PFS and OS univariate analysis. KM analysis found a significant difference in PFS across the three epitype groups, see **Figure 26A**. A pairwise log rank test found a significant difference (p-value<0.01) in PFS with the n-CLL (median: 2 years) have a significantly poorer PFS than i-CLL (median: 3 years) or m-CLL patients (median: 2.8 years). From the KM plot, the percentage of cases with no progression event at 5 years was 14%, 25% and 27% for n-CLL, i-CLL and m-CLL patients, respectively. The pairwise log rank test in

the KM analysis identified that m-CLL patients (median: 9.8 years) had a significantly (p-value<0.01) greater OS than compared to n-CLL (median: 5.6 years) or i-CLL patients (median: 5.8 years) (**Figure 26B**). The m-CLL also had a greater 10-year survival of 46% compared to 15% of n-CLL and 25% of i-CLL patients.

KM plots of the three TL groups identified the TL-L (median PFS&OS: 3.85 and 9.65 years) as having a significantly (p-value<0.01) better PFS and OS compared to the TL-I (median PFS&OS: 2.35 and 6 years) and TL-S (median PFS&OS: 1.95 and 4.95 years), see **Supplementary Figure 4**. At 5 years, 39% of patients with TL-L had not progressed, whereas only 10% and 21% of TL-S and TL-I had not progressed. Similarly, the 10-year survival rate was only 15% and 19% for TL-S and TL-I patients, respectively, compared to 47% of TL-L patients.

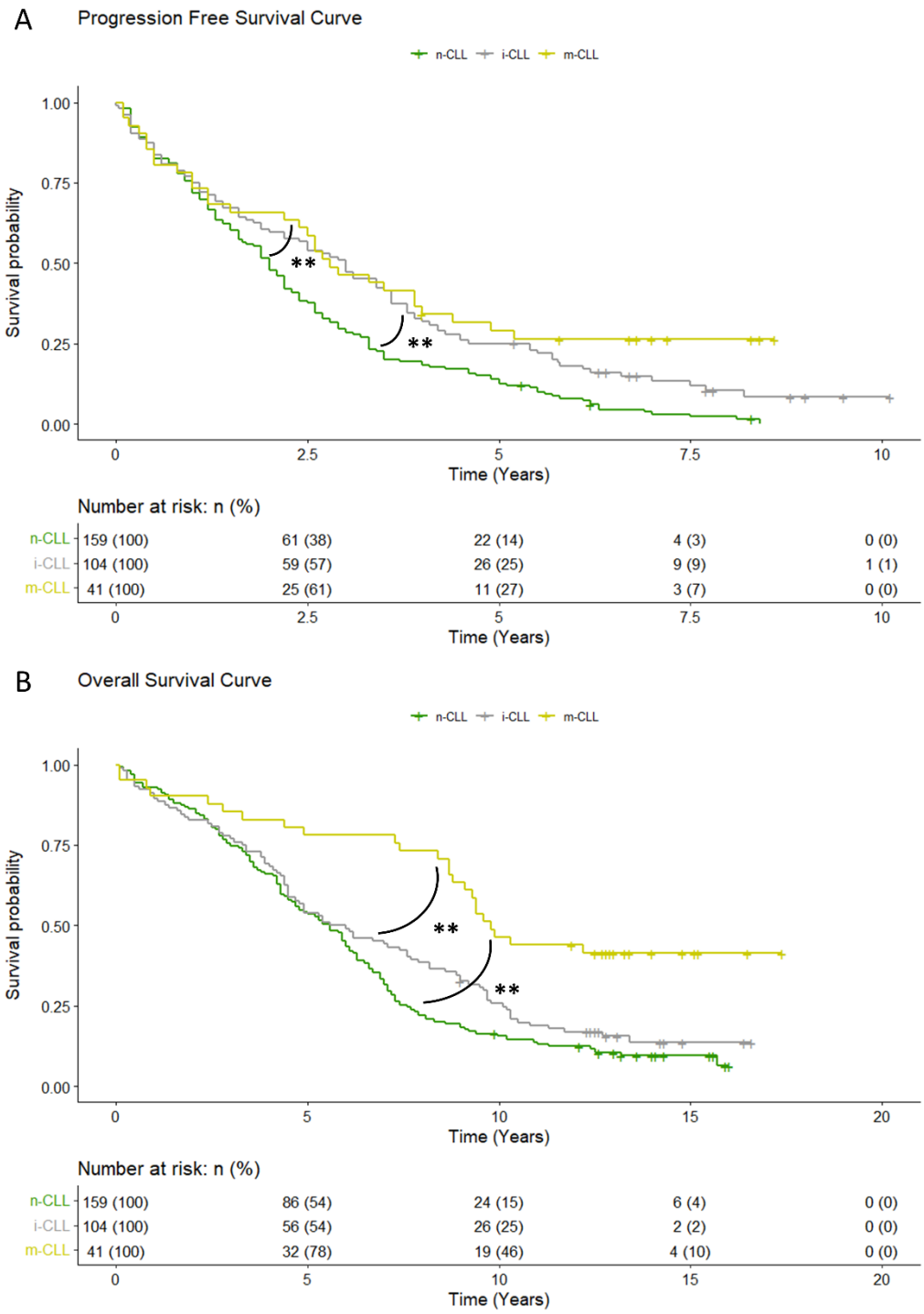

Figure 26- Kaplan-Meier plot of the three epitype groups for PFS (A) and OS (B) for the cohort of 304 CLL4 patients. A pairwise log rank test was employed to compare survival plots, p-value<0.01 is indicated by two astericks (**). The table shows the number and percentage of cases in each epitype group that have not had an event, i.e progressed or died, at a point in time. The number of PFS events for the n-CLL, i-CLL and m-CLL patients was 157/159, 92/104 and 30/41, respectively. The number of OS events for the n-CLL, i-CLL and m-CLL patients was 144/159, 88/104 and 24/41, respectively.

Of the 11 variables analysed in the cox regression univariate analysis, the most powerful predictor of survival was *TP53* aberration, which indicated an increased risk of progression (HR: 3.61, 95%CI: 2.39 to 5.44, p-value<0.001) and death (HR: 3.66, 95%CI: 2.4 to 5.57, p-value<0.001). Patients with *TP53* disruption had a shorter PFS (median: 0.3 v.s 2.5 years) and OS (median: 1.5 vs. 6.3 years) compared to patients without. Similar to the KM analysis, the TL-S (HR: 2.36, 95%CI: 1.7 to 3.29) and TL-I group (HR: 1.81, 95%CI: 1.26 to 2.6) had a significantly (p-value<0.001) poorer PFS compared to the TL-L, which was used as the reference. This trend was also found in OS with a significantly (p-value<0.001) shorter OS being shown in TL-S (HR: 2.66, 95%CI: 1.87 to 3.76) and TL-I (HR: 2.11, 95%CI: 1.43 to 3.12) groups compared to TL-L, see **Figure 27**. PFS univariate analysis of the DME variable found there was a significant difference between m-CLL, the reference, and n-CLL (p-value<0.001) but not between m-CLL and i-CLL (p-value>0.05). The n-CLL patients were reported to have nearly double the risk of progressing than m-CLL patients (HR: 1.96, 95%CI: 1.32 to 2.9). Other covariates that were significant in predicting a poorer PFS are patients with a biallelic *ATM* dysfunction compared to *ATM* wild type patients, and U-CLL patients compared to M-CLL. Specifically, the median PFS of patients with biallelic *ATM* inactivation was 1.47 compared to 3.02 years of wild type patients (HR: 2.42, 95%CI: 1.12 to 5.2, p-value<0.05). Median PFS of 163 U-CLL cases was 1.9 years compared to 3.4 years for 104 M-CLL patients (HR: 2, 95%CI: 1.5 to 2.6, p-value<0.001) (**Figure 27**). Additionally, the treatment arm patients were enrolled in was found to be significant (p-value<0.001) in PFS univariate analysis, with the FC treated (HR: 0.54, 95%CI: 0.4 to 0.73, median: 3.84 years) patients have a greater PFS compared to the FDR treatment arm (median: 2.36), which was used as the reference group.

After *TP53* aberration, DME emerged as the second greatest predictor of OS with a reported HR of 2.8 and 2.2 for the n-CLL and i-CLL epitype, see **Supplementary Table 5 and 6**. Both n-CLL and i-CLL epitype had a significantly (p-value<0.001) shorter OS compared to m-CLL patients (median: 5.6, 5.8 and 9.8 years, respectively). 91% of n-CLL and 85% of i-CLL experienced an OS event compared to 59% of m-CLL patients. The univariate analysis of the TL covariate using OS endpoint found a significant (p-value<0.001) difference between TL-L and TL-S and TL-I, **Figure 27**. Both TL-S and TL-I patients have over double the risk of death compared to patients with TL-L with a reported HR of 2.66 and 2.11, respectively. The *IGHV* mutation status covariate also was significant in predicting OS, with U-CLL having a greater risk of death than M-CLL patients (HR: 2.3, 95%CI: 1.73 to 3.06, p-value<0.001). The presence of *SF3B1* mutation (median:4.6 years) was found to predict a shorter OS compared to wild type (median: 6.95 years) patient (HR:1.77, 95%CI:1.31 to 2.38, p-value<0.001). Median survival of the subgroups within the *ATM* dysfunction covariate was 4.93, 5.3, and 7.04 years for the biallelic, del11q and wild type patients. However, only a significant difference in OS between patients with a del11q event compared to wild type patients was

reported (HR: 1.65, 95%CI: 1.16 to 2.34, p-value<0.01). This suggests that patients with a del11q event have over a 50% increase in risk of death compared to wild type patients. Age, as a continuous variable, was also a significant covariate (p-value<0.001) in OS, with increased age predicting a shorter OS (HR: 1.05, 95%CI: 1.04 to 1.07), see **Figure 27**. Of the 13 covariates included, only 8 were significant in either/or the PFS or OS univariate analysis using this discovery cohort. These were as follows; *TP53* aberration (*TP53*ab), *ATM* dysfunction, TL, *IGHV* mutation status, epitype, treatment arm, *SF3B1* mutations, and age.

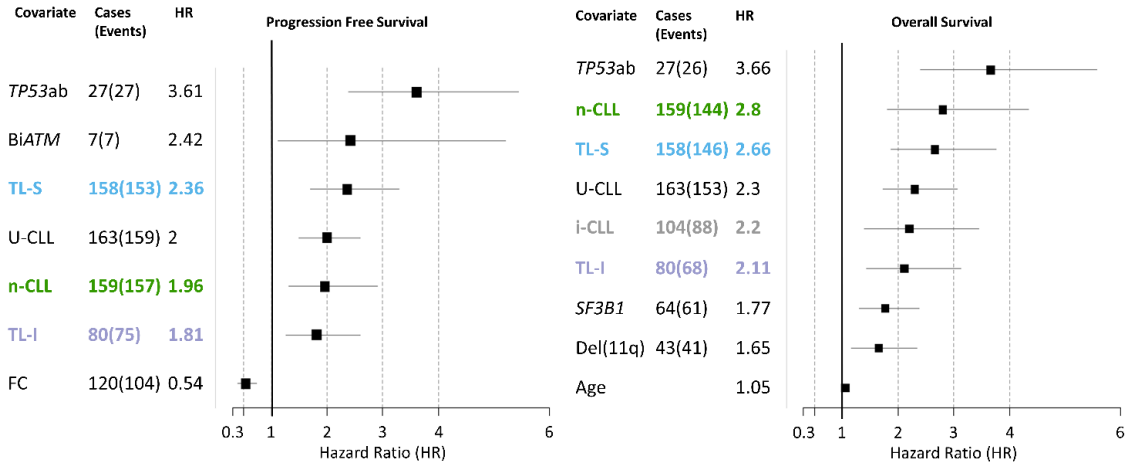

Figure 27- Forest plot including the variables that were significant in the univariant analysis using PFS and OS when using the 304 CLL4 cohort. The TL and epitype subgroups are coloured and shown in bold. For each covariate, number of cases, number of events and the hazard ratio is stated.

4.4.3.2 Validation survival cohort of 215 ARCTIC and ADMIRE clinical trial patients.

Within the univariate analysis both TL and DME variables were significant in predicting PFS and OS. KM analysis using a pairwise log rank test of the three DME groups identified a significant (p-value<0.01) difference in PFS between all the groups. KM plot shows that n-CLL (median: 3.87) patients had a significantly shorter PFS than i-CLL (median: 5.45 years) or m-CLL (median: 6.93 years) patients, **Figure 28A**. Additionally, a significant difference (p-value<0.01) was identified between the i-CLL and m-CLL patients, with the latter group having a greater PFS. After 5 years, 34% of n-CLL patients, 54% of i-CLL patients and 71% of m-CLL patients had not progressed. KM analysis of OS across the three epitype groups only found a significant difference (p-value<0.01) between n-CLL (median: 6 years) and m-CLL (median: 7.03 years) patients, each group had a 5-year survival of 65% and 83%, respectively **Figure 28B**. I-CLL patients had a median survival of 6.74 years and a 5-year survival rate of 75%.

The KM analysis, including a pairwise log rank test of the three TL groups showed a significant difference in PFS, with the TL-L group having a greater PFS than TL-S or TL-I (p-value<0.01), **Figure**

29A. The median PFS for the three TL groups was 3.84, 4.05 and 6.06 years for TL-S, TL-I and TL-L. After 5 years, 33% and 32% of TL-S and TL-I cases had not progressed, however 65% of TL-L had not progressed after 5 years. KM analysis of OS also found a significant difference between the TL groups. However, only a significant (p-value<0.05) difference in survival was found between TL-L (median: 6.99 years) and TL-S (median: 5.8 years) and not with the TL-I group (median: 6.28 years), **Figure 29B**. The 5-year survival for the three TL group was 60%, 69% and 79% for TL-S, TL-I and TL-L, respectively.

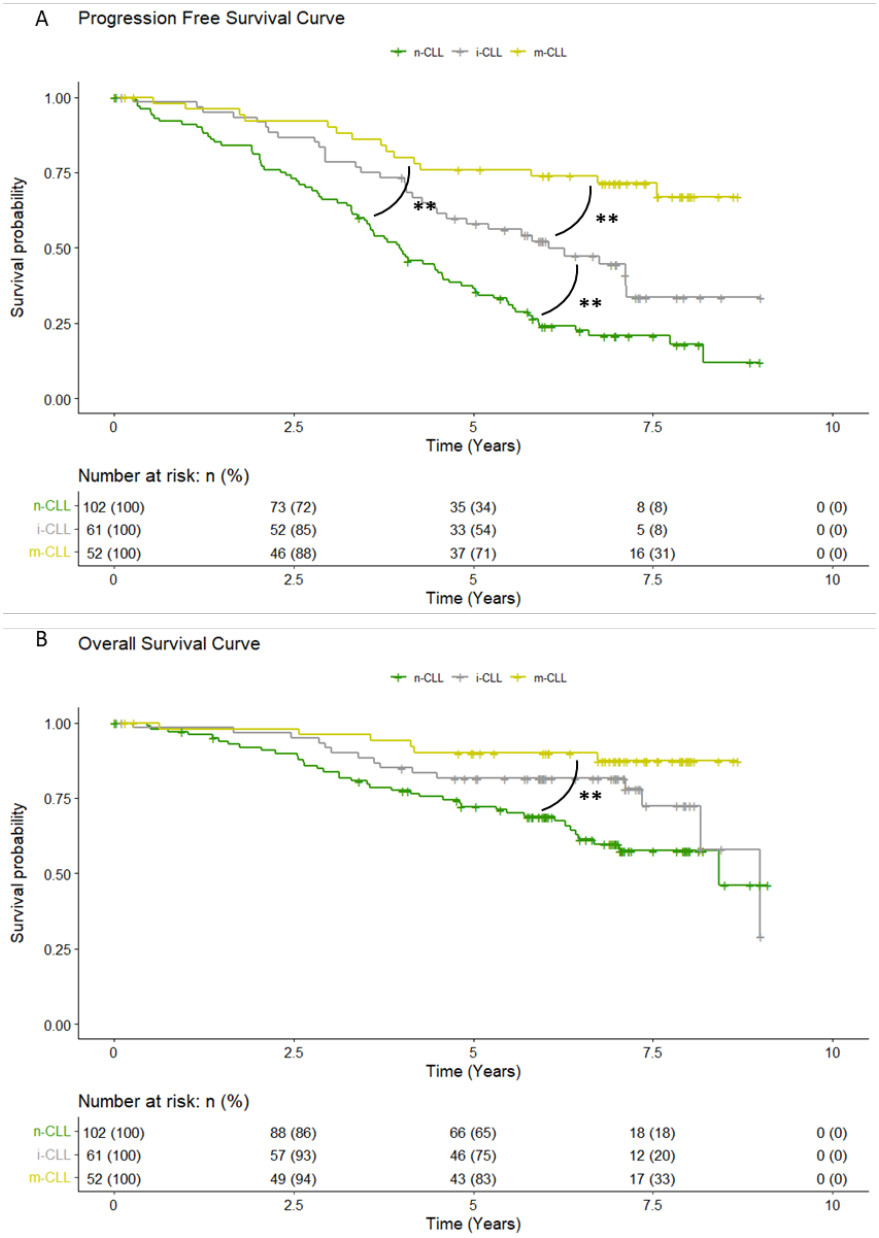

Figure 28- Kaplan-Meier plot of the three epitype groups for PFS (A) and OS (B) for the cohort of 215 ARC/ADM patients. A pairwise log rank test was employed to compare survival plots, p-value<0.01 is indicated by two astericks (**). The table shows the number and percentage of cases in each epitype group that have not had an event, i.e progressed or died, at a point in time. The number of PFS events for the n-CLL, i-CLL and m-CLL patients was 78/102, 34/61 and 15/52, respectively. The number of OS events for the n-CLL, i-CLL and m-CLL patients was 38/102, 15/61 and 6/52, respectively.

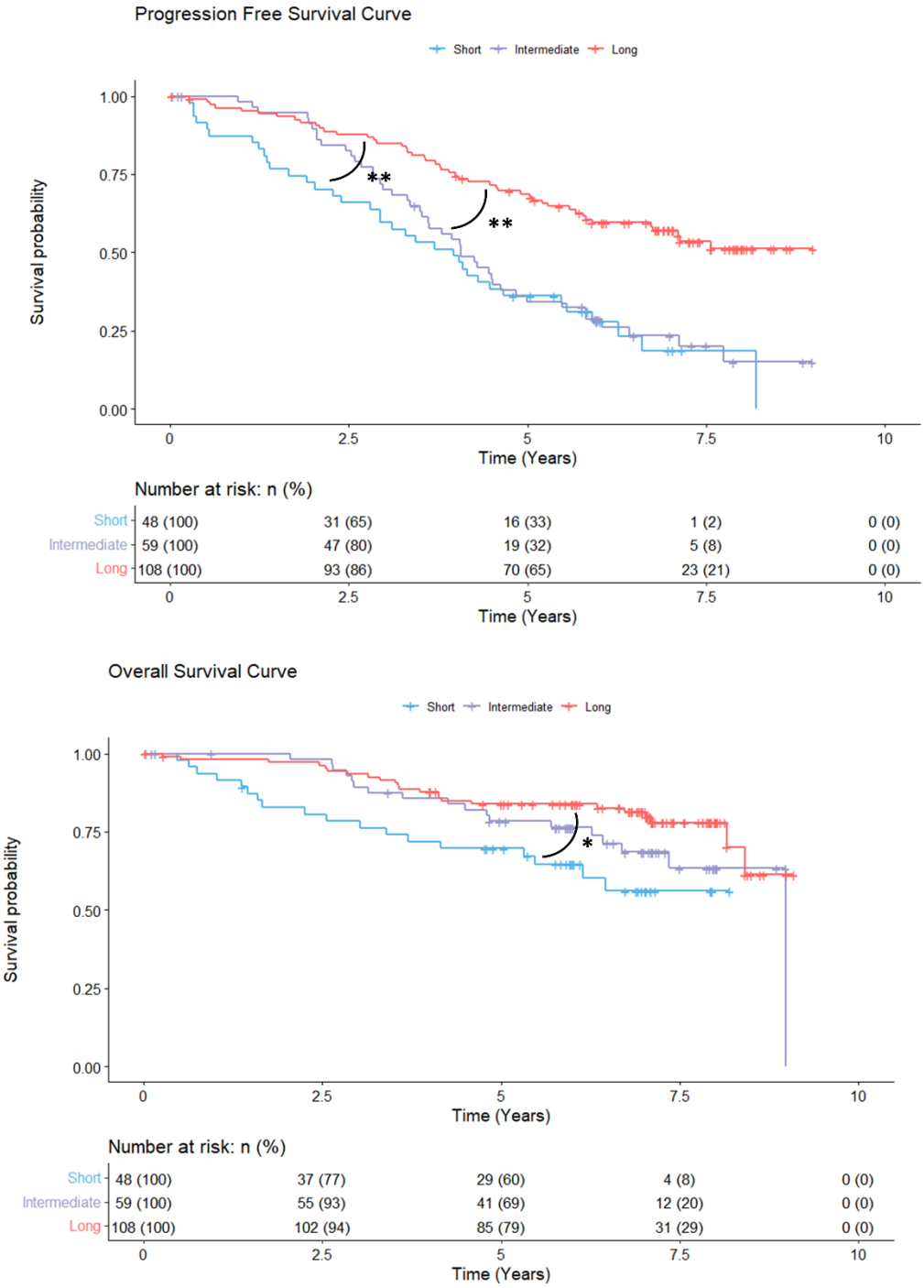

Figure 29- Kaplan-Meier plot of the three TL groups for PFS (A) and OS (B) for the cohort of 215 ARC/ADM patients. A pairwise log rank test was employed to compare survival plots, p-value<0.05 is indicated by an asterick (*) and a p-value<0.01 is indicated by two astericks (**). The table shows the number and percentage of cases in each epitype group that have not had an event, i.e progressed or died, at a point in time. The number of PFS events for the TL-S, TL-I and TL-L patients was 36/48, 44/59 and 47/108, respectively. The number of OS events for the TL-S, TL-I and TL-L patients was 18/48, 18/59, and 23/108, respectively.

Of the 12 covariates included in the cox regression univariate analysis, the DME was found to be the strongest predictor of PFS and OS. Specifically, n-CLL patients had a significantly shorter PFS

and OS compared to m-CLL patients. For PFS, the n-CLL patients had over four times the risk of progressing than the reference group, m-CLL epitype (HR: 4.47, 95%CI: 2.56 to 7.82, p-value<0.01), see **Figure 30**. i-CLL patients also had a significantly poorer PFS compared to m-CLL patients (HR:2.4, 95%CI: 1.3 to 4.41, p-value<0.001). Across the three epitype groups, 77% of n-CLL, 56% of i-CLL and 16% of m-CLL patients progressed during follow up. Other covariates that had a significant impact of PFS included *TP53* aberration (HR: 4.39, 95%CI: 2.69 to 7.17, p-value<0.001) with patients with a *TP53* aberration (median: 2.09 years) have a poorer PFS than patients without (median: 5.45 years), see **Supplementary Table 7**. The covariate *ATM* dysfunction was also significant, with both biallelic (median: 3.36 years) and del11q (median: 3.82 years) patients having a significantly (p-value<0.001) shorter PFS compared to wild type patients (median: 4.98 years). TL was also significant in the PFS univariate analysis, TL-S (median: 3.84 years) and TL-I (median: 4.05 years) had significantly shorter PFS compared to TL-L (median: 6.06 years), the reference group. Patients with TL-S have nearly 3 times high risk of progressing than TL-L (HR: 2.87, 95%CI: 1.85 to 4.46, p-value<0.001). Similarly, TL-I patient had double the risk of progressing than TL-L patients (HR: 2.45, 95%CI: 1.62 to 3.71, p-value<0.001). Across the three TL groups 75% of TL-S, 75% of TL-I and 44% of TL-L had progressed during the clinical trial follow up. Finally, *IGHV* mutation status had a significant (p-value<0.001) difference in PFS, U-CLL patients had a poorer PFS (median:4.09 years) compared to M-CLL (median: 6.76 years) patients (HR: 2.76, 95%CI:1.81 to 4.21).

As mentioned above, the epitype covariate was significant in the OS univariate analysis. n-CLL patients have a significantly shorter OS compared to m-CLL patients (HR: 3.95, 95%CI: 166 to 9.35, p-value<0.05), **Figure 30**. Across the three epitype groups, 37% of n-CLL, 25% of i-CLL and 12% of m-CLL have died within the follow up period. The univariant analysis did not find a significant difference in OS between the i-CLL (median: 6.74 years) and m-CLL (median: 7.03 years) groups. TL was also significant in the univariate analysis, with TL-S patients having a significantly shorter OS compared to TL-L patients (HR: 2.56, 95%CI: 1.37 to 4.79, p-value<0.05) but no significant difference between TL-I and TL-L was found (p-value>0.05). A further significant covariate was *TP53* aberration (HR: 3.77, 95%CI:1.94 to 7.33, p-value<0.001), as patients with *TP53* aberration (median: 3.62 years) had a shorter OS compared to patients without (median: 6.83 years). U-CLL patients were found to have a significantly poorer OS compared to M-CLL patients (median: 6.05 vs. 6.99 years, p-value<0.05) and the reported HR of this covariate was 1.81 (95%CI: 1.01 to 3.26). Finally, age also was significant in the OS univariate analysis (HR: 1.04, 95%CI: 1.01 to 1.07, p-value<0.05) this shows that as a patients age at diagnosis increases OS decreases, see **Supplementary Table 8**. From the univariate analysis which included 12 covariates, 6 were found to be significant in predicting PFS or OS in this validation cohort. These were as follows; *TP53*

aberration (*TP53*ab), *ATM* dysfunction, TL, *IGHV* mutation status, epitype, and age. The presence of a IGLV3-21^{R110} mutation was not found to impact either PFS (median: 4.53 vs. 4.38 years) or OS (median: 6.95 vs. 6.55 years) in the univariate analysis of the ARC/ADM cohort.

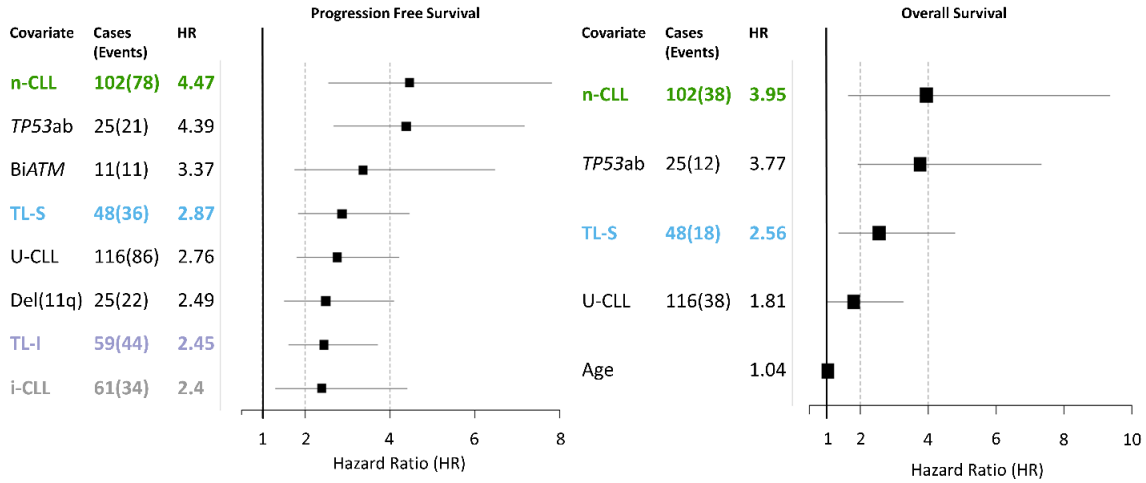

Figure 30- Forest plot including the variables that were significant in the univariant analysis using PFS and OS when using the 215 ARC/ADM cohort. The TL and epitype subgroups are coloured and shown in bold. For each covariate, number of cases, number of events and the hazard ratio is stated.

4.4.3.3 I-CLL cases can be further stratified by TL in univariate analysis.

To further investigate survival trends, I completed a subgroup analysis across different metrics, in particular TL and DME, whereby patients in one TL subgroup were stratified by epitype and vice versa. Because the i-CLL epitype was identified to have survival outcomes somewhere between these two previously reported good and bad survival trends of the n-CLL and m-CLL epitype, we wanted to see if TL could identify clinically relevant subgroups within i-CLL patients. It was found that the i-CLL only ARC/ADM patients could be further stratified by TL (p-value<0.01), with the TL-L group predicting a greater PFS (median PFS: 6.12 years) compared to TL-S (median PFS: 3.8 years) or TL-I (median PFS: 4.35 years), **Figure 31**. Additionally, within the TL-L only ARC/ADM patients the n-CLL indicated a significantly shorter PFS (p-value<0.01) and OS (p-value<0.05), see **Supplementary Figure 5**. These survival trends were also found when assessing i-CLL and TL-L only patients in the CLL4 cohort.

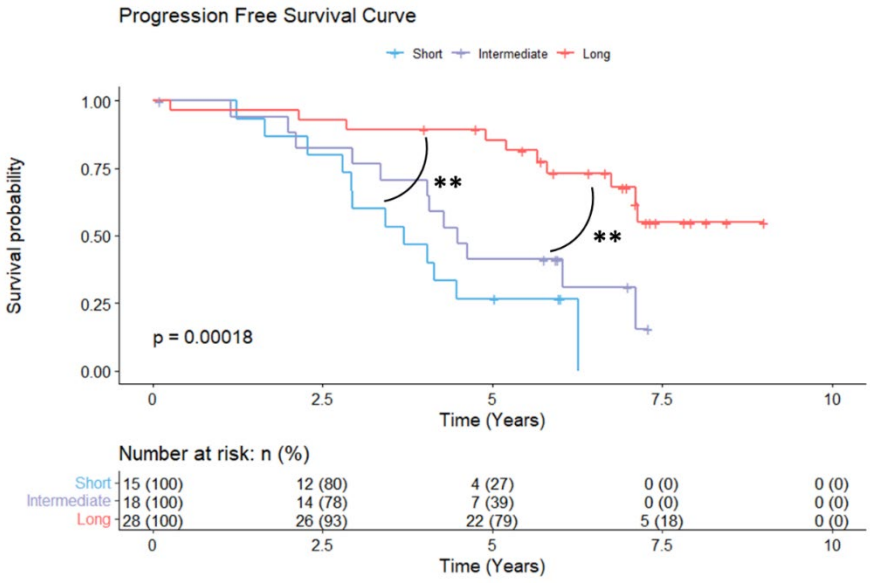

Figure 31- Kaplan-Meier plot of the three TL groups for PFS using the cohort of 61 ARC/ADM patients with a i-CLL epitype. A pairwise log rank test was employed to compare survival plots, p-value<0.01 is indicated by two astericks (**). The table shows the number and percentage of cases in each epitype group that have not had an event, i.e progressed or died, at a point in time. The number of PFS events for the TL-S, TL-I and TL-L patients was 12/15, 12/18 and 10/28, respectively.

4.4.4 Both TL and epitype are independently significant in PFS and OS in chemo(immuno-) therapy treated CLL patients

A multivariate Cox regression was used to examine the impact of epitype and TL on PFS and OS while also controlling for confounding variables. The eight covariates that were found to be significant in the univariant analysis were included in the MVA. The eight covariates that were included in the first model were TL, epitype, *TP53* aberration, *ATM* dysfunction, *IGHV* mutation status, age, *SF3B1* mutation and treatment arm. The variable *ATM* dysfunction was coded to include biallelic, which are patients with both a deletion and mutation of the *ATM* gene, del11q and wild type patients. Starting the same 8 covariates, a stepwise backwards elimination process was applied whereby the least significant variable was removed. Before the least significant variable could be removed from the first model to create the second model, a likelihood ratio was calculated to compare the two models to prove that removing the variable would not impact the significance of the model. This process was repeated until a final model was reached that contained variables that all significantly impacted survival. The final CLL4 PFS model was based on 246 cases with 221 events whereas the OS model was based on 246 cases with 205 events. The final ARC/ADM PFS model was based on 138 cases and 86 events whereas the OS model was based on 176 cases and 45 events.

Within the two final PFS models the TL-S category could independently predict a poorer PFS in both cohorts (CLL4 HR: 2.14, 95%CI: 1.39 to 3.3, p-value<0.001, ARC/ARM HR: 2.18, 95%CI: 1.17 to 4.05, p-value<0.01), see **Figure 32**. Whilst the TL covariate remained in both final PFS models, it was only the TL-S subgroup that had a significant impact on PFS and TL-I was found to not impact survival (CLL4 HR: 1.42, 95%CI: 0.9 to 2.25, p=0.13, ARC/ARM HR: 0.92, 95%CI: 0.51 to 1.66, p-value=0.78). Within the CLL PFS final model, DME remained in the model with both n-CLL and i-CLL predicting a significantly shorter PFS. n-CLL patients had over twice the risk of progressing than m-CLL patients, as indicated by the HR of 2.35 (95%CI: 1.37 to 4.05, p-value<0.01), see **Figure 32**. Whilst the DME covariate remained in the final PFS CLL4 cohort, this covariate did not remain in the ARC/ADM PFS model. Additional covariates that retained independent importance for PFS in the CLL4 cohort included *TP53* aberration, *SF3B1* mutations and treatment arm, see **Supplementary Table 9**. In fact, the highest increase in risk of progression was for patients with *TP53* aberration. Patients with *TP53* aberration were nearly at 4 times higher risk of progressing if they had *TP53* aberration than if they did not (HR: 3.38, 95%CI: 2.13 to 5.37, p-value<0.001) which greatly impacted the median survival of the cases with *TP53* aberration (median: 0.3 vs. 2.5 years). The presence of a S*F3B1* mutation was found to have an independent negative impact on PFS, with patients with this mutation having a 50% increase in risk of progression than wild type patients (HR: 1.55, 95%CI: 1.13 to 2.13, p-value<0.01). Finally, CLL4 patients in the treatment arm FC had a significantly longer PFS compared to patients treated with FDR (HR: 0.47, 95%CI: 0.33 to 0.68, p-value<0.001). Within the validation cohort of 215 ARC/ADM patients, TL retained independences in the final PFS model, as detailed above, however the epitype variable was removed as did not reach significant level (p-value>0.05)**.** Additional covariates that were independent markers of PFS included *TP53* aberration, *ATM* dysfunction, and *IGHV* mutation status, see **Supplementary Table 9 and 11**.

When assessing the multivariate OS models across the two cohorts, the epitype covariate retained independence in both. Specifically, n-CLL patients in the CLL4 cohort had two times the risk of death than m-CLL patients (HR: 2.07, 95%CI: 1.15 to 3.73, p-value<0.05). The n-CLL patients in the ARC/ADM cohort had a more than three times the risk of death than m-CLL patients (HR: 3.4, 95%CI: 1.14 to 10.12, p-value<0.05) and was the strongest predictor of death in this model, see **Figure 32**. Similarly, the TL covariate also remained in both the final CLL4 and ARC/ADM OS model. CLL4 patients with TL-S had a significantly poorer OS compared to TL-L patients (HR: 2.4, 95%CI: 1.51 to 3.81, p-value<0.001). Moreover, in the CLL4 model, TL-I also had a significantly shorter OS compared to TL-L patients (HR: 1.76, 95%CI: 1.08 to 2.86, p-value<0.05). Conversely, whilst the TL variable remained in the final ARC/ADM OS model, the TL-S and TL-I subgroups did not have a significant impact (p-value>0.05) on OS however the covariate was important in the

model itself and therefore could not be removed. Along with epitype and TL, the *TP53* aberration covariate retained independence in the ARC/ADM OS model (HR: 3.28, 95%CI: 1.64 to 6.55, p-value<0.001) (**Supplementary Table 12**). Whereas further covariates that were independent markers of OS in the CLL4 model included *TP53* aberration, *SF3B1* mutation, age and treatment arm (**Supplementary Table 10)**. The MVA found that both TL and DME independent predictors of PFS and OS across a discovery and validation clinical trial cohorts.

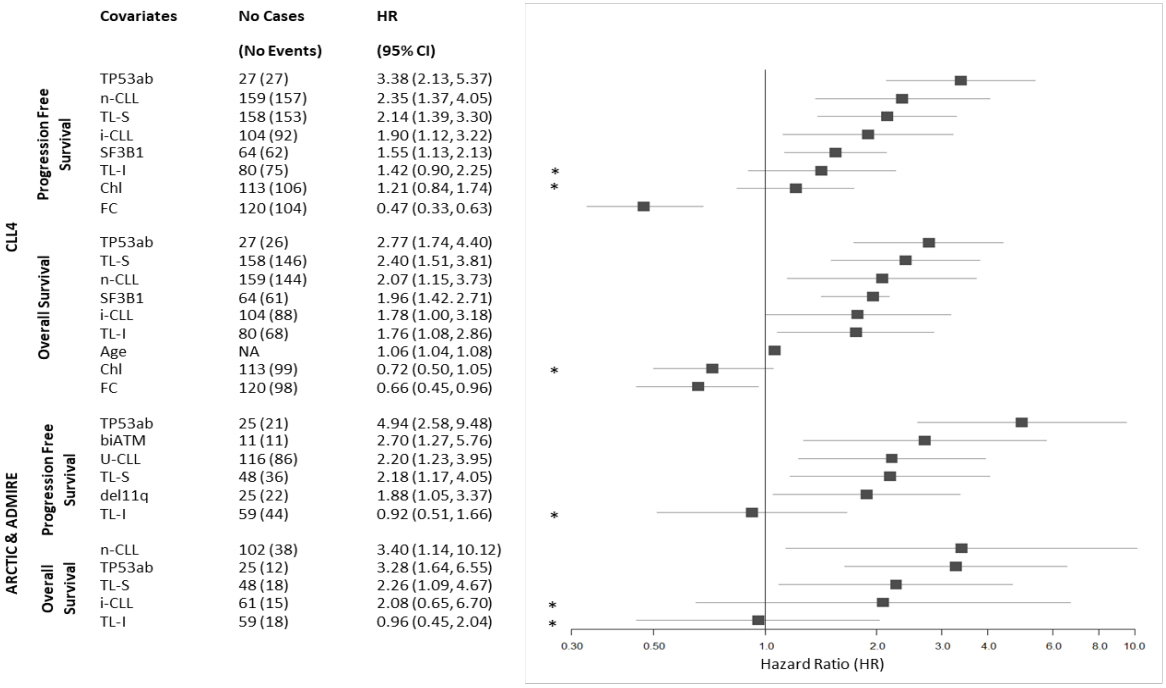

Figure 32- Forest plot including the variables that remained significant in the final multivariable models after a stepwise backwards elimination process was applied to the CLL4 and ARCTIC/ADMIRE cohorts. Asterisks highlight factors within a categorical variable that were not significant, as the confidence interval (CI) included 1, but the categorical variable itself was significant as the model had a better goodness of fit when the variable remained, for example the TL-I factor in the TL categorical variable. Abbreviations: TL-S- Short Telomere Length, TL- I-Intermediate Telomere Length, TL-L-Long Telomere Length, U-CLL- Unmutated IGHV genes, TP53ab- TP53 Aberration, Tri12-Trisomy 12, biATM- Biallelic ATM inactivation, Chl-Chlorambucil, FC-Fludarabine plus Cyclophosphamide, SF3B1- *SF3B1* mutation, NOTCH1-*NOTCH1* mutation

4.4.5 TL and DME alone and in combination are strong predictors of PFS and OS

To further quantify the clinical impact of epitype and TL, a sensitivity-specificity analysis was conducted. This allowed us to determine the likelihood ratios (LR+/LR-) of three biomarkers—epitype, TL, and *TP53* aberration status—in predicting the presence or absence of PFS and OS events in cohorts of 304 CLL4 and 215 ARC/ADM patients. For *TP53* aberration assessment, cohorts were restricted to 250 and 176 patients for CLL4 and ARC/ADM cohorts, respectively, due

to limited data availability. Notably, due to zero false positive rates, the LR+/LR- for PFS events in the CLL4 cohort could not be calculated solely for *TP53* aberration status. This type of analysis takes into account the sensitivity of the variable, which is the probability that the biomarker will indicate progression or death in cases that have a PFS or OS event. Also, by calculating the specificity of the biomarker, it shows the fraction of patients that have not progressed or died that were indicated by the biomarker to have a short PFS and OS.

All three biomarkers exhibited discriminatory power to varying degrees, with TL and epitype emerging as the strongest predictor of PFS events in the CLL4 cohort (LR+/LR-: 7.30) and ARC/ADM cohort (LR+/LR-: 5.42), respectively (**Table 4**). The combined TL-S/TL-I group correctly predicted the 228/278 patients who did not have a PFS event (sensitivity of 82%), while 16/26 TL-L patients did have a PFS event during follow-up (specificity of 61.5%). Within the ARC/ADM cohort, the greatest predictor of a shorter OS (presence of an OS event) was epitype, specifically the combined n-CLL/ i-CLL group (LR+/LR-:3.69). *TP53* aberration was the second strongest predictor of an OS event (LR+/LR-: 3.30), while TL had a lower predictive power (LR+/LR-: 1.87) (**Table 5**). Similarly, in the CLL4 cohort, TL had the lowest LR+/LR- ratio (LR+/LR-: 5.10), with *TP53* aberration exhibiting the strongest predictive power of an OS event (LR+/LR-: 5.68). The combined n-CLL/i-CLL epitype group correctly predicted the 232/256 patients who did not have an OS event (sensitivity of 90.6%), while 17/48 m-CLL patients did have an OS event during follow-up (specificity of 35.4%) with a reported LR+/LR- of 5.3.

Table 4- Sensitivity and specificity analysis of significant biomarkers to predict PFS events across the two clinical trial cohorts

BIOMARKER (POSITIVE TEST€)	SENSITIVITY	SPECIFICITY	ACCURACY	LIKELIHOOD RATIO (LR+)¶	LIKELIHOOD RATIO (LR-)¶	LR+/ LR-
			CLL4 cohort (n=304*)			
Telomere length (Short + Intermediate)	82.0% (228/278)	61.5% (16/26)	80.3% (244/304)	2.13	0.29	7.30
Epitype (n-CLL + i-CLL)	89.2% (248/278)	42.3% (11/26)	85.2% (259/304)	1.55	0.26	6.06
TP53^ (abnormal)	12.0% (27/225)	100% (25/25)	20.8% (52/250)	NE[#]	0.88	NE[#]
			Arctic & Admire cohort (n=215*)			
Telomere length (Short + Intermediate)	63.0% (60/127)	69.3% (61/88)	65.6% (141/215)	2.05	0.53	3.85
Epitype (n-CLL + i-CLL)	88.2% (112/127)	42.0% (37/88)	69.3% (149/215)	1.52	0.28	5.42
TP53~ (abnormal)	19.6% (21/107)	94.2% (65/69)	48.9% (86/176)	3.39	0.85	3.97

Footnote: *With data for telomere length and methylation based epitype. ^ n=250 with data for telomere length, methylation based epitype and TP53 dysfunction. ~ n=176 with data for telomere length, methylation based epitype and TP53 dysfunction. €The presence of a biomarker condition with a poorer outcome is used to predict the occurrence of PFS events. In the case of telomere length, the better outcome group is the Long telomere group. ¶ LR^+=sensitivity ÷ (1-specificity); LR^-= (1-sensitivity) ÷ specificity. #NE: not estimable because 1-sensitivity (false negative rate) is zero.

Table 5- Sensitivity and specificity analysis of significant biomarkers to predict OS events across the two clinical trial cohorts.

BIOMARKER (POSITIVE TEST€)	SENSITIVITY	SPECIFICITY	ACCURACY	LIKELIHOOD RATIO (LR+)¶	LIKELIHOOD RATIO (LR-)¶	LR+/ LR-
			CLL4 cohort (n=304*)			
Telomere length (Short + Intermediate)	83.6% (214/256)	50.0% (24/48)	78.3% (238/304)	1.67	0.33	5.10
Epitype (n-CLL + i-CLL)	90.6% (232/256)	35.4% (17/48)	81.9% (249/304)	1.40	0.26	5.30
TP53^ (abnormal)	12.4% (26/209)	97.6% (40/41)	26.4% (66/250)	5.10	0.90	5.68
			Arctic & Admire cohort (n=215*)			
Telomere length (Short + Intermediate)	61.0% (36/59)	54.5% (85/156)	56.3% (121/215)	1.34	0.72	1.87
Epitype (n-CLL + i-CLL)	89.8% (53/59)	29.5.0% (46/156)	46.0% (99/215)	1.27	0.34	3.69
TP53~ (abnormal)	26.7% (12/45)	90.1% (118/131)	73.9% (130/176)	2.69	0.81	3.30

Footnote: *With data for telomere length and methylation based epitype. ^ n=250 with data for telomere length, methylation based epitype and TP53 dysfunction. ~ n=176 with data for telomere length, methylation based epitype and TP53 dysfunction. €The presence of a biomarker condition with a poorer outcome is used to predict the occurrence of PFS events. In the case of telomere length, the better outcome group is the Long telomere group (>75 percentile). ¶ LR^+=sensitivity ÷ (1-specificity); LR^-= (1-sensitivity) ÷ specificity. #NE: not estimable because 1-sensitivity (false negative rate) is zero.

Additionally, we evaluated LR+/LR- ratios when TL and epitype were used together as predictors, to further examine the relative discriminatory power of the TL and epitype subgroups by combining the two biomarkers. The outcome of this analysis was similar to the single marker sensitivity and specificity analysis as when n-CLL/i-CLL or TL-S/TL-I groups were included in the predictor, a PFS or OS event is more likely to occur, as shown by a >1 LR+/LR- ratio, see **Table 6**. From this analysis, when n-CLL/i-CLL variable was combined with the TL-S/TL-I variable, a greater LR+/LR- ratio was reported in the PFS and OS analysis. For example, the LR+/LR- ratio for the sole

epitype variable (n-CLL&i-CLL) as a predictor for PFS event was 5.3 which is interpreted as a PFS event being over 5 times more likely in the n-CLL&i-CLL group compared to the control (m-CLL group). However, when both TL and epitype were combined (n-CLL&i-CLL(TL-S&TL-I)) as the predictor a LR+/LR- ratio was 13.08, see **Table 4** and **Table 6**. However, the recorded LR+/LR- ratios varied across the cohorts, emphasizing the need for further analysis with expanded sample sizes. Furthermore, n-CLL/i-CLL combined with TL-S/TL-I had a higher accuracy in predicting a PFS event than when either variable was assessed alone. For example, in the ARC/ADM cohort, n-CLL/i-CLL alone had an accuracy of 69.3% compared to in combination with TL-S/TL-I variable, it had an accuracy of 77%. This improvement in the accuracy when using a combined TL and epitype variable as a predictor, was also found in OS. This analysis suggests that a biomarker that combined both the TL and DME variable has a greater predicting power than when these variables are used alone.

Table 6- Sensitivity and specificity analysis using two biomarkers, telomere length and epitype as predictors of PFS and OS when using separate CLL4 and ARCTIC/ADMIRE cohorts.

		CLL4 Cohort						Arctic & Admire cohort					
		m-CLL(TL-L)		m-CLL(TL-S&I)		n-CLL&i-CLL(TL-L)		m-CLL(TL-L)		m-CLL(TL-S&I)		n-CLL&i-CLL(TL-L)	
PFS	n-CLL&i-CLL(TL-S&I)	91.6%	90.0%	95.6%	93.7%	87.9%	86.7%	88.2%	77.0%	93.8%	74.8%	67.0%	63.8%
		54.5%	**13.08**	50%	**21.8**	66.7%	**14.53**	59.3%	**10.91**	18.5%	**3.41**	56.9%	**2.67**
	n-CLL&i-CLL(TL-L)	60%	54.5%	75%	63.6%			78.7%	63.9%	88.1%	55.3%		
		37.5%	**0.9**	33.3%	**1.5**			52.5%	**4.08**	14.7%	**1.28**		
	m-CLL(TL-S&I)	33.3%	39%					33.3%	71.2%				
		54.5%	**0.6**					86.5%	**3.20**				
OS	n-CLL&i-CLL(TL-S&I)	93.2%	86.7%	95.8%	88.7%	88.4%	82.9%	87.5%	51.8%	97.2%	41.1%	66.0%	50.9%
		37.9%	**8.35**	25.0%	**7.59**	41.9%	**5.48**	37.4%	**4.18**	12.7%	**5.08**	43.6%	**1.51**
	n-CLL&i-CLL(TL-L)	64.3%	57.6%	75.0%	60.0%			78.3%	50.9%	94.7%	35.5%		
		45.8%	**1.52**	31.6%	**1.38**			43.5%	**2.78**	15.8%	**3.38**		
	m-CLL(TL-S&I)	37.5%	48.8%					16.7%	73.1%				
		64.7%	**1.10**					80.4%	**0.82**				

Footnote: Both telomere length and epitype have been used as predictors of PFS and OS in both the CLL4 and ARCTIC/ADMIRE cohorts. By grouping the two variables and combining short/intermediate TL or long TL with n-CLL/i-CLL or m-CLL, four groups were produced that where then compared in a pairwise fashion, for example comparing m-CLL (TL-short & intermediate) against m-CLL (TL-long). The positive predictor group is shown on the first column and are being compared to the groups shown along the top. For each comparison sensitivity (%), accuracy (%), specificity (%) and diagnostic odds ratio (shown in bold) has been calculated and displayed.

4.5 Discussion

In summary, our analysis, for the first time, investigated both TL and methylation based epitype as prognostic biomarkers within a discovery and validation CLL cohort. We were able to ascertain

that TL and epitype are significant associated, specifically with a concordance between patients with TL-S and a n-CLL and TL-L patients with m-CLL being identified. This finding is consistent with previous work that found a high percentage of n-CLL and m-CLL patients with TL-S and TL-L, respectively (195). This project advanced on previous TL or DME statistical analysis that had been published, as it used a cohort of 519 clinical trial patient that had a wealth of molecular characterisation, so many established CLL biomarkers could be assessed alongside TL and epitype. This not only allowed us to examine how these two-novel biomarker interact with each other, but also investigated the biological context and characteristics of these TL and epitype subgroups. Furthermore, we were able to examine the clinical significance of TL and DME together within a discovery and validation study design. Whilst the impact of TL and DME on survival outcomes has been shown previously, we were able to investigate the independent impact each biomarker has on clinical progression through the construction of multivariate models, whilst controlling for confound variables. Completing this type of statistical and survival analysis is typically more useful as these CLL biomarkers do not occur in isolation, and patients will usually have a more complex combination of many of them. Therefore, by examining these biomarkers at the same time we aim to build a more representative idea of true clinical utility of this data.

Firstly, as discussed above, TL and epitype were found to be significantly associated in the cohort of 519 patients used for this chapter. Association plots also identified that both the TL-S and n-CLL epitype subgroup co-occurred with many poor risk factors such as *TP53* aberration and IGHV-U status. Similar associations were found in published work, for example a cohort of 211 CLL patients found 97% of the n-CLL patients also had unmutated *IGHV* genes (194). DNA methylation is a known hallmark of cancer cells, but it has also been identified as a tissue-of-origin signature and thus can reflect the development state of the B cell from which the tumour has arisen from (194). As both methylation based epitype and *IGHV* mutational status reflect this cellular origin of the tumour, unsurprisingly there is a strong correlation between these two classification systems. Additionally, a correlation between TL and *IGHV* status has been reported both in the literature, specifically unmutated *IGHV* status is associated with shorter telomeres (189,276). Published work has also found an increase in telomerase activity in unmutated patients (277). One theory behind this difference is that it may reflect the TL present in the cell at time of initial transformation and therefore represent the proliferative histories of the precursor cells. For example, *IGHV* mutated CLL has arisen from cells that have undergone the germinal centre reaction where increased telomerase activity elongates their telomeres. The increased activity of telomerase identified in U-CLL has been hypothesized to be a compensatory action of the cell, which had excessive loss during clonal expansion and the enzymatic action ensures cell survival by avoiding the telomere length threshold at which cell senescence is triggered (276). Together, this evidence supports

disregarding the previous theory that CLL is caused by the accumulation of long-lived resting B-cell and supports the involvement of B-cells with extensive proliferative histories.

This chapter found that TL-S were associated with both del11q and *ATM* biallelic inactivation events, as previously published (278,279). Conversely, the i-CLL epitype has been reported in the literature to be composed of mainly stereotype subset #2 (*IGHV3-21*/*IGLV3-21*) and is enriched for *ATM* dysfunction, *SF3B1* mutations and the recently identified IGLV3-21^{R110} mutation (131,279–281). However, within our cohort of i-CLL patients, no significant association was found with either biallelic *ATM* dysfunction or del11q events. Additionally, the *ATM* dysfunction reported in subset #2 was also associated with shorter telomeres, which was not captured in the i-CLL patients of our cohort (280). Whereas a significant enrichment of *SF3B1* mutations in i-CLL patients (p-value<0.05) was identified in our results as 30% (n=46/153) of i-CLL patients had a *SF3B1* mutation compared to just 22% of n-CLL or 17% of m-CLL patients. This association between stereotype usage, DNA methylation profiles, gene expression and genetic aberrations reported in the literature and within this cohort suggests that interactions within the tumour microenvironment with particular BCR stereotypes may result in a selection of certain genetic alteration that, in combination, effect the evolution and clinical outcome of the disease.

As mentioned before, the i-CLL epitype has been reported to have a biased toward expressing IGLV3-21 (131). Recent research has reported in CLL cells with IGLV3-21 stereotype a single G>C substitution a splice site can occur during somatic hypermutation, which alters the glycine to arginine (R) at position 110 (282). This single point change in the IGLV3-21 genes allows for self-recognition between a R110 mutated BCR and BCR in neighbouring CLL cells causing cell autonomous signalling, independently of any antigen stimulation. A published cohort of 584 CLL cases not only found that these IGLV3-21^{R110} mutations were enriched in the i-CLL epitype but it also conferred an aggressive disease with poor survival (283). These cases had a phenotype like that of n-CLL patients that was largely independent of *TP53* dysfunction and had a specific transcriptomic signature including *WNT5A/B* overexpression. Wnt-5a bind to the ROR1 and ROR2 receptor causing the activation of the wnt pathway, also known as the planar cell polarity pathway, which in CLL is involved in modulating the chemotactic response and dictates the migratory properties of the cell. Therefore, it is suggested that an overexpression of *WNT5A/B* in CLL contributes to an increased cell motility, decreased response to chemokines and presents as a more aggressive disease (283). Our research was also able to identify a significant concordance between the IGLV3-21^{R110} mutation and i-CLL, as 13/14 (93%) of the patients with the mutation also had a i-CLL epitype. Additionally, for the first time, we found that the IGLV3-21^{R110} mutation status significantly vary across TL groups (p-value<0.05), as the majority of mutated cases also had TL-S (58%). Moreover, the median TL was shorter in the IGLV3-21^{R110} mutated cases compared to

wild type patients (median 2.8 v.s. 3.7 kb). When assessing the clinical impact of IGLV3-21 patients harbouring the R110 mutation in our univariate analysis, no significant difference between the mutated and wild type cases was found. Stereotype data was available on a limited number of cases (86/215) from the ARC/ADM cohort, with only 14 patients being detected to have an IGLV3-21^{R110} mutation. At present, insufficient data for this variable precludes further downstream analysis. And as IGLV3-21^{R110} was not included in the multivariant analysis, we were unable to account for the R110 mutation and rule out its potential impact, specifically in the i-CLL cases, which this study found to be useful in risk-stratifying IGHV-mutated patients.

Conversely, a strength of this study is the novelty of reporting on both TL and DME variables within a clinical trial CLL cohort. Univariate analysis found that both TL and epitype were significant for predicting PFS and OS events, this result has also been reported in various published literature (185,195). Similarly, sensitivity and specificity analysis found that both TL and epitype were useful as single predictors but were, in some cases, more useful when combined together. Strefford (2015) also found from a sensitivity and specificity analysis that combined TL-S and TL-I group were the best predictors of a PFS event (185). In our data, the TL-S and TL-I group was the greatest predictor of a PFS event in the CLL4 cohort, however within the ARC/ADM data both the n-CLL and i-CLL group and *TP53* aberration were a found to be a stronger predictor. Likewise, for OS, both *TP53* aberration and the n-CLL and i-CLL epitype group were stronger predictors of a death event than TL. The results from when TL and epitype were used in combination as predictors were similar to when the variables were used as single predictor, further detail identifying specific correlation between the unique subgroups was not found. This is potentially due to a lack of power when using subgroups of a small cohort size. Further expansion of the cohorts used in this study will allow greater numbers in the subgroup that we wish to drill down into further.

To further examine the relationship between TL and epitype, a subgroup univariate analysis was undertaken. This identified that the i-CLL group, that has a survival outcome greater than the n-CLL cases but poorer than m-CLL, can be further stratified by TL with TL-L predicting a lower risk of progression. This has important implication for the management of CLL patients enrolled in chemo(immuno-)therapies as it has been reported that 20-30% of M-CLL cases, although a good risk factor, are associated with a poor outcome after first line FCR treatment (125,284). The outcome of these patients is not explained by current poor-risk factors, such as TP53 aberration. Therefore, if the i-CLL epitype, which accounted for 51% of the M-CLL cohort, could identify patients destined to have a poorer outcome than m-CLL patients (40% of M-CLL patients), the epitype biomarker could be useful in treatment decisions to improve patient outcome. Whilst the potential importance of the i-CLL epitype in further risk stratifying the M-CLL group has been

supported in previous research (195). We were able to further this idea by showing that the i-CLL epitype could be further dichotomized by the TL variable. Specifically, i-CLL patients with TL-L were shown to have a significantly greater PFS, compared to i-CLL patients with TL-S or TL-I. Therefore, TL-L and the i-CLL epitype have potential use as prognostic biomarkers in identifying M-CLL patients that are destined to have prolonged survival after commencement of a chemo(immuno-) based therapy.

Due to the extensive follow up data available for CLL4 and ARC/ADM clinical trial cohorts, up to 17 and 9 years respectively. We were able to build sophisticated survival models to assess the independent impact of TL and epitype, whilst controlling for confounding variables. Overall, both epitype and TL were found to provide independent prognostic information in both the discovery and validation cohorts. Final multivariate models identified n-CLL as an independent prognostic marker of poor OS across both cohorts and a marker of poor PFS in the CLL4 cohort. Including the TL covariate into models identified that patients with TL-S were independently associated with a shorter PFS and OS. Previous research using a CLL8 cohort of 620 patients also identified short telomeres as being significantly associated with poor PFS but only remained significant in the OS model when certain covariates were not included in the backwards elimination process (285). Within our OS ARC/ADM model, TL-S did not remain significant but in the CLL4 cohort it did retain independence. One explanation of this result is that the two cohorts have used two different techniques for measuring TL: MMQPCR and STELA. These techniques differ in running costs and labour intensity, which are relevant factors in biomarker validation, with the MMQPCR technique having a decreased cost and higher throughput (286). However, these two techniques have been previously compared with a high concordance reported (185). Additionally, across the PFS endpoint TL measured from both techniques remained significant. An alternative explanation is that as the ARC/ADM cohort also has less follow up data available, the prognostic significance of TL could not be captured in the OS endpoint.

This chapter had two main aims, which were addressed in the results. Firstly, to describe the biological associations and features of the TL and DME subgroups and to investigate the relationship between the TL and DME biomarkers. Secondly, identify the clinical merit and relative power of these two biomarkers using CLL patients enrolled in CIT trials. Whilst the aim of identifying the clinical importance of TL and DME was able to be achieved through the completion of univariate analysis and by building sophisticated multivariate models, the hypothesis that patient outcome is more significantly associated with TL than DME should be rejected. The results from including both TL and DME in survival analysis for the first time, suggested that both TL and DME have a prognostic impact and, in fact, combining the two variables could identify a unique

cohort of patients destined to have poor prognosis, which is not explained by current clinical biomarkers.

In conclusion, this analysis is the first of its type to directly compare the prognostic impact of the TL and epitype variables in a large cohort of CLL clinical trial patients that have extensive molecular characterisation and extended follow up data available. We were able to further describe the biological context of the TL and epitype subgroups, as well as examine the relationship between two biomarkers. Results of this work have indicated that TL and epitype have additional prognostic value compared to previous reported and established biomarker for predicting PFS and OS in CIT treated patients. Importantly, this work grants us further insight into the clinical outcome of the subset of M-CLL patients with a poor prognosis, that is not capture by current biomarkers. Application of this work would allow further risk stratification of CLL patients, ensuring the M-CLL patients who are likely to respond poorly to CIT are given alternative treatments, such as targeted agents, to improve patient's response and survival.

Chapter 5 Data generation for the assessment of genomic complexity within CLL

5.1 Synopsis

This chapter describes the laboratory and bioinformatic work that I undertook to generate new data points for clinical trial patients that were missing certain datasets. The content of this chapter complements what is described in the methodology and it gives detail about the process of optimising the experimental procedures and bioinformatic pipelines used. Results from the main steps of HS2 raw sequencing analysis are reported, as well as a description of how the bespoke probe panel was designed. The optimization of the MMQPCR data analysis and CNA calling ability of the sWGS bioinformatic pipeline, completed by myself, are also discussed below in this chapter.

5.2 Introduction

During my PhD program I have aimed to generate the largest possible cohort of clinical trial CLL patients that have extensive biological and molecular characterisation with considerable follow up data available. This cohort will then be used to examine the prognostic and predictive ability of the GC biomarker which has been extensively reported to be clinically valuable in the current CLL literature but have yet to be validated. Firstly, the availability of published data for patients in the three clinical trials was verified, allowing a clear idea of the patients that were missing certain data points. Gene variant, TL and CNA data have been previously generated for different subsets of the CLL4 and ARC/ADM cohorts, during various projects and using different techniques. Both the CLL4 and ARC/ADM cohort had previously established variant data generated using two different TruSeq custom probe panel (159,249). CNA data for the two clinical trial cohorts was compiled using two distinct SNP technologies; the Illumina HumanOmni 2.5-8 BeadChips (ARC/ADM) and Affymetrix SNP6.0 array (CLL4) (144,249). Furthermore, two methodologies were previously used to generate TL data for the CLL4 and ARC/ADM cohort, namely MMQPCR and STELA, respectively (185,189).

Once this step was completed, I then planned experimental work to generate new data points with the aim of filling the gaps in datasets, thus allowing more patients to meet the inclusion criteria for the GC project. For the generation of copy number, TL and genetic variant data the techniques of sWGS, MMQPCR and HS2 target enrichment sequencing were employed,

respectively. For each technique I completed the laboratory protocols, ran samples, analysed the raw data generated and manually curated the output from the data analysis steps. Additionally, Infinium HumanMethylation450 (450k) array was employed to generate CNA data for a cohort of 31 ARC/ADM cases, see 3.4.5.1. 450k array data was previously generated for a prior methylation project, however due to similarities to SNP arrays in the principle and chemistry of the technique, CNA profiles can be inferred (287). 450k array data was available for a cohort of 280 ARC/ADM cases however only 31 cases met all inclusion criteria and were used in this project. As no laboratory work was completed as this 450k array data was given to be used in this project and no significant optimisation of the bioinformatic pipeline was required, this data set will not be discussed in detail in this chapter. I completed the analysis of the raw 450k array data as well as manually inspecting and curating the CNA called. This data was integrated to create a cohort of 495 clinical trial patients used in subsequent chapters.

5.2.1 Principles behind techniques employed to generate data

The principles of the techniques utilized for the generation of new data, as well as technologies that were used by others to generate the data I included in the assessment of GC chapter, are described.

5.2.1.1 Microarrays

Previously produced CNA data generated using various types of microarrays. The principle behind these microarray techniques is similar to FISH in the sense of specific probes are designed to bind to complementary sample DNA sequences. However, microarrays assess the entire genome for imbalances, at a greater resolution and does not require cells to be in metaphase. There are two main types of microarrays; aCGH and SNP array. Both the SNP 6.0 and HumanOmni 2.5-8 array are examples of the latter. aCGH is a technique that allows genome-wide screening for CNV using both a test sample from a patient, and a control sample. The fluorescent signal intensity of the sample DNA compared to the control DNA can be assessed by a linear plot, allowing chromosomal abnormalities such as deletions, duplication, amplification and aneuploidies to be identified. aCGH also has the additional ability to detect submicroscopic chromosomal abnormalities such as subtelomeric and pericentromeric rearrangements (288). (289). Whilst aCGH has a much higher resolution compared to FISH, this is heavily influenced by the size of probes and the genomic distance between the probes. Unlike aCGH, SNP arrays do not require a control sample and the probes are designed to be complementary of known single nucleotide differences. For each SNP, two forms of the hybridization probe are designed, one for each of the known alleles. The genotype of the SNP can be determined by the signal intensity ratio of these two probes.

Additionally, any deletion or duplications at these sites can be inferred from decreases or increases of the total measured intensities. Whilst aCGH measures a relative fluorescence signal, SNP array gives an absolute measurement. This array is able to detect the chromosomal abnormalities the aCGH can but can also report on LOH events and copy-neutral anomalies (290). A further microarray used to generate CNA data was a 450k methylation microarray. The Illumina Infinium HumanMethylation450K BeadChip array is a technology that profiles CpG DNA methylation. The biochemical principles are similar to the Infinium SNP arrays, used in CNA experiments, and therefore CNA detections are a zero-cost byproduct of methylation studies (264). Sodium bilsufite is used, as it selectively changes unmethylated cytosines to uracils but does not affect methylated cytosines. By PCR amplifying this bisulfite converted DNA, the uracils are converted to thymines. Therefore, two probes are designed for each CpG site, one being a methylated (C) and one being a unmethylated (T) query probe. The relative ratio of C/T probe signal intensity in bisulfite converted DNA residues is used to define a specific locus methylation state. This principle has been applied to infer copy number with the total probe intensity (methylated and unmethylated) being used to detect copy number changes. Due to the higher number of probes used in this technology compared to SNP arrays, this technology can provide a high-density coverage of the genome. However, problems have been reported with using 450k array technologies including the impact of probe effect as well as with technical artifacts (287).

5.2.1.2 Next generation sequencing

NGS technology can be used for the sequencing of both DNA and RNA, allowing for genetic variants to be detected. Three main types of NGS are TS, WGS and WES, see **Figure 33** for a visual summary of the three techniques. The technology can sequence thousands of genes or even the whole genome in a massively parallel process that is much more rapid and efficient than Sanger sequencing. Unlike previous techniques that used DNA chain growth termination and relied on gel electrophoresis and radioactive labelling, NGS involves reading sequences from multiple fragments simultaneously (291). The main steps include DNA fragmentation, library preparation, massive parallel sequencing, bioinformatic analysis, and variant annotation and interpretation.

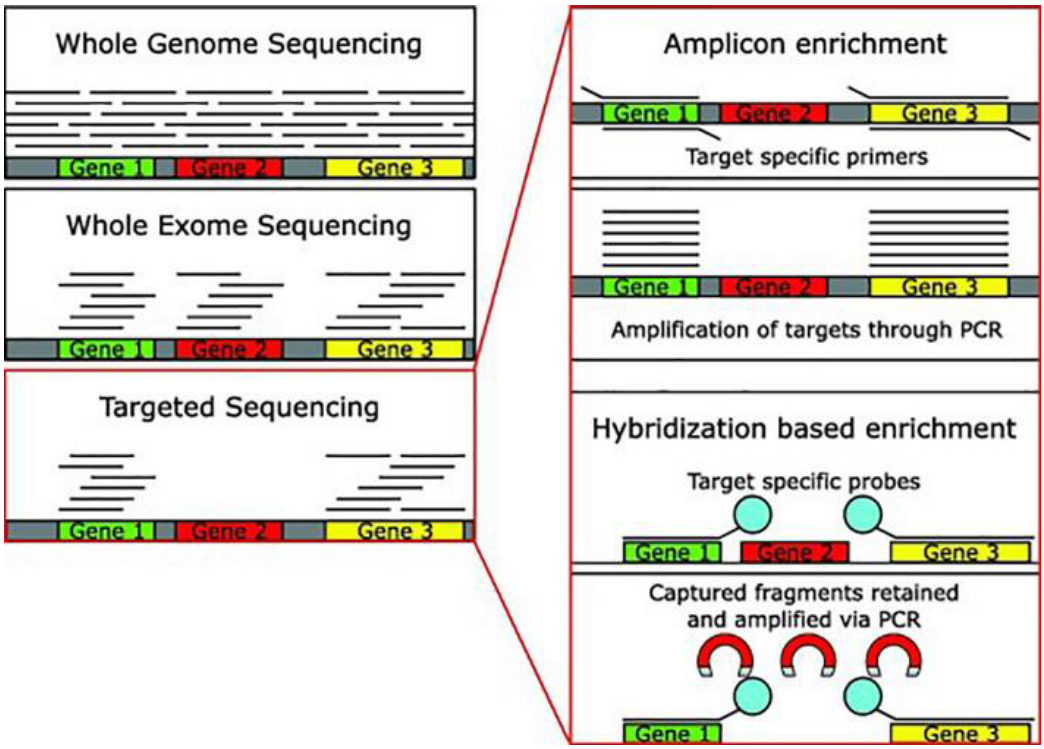

Figure 33- Schematic overview of the three main types of next generation sequencing: Whole genome, whole exome and targeted sequencing. For targeted sequencing, the two target enrichment approaches are detailed, from (291).

5.2.1.2.1 Targeted next generation sequencing

For targeted NGS, a crucial step is the target enrichment of the desired sequences which ensures the high sensitivity and specificity sequencing of the target. Two methods for target enrichment are available, namely hybridization capture assay and amplicon assay. Hybridization capture uses biotinylated probes that are designed to be complementary to targeted sequences of interest, once hybridized these probes are captured using streptavidin-coated magnetic beads. Whereas amplicon assay PCR amplifies the target DNA sequences and it is these PCR products that act as the DNA segments that are used in library preparation (292). The technique has a sequencing DOC of 1000x of higher, which is greater than Sanger sequencing and other non NGS base techniques. Additionally, it is able to detect variants at a VAF of around 0.1-0.2% which is useful for detecting minimal residual disease (212).

The SureSelect XT HS2 target enrichment system and Illumina TruSeq Custom Amplicon technology was used to generated variant data. The Agilent SureSelect XT HS2 DNA target enrichment system utilises the hybridization capture method for target enrichment of a custom probe panel containing genes or region of interest. After the custom probe panel is hybridized to the fragmented DNA sample, streptavidin-coated magnetic beads are used to capture the hybridized DNA. Similarly, Illumina's TruSeq approach also uses the hybridization capture method

for target enrichment of a custom probe panel. A further feature of the HS2 target enrichment technology is the use of 384 unique dual indexing which allowed the sequencing to be multiplexed, thereby reducing sequencing costs. Additionally, the HS2 system includes molecular barcodes which are integrated into both ends of each DNA fragment during library preparation, **Figure 34**. These MBCs are then identified during preprocessing steps and used for trimming and PCR duplicate read identification. These duplicates are merged or removed to create consensus reads which are used for downstream analysis.

Figure 34- Each DNA fragment within the HS2 sequencing library contains a target insert (blue) with a duplex molecular barcode attached on each end (brown), surrounded by Illumina paired-end sequencing elements (black), unique dual sample indexes (red and green) and the library PCR primers (yellow). From (255)

NGS can also be used for whole genome and whole exome sequencing. WGS does not target specific DNA sequences and instead investigates the complete genome, including the coding, non-coding, and mitochondrial DNA. Whereas WES examines only the protein-coding sequences of the genome. As TS examines only a specific panel of genes and coding regions, these sequences can be examined at a much greater sequencing depth than WGS or WES. Whereas WGS and WGS can be employed in the discovery of new genomic variants associated with cancer as it has a more comprehensive coverage as is it is not limited to a panel of genes. The trade-off between a greater breadth of profiling is a poorer depth of sequencing as WGS and WES has a sequencing depth of 30-60x and 100-200x, respectively (212).

5.2.1.2.2 Shallow whole genome sequencing

Several techniques have been developed to infer copy number from WGS data, such as depth of coverage (DOC), assembly-based or read-pair methods. Scheinin et al (2014) published a robust and cost-effective methodology that can identify CNAs with only a ~0.1x coverage (213). This method (sWGS) produces CNA profiles using the principles of DOC method. The DOC method for extrapolating copy number for WGS data uses observed whole genome sequence depth to infer copy number and relies on the assumption that the DOC across the genome is consistent (266).

sWGS is a multiplexed, single-read methodology which generates a small sequencing output and therefore only requires small quantities of input DNA and has comparatively low running costs.

5.2.1.3 Monochrome multiplex quantitative PCR and STELA

The MMQPCR technique has been developed from a similar assay which measured a telomere (T) signal in experimental sample DNA in one well, and a selected single copy gene (S) signal from another well and compared it to a reference DNA to calculate a relative T/S ratio that is proportional to the average TL of the experimental sample. The addition of a multiplex element to the assay improves the throughput whilst lowering the cost. Similarly to the original assay, a T/S ratio is calculated however both the T and S signal can be collected from the same well using a single DNA-intercalating dye, SYBR green. At first, the C_t of the more abundant target sequence, the telomere signal, is collected and as the temperature increases during the PCR cycle the telomere product is completely melted off and thus the T signal returns to baseline, and the S signal can then be measured (258). This difference in melting temperature (T_m) is achieved by the addition of primers which place GC-clamps on either ends of the single copy gene (highlighted below in **Table 7**) and by keeping the genomic sequence part of the primer short (non-highlighted section of the albumin sequence), raising its T_m. The primers for the telomeric amplification were designed to generate a short, fixed length product. This was achieved by having the telg primer only be able to prime DNA synthesis on telomeric sequences. The telc primer has a mismatched based at its 3' end which means it can only prime to the telg primer extension (3bp overlap) thereby enabling the generation of a fixed length PCR product that is 3bp shorter than the sum of the two primer lengths used (258). Research has found that the correlation of T/S ratios with terminal restriction fragment lengths, another PCR-based technique that is measured using a Southern blot, was stronger with the novel MMQPCR assay (coefficient of determination [R^2]=0.844) compared to the original technique (R^2=0.677)(258,293). The output from the MMQPCR assay is a TL relative to a standard used in the serial dilution and tells us if the sample DNA has longer or shorter telomeres compared to the standard used. In this case the standard used is a commercially available cell line K562 which has TL of 6.5 kb.

Table 7- Details about the primers used in MMQPCR (258)

Primer	Gene	Sequence	Tm	Product size
telg	Telomere	ACACTAAGGTTTGGGTTTGGGTTTGGGTTTGGGTTAGTGT	74°C	79bp
telc	Telomere	TGTTAGGTATCCCTATCCCTATCCCTATCCCTATCCCTAACA	74°C	79bp
albu	Albumin	CGGCGGCGGGCGGCGCGGGCTGGGCGGAAATGCTGCACAGAATCCTTG	88°C	98bp

albd	Albumin	GCCCGGCCCGCCGCGCCCGTCCCGCCGGAAAAGCATGGTCGCCTGTT	88°C	98bp

A further technique used to measure TL is STELA, also known as single telomere length analysis. This technology uses a PCR-based approach that analyzes telomeres and reports an absolute TL value, unlike MMQPCR (294). However, compared to MMQPCR, STELA is a more expensive and labor-intensive technique for measuring TL.

Work completed within the University of Southampton has compared the output from MMQPCR to the output from STELA. Originally 111 CLL4 cases with both STELA and MMQPCR data were compared and found to have an excellent correlation (Spearman correlation 0.8) (185). Within this cohort of 111 CLL4 cases, a patient sample was used as the standard to create the standard curve used within the MMQPCR. Therefore, this work was revised using 86 of the previously used cohort of CLL4 samples, but a commercially available cell line was used as the standard. Using this new standard, a strong correlation was again found between the two techniques (Spearman correlation 0.816).

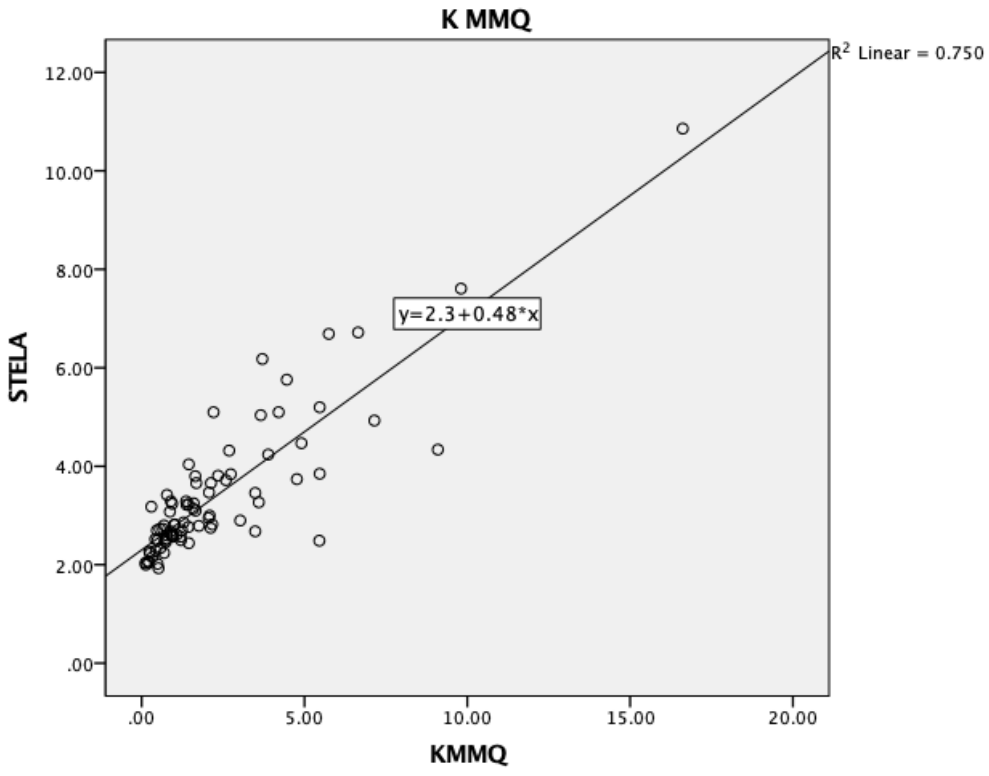

Figure 35- Statistical comparison of two techniques for inspecting telomere length. The Spearman correlation found a high correlation between the two techniques based on a cohort of 72 CLL patients. The linear regression equation shown allows the conversion of a relative telomere length to an absolute with x representing the output from the MMQPCR technique. The coefficient of determination (R^2) is calculated which reported on how much of the variation in the outcome variable is explained by the model, i.e R^2 =0.75 is 75%.

A validation cohort of 72 samples were reanalysed using the MMQPCR technique with the commercially available standard. A Spearman's correlation of 0.75 was reported when comparing this newly generated data to the original STELA data. From this a linear regression equation was calculated which allows the conversion of the MMQPCR result to an absolute TL value, see **Figure 35**.

5.3 Methodology

The three main experiments I completed in this chapter are as follows; MMQPCR, HS2 target enrichment and sWGS, to generate TL, variant and CNA data, respectively. The laboratory protocols and data analysis steps involved in generating this data are given in detail in Chapter 3. Results from the analysis of HS2 raw sequencing data is included in this chapter. The bioinformatic pipeline used to generate these results is described in 3.4.4. For the MMQPCR and sWGS experiments, discussed here are the optimizations steps that resulted in the final methodology reported in 3.4.3 and 3.4.5.

5.4 Results and discussion

Results from the analysis of newly generated data, produced from either the MMQPCR, HS2 target enrichment or sWGS technique are described in this chapter. Additionally, the process of optimizing the experimental procedures and bioinformatic pipelines is also reported and discussed below, starting with a description of how the three experimental cohorts were designed.

5.4.1 Data consolidation and cohort design

An aim of my PhD has been to create the largest possible clinical trial cohort of CLL patients with clinical, survival, gene variant, TL and copy number data available. Therefore, the first step in this task was to assess the total clinical trial cohorts, to ascertain where there were insufficiencies in the previously generated available data. **Figure 36** shows the number of patients included in each of the three experimental cohorts to generate copy number, TL, and variant data. **Figure 36** also illustrates the steps involved to generate this data and where samples have been excluded from the cohort are shown, for example removing ten cases from the HS2 experimental cohort as they failed library preparation. It is important to note that not all patients that required a specific datapoint could be included in the specific experimental cohort, for various reasons. One such reason being that these clinical trials are historic and extensively studied in previous research with only a finite DNA sample per patient available. Therefore, often there was insufficient sample

available, or the DNA had degraded over time resulting in the clinical trial patient not being included in the project. Therefore, a vital step in designing the three experimental cohorts involved completing quality control checks on the DNA patient samples located in the University of Southampton -20^{o}C sample storage freezer. Quality control checks were completed using the Qubit fluorometer to measure the concentration of the stock DNA patient samples. In the cases where a stability of the DNA sample was in question, the NanoDrop spectrophotometer was used to assess if the DNA had degraded, which would result in exclusion from the experimental cohort. The final experimental cohort of sWGS, MMQPCR, and HS2 were 177, 83, and 52 CLL clinical trial patients, respectively. It should be noted that some patients were included in more than one of the experimental cohorts as lacked more than one datapoint. The next steps using these cohorts are outlined in further detail below.

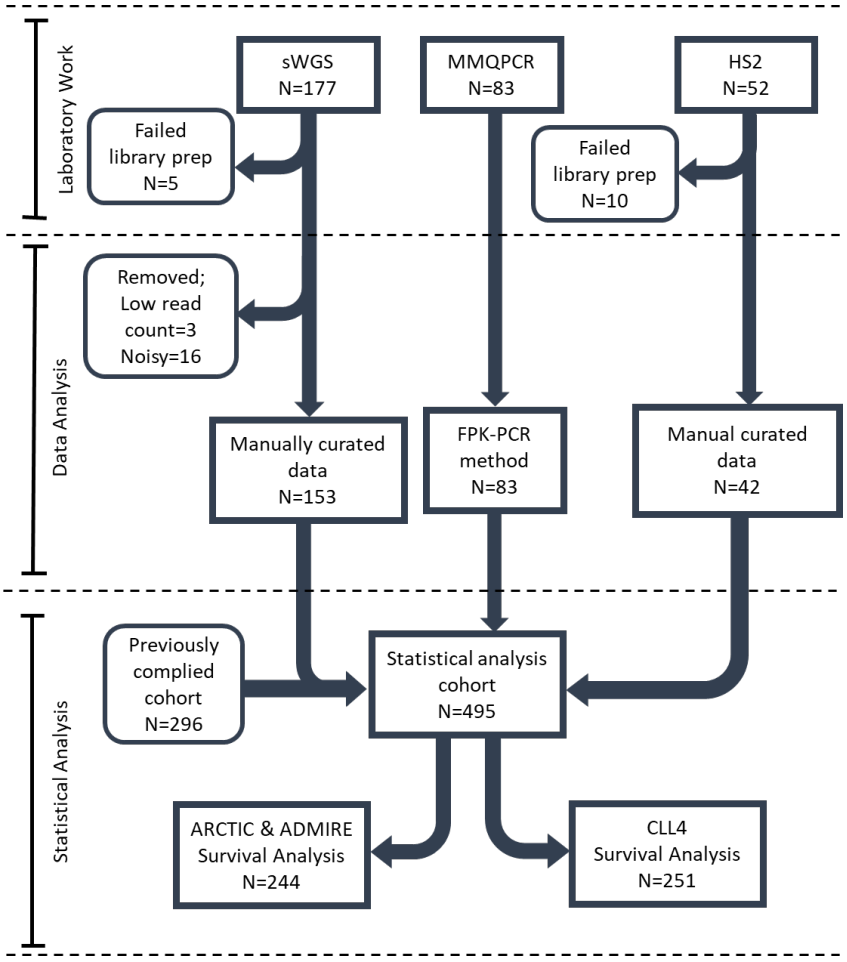

Figure 36- Flow diagram showing the cohorts and steps used for the generation of the three new datasets that are then integrated with pre-existing data.

5.4.2 Generation of Telomere Length Data

5.4.2.1 Experimental Protocol

This protocol was adapted from another the published work of Cawthon et al, 2009 (258). A cohort of 83 cases (CLL4:71 & AA:12) that were missing TL data formed the experimental cohort. Furter detail on the experimental protocol is given in 3.4.3.

5.4.2.2 Data analysis and pipeline development

During the analysis of the newly generated MMQPCR data for 83 samples it was noted that the old analysis pipeline relied on a web-based software called PCR miner. It requires raw fluorescence data as input and performs Ct calculation across various steps. Firstly, a four-parameter logistic model is used to fit the raw fluorescence data, as a function of cycles, to identify the exponential phase of the reaction. Then a three-parameter simple exponent model and iterative nonlinear regression model is used to fit the exponential phase. Within the exponential section of the curve, the PCR miner method identifies candidate regression values using the *p-value* of regression and then uses a weighted average to calculate the final efficiency for quantification. Whereas to calculate the Ct values the first positive maximum of the second derivative of the five-parameter logistic model is used (295).

Due to PCR miner being a web-based software I wished to 'future proof' the data analysis protocol by changing to an alternative method for QPCR data analysis. When I originally went to complete the analysis the PCR miner web domain was unavailable, and it was uncertain if this software would become available again. Therefore, I solved this problem by finding and implementing an alternative technique which was found to be comparable to the old method and possibly supersedes it. This not only allowed me to analyze the data I had just generated using the MMQPCR technique but also was used by another student in the group to analyze their data and will be used in the future by others in the Cancer Genomic research group.

Examination of the literature identified a variety of different methods for QPCR analysis, one such method that was comparable to PCR miner was FPK-PCR. Similarly to PCR-miner it performs a Ct calculation using raw fluorescence data however is R based technique that employs the R package 'minpack.lm'. The FPK-PCR method estimates the initial target quantity using a bilinear and four-parameter logistic model (296). Due to it being a R based technique it avoids the reliance on a webpage that may become unavailable if the web domain is not maintained. Additionally, the data retabulating steps that preceded the Ct calculation step were also converted to be produced in R whereas previously had been completed manually in excel. To assess the new FPK-PCR method an old dataset of 20 cases we processed with PCR miner was used. The concordance of

the two methods were assessed before FPK-PCR method was used to analysis the 83 new cases that had MMQPCR data generated. Comparing the absolute TL given when PCR miner or FPK-PCR were employed found a high level of concordance between the two methods with an average difference between to two values of +/-0.00989. Spearman's correlation coefficient was employed and found a highly significant positive correlation between the two results given from the two methods investigated (p-value=0.000006), see **Figure 37**. Due to this result the FPK-PCR method replaced PCR miner in the processing of MMQPCR data and was used to analysis the cohort of 83 outlined above.

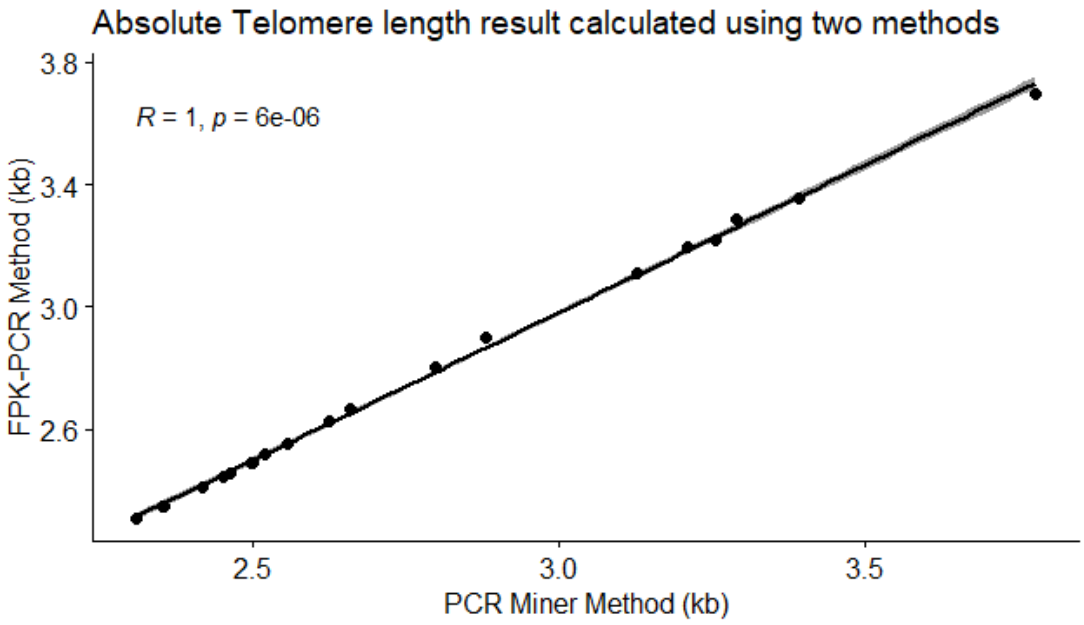

Figure 37- Scatterplot of the 20 samples used to compare the two methods for Ct calculation: PCR miner and FPK-PCR.

Once the Ct calculations were completed within R studio, a macro enabled excel spreadsheet was used which calculated relative TL for each sample. The final step involved converting the relative TL value into an absolute value, using the linear regression equation developed during a series of projects described above. The process from setting up the PCR reactions to the analysis of generated data meet the requirements for quantitative PCR assay as outlined by MIQE (297)

5.4.3 Generation of genetic variant data

5.4.3.1 Experimental Protocol

To generate novel variant data for the cases that lacked this dataset, the Agilent SureSelect XT HS2 DNA target enrichment system was used to for DNA library preparation and targeted enrichment for sequencing on an Illumina platform. To generate this dataset, the SureSelect HS2 XT target enrichment library preparation and the Illumina NovaSeq 6000 system was used. The

experimental procedure can be broken down into; custom probe design, DNA library preparation, hybridization capture for target enrichment, pooling and sequencing using Illumina based technologies (**Figure 16**). A cohort of 52 patients (CLL4:32 & AA:20) was identified for library preparation, see **Figure 36**. However, only 42 samples (CLL4:24 & AA:18) had a successful library preparation and therefore were included in the DNA library pool and sequenced.

5.4.3.1.1 Probe Design

This system requires custom probe production that are designed to target a panel of selected genes and genomic regions (255). These targets were selected by myself by looking at gene panels previously used and by investigating the current CLL literature for any novel targets of interest. From this, a panel of 72 genes and genomic regions were selected and had probes designed against, see **Supplementary Table 2** for the full list. 62 of these targets were part of a custom probe design created in 2018 for a previous target sequencing experiment. This probe design included various established CLL and lymphoid malignancy gene panels as well as any additional genes or genetic regions that were reported in the literature, at the time of probe design. To update the probe design I completed a literature search in 2021, with any new genes or genetic regions reported in CLL published research were considered to be added to the probe design. This literature search identified 10 new genes, that were reported to have importance in CLL biology. These 10 genes were added to the 2018 probe design of 62 targets, resulting in a panel of 72 genes and genomic regions. The probes were designed with Agilent's SureSelect DNA design tool, whereby a machine learning algorithm selects the probe sequences and calculates the probe coverage of the gene or genomic region. A few targets had lower coverage when using this machine learning algorithm and therefore required manual inspection to improve coverage before the probes were produced, which was completed by Agilent after a discussion with myself, see **Supplementary Table 2**. It is important to note that the new variant data produced during this experiment will be integrated with previously generated data for the CLL4 and ARCTIC/ADMIRE clinical trial cohorts. Variant data for these two cohorts were previously generated in two separate experiments using two separate TruSeq custom panel for target enrichment sequencing. These TruSeq panels, along with the HS2 custom panel, differed in size and in the selection of genes and genomic regions included, see **Figure 38**. However, there was an overlap of 9 targets that were included in all three panels, which will therefore be the focus of downstream analysis.

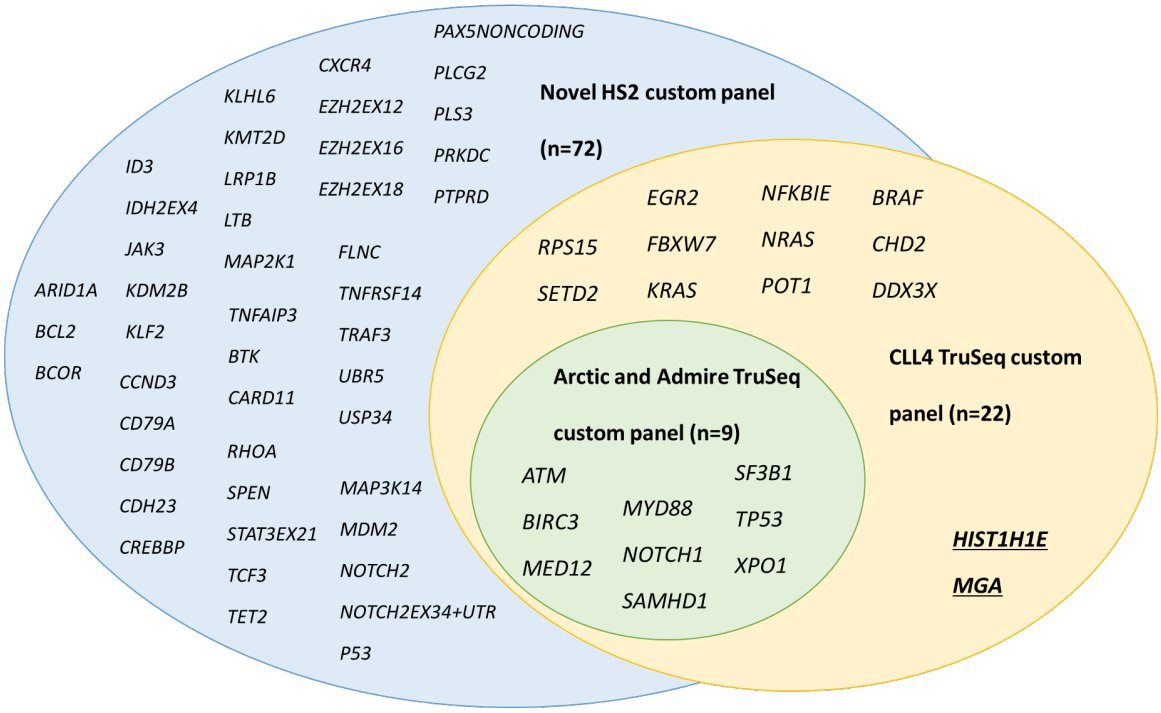

Figure 38- A outline of the two TruSeq custom panels used for the Arctic/Admire (green) and CLL4 (yellow) cohort as well as the more recent HS2 custom panel (blue). The 9 targets included in the Arctic/Admire panel were also included in the CLL4 TruSeq and HS2 panel. 20 of the 22 targets of the CLL4 TruSeq panel were included in the HS2 custom panel, 2 targets (shown in bold and underlined) were not included. The HS2 custom panel had 72 targets, not all are shown in the figure as multiple targets were included for a single gene and therefore have been simplified by only including the gene name.

5.4.3.1.2 Library Preparation

Once probe development was completed, preparation of DNA libraries was completed with the SureSelect XT HS2 DNA system. An overview of the main steps of the protocol is shown in **Figure 39**, further detail is discussed in 3.4.4. As mentioned above, only 42 of the 52 cases passed the DNA library preparation and therefore only 42 samples were pooled together and sequenced. The minimal sequencing data required for the specific probe design used was calculated by doubling the recommended minimal sequencing and multiplying by the number of samples included in the final pool, for this experiment it was 6.29 Gb of sequencing was required. The pooled library was then sequenced on the NovaSeq 6000 Illumina platform using v1.5 chemistry. The generated raw sequencing data, in the form of FASTQ files were then analysed using a bioinformatic pipeline.

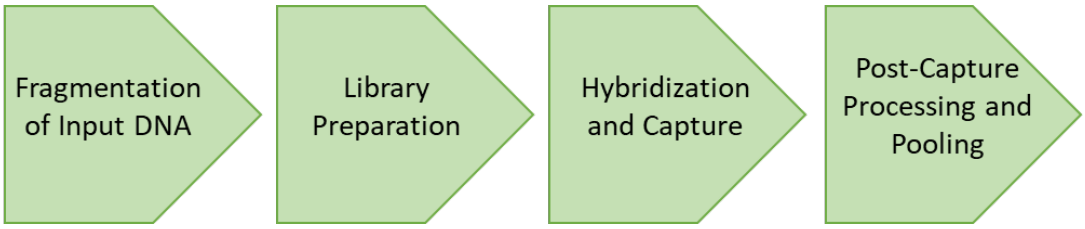

Figure 39- The main experimental steps involved in generated novel variant data using the SureSelect XT HS2 DNA system, from (255)

5.4.3.2 Data analysis and manual curation

Analysis of the generated data can be divided into three main sections, first preprocessing, alignment and variant calling was completed within the University's high-performance computing cluster IRIDIS 5, then variant filtering was completed using RStudio within the R environment, and finally manual curation of the final filtered list of variants was completed using the IGV software, see 3.4.4.

5.4.3.2.1 Results from the preprocessing, alignment and variant calling steps

Raw sequencing data is inputted into the bioinformatics pipeline in the form of two FASTQ files, due to the paired-end run. FASTQC software (version 0.11.9) was used to assess the sequence quality of the FASTQ files. These outputted files were merged together using MultiQC, to allow easier comparisons of all samples. An example of the FASTQC output is given in **Figure 40**, the per sequence quality score report identifies sequences runs with low quality values that may have been caused by technical problems with the sequencing run. The plot shows the FASTQC check of per sequence quality score, with all samples passing with a sufficient mean sequence quality (green zone). A warning is given when the most frequently observed mean quality is below 27 (orange zone), this reflects an 0.2% error rate. A FASTQ file is failed if the most frequently observed mean quality is >20 (red zone), which equates to an error rate of 1% (298). However, all FASTQ files passed this check and all other FASTQC checks.

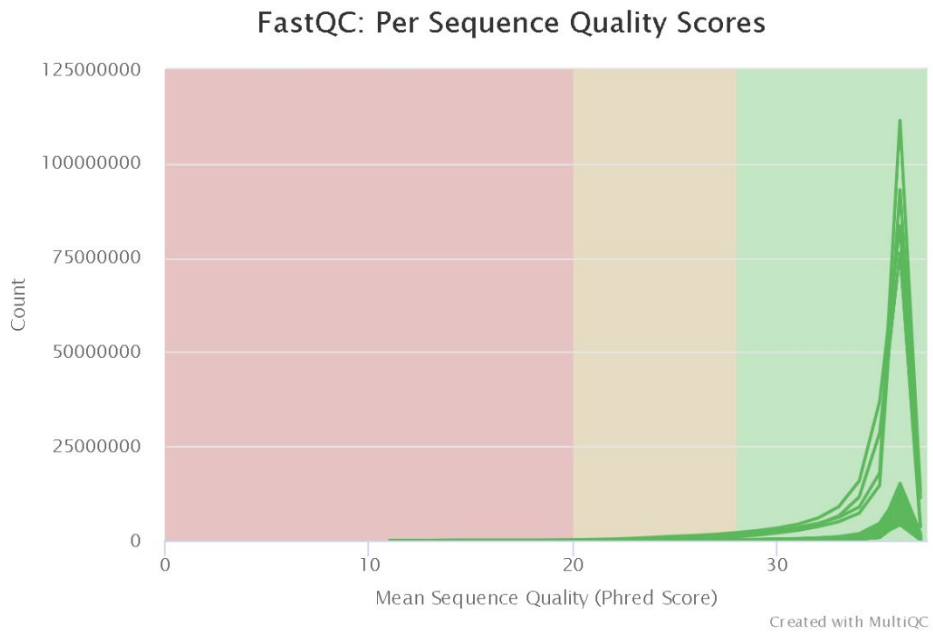

Figure 40- Figure of per sequence quality score was generated by the MultiQC tool by merging all FASTQC files together.

Mosdepth (version 0.3.4) was used to calculate genome-wide sequencing coverage, again MultiQC was used to merge all output files into a single report of all samples for easier examination. Mosdepth was used to produce coverage summaries across capture regions, specifically across the 72 target regions of interest. To examine the DOC at each of the targets the mean depth was calculated across all regions of the target and across all patients, this data was extracted from each mosdepth file created for each sample and was graphically represented in a scatter plot created in RStudio (**Figure 41**). Of the 72 targets, only two, BTK and PLS3, had a mean depth lower than 1000. Overall, there was sufficient sequencing depth of all targets across all samples for confident variant calling.

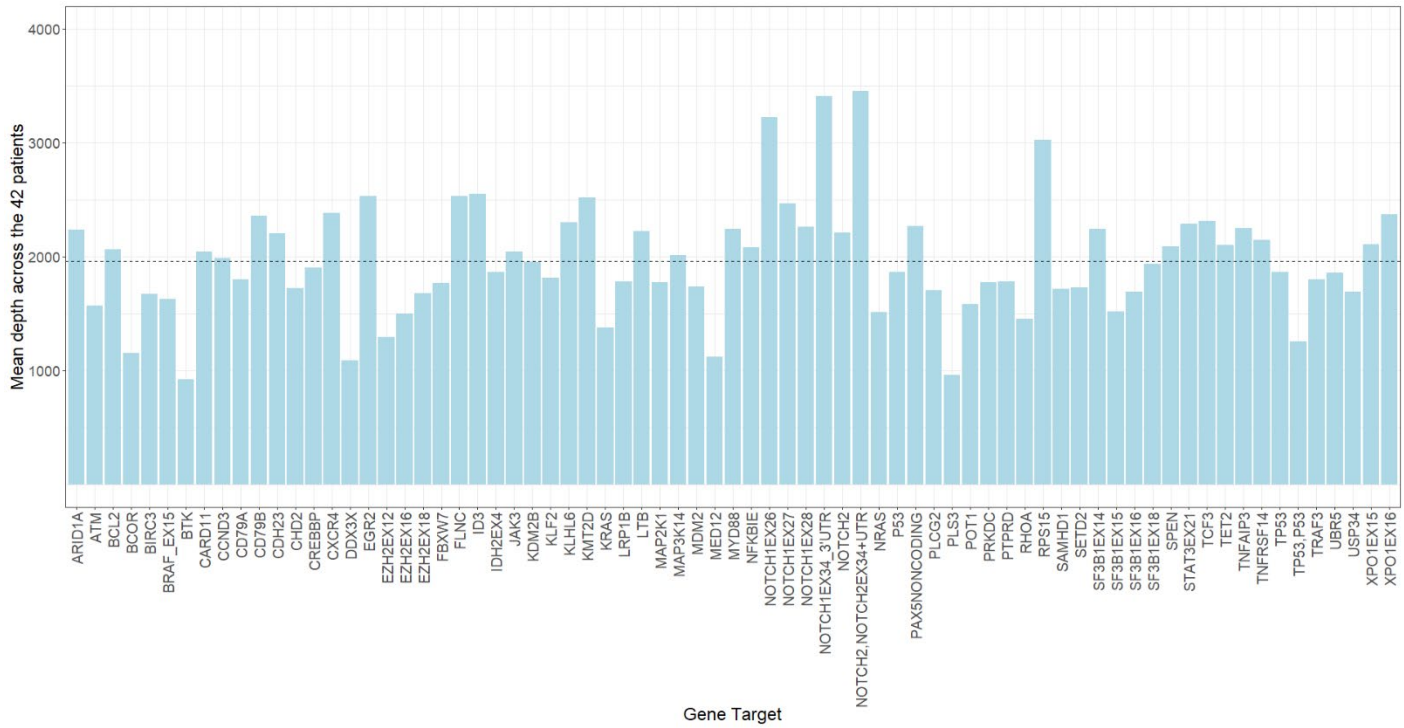

Figure 41- The mean depth of the gene target, across all regions and all patients. The mean sequencing depth of the 72 targets is shown by a horizontal dashed line.

5.4.3.2.2 Results from variant filtering steps

The output from the preprocessing and alignment stages of data analysis was a maf object that showed a total of 1272 variants had been called, these included frame shift deletions, nonsense mutations, splice sites and 3'UTRs (synonymous mutations). Filtering using the gnomAD genome database with an inclusion criteria of <0.001 allele frequency (0.1% allele frequency) resulted in a list of 176 variants remaining. Similarly, the gnomAD exome database with a <0.001 allele frequency cut off was applied, removing a further 7 variants resulting in a final filtered list of 169 variants across the 42 patients. These two population databases were used to remove likely germline variation, as matched germline samples were not available on a per sample basis.

Using the maftools package, graphical summaries of these variants could be made to examine the final filtered variant list. Below (**Figure 42**) is an oncoplot showing the 10 most mutated genes across the 42 samples. *SF3B1, BIRC3* and *NOTCH1* were the most frequently mutated genes each being present in 10, 9 and 9 patients, respectively.

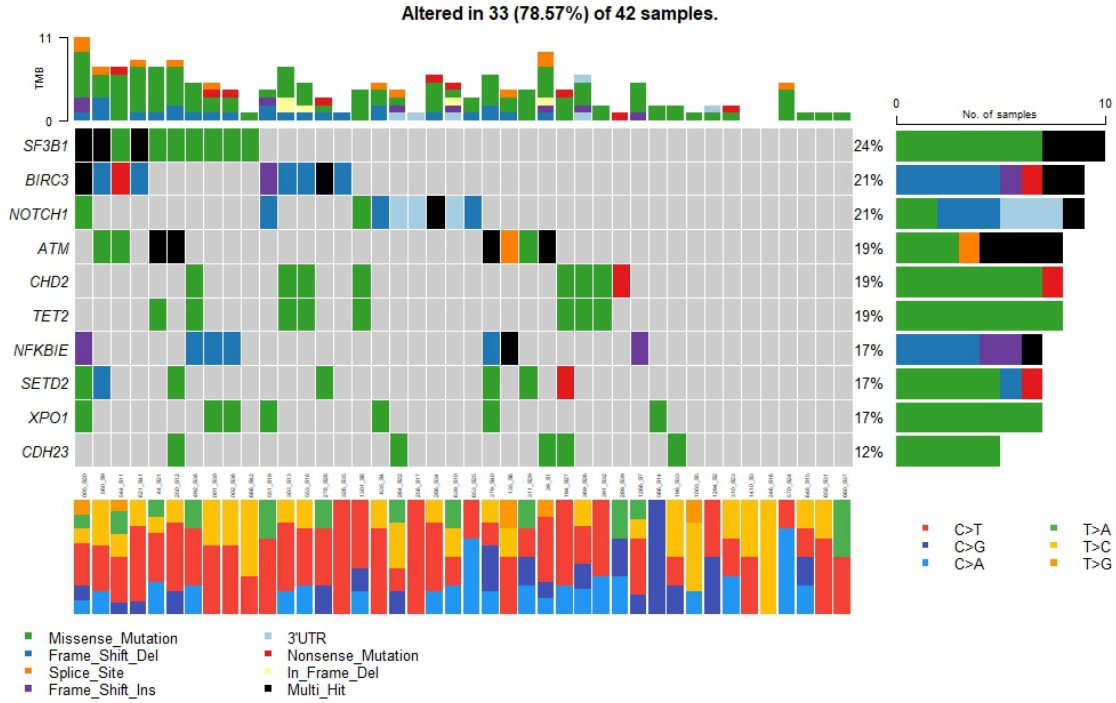

Figure 42- Oncoplot of the top 10 most frequently mutated genes across the 42 samples. The rows represent each of the 42 patients included in this analysis. The colour indicates the type of variant, for example 3'UTR or a missense mutation.

Lollipop plots of various genes allowed further examination of the filtered variants, for example the *BIRC3* gene frequently (n=5) had a frame shift deletion resulting in a Q547fs protein change (**Figure 43**). Due to the frequency of the variant, there was uncertainty around whether this was a true variant and therefore this variant was manually inspected further.

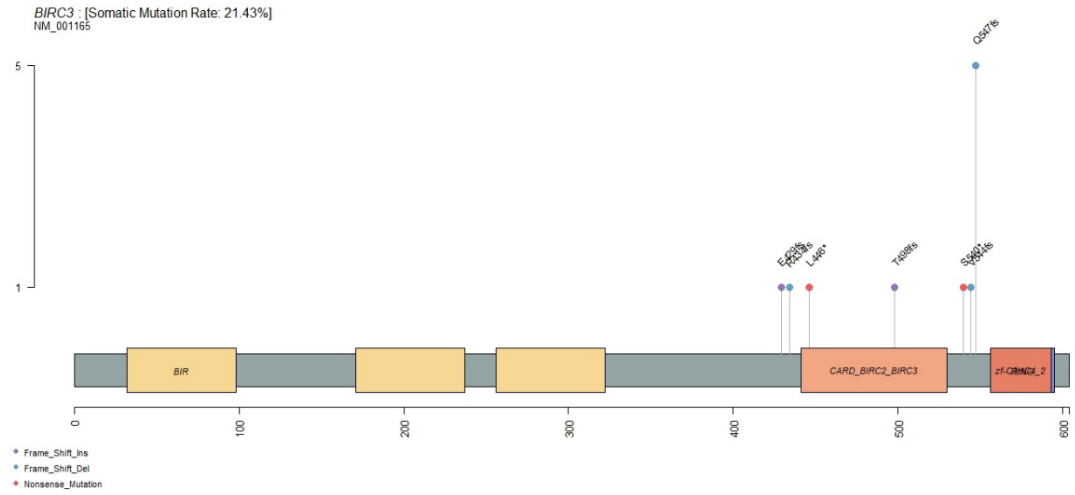

Figure 43- Lollipop Plot of the *BIRC3* gene, showing the 11 variants identified in the gene.

5.4.3.2.3 Results from manual curation steps

As highlighted above in **Figure 38**, the three target sequencing panels used to generate the variant data for the ARC/ADM and CLL4 cohort in this project are integrated together, only 9 genes are present in all. Therefore, variants that were not one of the 9 gene targets present in all probes were removed (n=100), resulting in 69 variants that progressed to the final stage of manual curation where IGV software was used.

The final step in manual curation is visual inspection of the variant and its surroundings using the IGV software. Established criteria for distinguishing true somatic variants were used (261); which included assessing if the change was present on both the positive and negative strand, what percentage of the reads had the change, if the surrounding reads have many changes (noisy reads) or if the variant was present at the end of the gene or frequently at the end of a read. **Figure 44** shows two examples of variant visual inspection using IGV. **Figure 44A** is the view of a *TP53* gene variant that has passed IGV inspection as the missense mutation is present on many of the reads (VAF 40%), was found similarly across both the positive and negative strand (382+ vs. 533-) and the variant was not frequently occurring at the end of a reads. Furthermore, the immediate surrounding area was not laden with other changes or variants. Whereas **Figure 44B** shows a *POT1* missense mutation that failed IGV inspection as it had a low VAF (4%), was in a bad position at the end of the *POT1* gene and many of the missense mutations (C<T) were at the end of reads. Applying these criteria during visual inspection of each variant allowed a further 20 variants to be disregarded, resulting in a final list of 49 variants across the 42 patients included in this analysis. The most commonly mutated gene was *SF3B1* (8/42, 19%), followed by *XPO1* (7/42, 16.7%) and then *NFKBIE* (6/42, 14.3%). Three clinically important genetic variants in CLL: *TP53, ATM* and *NOTCH1* were found in 2, 4 and 4 patients, respectively.

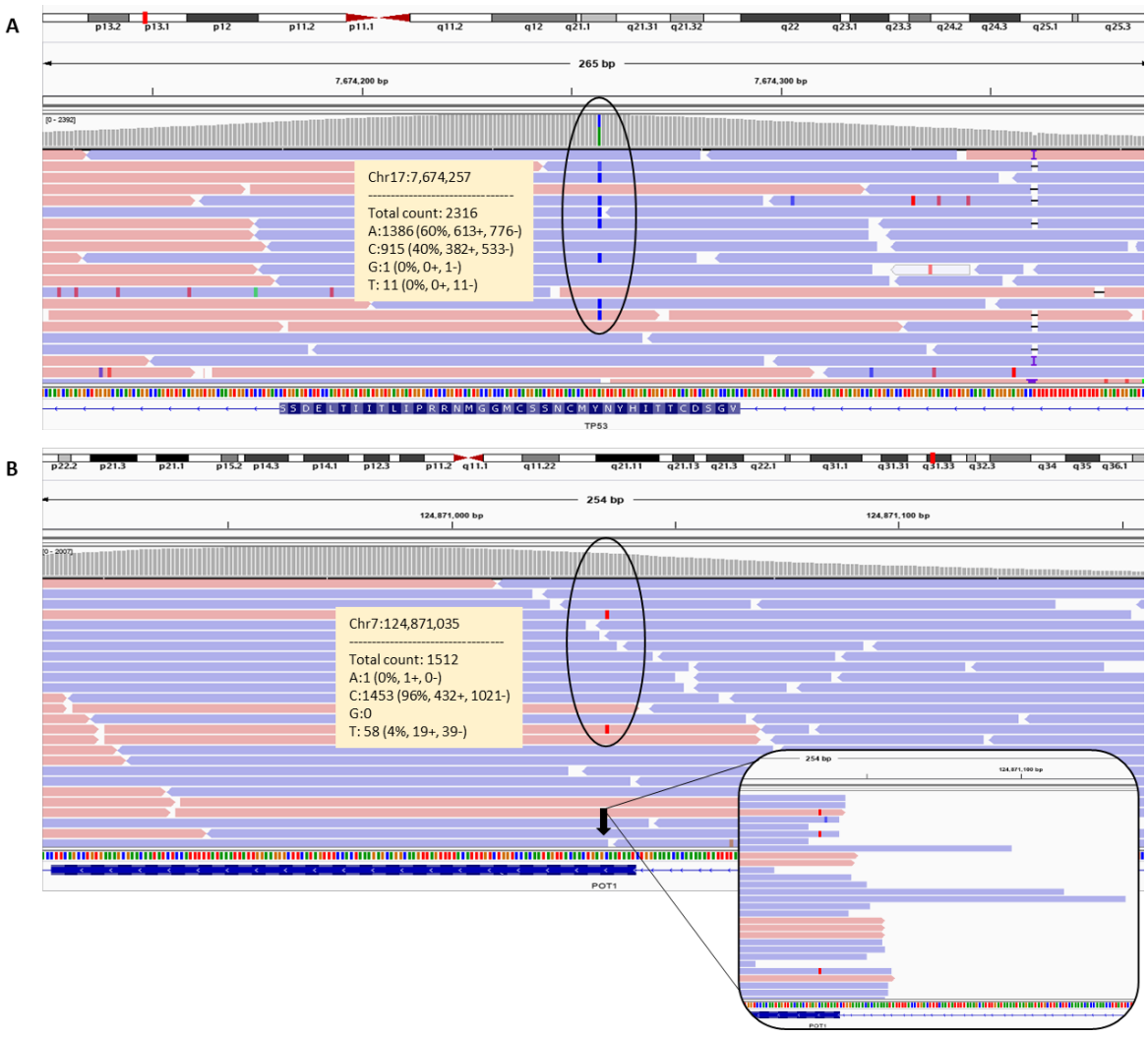

Figure 44- Output from two variant assessment using IGV. A. A region containing a missense mutation in the *TP53* gene (A>C), an example of a variant that would pass IGV visual assessment. B. Assessment of a region containing a POT1 missense mutation (C>T), this variant did not pass visual inspection criteria as had a low variant allele frequency (4%) and was in a bad position at the end of the POT1 gene with many of the variants being identified at the end of reads.

5.4.4 Generation of copy number aberration data

The generation of copy number aberration data through shallow whole genome sequencing was completed in various stages. Firstly, a cohort of 70 clinical trial patients were identified as requiring this datatype and therefore underwent library preparation using Agilent SureSelect Whole Genome Library prep and multiplexed sequencing on the Illumina NovaSeq. Subsequently, a second batch of 107 clinical trial patients also underwent library preparation for sWGS. Of these cases 5 failed library preparation so only 102 cases were sequenced. Below (**Figure 45**) is a schematic of the main steps in generating this sWGS data across the two main cohorts, highlighting where samples had to be excluded and the final numbers reached.

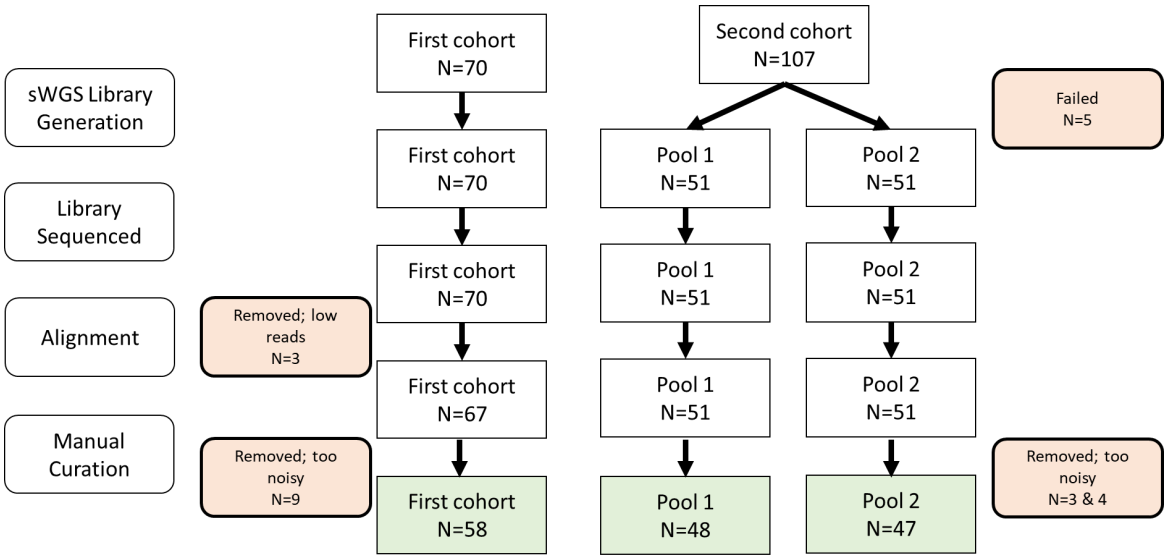

Figure 45- Overview of the steps involved in generating copy number aberration data using shallow whole genome sequencing. Highlighted in red shows the number of cases removed from the experimental pipeline and the reason for the exclusion. Highlighted in green shows the final cohorts of patients with successful data generation completed.

5.4.4.1 Library preparation

The SureSelect library preparation kit was used to generate a DNA library for each patient included in the CNA experimental cohort. Greater detail of the library preparation process and the sequencing completing using the Illumina NovaSeq 6000 platform, is given in 3.4.5.2

5.4.4.2 Pipeline development for improved CNA calling

Sequencing data generated from sWGS DNA libraries were analysed using an in-house bioinformatic pipeline (described in 3.4.5.2) but required optimizations, which will be discussed.

Work was undertaken to develop the Rstudio based pipeline and improve the CNA calling ability of the analysis. This work involved altering the bin sizes, deciding on various cut offs and classifications and defining the manual curation process. The first cohort of 70 cases with sWGS data was used to complete this work. Subsequently the optimized pipeline was applied to the remaining cohort of 102 patients.

A parameter that was explored was the size of bins created as the first step of the QDNAseq analysis. There is no specific bin size as using a large bin size will have less noise but will have a lower resolution, with smaller bins having greater resolution but will suffer more from technical noise. Additionally, bin size depends on the type of analysis and how it will be used and therefore should be chosen in relation to the sequencing depth. Examining the current literature, a wide

range of bin sizes have been employed for the analysis of sWGS data including 5 kb, 15 kb, 20 kb, 30 kb and 100 kb (213,299–301).

To examine what the optimal bin size is for this data, I compiled a subgroup of six samples and applied various different bin sizes and compared the results generated from the analysis. These size cases were chosen to try and be representative of the greater cohort, for example samples with low and high levels of noise were included. Originally a 5 kb bin size was applied to this cohort. This resulted in many CNAs being called even after the +/-0.2 log2 ratio cut off being applied. Additionally, the copy number called plots showed significant noise making it hard to be confident in the small CNA that were being called when they were visually inspected during the manual curation step (see **Figure 46A**).

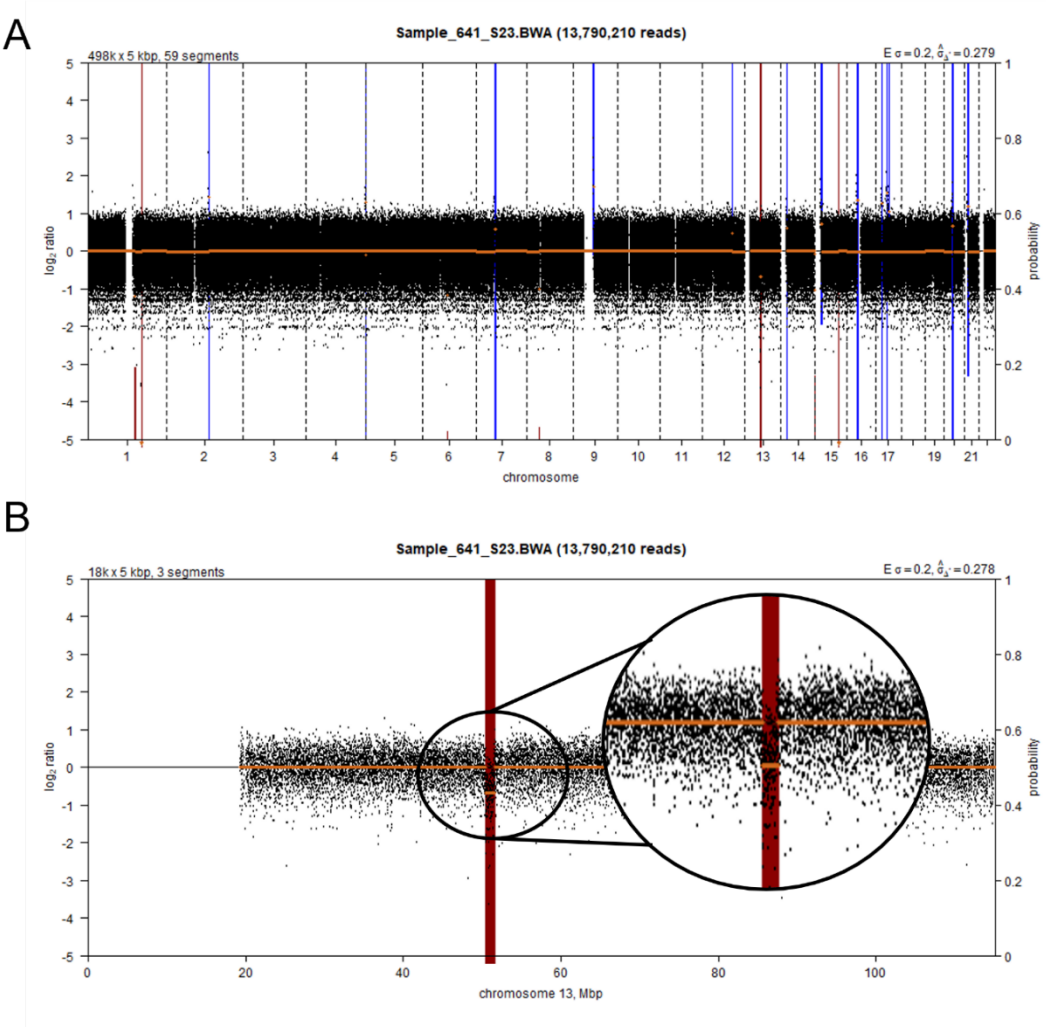

Figure 46- Copy number called plot of sample 641 with bin size of 5 kb. A. Shows each 5 kb bins plotted across the whole genome. Considerable noise is present in the plot with many small insignificant CNAs being called but after visual inspection will be removed because it is difficult to distinguish from the technical noise variation. B. Chromosome 13 showing a del13q event that is identified using 5 kb bins even when the plot is noisy.

A more stringent bin size of 50 kb was employed and found that this removed a lot of the noise present however when assessing the copy number called plots the data points became very sparse and made visual inspection difficult, see **Supplementary Figure 6**. Finally, a bin size of 30 kb was used and was found to be a good compromise between removing technical noise, making the manual curation more manageable, but whilst keeping good resolution which allows smaller CNAs that were removed during the filtering process to be confidently identified during manual curation. For example, sample 641 has a del13q event which was constantly identified at all bin sizes (see **Figure 46B** and **Figure 47B**). However, when using bin size 30 kb compared to 5 kb, many of the smaller called CNAs were removed across the genome as shown in **Figure 47A**. On visual inspection at bin size 5 kb, these would be removed as cannot be distinguish against the considerable noise of the plots. Thereby using the larger bin size, these called CNAs are being removed as part of the filtering, thus making the manual curation step less time consuming. A further reason for selecting a bin size of 30 kb is that similar bin sizes (20 kb and 30 kb) have been frequently used in publications using sWGS data (299,301).

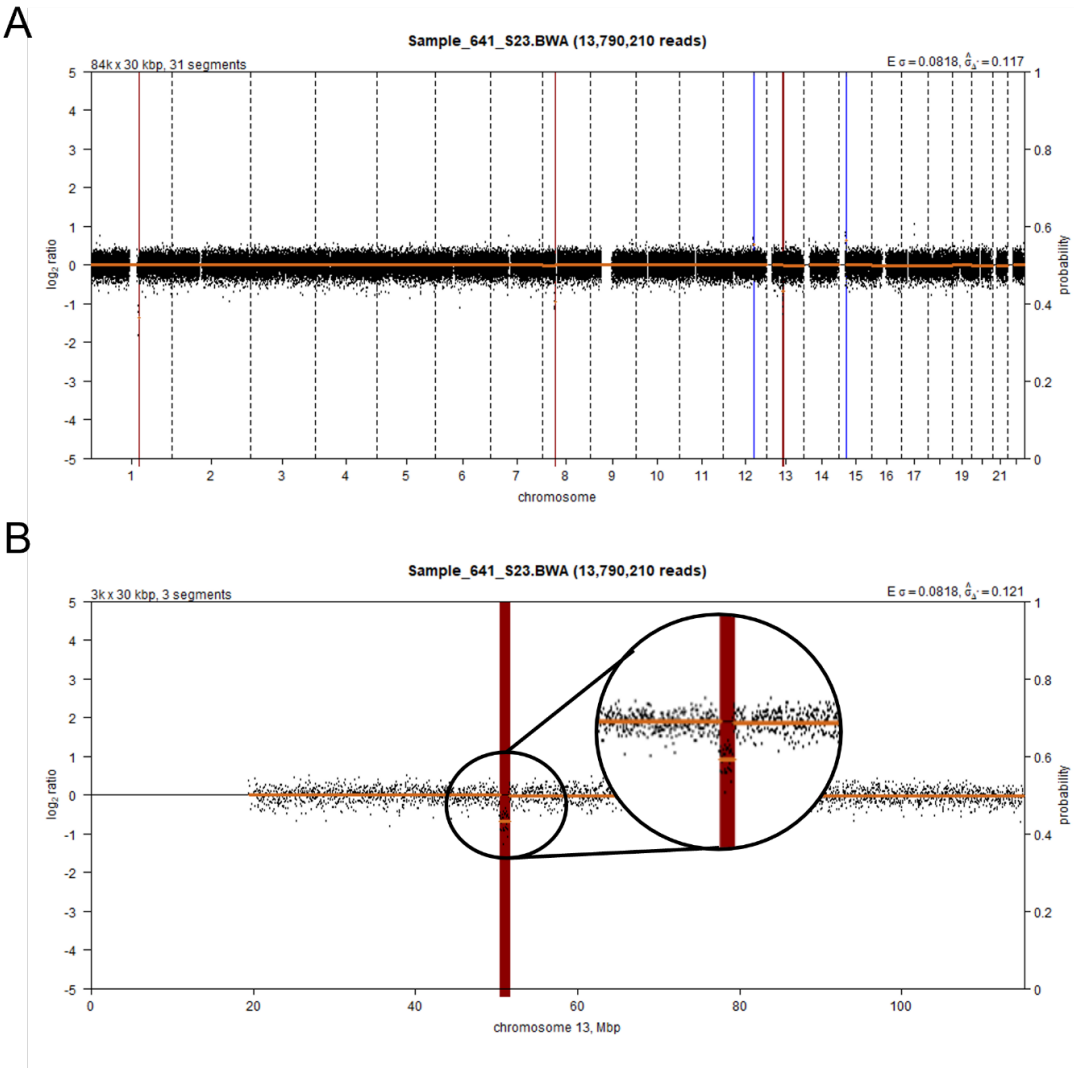

Figure 47- Copy number called plot of sample 641 with bin size of 30 kb. Shows each 30 kb bins plotted across the whole genome. A few small CNAs are being called across the genome which did not pass the filtering steps and were easily accepted or rejected during manual curation B. Chromosome 13 showing a del13q event that is identified clearly using 30 kb bins.

Overall, completion of this work generated 153 new cases of CNA data which will be integrated with previously generated data for the CLL4 and ARC/ADM cohorts. Furthermore, undertaking the experimentation with certain aspects of the data analysis allowed greater certainty in the CNA calling ability of the pipeline.

5.5 Conclusion

Overall, completion of the work outlined in this chapter resulted in 273 new data points being generated. As a result, 199 new patients now met inclusion criteria for the project outlined in the chapter below. Therefore, the cohort that will be used included a total of 495 CLL patients from

CIT clinical trials that all had CNA, TL and variant data available. This cohort was then employed to describe the biological context of GC and assess its clinical utility as a prognostic biomarker with CLL.

Chapter 6 Evaluation of Genomic Complexity within a Discovery and Validation Cohort

6.1 Synopsis

This chapter is cumulative effort of the experimental and computation work outlined in the previous chapter, as the cohort complied in Chapter 5 was utilised in this project. For this chapter, I undertook the laboratory and analytical work for create novel CNA, somatic variant and TL data using sWGS, HS2 and MMQPCR techniques, respectively. Furthermore, I completed the analytical work to infer copy number profiles for a cohort of ARCTIC and ADMIRE patients which has 450k array data already available. The various datasets, generated by me or by others previously, were then collated together and used in statistical and survival analysis, all of which was completed by myself. Within this chapter the novel biomarker GC was assessed within a CIT clinical trial cohort of 495 patients. Evidence is given which suggests the GC is an important prognostic marker in CLL and an in-depth description of the biological background of GC and its association with a breath of genomic variables is given, many for the first time.

6.2 Introduction

As depicted in the systematic review completed in Chapter 2, there is a growing evidence base that concludes that GC is an important prognostic and predictive biomarker which has great utility in the risk stratification of CLL patients enrolled not only in CIT but also targeted agent treatment regimes (103,198,204,232–234,238). Whilst the overarching conclusion is that GC is a clinically powerful biomarker, this is predicated on research that has used a variety of technologies for its detection and even using different definitions of the GC metric. Whilst this chapter is not able to empirically state what the most appropriate technology and metric is for the GC biomarker, an evaluation of the four genomic technologies used within this work will be completed and other metrics of GC will be considered, i.e CNA count and dosage. Furthermore, there is disparity between the clinical utility of different GC groups, i.e. ≥3 CNAs and ≥5 CNAs, with some publications reporting that ≥3 CNAs is a useful cut off to describe GC whereas others only find a cut off of ≥5 CNAs has independent prognostic ability (103,238). It has been suggested that a biological heterogeneity maybe underpinning this variation, with different biological pathways and interactions driving the contrasting levels of GC and leading to a different clinical presentation and patient outcome. Thus, an aim within this chapter was to assess the biological composition and describe the genomic profile of three GC groups; low (0-2 CNAs), intermediate (3-4 CNAs) and

high (≥5 CNAs). Finally, this project aimed to investigate the survival impact of GC in the context of numerous other established CLL biomarkers, many for the first time, using a discovery (CLL4) and validation (ARC/ADM) CIT clinical trial cohorts. The inclusion of the GC, TL and DME biomarker within a single survival model has, to my knowledge, not been completed before.

6.3 Methodology

A cohort of patients enrolled in either the CLL4, ARCTIC or ADMIRE clinical trials was constructed and used in this chapter. The assembly of this cohort, whereby previously published data and newly generated data was augmented together, is explained in greater detail in Chapter 3 and Chapter 5. A cohort of 495 patients was used for the statistical analysis of GC. Whereas separated CLL4 (n=251) and ARC/ADM cohorts (n=226) were used for survival analysis due to having very different amounts of follow up data. 18 ARC/ADM cases were excluded from the survival analysis cohort due to concerns about the CNA data generated from the 450k array. Inclusion criteria for this project was dependent on if a patient had available CNA, variant and TL data. Furthermore, many patient characteristics and clinical biomarkers, such as age, gender, CD38 expression, Binet stage and *IGHV* mutation status were reported on as part of the clinical trial.

6.3.1 Data analysis

Extensive details on the methodology and optimization of the analysis of CNA and variant data are given in 3.4.5 and 3.4.4. Analysis of this data was completed firstly using IRIDIS5, the supercomputing system at the University of Southampton. Analysis was then completed within the R environment using R studio (version 4.3.0). An oncoplot and lollipop plots were constructed using the R package “maftools” (version 3.19). Both nonsynonymous and synonymous variants were included in the analysis, specifically the 3’UTR *NOTCH1* variants were included. The analysis of TL data generated using the MMQPCR technique is given in 3.4.3. sWGS and 450k array CNA data was generated using two bioinformatic pipelines described in detail in 3.4.5.1 and 3.4.5.2. Optimization of the MMQPCR, HS2 and sWGS pipelines is discussed in great detail in 5.4.2, 5.4.3 and 5.4.4.

6.3.2 Statistical analysis

Statistical analysis was completed using R studio within the R environment (version 4.3.0). Various graphs and diagrams, such as bar charts, scatter plots, and Sankey diagrams, were constructed using R studio. Packages used were “ggplot2”, “networkD3”, “dplyr” “plyr” and “table1”. Packages “viridis” and “RColorBrewer” were used to annotate the figures with specific colour schemes. GC

was defined using the three subgroups utilised in Leeksma 2020 study, with low, intermediate and high GC being defined as 0-2 CNA, 3-4 CNAs and ≥5 CNA, respectively (103). But CNA count and dosage, as continuous variables, were also employed to investigate GC at certain points during the statistical analysis. *TP53* aberration was defined as the presence of a del17q and/or *TP53* mutation. *ATM* disruption variable was divided into biallelic *ATM* inactivation, sole del11q (CN loss of *ATM*), sole *ATM* mutation and *ATM* wild type patients. Similarly, *BIRC3* disruption was assessed by the presence of a biallelic *BIRC3* loss, sole CN loss of *BIRC3*, sole mutation of *BIRC3* or *BIRC3* wild type. Comparisons of the genomic technologies; sWGS, HumanOmni array, SNP 6.0 array and 450k array, with FISH data found a high concordance for calling the four recurrent CLL CNAs, **Table 10**. Therefore, the presence of the four recurrent CNAs; del17p, del11q, trisomy 12 and del13q, was reported using CNA data generated using the four genomic technologies and not with FISH data.

6.3.3 Survival analysis

A post hoc power analysis was completed to identify the sample size which is sufficient to capture survival trends that are being studied in this chapter. A sample size calculator for designing clinical research was employed to calculate the number of cases required to have sufficient power for survival analysis. The software required the input of certain parameters for example; a type 1 errors rate of 0.05 and a type 2 error rate 0.2 (302). As there were three GC groups included in the analysis, multiple power calculations were needed with each comparing two of the groups, for example low vs. intermediate GC and low vs. high GC. For each comparison the proportion of subject in each group were required to be inputted into the calculation. Finally, a relative hazard was needed and for this value published work was examined to identify a HR for each pairwise comparison and each survival endpoint was needed. The published work the HR were extracted from needed to include the same three GC classifications. For PFS, the HR reported in the Kater et al paper was employed (233). For OS, the HR reported in the Leeksma et al paper was used (103). However in the Leeksma paper, whilst they employed the same GC classifications, no comparison was reported between patients with intermediate and high GC and therefore this power calculation could not be completed.

Included in the univariate and multivariate survival analysis was the covariate treatment arm. As the treatment regime patients were enrolled in differed across the two clinical trial cohorts. CLL4 patients were divided into one of the following; Fludarabine plus Cyclophosphamide (FC), Chlorambucil (Chl) or Fludarabine (FDR). Whereas the ARC/ADM clinical trial patients were enrolled into either fludarabine, cyclophosphamide and rituximab (FCR), the addition of mitoxantrone to FCR (FCMR), mitoxantrone with low-dose rituximab (FCMminiR) or finally a

regime that started on FCMminiR but then crossed over to FCR following medical recommendations (FCMminiR/FCR). Additionally, *BIRC3* disruption was assessed differently in the survival analysis compared to the statistical analysis, with only cases of *BIRC3* biallelic loss being compared against patients without a biallelic *BIRC3* loss.

Univariate analysis was completed using a KM analysis with a log rank test as well as a Cox regression analysis, whereby each covariate was individually entered. The median PFS and OS for each subgroup of every variable was calculated. This analysis was completed using R Studio within the R environment (version 4.3.0) using “survival”, “survminer”, “survivalAnalysis” and “ggplot2” packages. The results from the univariate analysis guided which covariates were included in the primary multivariate models as only variables that were significant in the univariate analysis (p-value<0.05) were included. A stepwise backwards elimination process was applied, using a likelihood statistic to test whether it was appropriate to remove a covariate from the model, until a final model was reached.

6.4 Results

6.4.1 Examining variant and copy number data for the statistical cohort of 495 patients

Across the 495 patients, 211 did not have any variants present in the 9 genes of interest. A total of 426 variants were recorded across the remaining cohort of 284 patients. Therefore, on average a patient had 0.86 variants (0-6). The most frequently mutated gene was *SF3B1* with 111 patients, or 22% of the cohort, carrying a mutation in the gene. The *NOTCH1, ATM* and *TP53* gene was mutated in 15%, 11%, and 9% of patients, respectively (**Figure 48**). The most common variant classification type identified in the data was a missense mutation, frameshift deletions and nonsense mutations accounting for 258, 105 and 29 of the 426 recorded variants. Included in the analysis were 7 cases of a 3’UTR *NOTCH1* mutation.

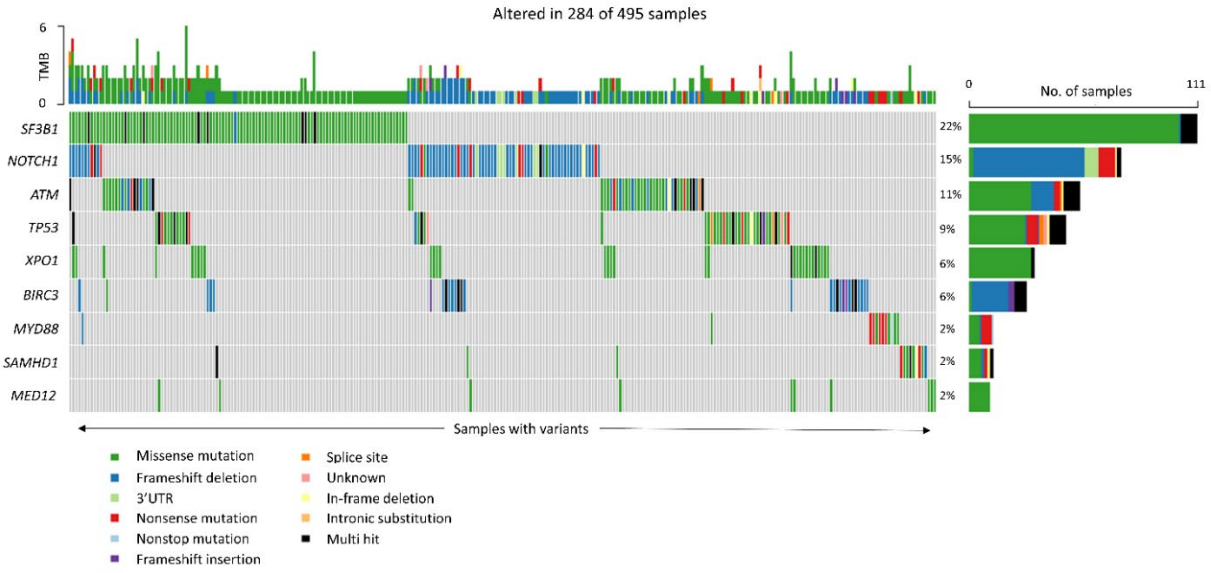

Figure 48- Oncoplot shows the overview of somatic mutations in the total clinical trial cohort of 495 CLL patients.

Frequently, a gene had a greater number of variants than the number of patients, which indicates there are cases where a patient may have one or more genetic variant. For example *SF3B1* mutations are present in 111 patients but have a recorded 121 variants. Similarly, a total of 65 variants in the *ATM* gene are recorded across 65 patients and a total of 59 *TP53* variants have been identified across 47 patients. The lollipop plots of the four most commonly mutated genes shown in **Figure 49**, displays the distribution of variants and highlights the common and rare variants identified within our cohort. For example, the most common *SF3B1* variant involved K700E which had a recorded 54 cases (45%). Within CLL, this K700E has been found to be the most frequently mutated site with it being identified in 50% of reported cases with a *SF3B1* mutation (303). Similarly in the *NOTCH1* gene, the most common mutation site is the p.P2514fs, also known as a deltaCT mutation, with 31 of the reported *NOTCH1* mutations (42%), which is concordant with the CLL literature. Next the compiled copy number data used in this project was examined.

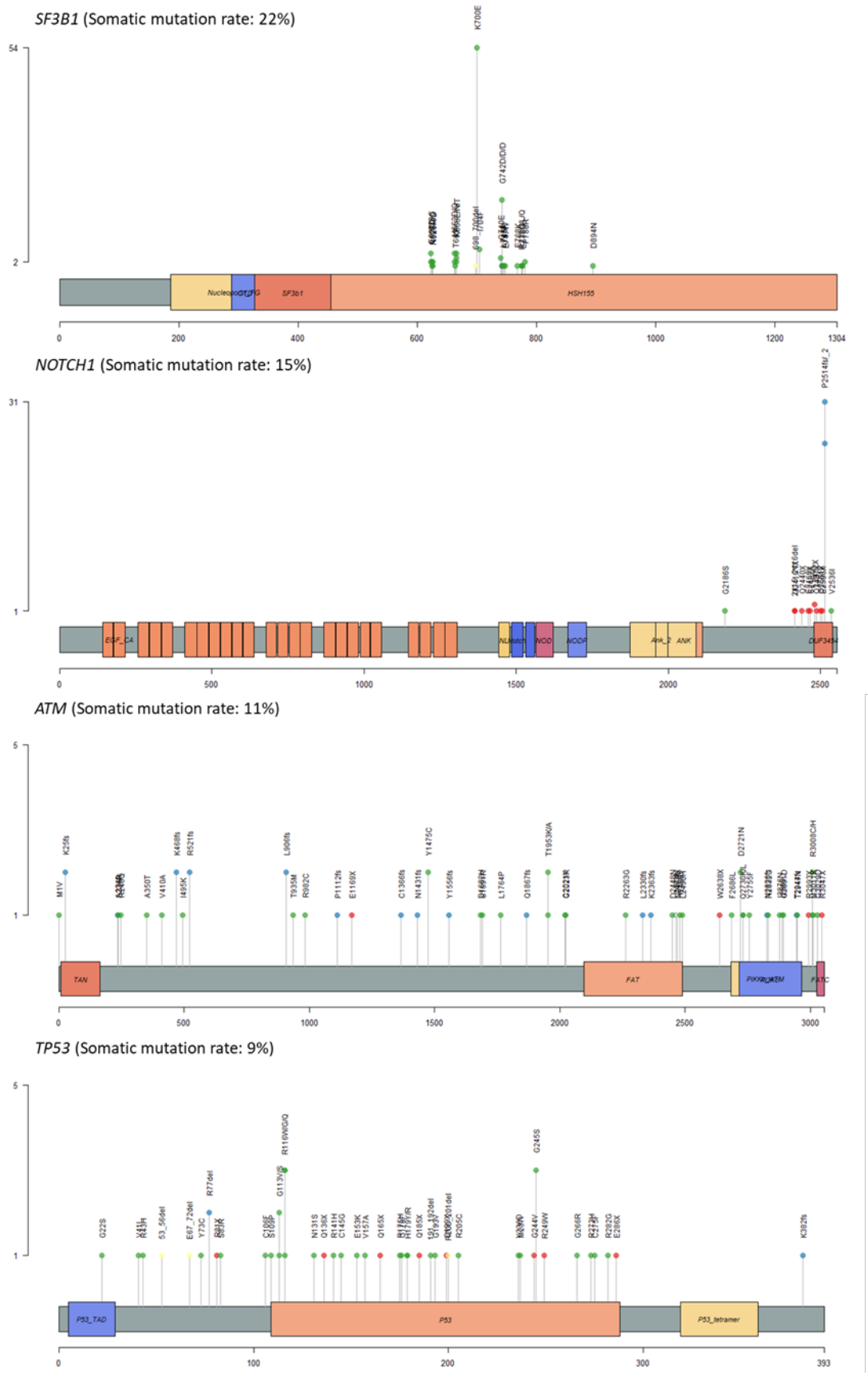

Figure 49- Lollipop plots of the four most frequently mutated genes across the 495 CLL patients.

Of the 153 cases that had sWGS data generated for, 8 were not included in the final cohort of 495 patients as lacked variant data as failed the HS2 library preparation or sequencing (**Figure 36**).

Therefore, of the 495 cases 144, 108, 212, and 31 were generated from sWGS, SNP6 array, HumanOmni array and 450k array, respectively.

All raw CNA was aligned to the hg19 reference genome. Once all data was collated, I completed a UCSC genome liftover to the hg38 reference genome. During this step, a small percentage of the CNA events failed the liftover. This is due to certain regions not being well-conserved between the two genomes. As I was unable to be certain of their start and stop location but required all data of the cohort to be updated to a more recent human reference genome, these cases were excluded from any downstream analysis. Across the 495 cases there were 1595 CNAs. Of them 68 failed the liftover and a further 59 were removed as they were cnLOH events. The cnLOH were removed as not all techniques employed in the cohort were able to measure these events and thus were removed to standardise the analysis. This meant a remaining 1468 copy number changes were reported and included in this analysis.

Assessment of these 1468 revealed that 62 were aneuploidy, most commonly of chromosome 12 (n=58). However further inspection of the 450k array data, specifically of the CNA plots similar to those shown in **Figure 47A**, identified an additional 4 cases with trisomy 12 events, increasing the total number of aneuploidy events to 66 with 62 of them being trisomy 12. These were not included in the CNA count or GC calculations.

I also used the hg38 location of certain genes to classify different CNAs. For example, *TP53*, *ATM*, *DLEU2* for del17p, del11q and del13q events, respectively. Additionally, I assessed whether the CNA event impacted other relevant genes; *BIRC3*, *RB1* and *RNASEH2B* (**Table 8**). Locations of the genes were reported from the UCSC genome browser (Hg38). When defining biallelic del13q I have included the diminished X2 and homozygous loss events and when the log -2 ratio as less the -1 (n=51). Furthermore, to examine del13q events with greater granularity I also classified these cases based on the two del13q classes and types. Class 1 and type 1 del13q copy number deletion overlaps the *DLEU2* gene as this is in the MDR of del13q. Class 2 deletions are larger and has a target region that includes the *DLEU2* and *RNASEH2B* gene. Similarly type 2 deletion targets a region including the MDR and the *RB1* gene.

Table 8- Genomic regions from the GRCh38 reference genome used to annotate the copy number data with important CNAs.

Gene	Hg38 location (Hg_start-Hg_stop)	Number	Cases (%)
TP53	7668421-7687490	21	21 (4)
ATM	108223067-108369102	89	89 (18)
BIRC3	102317484-102339403	76	76 (15)
DLEU2	49982552-50125541	258	234 (47)
RNASEH2B	50909791-50956762	176	172 (35)
RB1	48303751-48481890	133	131 (26)

As mentioned above, CNA count, excluding aneuploidy events, was used to define the GC metric used in this project. Mainly three classifications of low, intermediate and high GC were used within this chapter. However, CNA count as a continuous variable was also employed to examine biological associations with GC. Similarly, dosage, the total size of the genomic region impact by the CNAs excluding aneuploidy (Mb), was also investigated.

6.4.2 Assessing the prevalence of genomic features across the cohort

The distribution of the three GC groups across the total cohort of 495 patients is shown below in **Figure 50**. The majority of patients were defined in the low GC groups (62%) with only 22% having intermediate GC and 16% having high GC. When excluding aneuploidy events, a total of 1406 CNA was recorded across the cohort with an average of 2.8 CNA per patient (range: 0-26 CNA). Furthermore, on average a patient reported a dosage of 30 Mb (range: 0-303.44 Mb).

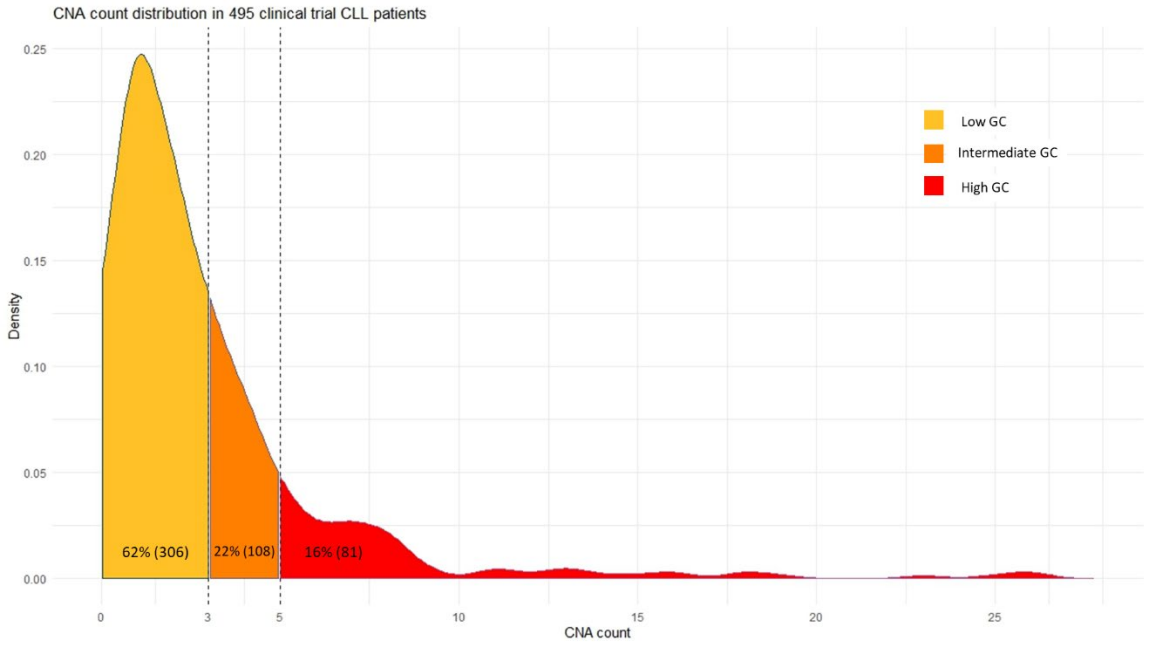

Figure 50- Density curve of CNA count across the total cohort of 495 CLL clinical trial patients. The three GC classification groups are coloured with the number of patients and percentage of the cohort each group has is also given.

A table of variables important in this project is shown below, showing the prevalence of various variables across the two clinical trial cohorts that were combined for statistical analysis completed in this chapter. A chi squared test identified a significant (p-value<0.01) difference in GC groups across the two cohorts and a Wilcoxon rank sum test also identified significant difference in CNA count (p-value<0.01) and dosage (p-value<0.05) across the two cohorts. This difference across the two clinical trial cohorts will be examined in greater detail below. No significant difference in gender, *IGHV* mutation status, *TP53* dysfunction, *BIRC3* disruption, trisomy 12 events, del13q events, mutation count, *SF3B1* and *NOTCH1* mutations was found across the cohorts.

Table 9- Baseline clinco-biological variables of the ARCTIC, ADMIRE and CLL4 trials

Variable	**ARCTIC & ADMIRE N (%)**	**CLL4 N (%)**	**Concordance P-value**
Total number of patients	244	251	
Age, median years (range)	63 (36-80)	64 (42-86)	<0.01
Gender			
Male	183 (75%)	184 (73.3%)	0.67
Female	61 (25%)	67 (26.7%)	
Binet Stage			
A	35 (14.4%)	64 (25.5%)	<0.01
B	127 (52%)	110 (43.8%)	
C	82 (33.6%)	77 (30.7%)	
IGHV Mutational Status			

IGHV-U	129/218 (59.2%)	141/221 (63.8%)	0.32
IGHV-M	89/218 (40.8%)	80/221 (36.2%)	
TP53 Aberration			
Absent	218 (89.3%)	227 (90.4%)	0.69
Present	26 (10.7%)	24 (9.6%)	
ATM Disruption			
Absent	177 (72.6%)	193 (76.9%)	<0.05
CNA	30 (12.3%)	41 (16.3%)	
Mutated	24 (9.8%)	12 (4.8%)	
Biallelic	13 (5.3%)	5 (2%)	
BIRC3 Disruption			
Absent	201 (82.4%)	203 (80.9%)	0.62
CNA	27 (11.1%)	36 (14.3%)	
Mutated	9 (3.7%)	7 (2.8%)	
Biallelic Loss	7 (2.9%)	5 (2%)	
Trisomy 12			
Absent	207 (84.8%)	226 (90%)	0.08
Present	37 (15.2%)	25 (10%)	
Del13q			
Absent	115 (47.1%)	145 (57.8%)	0.05
Monoallelic	104 (42.6%)	81 (32.3%)	
Biallelic	25 (10.2%)	25 (10%)	
SF3B1 Mutation			
Absent	193 (79.1%)	191 (76.1%)	0.71
Present	51 (20.9%)	60 (23.9%)	
NOTCH1 Mutation			
Absent	209 (85.7%)	212 (84.5%)	0.71
Present	35 (14.3%)	39 (15.5%)	
Epigenetic Subgroup			
n-CLL	103/220 (46.8%)	115/226 (50.9%)	<0.01
i-CLL	61/220 (27.7%)	83/226 (36.7%)	
m-CLL	56/220 (25.5%)	28/226 (12.4%)	
Telomere Length Group			
Short	56 (23%)	137 (54.6%)	<0.01
Intermediate	62 (25.4%)	61 (24.3%)	
Long	126 (51.6%)	53 (21.1%)	
Telomere Length, median length kb (range)	3.63 (1.13-7.68)	2.88 (1.93-10.24)	<0.01
CNA count, median count (range)	2 (0-26)	2 (0-23)	<0.01

Dosage, median size Mb (range)	9.09 (0-303.44)	4.25 (0-268.93)	<0.05
Mutation Count			
0	95 (38.9%)	116 (46.2%)	0.42
1	97 (39.8%)	87 (34.7%)	
2	35 (14.3%)	34 (13.5%)	
≥3	17 (7%)	14 (5.6%)	
Genomic Complexity			
Low GC	134 (54.9%)	172 (68.5%)	<0.01
Intermediate GC	63 (25.8%)	45 (17.9%)	
High GC	47 (19.3%)	34 (13.5%)	

Footnote: CNA data used in variables are generated from genomic techniques, not FISH. Continuous variables were summarised as median and range, and categorical variables were shown as proportions. A chi squared was to test the concordance between categorical variables and a Wilcoxon rank test was used for continuous variables.

A significant difference between the two cohorts was identified across the TL groups and the continuous TL variable (p-value<0.01). To further inspect this difference, the results of the two technologies employed to generate TL data were examined. For the generation of the TL data in the CLL4 cohort, the MMQPCR technology was employed. Whereas the STELA technique was used predominantly to generate the ARC/ADM TL data. However, it is important to note that 11/244 ARC/ADM patients had TL generated using the MMQPCR technology as part of the 60 cases that had TL data added during this project. A density plot displaying the distribution of the TL results given from each technology shows that there is a difference in the mean and median TL given by each technology, see **Figure 51** and **Table 9**. The median TL of the MMQPCR cohort (mean: 2.87 kb) was significantly shorter than the median TL of the STELA cohort (mean: 3.66 kb) (p-value<0.001). Whilst the MMQPCR technology had a shorter mean and median TL compared to the STELA data, this cohort had a large spread of TL recorded, with the results ranging from 1.93 kb to 10.24 kb. This difference in TL recorded across the cohorts also was found in the TL groups, with the majority of ARC/ADM patients being reported as having TL-L (51.6%) whereas the CLL4 patients were predominantly in the TL-S (54.6%).

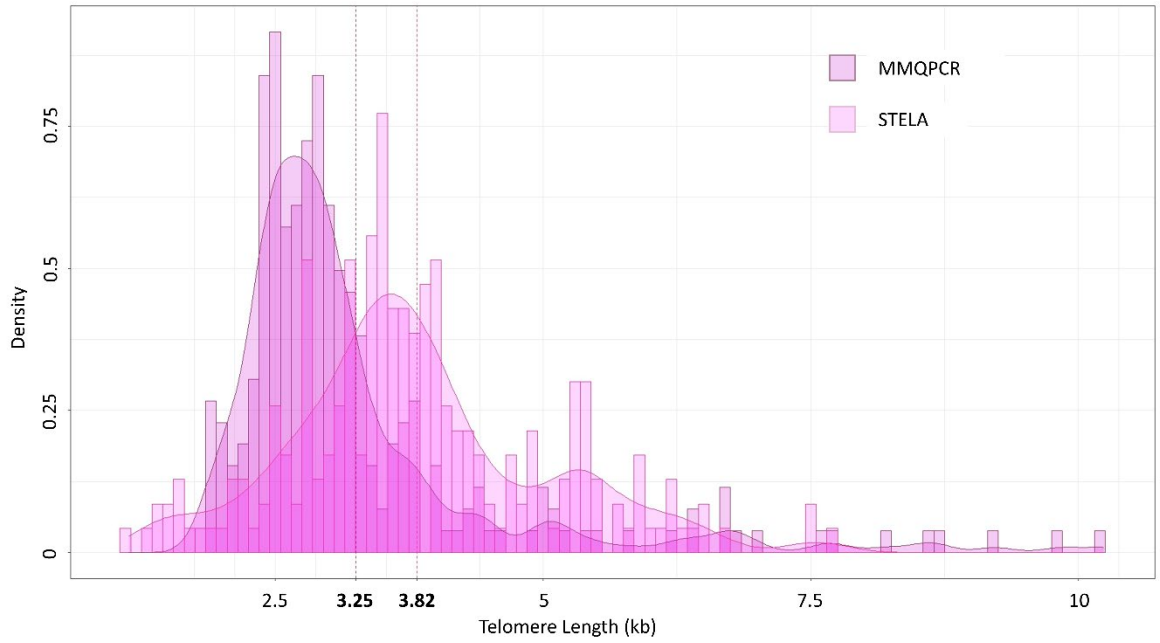

Figure 51- Density plot of the TL measurements across the two TL technologies; MMQPCR and STELA. The mean TL from MMQPCR (3.25kb) and STELA (3.82kb) technologies are annotated and shown in bold.

To further examine the difference between the two technologies a sub cohort of 80 CLL4 patients that had TL generated by both MMQPCR and STELA was used. A Kendall's rank correlation test found a significant positive correlation between the recordings from the two technologies (0.657 correlation coefficient, p-value<0.001), see **Supplementary Figure 7.** Therefore, even though a significant difference in TL was identified across the two cohorts, the reported high correlation between the two technologies suggests that the difference across the cohorts is due to patient variation and not due to biases within the technology used. Therefore, the two clinical trial cohorts were combined for the following statistical analysis completed below.

6.4.3 The prevalence of many established biomarkers shows biases towards certain GC subgroups.

Firstly, a oncoplot which included many important genomic features was constructed to investigate how the three GC group lie in the context of other established CLL biomarkers. The somatic landscape shown in the tumour mutational burden (TMB) graph of the oncoplot (**Figure 52**), highlights that as GC increases so does TMB. Additionally, the number of cases with zero TMB decreases as GC increases, for example 42/306 patients with low GC and 13/108 of intermediate GC have zero TMB compared to only 4/81 of patients with high GC.

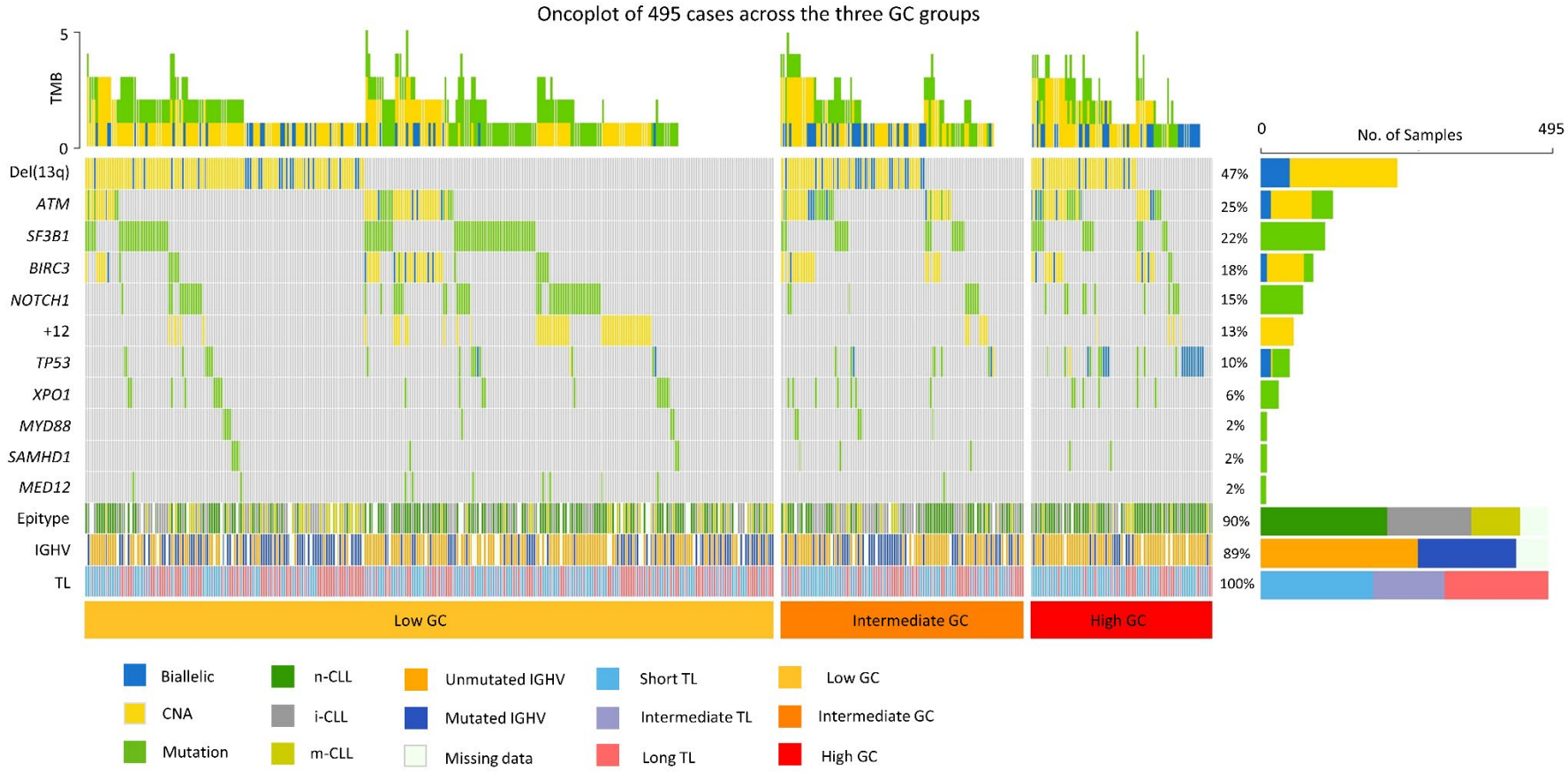

Figure 52- Oncoplot of a variety of genomic features including CNAs and mutations as well as the *IGHV* mutation status, epitype and TL variables. The three GC groups were used to order the samples. Del13q were coloured to include both biallelic and monoallelic disruptions. Similarly, the *TP53*, *ATM* and *BIRC3* rows were coloured to show if patient had a copy number deletion that overlapped this gene (CNA), a mutation of this gene (Mutation), or both a deletion and mutation (Biallelic). *IGHV* status and epitype was not reported for all 495 and this missing data is coloured in the *IGHV* mutation status and epitype row. Tumour mutation burden (TMB) was calculated from the mutation and CNA data.

Of the 10% of the total cohort that had *TP53* aberration (n=50), 46% were in the high GC group and 18% had intermediate GC, whereas 36% had low GC. Interestingly, of the 23 cases with *TP53* aberration and high GC, in 9 cases this *TP53* aberration was the only genomic change reported. Examining the least commonly mutated genes, *XPO1* and *SAMHD1* were found to have an even distribution across the three GC groups. For example, the percentage of cases in low, intermediate, and high GC group with a *XPO1* mutation was 6.2% (19/306), 6.8% (7/108), and 7.4% (6/81), respectively. Whereas the *SAMHD1* gene was mutated in 2.3%, 2.8% and 2.5% of low, intermediate, and high GC cases, respectively. Trisomy 12 events were more frequent in the low GC group (17%) than the intermediate (5.6%) or high group (4.9%). Additionally of the 62 trisomy 12 events, 24 patients also had a *NOTCH1* mutation (38.7%). Examining this cohort of 24 patients, most (n=20) were in the low GC group. Similarly, of the 125 cases which had either a mutation, CNA loss or both (biallelic) of *ATM*, 76 cases also had either a *BIRC3* mutation and/or CNA loss. The cases where both *ATM* and *BIRC3* was disrupted were more frequent in patients with high GC (24.7%) or intermediate GC (18.5%) than patients with low GC (11.7%). Finally, the oncoplot in **Figure 52** shows a higher prevalence on U-CLL in the high GC group and a bias toward certain TL and epitype groups across the three GC groups. Therefore, further assessment of GC association with *IGHV* mutation status, TL and epitype was completed below.

6.4.4 Increasing GC is negatively correlated with TL and closely connected with many biomarkers that reflect the proliferative history of CLL

The three GC groups were found to have a significant difference in the proportion of U-CLL and M-CLL cases (p-value<0.001). Specifically, most patients with high GC also had a unmutated *IGHV* status (83%, n=62) compared to only 17% of patients having M-CLL (n=13). The high GC group had a significantly greater proportion of U-CLL cases than either low or intermediate GC, with both of these groups having only 57% of cases with U-CLL, see **Figure 53**. Similarly, a significant difference across the three GC group was also found when examining TL and epitype.

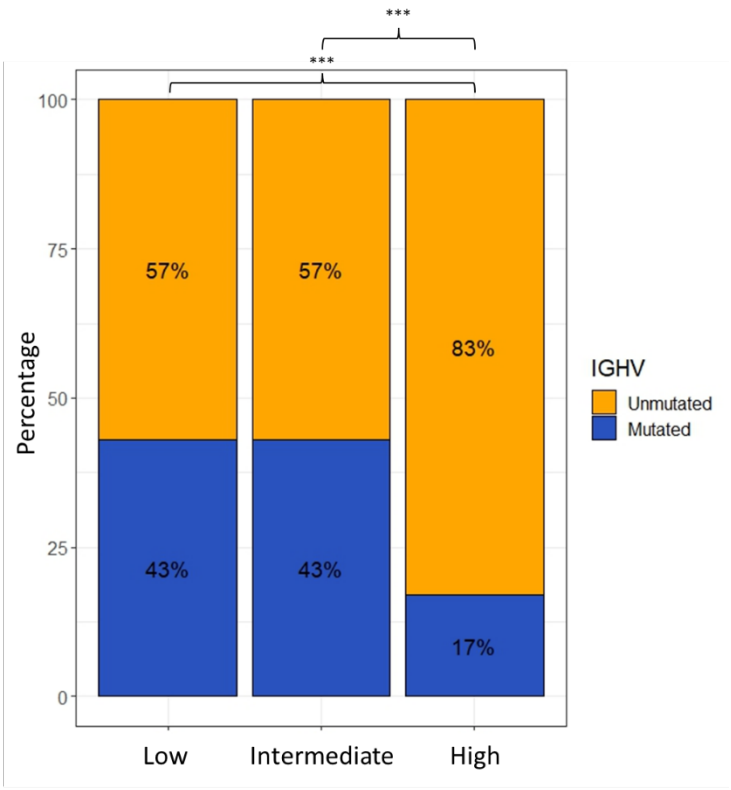

Figure 53- Stacked bar chart of the proportion of U-CLL and M-CLL cases in each of the three GC groups. A pairwise chi squared was employed to test the significance difference in the *IGHV* status prevalence across the three GC groups, p-value<0.001 shown by three asterisks (***).

Figure 54A displays the significant difference in the cases of n-CLL, i-CLL and m-CLL across the three GC groups. The low GC against both intermediate and high GC were significantly difference in proportion of the three epitype groups (p-value<0.05). Specifically, the low GC group had 82 i-CLL cases (31%) but the intermediate GC group had 45 cases (44%), but had similar proportions of n-CLL (47% vs. 41%) and m-CLL (22% vs 15%). In fact, the largest epitype group in the low GC group was n-CLL epitype (47%) whereas the i-CLL had the highest proportion of the intermediate GC group (44%). Comparing low to high GC groups, the n-CLL cases seemed to differ the most with it accounting for 64% of the high group whereas only representing 47% of the low GC group. Between the intermediate and high GC group epitype varied greatly (p-value<0.01). m-CLL cases were present in similar proportions of the intermediate and high groups, 15% and 14% respectively. But the high group was composed mainly of n-CLL cases (50/78) whereas the i-CLL epitype (45/102) was the most prevalent in the intermediate GC group. TL across the three GC group differed, with the high group having a significant difference against low (p-value<0.01) and intermediate (p-value<0.05). As **Figure 54B** shows, low and intermediate GC cases have a similar proportion of the three TL groups. However the largest proportion of low is the TL-L (39%) followed by TL-S (35%), whereas the greatest proportion of intermediate was TL-S (38%) followed by TL-L (35%). However the high GC group is mainly composed of TL-S (67%) with a smaller

portion of both the TL-L (26%) and TL-I (17%) groups. This relationship between TL and GC was also found when TL was assessed as a continuous variable and plotted against CNA count, a continuous variable. A Kendall's rank correlation test found a significant (p-value<0.001) negative correlation (coefficient; -0.12) between the two continuous variables, scatterplot is shown in **Figure 55**. Therefore, as CNA count increases TL decreases which is concordant with the trends identified between the TL and GC categorical variables, **Figure 54B**. A Sankey plot was also compiled to examine the relationship between GC, epitype and TL (**Supplementary Figure 8**). The nodes and links of the Sankey diagram illustrates that patients with high GC typically also had TL-S and the n-CLL epitype. An even distribution of the intermediate GC across the TL groups was found as intermediate GC accounted for 21%, 24% and 21% of TL-S, TL-I and TL-L group, respectively. Conversely, the intermediate GC patients accounted for 19%, 31% and 18% of n-CLL, i-CLL and m-CLL cases, again highlighting the association between intermediate GC and i-CLL epitype. The biological characteristics of the three GC groups are further examined below through assessing their association with additional biomarkers.

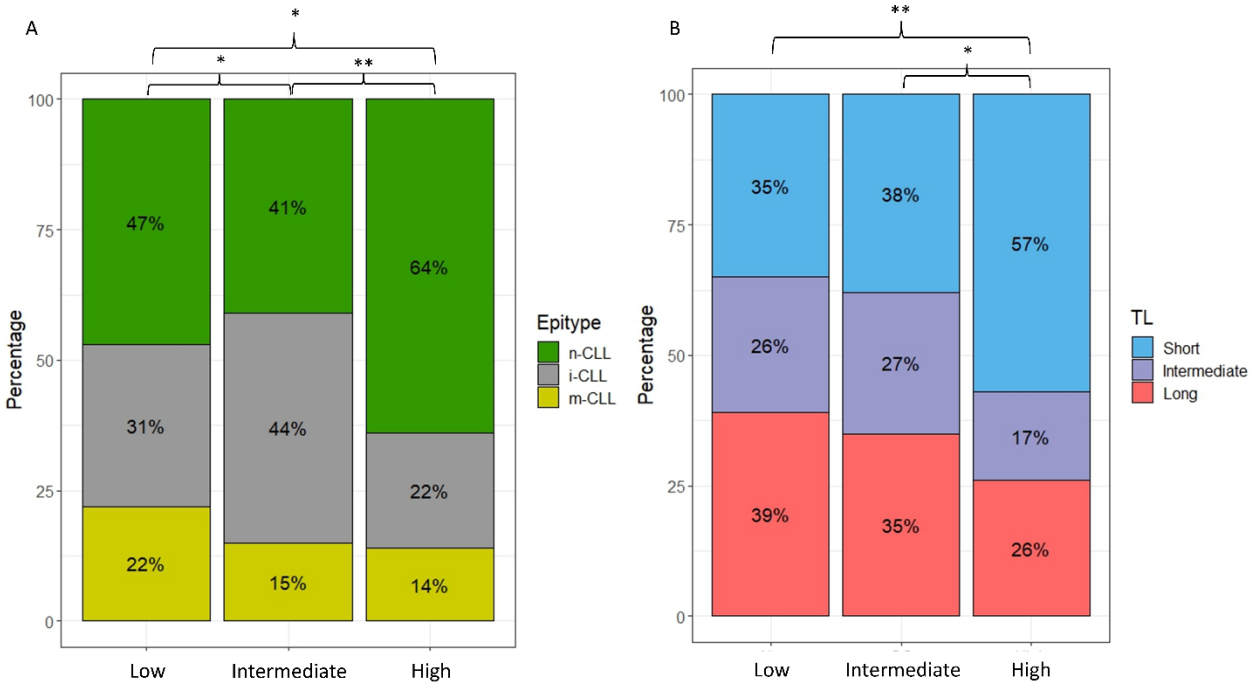

Figure 54- Stacked bar chart of the proportion of the three epitype (A) and TL (B) groups in each of the three GC groups. A pairwise chi squared was employed to test the significance difference in the *IGHV* status prevalence across the three GC groups, p-value<0.05 is shown by a single asterisk (*) and a p-value<0.01 is shown by two asterisks (**).

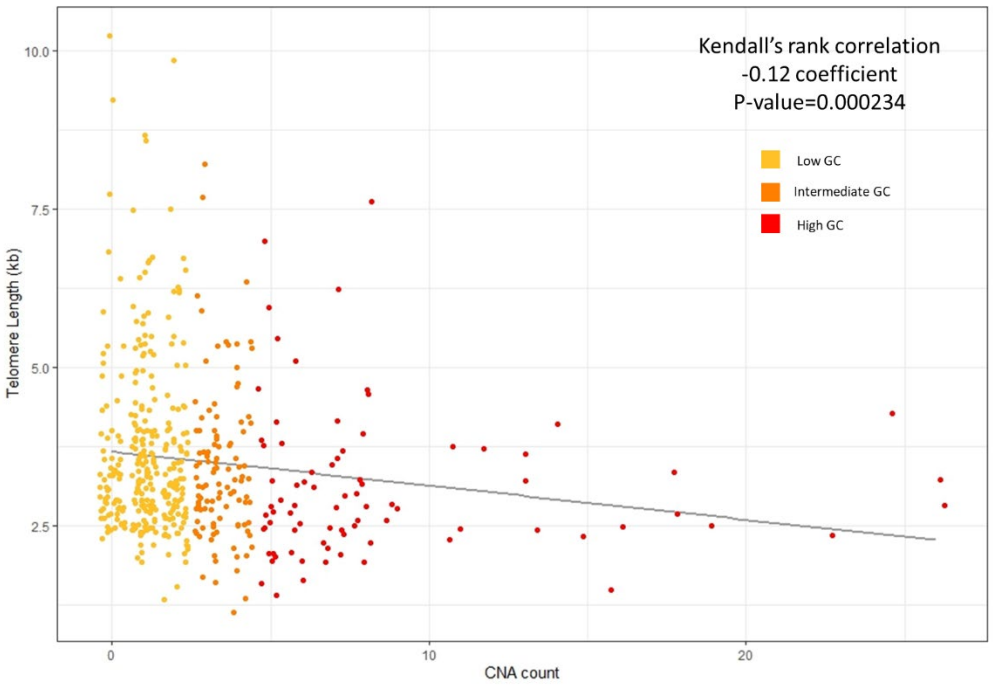

Figure 55- Scatter plot of CNA count against TL, both as continuous variables, for 495 CLL patients. The points are coloured based on the three GC classification groups; low, intermediate and high. A Kendall's rank correlation test was used to compare the TL given by the two metrics for each patient.

6.4.5 High GC is linked with the presence of *TP53* aberration and various other poor risk biomarkers

Firstly, mutation count, the number of mutations recorded per patient from the screening of the 9 genes, was assessed. Please note that in some cases more than one variant was reported in a gene, all variants were included in mutation count. A significant (p-value<0.05) difference in mutation count was found between the high GC group against low or intermediate GC, see **Figure 56**. The low and intermediate GC group had a mean mutation count of 0.86 (range: 0-6) and 0.71 (range: 0-3) mutations whereas the high GC group, on average had 1.07 mutations (range: 0-3). However, when comparing mutation count against CNA count as a continuous variable, no significant difference in CNA count was found as mutation count increased, see **Supplementary Figure 9**.

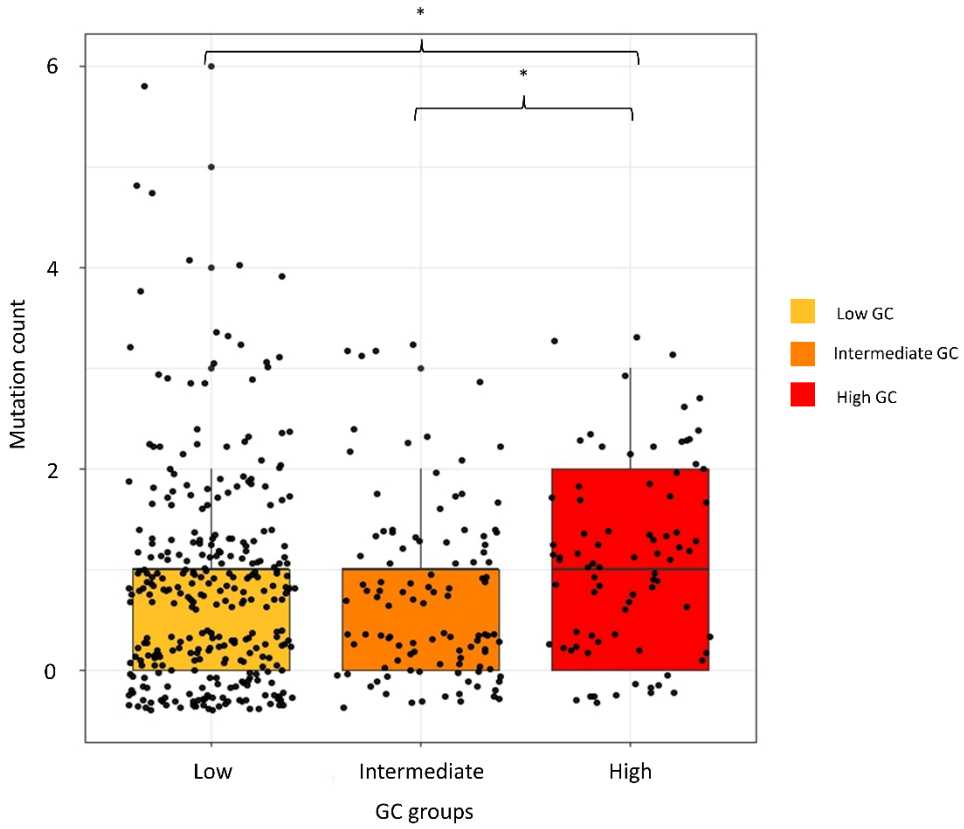

Figure 56- Boxplot showing the range of mutation count reported in each of the three GC groups; low, intermediate and high. A pairwise Wilcoxon test was utilised to examine the difference in mutation count between two GC groups, a p-value<0.05 is indicated by a single asterisk (*).

Further mutations and CNA events across the three GC groups were examined through the construction of a bar chart (**Figure 57**), illustrating the prevalence of various genomic disruption events across the three GC groups. Firstly, the most prevalent genomic disruption reported was del13q, occurring in 235 patients with 185 cases being a monoallelic loss and 50 being a biallelic loss. A significantly higher prevalence of del(13q) monoallelic events was reported in the high GC group compared to low GC patients (p-value<0.01). The monoallelic del13q event was present in 33%, 41% and 51% of low, intermediate and high GC patients, respectively. Whereas a biallelic del13q event was significantly more prevalent in patients with intermediate GC (19%) compared to low (8%, p-value<0.05) or high GC (7%, p-value<0.01). Next, *TP53* dysfunction, a *TP53* mutation and/or del17p event, was found to have a significantly (p-value<0.001) greater frequency in patients with high GC than either the intermediate or low GC patients, see **Figure 57**. 28% (n=23) of patients with high GC also had *TP53* dysfunction compared to only 8% and 6% of intermediate and low GC patients.

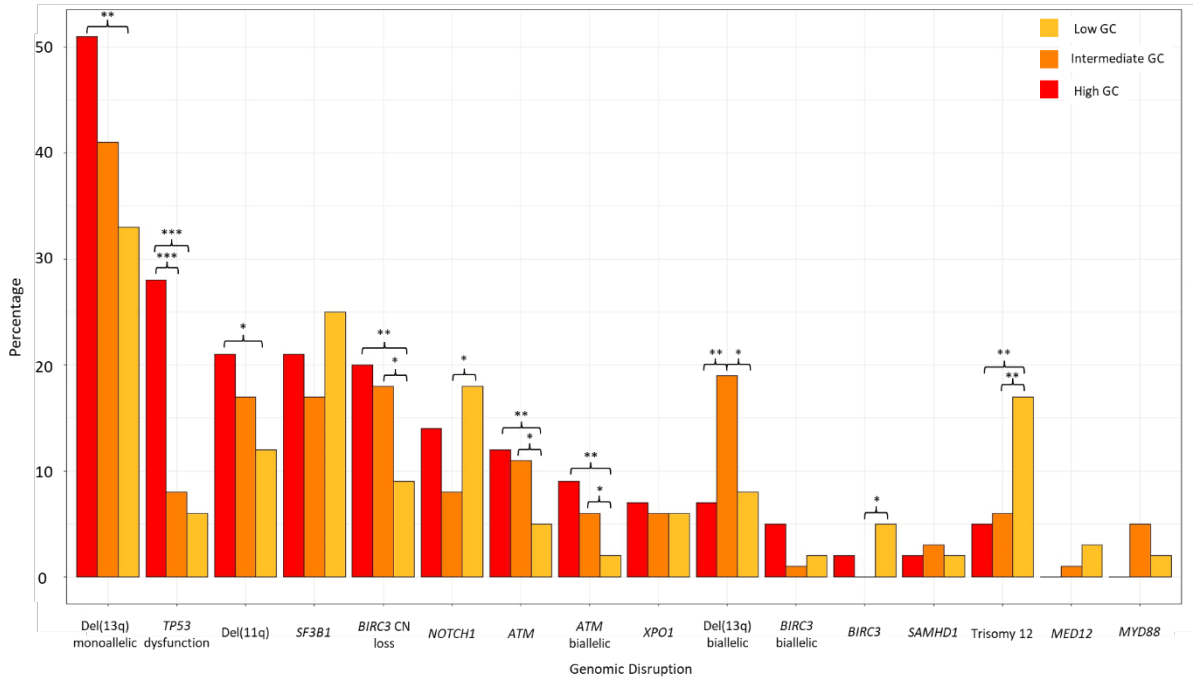

Figure 57- A bar chart illustrating the prevalence of various genomic disruptions, including mutations of genes, CNA, biallelic losses of genes, across the three GC groups (coloured bars). The y axis shows the percentage of low, intermediate, and high GC patients that have each genomic disruption. For example, 25% of patients with low GC also have a *SF3B1* mutation. Certain variables had many subgroups, for example *ATM*, del(11q) and *ATM* biallelic groups were cases with only a mutation of the gene, a copy number loss which overlapped the gene or both a mutation and copy number loss, respectively. A pairwise chi squared test was used to analyse the independence of mutation/CNA events across the three GC groups. For the comparison of GC groups with 5 or less events, a Fishers exact test was used instead. p-value<0.05 *, p-value<0.01 **, and p-value<0.001 ***.

Assessing the remaining two recurrent CNA events described in Dohners seminal paper, it was found that the frequency of both del11q and trisomy 12 cases differed across the GC groups (**Figure 57**). Specifically, a significantly greater proportion of the high GC group (21%) had del11q event compared to the low GC group (12%, p-value<0.05). No significant difference in del11q events was found between the intermediate group against low or high GC. Conversely, trisomy 12 had a significant greater prevalence in low GC patients compared to intermediate or high GC (p-value<0.01). Of the 306 patients with low GC, 52 patients also had a trisomy 12 event (17%) compared to only 6% of intermediate and 5% of high GC patients. The disruption of *BIRC3* and *ATM* were classified using the same system. For example, *ATM* signifies the number of cases with a mutation in that gene, del11q signifies the presence of the copy number loss that overlapped the *ATM* gene and *ATM* biallelic represents a patient with both a mutation and copy number loss of the gene. As previously mentioned, del11q events differed across the GC groups, however *ATM* mutations and biallelic *ATM* loss was also found to be significantly dominant in certain GC groups.

High GC had a significant greater proportion of *ATM* mutations and biallelic *ATM* loss than low GC patients (p-value<0.01). Similarly, intermediate GC had a significant greater proportion of *ATM* mutations and biallelic *ATM* loss than low GC patients (p-value<0.05). Assessment of *BIRC3* dysfunction identified that both high (20%, p-value<0.01) and intermediate GC (18%, p-value<0.05) group had a significantly greater proportion of *BIRC3* copy number losses event than the low GC group (9%). In contrast, no significant difference in the presence of biallelic *BIRC3* loss was found across the three GC groups and a greater prevalence of *BIRC3* mutations was identified in the low GC group compared to intermediate GC (p-value<0.05). Of the remaining 6 mutation groups, only a significant difference in *NOTCH1* (p-value<0.05) prevalence was found, with a greater percentage of the low GC patients having this mutation compared to high or intermediate GC group. Further examination of del13q events were investigated and is outlined below.

6.4.6 Increased GC was not affiliated with del13q subtypes, a finding reported in the literature

Published literature has further classified del13q events using two naming systems; class 1&2 and type 1&2 (144,304,305). Class 1 and type 1 del13q event are copy number losses that encompasses the MDR (*DLEU2*). The class 2 del13q events are much larger and impact not only the MDR but also the *RNASEH2B* gene whereas a type 2 event includes the MDR and the *RB1* gene. When comparing the reported CNA count of the 2 class groups and 2 type groups, no significant difference was found between the class groups or type group. However, patients with no del13q had a significantly smaller CNA count than patients with del13q (p-value<0.001) (see **Supplementary Figure 10**), irrespectively of the del13q subgroup. This result was also found when comparing the del13q subgroups and GC as a categorical variable as the distribution of the three GC groups was similar in the class 1, type 1, class 2 and type 2 (see **Supplementary Figure 11**). A final examination of the del13q cases where cases were classified not only based on class and type, but also if the deletion was monoallelic or biallelic. This analysis found there was a significantly higher percentage of low GC (64.7%) patients in the cohort of del13q cases which has a biallelic loss of both the MDR and *RNASEH2B* (p-value<0.05), see **Figure 58**. However, it is important to note that across the cohort of 495 patients, 17 cases have a biallelic loss of both genes (class2bi2) and only 11 cases where *DLEU2* was a biallelically lost in combination with a monoallelic deletion of *RNASEH2B* (class2bi). No significant difference in GC prevalence across the del13q type events, including the various monoallelic and biallelic subgroups, was found (**Supplementary Figure 12**).

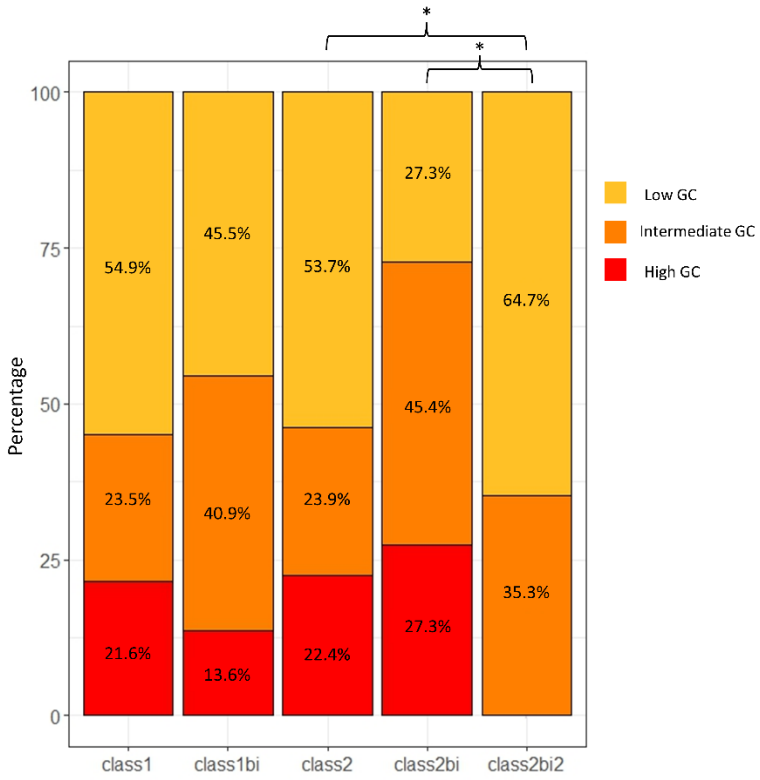

Figure 58- Stacked bar charting showing the distribution of the three GC groups across the different del13q subgroup. A pairwise chi squared was employed to test the significance difference in the GC prevalence across the five del13q classes, p-value<0.05 is shown by a single asterisk (*)

6.4.7 GC significantly co-occur with many poor risk clinical biomarkers.

Associations between GC and many clinically relevant CLL biomarkers were examined by calculating the OR, which quantifies the strength of association between two variables. The findings from this analysis supported much of the work previously completed in this chapter, but also add further granularity in describing the biological composition of the three GC groups.

Firstly, this analysis confirmed what was reported in **Figure 56**, as a mutation count of 2 were strongly co occurred with high GC. However, this association with high GC was not found between the 31 cases where three or more mutations were identified. Similarly, previously reported trends between GC and the three TL and epitype subgroups were also identified (**Figure 54** and **Figure 55**). High GC and the n-CLL epitype were significantly associated (p-value<0.01). Furthermore, a significant co-occurrence between intermediate GC and the i-CLL epitype was also found (p-value<0.01). TL-S was strongly associated with high GC (p-value<0.01) and significantly mutually exclusive with low GC (p-value<0.05). Similarly, high GC was found to be significantly negatively associated with TL-L. No significant association between the TL-I variable and the three GC classifications was identified. *TP53* aberration was found to be significantly co-occurring with high GC, conversely, low GC was significantly mutually exclusive (p-value<0.01). Of the 81 patients with

high GC, 23 patients had a *TP53* aberration (28%) compared to 18 patients (6%) of the low GC patients that were reported to have a *TP53* aberration.

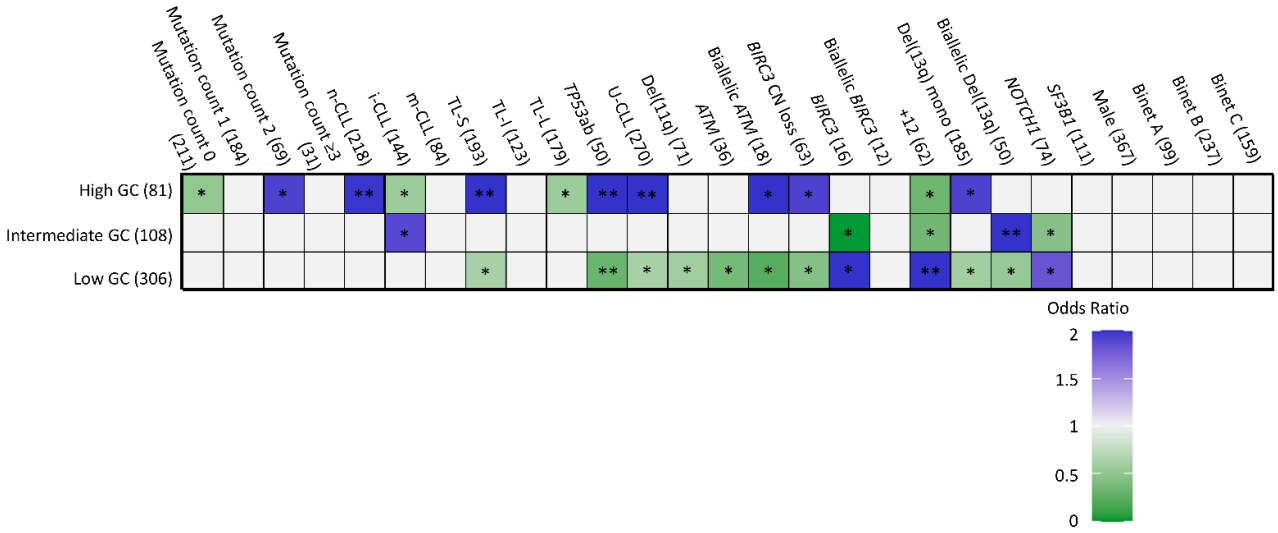

Figure 59- Association plot comparing GC against 13 clinical CLL biomarkers. The three GC subgroups are shown in the plot's columns and compared against all the variables, shown in rows, in a pairwise fashion. An odds ratio (OR) is calculated for each pairwise comparison of 27 subgroups from the 13 clinical variables. The OR quantifies the strength of association between two events, i.e. high GC and *TP53* aberration. A Fishers exact test was used to assess if the relationship between the two events was statistically significant. An OR with a p<0.05 is shown by an asterisk (*), an OR with a p<0.01 is shown by two asterisks (**), and p-values are corrected using false discovery rate (FDR) to account for multiple testing. A green-coloured square indicates an OR<1 and therefore the two variables are negatively associated, whereas a blue square indicates an OR>1 and therefore the two variables are positively associated.

The association plot reported that the presence of unmutated *IGHV* mutation status also co-occurred with high GC (p-value<0.01), which supports the previous finding reported in **Figure 53**. Trisomy 12 events were significantly associated with low GC (p-value<0.01) and significantly mutually exclusive with intermediate and high GC (p-value<0.05), as earlier reported (**Figure 57**). Assessing the presence of certain mutations identified that both *NOTCH1* and *BIRC3* mutations significantly co-occurred with low GC patients but were negatively associated with the intermediate GC (p-value<0.05), which is concurrent with previous analysis (**Figure 57**). *ATM* mutations and del11q events were significantly negatively associated with low GC (p-value<0.05), but not significantly associated with either intermediate or high GC (**Figure 59**). Conversely, biallelic *ATM* loss was negatively associated with low GC but strongly associated with high GC (p-value<0.05). The presence of a sole *BIRC3* copy number loss was also significantly associated the high GC group and mutually exclusive with low GC. Biallelic *BIRC3* loss was not significantly

associated with either of the three GC groups. Similarly, gender and Binet stage was not found to be statistically associated with GC.

6.4.8 450k array data reported, on average, significantly more CNA than the three other genomic technologies employed.

As mentioned above, a significant difference in CNA count, dosage and GC groups was found between the two clinical trial cohorts employed in this chapter. On average, the ARC/ADM cohort had a significantly greater CNA count per person than compared to the CLL4 cohort, with a mean CNA count being reported as 3.36 and 2.34, respectively (p-value<0.001), as illustrated in **Figure 60**. Whilst the median CNA count for both clinical trial cohorts was the same (2 CNA), the ARCADM cohort had a greater range of reported CNA count (0-26 CNA) than the CLL4 cohort (0-23 CNA). This translated into a significant difference in GC groups recorded for the two cohorts (p-value<0.01), with the proportion of CLL4 cases with low GC being greater than what was found when this GC classification was applied to the ARC/ADM cohort (low GC; 68% vs 55%), see **Supplementary Figure 13 and 14** and **Table 9**. As four different technologies had been used to generate CNA data, we wanted to further investigate if this difference between the two trial cohorts was due to technical biases of the technologies or due to normal patient variation.

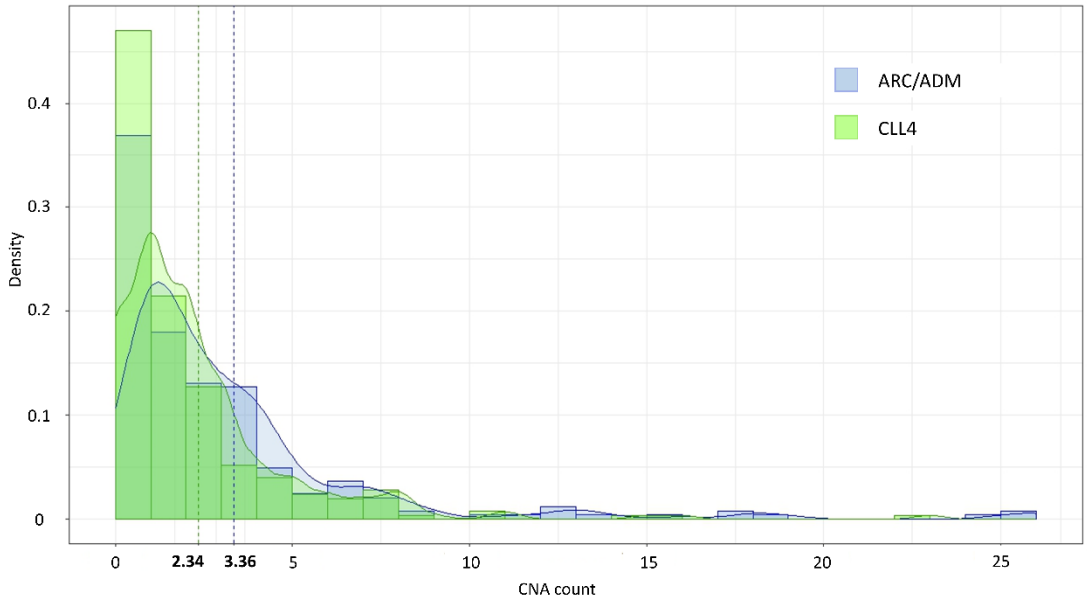

Figure 60- Density plot of CNA count across the two clinical trial cohorts; ARCTIC/ADMIRE and CLL4. The mean CNA count from CLL4 (2.34 CNA) and ARCTIC/ADMIRE (3.36 CNA) clinical trial cohorts are annotated and shown in bold.

A further density plot showing CNA count across the four technologies employed to generate CNA data was constructed, see **Figure 61**. 108 CLL4 patients had CNA generated using the SNP 6.0 array

technology and the remaining 143 cases were generated using sWGS technology. Whereas most of the ARC/ADM cohort CNA data was generated from HumanOmni array (n=212) with 450k data accounting for 31 patients and a single ARC/ADM clinical trial patient was processed using the sWGS technology. A pairwise Wilcoxon rank sum test identified a significant difference in CNA count between the 450k data and all three other technologies (p-value<0.001). The mean CNA count per patient was over double what the other technologies reported with 6.1 CNA per patient, compared to 2.99, 2.97 and 1.83 CNA reported in the SNP 6.0, HumanOmni and sWGS cohorts. Similarly, the 450k cohort had a greater median and a large range recorded (median: 5 CNA, range: 0-26 CNA). This caused the cohort of 31 patients with 450k array data to be mainly defined as having high GC (52%, 16/31). Across all other technologies, this high GC group was reported the least frequently with it only account for 15%, 20%, and 9% of the HumanOmni array, SNP 6.0 array and sWGS cohort, respectively.

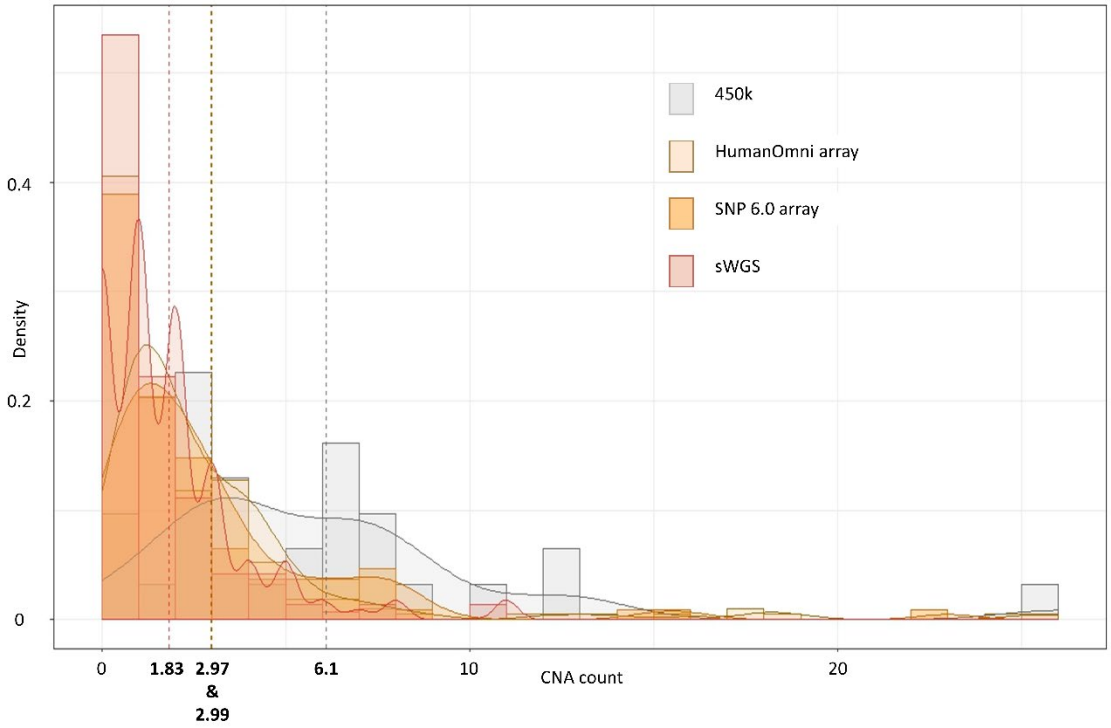

Figure 61- Density plot of CNA count across the four technologies used to generate CNA data; 450k, HumanOmni array, SNP 6.0 array, and sWGS. The mean CNA count from sWGS (1.83 CNA), HumanOmni array (2.97 CNA), SNP 6.0 array (2.99 CNA) and 450k array (6.1 CNA) are annotated and shown in bold.

Moreover, a significant difference in CNA count was found between patients in the sWGS group compared to the three other technologies (p-value<0.01). This technology, on average, detected less CNAs than the three other technologies and thus this group had a large percentage of patients that were classified in the low GC group (76%), see **Figure 61**. When comparing how this difference in CNA count influence the classification into the three GC groups, a significant

difference was found between sWGS and HumanOmni or SNP 6.0 array was found (p-value<0.05). However a greater statistical significant difference was reported when comparing the GC groups of the 450k array cohort to the three other technologies (p-value<0.001).

To further inspect these 4 cohorts that utilised differing technologies, the prevalence of certain patient variables were compared. The patient variables assessed included *TP53* dysfunction, *IGHV* mutation status, *ATM* disruption, *BIRC3* disruption, trisomy 12 and del13q events. Firstly, no significant difference across the four cohorts was identified when assessing *TP53* aberration or *IGHV* mutation status. A significant difference in the presence of del13q events (p-value<0.001) was found between SNP 6.0 array and the sWGS and HumanOmni array cohort, but not against the 450k array cohort. The SNP 6.0 array cohort reporting a del13q event in 31% of the cohort (33/108). Most strikingly, ATM disruption was significantly less prevalent in the sWGS cohort compared to all three other technologies (p-value<0.01). 20 patients out of 143 CLL4 patients with data generated by sWGS (14%) had either a mutation, copy number loss or biallelic loss of the *ATM* gene. Whereas, this variable was present in 35%, 27% and 32% of the SNP 6.0 array, HumanOmni array and 450k array cohorts. No patient variable was found to be significantly enriched or diminished in the 450k array cohort compared to the three other technologies.

The output of the four different genomic techniques was then compared against the available FISH data gathered as part of the clinical trial, see **Supplementary Table 13.** FISH data was not available for all 495 cases and comparisons between the FISH data and genomic arrays were completed on a subgroup of the cohort which had FISH data. **Table 10** reports a moderate to almost perfect concordance with FISH across sWGS, HumanOmni and SNP array for the detection of the four recurrent CNAs in CLL, del17p, del11q, trisomy 12 and del13q. A substantial concordance was found between FISH and 450k array data, except for the detection of del17p events in which a negative Cohen's kappa value was reported (-0.03). A negative result suggests that the two technologies tend to disagree with the reporting of del17p events. Calculating the percentage of agreement between a genomic technique and FISH data, a high percentage of agreement across all four techniques was found when detecting del17p, del11q and trisomy 12 events, compared to FISH data, see **Table 10**. For example, detecting del17p there was a 98%, 98%, 97% and 94% agreement with FISH when using SNP array, sWGS, HumanOmni array, and 450k array, respectively. A lower percentage of agreement is detecting del13q was found, however these are the most common CNA events but least prognostic (135). Overall, the genomic data was used instead of FISH array as all 495 had data from one of the genomic techniques and good concordance was found with FISH (**Table 10**). These techniques also gave greater resolution than FISH and reported breakpoint information about the CNAs, so dosage, a suggested GC metric, could be assessed.

Table 10- Concordance of the four genomic techniques employed in this thesis with FISH data.

	SNP Array		Cohen's Kappa	sWGS		Cohen's Kappa	HumanOmni Array		Cohen's Kappa	450k Array		Cohen's Kappa
Del17p	Yes	No		Yes	No		Yes	No		Yes	No	
Yes	5	1	0.82	5	2	0.83	8	5	0.71	0	1	-0.03 *
No	1	94	**98%**	0	123	**98%**	1	191	**97%**	1	29	**94%**
Del11q	Yes	No		Yes	No		Yes	No		Yes	No	
Yes	28	7	0.84	12	8	0.61	31	7	0.77	5	4	0.64
No	0	67	**93%**	4	107	**91%**	7	162	**93%**	0	22	**87%**
Trisomy 12	Yes	No		Yes	No		Yes	No		Yes	No	
Yes	9	2	0.84	13	5	0.79	5	1	0.90	4	1	0.85
No	1	90	**97%**	1	112	**95%**	0	74	**99%**	0	12	**94%**
Del13q	Yes	No		Yes	No		Yes	No		Yes	No	
Yes	30	27	0.44	59	18	0.60	48	7	0.73	5	3	0.63
No	3	42	**71%**	8	46	**80%**	3	23	**82%**	0	8	**81%**

Footnote: Cohen's kappa to test concordance between FISH and each of the four genomic technologies for the detection of copy number events; del17p, de;11q, Trisomy 12 and del13q. The magnitude of Cohen's kappa value is used to interpret the strength of the agreement; <0=Poor, 0.01-0.2=Slight, 0.21-0.4=Fair, 0.41-0.6=Moderate, 0.61-0.8=Substantial and 0.81-1=Almost perfect. * A negative value indicates that the two technologies tend to disagree with the result. FISH data was not available for all cases and therefore the sample size is smaller than the total cohort. Percentage in agreement is shown in bold (number of agreed yes and no cases/number of cases with FISH*100)

Overall, whilst the sWGS cohort reported significantly less CNA per patient, this did not greatly impact the GC classification. Furthermore, as this cohort was found to be significantly diminished in cases that have disruption of *ATM*, a gene heavily involved in DNA maintenance and genomic stability, it could be suggested that these patients truly have less CNA due to sufficient protection of *ATM* and its involvement in DNA repair. Therefore, suggesting the difference identified in the result for this technology is likely to be patient variation. Conversely, the 450k array cohort reported a much higher CNA count per patient compared to the other technologies used. As the prevalence of certain patient variables did not differ significantly against the other cohorts, there is no biological explanation of this difference in the CNA data reported. Instead it suggests a technical bias has skewed the data. Fortunately this cohort was the smallest technical cohort and comprised only 31 cases out of the 495 patients included in the statistical analysis. However, a decision to remove these cases and supplement, where possible, with HumanOmni array data was made for the following survival analysis, which was complete on separate ARC/ADM and CLL4 cohorts. Of the 31 patients that had CNA data generated using the 450k array technique, 13 cases also had HumanOmni array data available which was used instead. Therefore only 18 cases were removed from the 244 ARC/ADM clinical trial cohort, before survival analysis was completed. This resulted in a cohort of 226 ARC/ADM clinical trial patients, with all CNA data generated using the HumanOmni array technology.

6.4.9 GC has a significant impact on PFS and OS in a univariate analysis

To verify the impact of each clinco-biological variable, including GC, on PFS and OS a univariate analysis was completed on a separate CLL4 and ARC/ADM cohort. A total of 14 variables, including GC, was included in the univariate analysis. Theses variables were chosen based on published work of clinical biomarkers in CLL and availability of data for the cohorts used in the analysis. *ATM* disruption was defined with four groups; biallelic loss, sole del11q, sole mutation and wild type *ATM*. *BIRC3* biallelic loss was included but sole *BIRC3* mutation or deletion was not. *TP53* aberration included a cases with a del17p and/or mutation of *TP53* gene. CLL4 survival cohort was comprised of 251 cases. Survival data for the PFS and OS came from the 2010 and 2016 update, respectively. Median PFS for the 251 CLL4 clinical trial patients is 2.4 years (Range: 0-10.1 years) and the median OS is 6 years (Range: 0.1-17.4 years). The ARCTIC/ADMIRE cohort was comprised of 226 cases. Survival data for the PFS and OS came from the 2022 update. Median PFS for the 226 ARCADM clinical trial patients is 4.67 years (Range: 0.02-9 years) and the median OS is 6.43 years (Range: 0.02-9.1 years). Post hoc power calculations from the two cohorts, across both survival endpoints, shows sample size is sufficient to examine the clinical utility of GC, see **Table 11** and **Table 12**. The number of cases needed for each pairwise comparison was smaller than the

cohort size in each clinical trial cohort, except for PFS between intermediate and high GC. To capture the survival trends between these two cohorts an estimated sample size of over 960 patients is required, see **Table 11**. This power calculation was not able to be completed for OS due to the lack of an appropriate HR reported in the literature.

Table 11- The output from each pairwise power calculation for the PFS endpoint

		HR	Proportion	Number needed
CLL4	Low vs Intermediate	1.7	0.21 (45/217)	168
	Low vs High	1.9	0.17 (34/266)	135
	Intermediate vs High	1.2	0.43 (34/79)	963
ARC/ADM	Low vs Intermediate	1.7	0.27 (52/192)	141
	Low vs High	1.9	0.18 (34/192)	129
	Intermediate vs High	1.2	0.40 (34/86)	984

Table 12- The output for each pairwise power calculation for the OS endpoint

		HR	Proportion	Number needed
CLL4	Low vs Intermediate	1.67	0.21 (45/217)	180
	Low vs High	4.2	0.17 (34/266)	27
	Intermediate vs High	*	0.43 (34/79)	*
ARC/ADM	Low vs Intermediate	1.67	0.27 (52/192)	151
	Low vs High	4.2	0.18 (34/192)	26
	Intermediate vs High	*	0.40 (34/86)	*

6.4.10 Survival analysis in a discovery cohort of 251 CLL4 clinical trial patients

KM analysis identified no significant difference in PFS across the three GC groups, see **Supplementary Figure 15**. However, when assessing OS, a significantly poorer survival was reported in the high GC group compared to the low GC group (p-value<0.05), see **Figure 62**. The 5-year survival rate was 60%, 62% and 41% for the low, intermediate and high GC patients, respectively. Whereas results from a univariate cox regression analysis continuously identified a significant difference in survival between high GC and low GC subgroup (p-value<0.05). The median PFS for high GC patients was 1.01 years compared to 2.53 years for low GC patients. Similarly, the median OS for high patients was significantly shorter than low GC patients, 4.2 years compared to 6.25 years, see **Supplementary Table 14** and **15**.

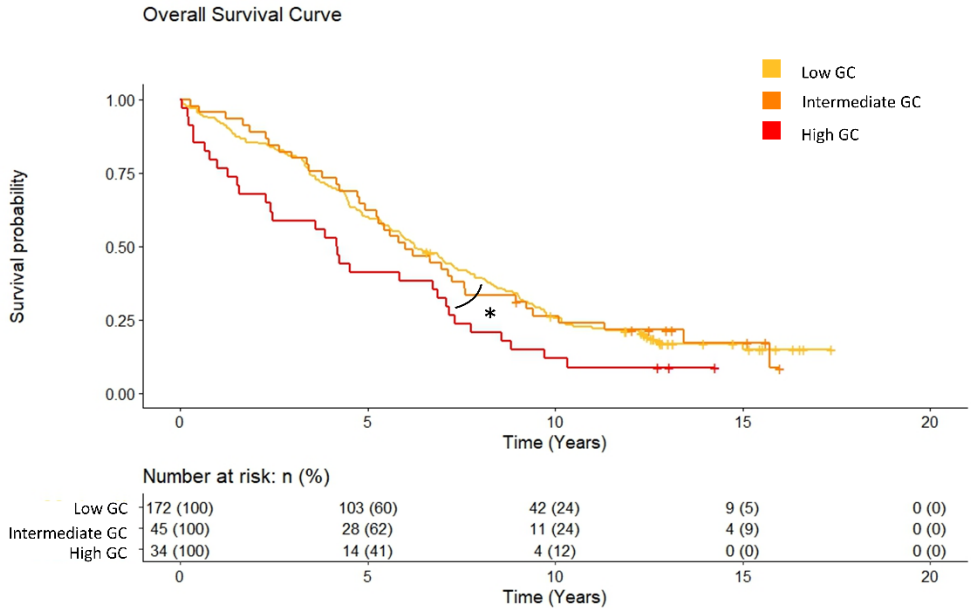

Figure 62- Kaplan-Meier plot of the three GC groups for OS using the cohort of 251 CLL4 patients. A pairwise log rank test was employed to compare survival plots, p-value<0.05 is indicated by a single asterisk (*). The table shows the number and percentage of cases in each GC group that have not had an event, i.e progressed or died, at a point in time. The number of OS events for the low, intermedite and high GC patients was 141/172, 37/45 and 31/34, respectively.

Other variables that were significant in the univariate analysis included *TP53* aberration, *IGHV* mutation status, TL and epitype. The presence of a *TP53* aberration resulted in a significantly poor PFS (HR: 3.72, 95% CI: 2.41 to 5.75, p-value<0.001) and OS (HR: 3.71, 95% CI: 2.38 to 5.78, p-value<0.001) compared to patients without. Likewise, in U-CLL patients had a significantly different PFS and OS than M-CLL (p-value<0.001). PFS was shorter in the U-CLL group compared to M-CLL (HR: 2.39, 95% CI: 1.74 to 3.27), with a median survival of 1.87 years and 3.59 years, respectively. Equally, U-CLL had a poorer OS than M-CLL patients (HR: 2.31, 95% CI: 1.67 to 3.19) with a reported median survival of 5.23 years and 8.94 years, respectively, see **Supplementary Table 15**. Across the three TL groups, a significant difference in PFS and OS was identified, with both the TL-S and TL-I patients having a significantly poorer survival compared to TL-L patients, which was the reference group. Specifically, TL-L had a median PFS and OS of 4.04 and 10.1 years which was significantly longer than TL-I patients (p-value<0.01) and TL-S patients (p-value<0.001). TL-I patients had median survival PFS and OS of 1.99 and 6.25 years, respectively, whilst TL-S patients have a median PFS and OS of 2.46 and 5.3 years, respectively. Epitype also had a significantly different PFS and OS, with the m-CLL patients having the greatest outcome compared to n-CLL or i-CLL patients. In the PFS analysis, a HR of 2.8 (95% CI: 1.67 to 4.69, p-value<0.001) was reported when comparing n-CLL patients against m-CLL patients, which is reflected in the median survival of 2.1 years for the 115 n-CLL cases and 3.7 years for the 28 m-CLL cases. Additionally, i-

CLL patients had a significantly poorer PFS than m-CLL patients (HR: 1.78, 95% CI: 1.05 to 3.02, p-value<0.05) Correspondently, this trend was also found in OS with both n-CLL and i-CLL patients having a significantly shorter OS than m-CLL patients (p-value<0.001). Median OS for these three epitype groups; n-CLL, i-CLL and m-CLL, were 5.86, 5.39 and 10.82 years, accordingly.

Examining the *ATM* disruption variable, a del11q event was the only significant subgroup in PFS analysis compared to patients with no disruption. Patients with del11q events were found to have a significantly poorer PFS than patients with no disruption to the *ATM* gene (HR: 1.97, 95% CI: 1.39 to 2.8, p-value<0.001, median: 1.51 vs. 2.53 years). Del11q patients also had a significantly poorer OS (HR: 1.5, 95% CI: 1.05 to 2.15, p-value<0.05, median: 5.56 years vs. 6.25 years). The presence of a biallelic *BIRC3* loss was only significant in the univariate OS analysis (HR: 2.73, 95% CI: 1.12 to 6.68, p-value<0.05), with a median OS of 3.32 years, which is significantly shorter than the patients without a biallelic loss (6.06 years).

Inspecting the survival trends within the mutation count variable showed that patients with greater than zero mutations had a significantly poorer PFS and OS. Specifically, a significant difference in PFS was identified in patients with ≥3, 2 or 1 mutations compared to patients with zero (p-value<0.01). The median survival for patients with a mutation count of ≥3, 2, 1 or 0 was recorded as 1.1, 1.43, 2.13, and 3.07 years, respectively. Similarly, patients with ≥3, 2 or 1 mutations compared to patients with zero had a significantly poorer OS. For example, the presence of 2 mutations lead to a significantly shorter OS (median: 4.47 years) than if zero mutations were recorded (median: 7.9 years, HR: 2.47, 95% CI: 1.64 to 3.72, p-value<0.001).

The presence of *SF3B1* or *NOTCH1* mutations did not have a significant impact on PFS in the univariate analysis, however both variables were reported to have a significantly poorer OS. Similarly, the variables age and trisomy 12 also were not significant in univariate analysis when the PFS endpoint was used but were significant in OS. As age at diagnosis increased, the risk of death increased (HR: 1.05, 95% CI: 1.03 to 1.07, p-value<0.01). The presence of a trisomy 12 also presented with a shorter OS, with a median survival of patients with a trisomy 12 event being 4.16 years compared to a median survival of 6.25 years for patients without a trisomy 12 event (p-value<0.05). Contrastingly, the univariate analysis of PFS for the three treatment groups identified a difference between the FC group and FDR group, with patients in the former having a significantly prolonged PFS (median: 3.69 years) than the latter (median: 1.69 years). No significant difference in OS across the three treatment arms was identified. Finally, del13q events, either a biallelic or monoallelic loss, was reported as significant in the PFS or OS univariate analysis, see **Supplementary Table 14** and **15**.

6.4.11 Survival analysis in a validation cohort of 226 ARCTIC and ADMIRE clinical trial patients

Firstly, this validation cohort also found a significant difference in OS, with patients in the high GC presenting with a poorer survival (median: 4.48 years) compared to patients with low GC (median: 6.82 years) (p-value<0.05). Conversely, unlike the discovery cohort, a significant difference was also found between intermediate and high GC groups (p-value<0.05), with the 5-year survival being reported as 79% and 47%, respectively, see **Figure 63B**. Furthermore, a significant difference in PFS across the three GC was found. The high GC patients had a significantly shorter PFS than either the low or intermediate GC group, **Figure 63A**. The high GC had a median survival of 2.53 years, whereas the intermediate GC patients were reported with a median survival of 4.86 years and the low GC group had 5.05 years median survival. The univariate cox regression analysis also discovered that the high GC group had a significantly poorer PFS and OS compared to the low GC group. A HR of 2.20 (95% CI: 1.27 to 3.22, p-value<0.01) was recorded for the high compared to low GC groups, using PFS as the survival endpoint, see **Supplementary Table 16**. Similarly, a HR of 2.21 (95% CI: 1.17 to 4.17, p-value<0.05) was reported in the OS analysis between high and low GC groups, see **Supplementary Table 17**.

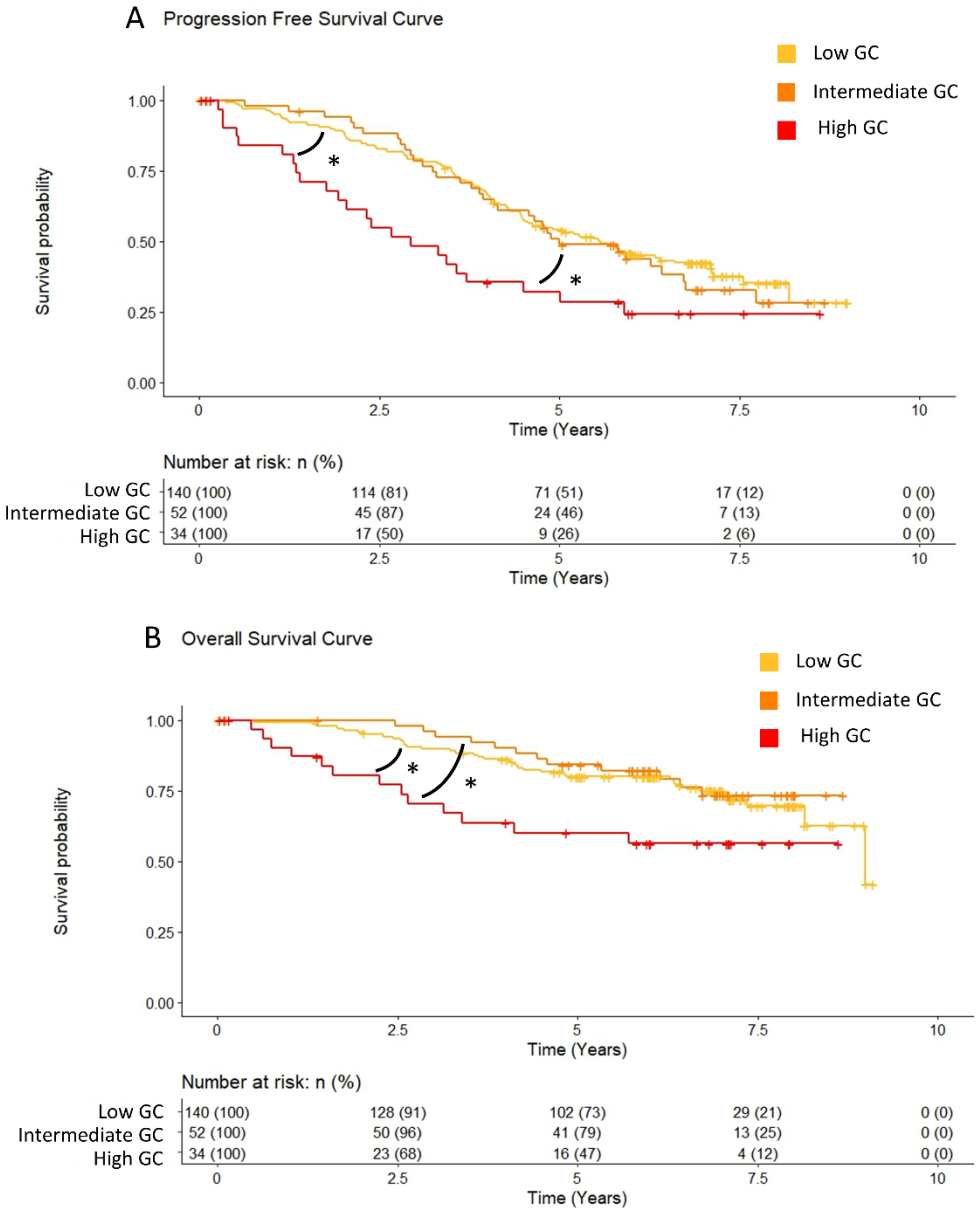

Figure 63- Kaplan-Meier plot of the three GC groups for A) PFS and B) OS, using the cohort of 226 ARCTIC/ADMIRE patients. A pairwise log rank test was employed to compare survival plots, p-value<0.05 is indicated by a single asterisk (*). The table shows the number and percentage of cases in each GC group that have not had an event, i.e progressed or died, at a point in time. The number of PFS events for the low, intermedite and high GC patients was 82/104, 33/52 and 23/34, respectively. The number of OS events for the low, intermedite and high GC patients was 37/104, 12/52 and 13/34, respectively.

The presence of a *TP53* aberration was found to have a significant detrimental impact on PFS and OS. Patient with a *TP53* aberration had a shorter PFS (median: 2.17 years) than patients with no aberration (median: 5.06 years) (HR: 4.65, 95% CI: 2.93 to 7.41, p-value<0.001). Likewise, patients with an aberration had a significant poorer OS (HR: 2.97, 95% CI: 1.58 to 5.59, p-value<0.001, median: 3.62 years) compared to patients who lacked this aberration (median: 6.69 years). As

previously shown, U-CLL patients had a significantly shorter PFS and OS compared to their counterpart, M-CLL patients (PFS, HR: 3.04, 95% CI: 2 to 4.61, p-value<0.001, OS, HR: 1.86, 95% CI: 1.04 to 3.33, p-value<0.05), see **Supplementary Table 16** and **17**.

Across the three TL groups a difference in PFS and OS was reported. TL-S patients had a significantly poorer PFS and OS compared to TL-L patients. The median PFS of TL-S, TL-I and TL-L patients was 3.7, 3.93 and 5.83 years, respectively. Similarly, median OS recorded for TL-S, TL-I and TL-L patients was 5.91, 5.99 and 6.92 years, respectively. The PFS HR comparing TL-S to TL-L patients was 2.57 (95% CI: 1.7 to 3.88, p-value<0.001) and the HR identified in the OS analysis was 2.55 (95% CI: 1.39 to 4.67, p-value<0.01). Whilst TL-I had a significantly poorer PFS compared to TL-L patients (PFS, HR: 2.21, 95% CI: 1.48 to 3.31, p-value<0.001), it was not significant in OS. In a similar manner, the three epitypes significantly differed in PFS, with n-CLL (HR: 4.35, 95% CI: 2.51 to 7.52, p-value<0.001) and i-CLL (HR: 2.09, 95% CI: 1.15 to 3.83, p-value<0.05) patients having a shorter survival than m-CLL patients. However, only a significant difference in OS was identified between n-CLL and m-CLL groups (HR: 4.69, 95% CI: 1.83 to 11.99, p-value<0.01).

Across both survival endpoints a significant difference in survival was reported in the mutation count variable. For PFS, the presence of ≥3, 2, or 1 mutation predicted a shorter survival compared to if a patient had zero with median survival times for each group being 2.61, 3.56, 4.48 and 5.83 years, respectively. Assessing OS identified a significant difference between ≥3 or 1 mutations and zero group with a reported HR of 3.68 (95% CI: 1.51 to 8.96, p-value<0.01) and 2.20 (95% CI: 1.11 to 3.69, p-value<0.05), respectively.

In PFS results only, *ATM* disruption was found to be significant in the ARC/ADM cohort. Specifically, patients with a biallelic loss of the gene had a median survival of just 3.36 years compared to 4.99 years reported in patients who were *ATM* wild type (HR: 2.1, 95% CI: 1.05 to 4.18, p-value<0.05) (**Supplementary Table 16**). Additionally, patients with a sole del11q event also had a poorer PFS of 4.02 years (HR: 2.1, 95% CI: 1.33 to 3.32, p-value<0.01). Conversely the age variable was only significant in the OS analysis, which found that as age at diagnosis increased the risk of death also increased (HR: 1.03, 95% CI: 1 to 1.07, p-value<0.05), see **Supplementary Table 17**.

The variables, treatment arm, *SF3B1* mutation, *NOTCH1* mutation, *BIRC3* biallelic loss, del13q and trisomy 12 events, were not found significant in either PFS or OS univariate analysis in this validation clinical trial cohort.

6.4.12 High GC is an independent predictor of poor survival within a multivariate analysis using a discovery and validation clinical trial cohort

The variables included in the first cox regression model were selected based on if they were significant in the univariate analysis, this resulted in 13 variables being selected. Therefore, the first PFS and OS models, in both cohorts, were comprised of GC, TL, epitype, *TP53* aberration, *ATM* disruption, *BIRC3* biallelic loss, *IGHV* mutation status, *SF3B1* mutation, *NOTCH1* mutation, mutation count, trisomy 12, age and treatment arm. *ATM* disruption variable was defined by four subgroups; biallelic loss of *ATM*, sole *ATM* mutation, sole del11q event and wild type, which was used as the reference group. Treatment arms differed across the two clinical trial cohorts as patients were enrolled into distinct treatment regimens and therefore the subgroups included in this covariate varied between the discovery and validation cohorts.

Firstly, the final PFS models for the CLL4 and ARC/ADM cohort were based on 198 and 202 cases with 176 and 121 events, respectively. The GC covariate remain significant in the final ARC/ADM PFS model with the high GC group independently predicting a shorter time till progression for patients (HR: 1.94, 95% CI: 1.15 to 3.27, p-value<0.05), see **Supplementary Table 20**. However, GC did not retain independent significant in the CLL4 PFS model and was removed from a previous iteration of the model during the stepwise backwards elimination process that was employed. Across both cohorts *TP53* aberration and epitype remained significant in the model (**Figure 64**). In the discovery cohort the presence of a *TP53* aberration had a greatest detrimental effect on PFS with patients being reported to have three times the risk of progressing than patients with a wild type *TP53* (HR: 3.13, 95% CI: 1.87 to 5.26, p-value<0.001), see **Supplementary Table 18**. *TP53* aberration was also significant in the validation cohort (HR: 2.60, 95% CI: 1.39 to 4.85, p-value<0.01). Conversely, the epitype covariate had a greatest impact on PFS in the ARC/ADM cohort with n-CLL patients (HR: 3.67, 95% CI: 2.08 to 6.47, p-value<0.001) and i-CLL patients (HR: 2.21, 95% CI: 1.20 to 4.07, p-value<0.05) independently predicting a significantly poorer survival than m-CLL patients. However, assessing the epitype covariate in the CLL4 cohort, only the i-CLL epitype was significant (HR: 2.34, 95% CI: 1.22 to 4.49, p-value<0.05).

Along with the GC, epitype and *TP53* aberration covariates as previously mentioned, mutation count retained independence in the final PFS ARC/ADM model. The results showed that the patients with three or more mutations had over twice the risk of progressing than patients with less mutations (HR: 2.59, 95% CI: 1.24 to 5.38, p-value<0.01).

The CLL4 PFS multivariate model also included *IGHV* mutation status, *ATM* disruption, TL and treatment arm. Results from this analysis reflected previous established clinical trends as unmutated *IGHV* patients were found to independently predict a poorer PFS (HR: 2.34, 95% CI:

1.36 to 4.04, p-value<0.001). Similarly, the presence of a sole del11q event was also found to predict a shorter PFS (HR: 1.62, 95% CI: 1.07 to 2.49, p-value<0.05), which has been reported in previous literature. The treatment arm covariate also remained in the final PFS model with the treatment group FC predicting a significantly longer PFS (HR: 0.3, 95% CI: 0.2 to 0.45, p-value<0.001), which corresponds with conclusions of the larger CLL4 clinical trial. Finally, the TL covariate remained in the final CLL4 PFS model and couldn't be removed as indicated by a significant likelihood ratio when comparing two models, one with TL and one without. However, neither TL-S or TL-I was significant in the model with a reported p-value of 0.17 and 0.78, respectively.

Subsequently, the final OS models identified many covariates that had an independent significant impact on patient survival. In both the two clinical trial cohorts, GC was found to have a significant impact on OS (**Figure 64**). In the ARC/ADM cohort, patients with high GC had over twice the risk of death than patients with low GC (HR: 2.44, 95% CI: 1.18 to 5.03, p-value<0.05), see **Supplementary Table 21**. Whilst the CLL4 cohort did find the high GC group had an independent detrimental effect on survival, it reported a HR of 1.6 (95% CI: 1.05 to 2.44, p-value<0.05) suggesting the difference in survival risk between high and low GC was less severe than the ARC/ADM cohort (**Supplementary Table 19**). Regardless, the GC covariate remained significant in both the discovery and validation final OS models, unlike PFS models in which it did not retain independent impact in the discovery cohort.

In accordance with the PFS final models, the OS models also reported that *TP53* aberration and epitype had a significant impact on survival in both the discovery and validation cohort, see **Figure 64**. The presence of *TP53* aberration was once again shown to independently predict a poorer survival, with these patients having around three times greater risk of death (CLL4, HR: 3.4, 95% CI: 2.05 to 5.64, p-value<0.001, ARC/ADM, HR: 2.72, 95% CI: 1.14 to 6.45, p-value<0.05). Epitype was also found to have an independent detriment impact on survival of CLL clinical trial patients. Specifically, n-CLL and i-CLL patient have a significantly poorer OS compared to m-CLL patients. In the discovery cohort, n-CLL was reported with a HR of 2.17 (95% CI: 1.18 to 3.99, p-value<0.05) whereas i-CLL had a HR of 2.19 (95% CI: 1.21 to 3.98, p-value<0.01). A comparable result from n-CLL and i-CLL subgroups was found in the validation cohort, see **Supplementary Table 21**.

In both OS final multivariate models, the covariates age and trisomy 12 were found to independently predict poor survival. For example, as age increased the risk of death also increased in both the discovery and validation cohort, each with a reported HR of 1.05 (p-value<0.01). The presence of a trisomy 12 event in CLL4 clinical trial patients also predicted an inferior survival compared to patients without a trisomy 12 event (HR: 1.74, 95% CI: 1.08 to 2.83,

p-value<0.05), see **Supplementary Table 19**. A concordant result was reported in the ARC/ADM patients (HR: 2.58, 95% CI: 1.15 to 5.79, p-value<0.05).

TL, *SF3B1* mutation, and treatment arm were covariates that were only present in the CLL4 OS model. Results showed that TL-S and the presence of a *SF3B1* mutation independently predicted a shorter OS with a recorded HR of 1.84 (p-value<0.05) and 1.79 (p-value<0.01), respectively. The treatment arm FC predicted a significantly longer OS (HR: 0.61, 95% CI: 0.41 to 0.89, p-value<0.05). Likewise, the mutation count covariate only remained significant in predicting OS in the validation cohort, with the presence of three or more mutation independently predicting a higher risk of death (HR: 3.52, 95% CI:1.18 to 10.5, p-value<0.05).

Overall, these results show that high GC was consistently important in predicting patients destined to have a poor survival, independently of many established poor risk CLL biomarkers.

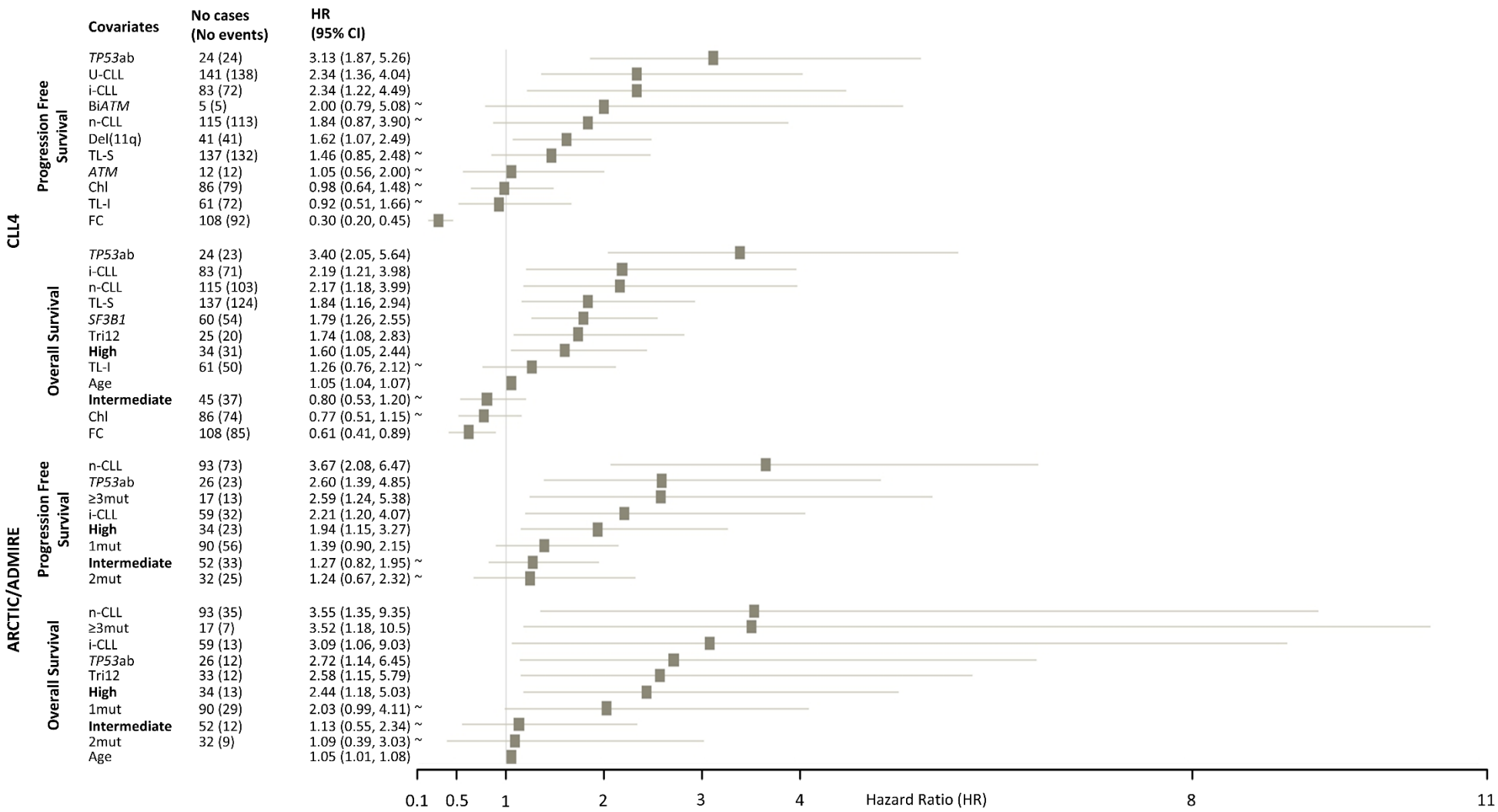
Covariates
No cases (No events)
HR (95% CI)
CLL4
Progression Free Survival
TP53ab 24 (24) 3.13 (1.87, 5.26)
U-CLL 141 (138) 2.34 (1.36, 4.04)
i-CLL 83 (72) 2.34 (1.22, 4.49)
BiATM 5 (5) 2.00 (0.79, 5.08) ~
n-CLL 115 (113) 1.84 (0.87, 3.90) ~
Del(11q) 41 (41) 1.62 (1.07, 2.49)
TL-S 137 (132) 1.46 (0.85, 2.48) ~
ATM 12 (12) 1.05 (0.56, 2.00) ~
Chl 86 (79) 0.98 (0.64, 1.48) ~
TL-I 61 (72) 0.92 (0.51, 1.66) ~
FC 108 (92) 0.30 (0.20, 0.45)
Overall Survival
TP53ab 24 (23) 3.40 (2.05, 5.64)
i-CLL 83 (71) 2.19 (1.21, 3.98)
n-CLL 115 (103) 2.17 (1.18, 3.99)
TL-S 137 (124) 1.84 (1.16, 2.94)
SF3B1 60 (54) 1.79 (1.26, 2.55)
Tri12 25 (20) 1.74 (1.08, 2.83)
High 34 (31) 1.60 (1.05, 2.44)
TL-I 61 (50) 1.26 (0.76, 2.12) ~
Age 1.05 (1.04, 1.07)
Intermediate 45 (37) 0.80 (0.53, 1.20) ~
Chl 86 (74) 0.77 (0.51, 1.15) ~
FC 108 (85) 0.61 (0.41, 0.89)
ARCTIC/ADMIRE
Progression Free Survival
n-CLL 93 (73) 3.67 (2.08, 6.47)
TP53ab 26 (23) 2.60 (1.39, 4.85)
≥3mut 17 (13) 2.59 (1.24, 5.38)
i-CLL 59 (32) 2.21 (1.20, 4.07)
High 34 (23) 1.94 (1.15, 3.27)
1mut 90 (56) 1.39 (0.90, 2.15)
Intermediate 52 (33) 1.27 (0.82, 1.95) ~
2mut 32 (25) 1.24 (0.67, 2.32) ~
Overall Survival
n-CLL 93 (35) 3.55 (1.35, 9.35)
≥3mut 17 (7) 3.52 (1.18, 10.5)
i-CLL 59 (13) 3.09 (1.06, 9.03)
TP53ab 26 (12) 2.72 (1.14, 6.45)
Tri12 33 (12) 2.58 (1.15, 5.79)
High 34 (13) 2.44 (1.18, 5.03)
1mut 90 (29) 2.03 (0.99, 4.11) ~
Intermediate 52 (12) 1.13 (0.55, 2.34) ~
2mut 32 (9) 1.09 (0.39, 3.03) ~
Age 1.05 (1.01, 1.08)
0.1
0.5
1
2
3
4
Hazard Ratio (HR)
8
11

Figure 64- Forest plot including the variables that remained significant in the final multivariable models of the CLL4 and ARCTIC/ADMIRE cohorts. A tilde (~) highlight factors within a categorical variable that were not significant, as the confidence interval (CI) included 1, but the categorical variable itself was significant as the model had a better goodness of fit when the variable remained, i.e TL-I factor in the TL variable. Abbreviations: TL-S- Short Telomere Length, TL- I-Intermediate Telomere Length, TL-L-Long Telomere Length, U-CLL- Unmutated IGHV genes, TP53ab- TP53 Aberration, Tri12-Trisomy 12, biATM- Biallelic ATM inactivation, Chl-Chlorambucil, FC-Fludarabine plus Cyclophosphamide, SF3B1- *SF3B1* mutation, 1mut- mutation count of 1, 2mut- mutation count of 2, ≥3mut- mutation of ≥3. High and Intermediate GC are shown in bold.

6.5 Discussion

This chapter has not only examined the biological context of the novel biomarker GC, but also analysed its clinical impact in a CIT therapy based clinical trial cohort. As previously discussed in Chapter 2, GC has been extensively reported in the CLL literature and it is proposed to be able to identify patients destined to have a poorer survival when given CIT and, as of recently, targeted agents regimes. However, the predictive power of GC in the context of targeted agents is not fully elucidated, with many conflicting reports being found across clinical trial using different target agent treatment options. Furthermore, because targeted agents are a newer development in the CLL treatment landscape, only recently larger scale clinical trials were constructed. Therefore, investigating the impact of GC in targeted agent treated patients is typically curtailed by a small sample size or limited follow up data. Nevertheless, GC has been shown extensively to be an important clinical biomarker in CLL.

Recently the ERIC suggested further consideration as to methodology recommendations and the clinical interpretation of GC is required before this biomarker can be validated. Furthermore, they also concluded that more robust evidence regarding the predictive value of specific genomic profiles within GC is needed to refine its risk stratification ability (306). In various haematological malignancies, such as acute myeloid leukaemia and acute lymphoblastic leukaemia, CK, defined as the presence of three or more CNA, has been found to have an independent prognostic and predictive power. However, the prognostic significance has been found to vary when a definition of 3 or 5 abnormalities was used to define CK (307–309). This variability in prognostic significance across different GC definitions was also found in CLL (103,222,225). This suggests that an underlying biological heterogeneity can influence the clinical relevance of GC. Therefore, a clinically applicable definition of GC is only possible when the biological context of the disease, such as the presence of other mutations, chromosomal abnormalities, cell of origin biomarkers, and various patient characteristics and therapeutic intervention is considered. Thus, this chapter aimed to assess GC in the context of many established biomarkers, to examine the biological composition and create a genomic profile for each of the GC subgroups; low, intermediate and high. Whilst published work has shown GC to be associated with various biomarkers, this has typically been on a limited number of biomarkers and usually as a biproduct of a larger clinical analysis. Therefore, this chapter is unique in the fact that GC was able to be assessed in a clinical trial cohort with extensive genomic characterisation, allowing GC to investigated alongside many genomic features.

Overall, a distinct biological profile was identified in the high GC patients. Whereas, across many variables, but not all, considerable similarities in the biological context of the low and intermediate GC patients were found.

Firstly, an association between GC and *TP53* aberration was confirmed in this analysis, with a significantly higher prevalence of *TP53* aberration in the high GC group being found. Biologically, the cellular environment of tumours with *TP53* aberrations can promote the acquisition of structural and numerical abnormalities due to the loss of the genes function which protects genomic stability through numerous mechanisms. This relationship has been regularly reported in the literature, for example Baliakas et al (2019), which identified a significant association between CK (≥3 structural and/or numerical aberrations) and *TP53* aberration (p-value<0.008) (103,238). They also identified a *TP53* aberration in 65% of the high CK (≥5 structural and/or numerical aberrations) group (p-value<0.001). Their MVA concluded that high-CK predicted a poor clinical outcome, independently of *TP53* aberration, clinical stage or *IGHV* mutation status. Conversely, they reported that CK only indicated a poor survival in patients that also had a *TP53* aberration. This finding was also reported in Delgado et al, which found that GC was a key predictor of survival from MVA using a cohort of patients with *TP53* aberration (HR:7.63, 95% CI: 1.62 to 33.3, p-value<0.05) (204). In a similar manner, the multivariate work completed in this chapter only found high GC to have an independent detrimental impact on survival, as shown in both the discovery and validation OS models. Conversely, the intermediate GC group did not remain significant in the multivariate models constructed in this chapter and perhaps this reflects the impact of *TP53* aberrations in the intermediate GC/CK group. Median PFS for ARC/ADM intermediate GC patients with and without *TP53* aberrations was 2.76 and 5 years (p-value<0.001), respectively, suggesting that intermediate GC could be further stratify by *TP53* aberration (**Supplementary Figure 16**). Whilst the OS was greater for patients with intermediate GC without *TP53* aberration (median: 6.72 years) compared to intermediate GC patients with *TP53* aberration (median: 5.99 years), this difference was not significant (p-value=0.71). Similarly, the CLL4 cohort reported no significant difference in median PFS and OS for intermediate GC patients with or without *TP53* aberration (p-value>0.05). These expected survival trends were not consistently identified perhaps due to limitations of sample size during subgroup analysis. By drilling down into specific subgroups, i.e intermediate GC, the number of patients with *TP53* aberration were very small (ARC/ADM: 3 and CLL4: 6), with the majority, as previous stated, being present in the high GC patients. Therefore, further work expanding the cohort size used in survival analysis may allow the presence of genomic features that have low prevalence to be examined.

As mentioned in 1.4, *TP53* aberration is one of the two CLL genomic biomarkers that have been approved for use in the clinical setting. The iwCLL guidelines suggests newly diagnosed patients

should always be screened for the presence of *TP53* aberrations and to identify the *IGHV* mutation status (84). In this chapter, as high GC was found to predict poorer OS, independently of *TP53* aberrations and *IGHV* mutation status, it suggests that this biomarker represents a clinically relevant CLL population that is not captured by currently validated clinical biomarkers.

Both reported in this chapter and in CLL literature is a distinct *IGHV* gene usage across GC, with an association being found, between high GC, intermediate GC, and U-CLL (103,238,310). My research has found that not only does the high GC patients have a greatest percentage of U-CLL cases, but also the low GC was significantly associated with M-CLL cases. Research published in 2019, concluded that a combination of these two biomarkers refined the prognostic stratification of CLL and gave greater clinical insight. Specifically in identifying M-CLL patients with low GC which are predicted to have a prolonged survival after treatment with chemoimmunotherapy, with 90% of these patients reported as alive after 10 years (p-value<0.0006) (311). This research group also investigated the clinical significance of a major structural aberrations, such as unbalanced translocations, ring or marker chromosomes, and suggested a GC metric which included them should be considered. They found that CK patients with major structural abnormalities were associated with more cases of *TP53* aberrations, shorter OS, and chemo-refractoriness. Analysis of mRNA expression profiles of these cases also found they had deregulation of cell cycle control and DNA damage response genes (312). This finding highlights how the inclusion criteria of different GC metrics can be developed and altered to reflect different biology and clinical responses, resulting in a better risk stratification of CLL patients.

25 years ago, CLL research reported that the *IGHV* mutation status dichotomizes patients into two clinically important groups, U-CLL and M-CLL (123). Since then, extensive research has tried to uncover the biological reasoning behind this distinct difference in clinical presentation. It is suggested that the cell of origin differs between U-CLL and M-CLL patients, with the latter arising from the B cell post germinal centre reaction and the former occurring from a pre germinal centre reaction B cell. Published work studying the epigenome of the two CLL subtypes found distinct differences in DNA methylation patterns between U-CLL and M-CLL (273). Furthermore, between the two subgroups, a difference in BCR reactivity and thus levels of proliferation, has been reported. Specifically, the U-CLL cases are found to have increased ability in phosphorylating downstream signalling pathways, such as Syk, triggering cell proliferation and survival. Conversely M-CLL has been reported to have decreased ability to activate BCR signalling pathways even to the point of signal anergy (124). The theory that U-CLL tumours have a greater proliferative history, due to these CLL cells having a greater BCR signalling capabilities, is supported by the finding of significantly shorter telomeres in these cases compared to M-CLL (276). The rate at which a cell proliferates will influence the rate at which mutations and chromosomal

abnormalities can accumulate. Furthermore, greater proliferative activity allows for greater clonal selection, an important mechanism in the tumorigenesis process (313,314). Thus, the significant association between high GC and U-CLL patients reported here and previously, is possibly explained by the difference in BCR signalling capabilities leading to a greater proliferative history in U-CLL. More recently, work reporting on the phenomenon of BCR stereotypes also reinforces the theory that BCR signalling plays an essential role in CLL presentation and progression. BCR stereotypes have also been reported to have unique methylation patterns. Specifically, subset #2, the largest stereotyped subset, the BCR is encoded by IGHV3-21 and IGLV3-21 genes, it is the predominate stereotyped subset in i-CLL epitype cases and most cases have mutated *IGHV* status (128,195). In survival analysis, subset #2 has been found to predict a poor survival, independently of *IGHV* mutation status. Furthermore, as previously mentioned, an association between the i-CLL epitype and IGLV3-21^{R110} mutation has been reported, with the mutation being shown to confer an aggressive disease with inferior survival (131,315). This chapter was able to, for the first time, show a significant association between the i-CLL epitype and GC (**Figure 54** and **Figure 59**). Possibly this association is due to significant enrichment of IGLV3-21^{R110} in the i-CLL epitype (131). The higher *WNT5A* expression levels reported in IGLV3-21^{R110} cases have been associated with increased proliferation and chemotaxis of the CLL cell (316). In a similar fashion to U-CLL, this increased proliferation reported in IGLV3-21^{R110} cases allows the quicker accumulation of genomic abnormalities. This is supported by research, as i-CLL patients expressing IGLV3-21^{R110} were found to have a greater total number of driver alterations (median: 2.8) than i-CLL without an R110 mutation (median: 1.9, p-value<0.05) and m-CLL (median: 1.5, p-value<0.001), but still less than the n-CLL epitype (median: 3.6, p-value<0.05) (131). Therefore, this suggests the relationship identified between i-CLL and intermediate GC in this chapter, could be confounded by the presence of IGLV3-21^{R110}. To fully understand this association between i-CLL and GC, the generation of stereotype data for the cohort used in this chapter is needed so the IGLV3-21^{R110} variable can be included in downstream analysis.

This chapter found a significant enrichment of both trisomy 12 events and *NOTCH1* mutations in the low GC group (**Figure 57** and **Figure 59**). In fact, the presence of trisomy 12 was frequently found in combination with a *NOTCH1* mutation, as out of the 52 low GC cases with trisomy 12, 20 also had a *NOTCH1* mutation (38%). Association between *NOTCH1* mutations and trisomy 12 has been previously reported in CLL literature (142,317,318). These patients have been found to present with a more aggressive disease, more likely to progress to Richter transformation and respond poorly to chemoimmunotherapy (142,318). Subgroup analysis of my CLL4 survival cohort, identified that the 10 low GC cases with both trisomy 12 and *NOTCH1* had shorter PFS (median: 1.87 vs. 2.54 years, p-value=0.09) and significantly shorter OS (median: 3.39 vs. 6.61 years, p-

value<0.05) compared to low GC patients without both a trisomy 12 and *NOTCH1* mutation, see **Supplementary Figure 17**. Furthermore, both the *NOTCH1* and trisomy 12 covariate were significant in the CLL4 univariate OS analysis (**Supplementary Table 15**). In both the discovery and validation multivariate OS models, the covariate trisomy 12 remained significant and it predicted a shorter OS independently of covariates including GC, *TP53* aberration, *IGHV* mutation status and epitype (**Figure 64**). Therefore, perhaps the presence of both trisomy 12 and *NOTCH1* mutations can be used to further risk stratify the low GC group, identifying patients that may have a more aggressive disease and poor response to treatment that is not currently being predicted by the GC biomarker. However additional work is needed to fully examine the heterogenous low GC group further to assess the role trisomy 12 and *NOTCH1* plays in disease presentation and progression.

Conversely, a biomarker that has been previously reported to be associated with GC was not found to be in this chapter. Large del13q events can be further classified based on whether the deletion overlaps the *RB1* (type 2) or *RNASEH2B* (class 2) gene. The former has been shown to be associated with elevated levels of GC. Moreover, del13q size has been reported to be an independent predictor of GC (305). By contrast, a previous examination of class 2 del13q events found considerable genomic heterogeneity within these cases and, in one cohort analysed, an association with GC, defined as ≥3 CNAs, was found. However, two additional cohorts also examined in the paper did not find an association between class 2 del13q events and GC, and instead found the presence of mono- or biallelic del13q was more important (144). The results of this chapter found no significant difference in GC, either assessed as a categorical or continuous variable, across either the type (type 1 and 2) or class (class 1 or 2) del13q definitions. However, as similarly previously reported, a significant association of mono- and biallelic del13q with GC was found. Specifically, monoallelic del13q events were more common in high GC patients whereas biallelic del13q events were associated more with intermediate GC, **Figure 59**. However, del13q events, either mono- or biallelic loss, were not found to impact PFS or OS in the univariate analysis and therefore were not assessed in the MVA. This suggests that the relationship between the size of del13q and GC in CLL is an intricate interaction that is potentially influenced by unknown extraneous variables (144).

Finally, whilst the clinical utility of GC could not be empirically tested in the project. The extensive characterisation of the patients included in this work has allowed a comprehensive examination of the biological context of the three GC groups. Therefore, survival analysis completed here surpasses much of the reported literature, as it includes many biomarkers into the univariate and multivariate work. Given the fact that the biomarkers typically do not occur in isolation, including as many elements into the construction of multivariate models will mean the conclusion from this analysis are more representative of CLL biology.

As highlighted before in Chapter 2, GC, measured and detected in various ways, has been identified as a prognostic biomarker in many CLL populations. For example, Herling et al (2016) identified that CK (≥3 aberrations), detected by conventional karyotyping, had a significant independent impact of OS (HR: 2.7, 95% CI: 1.4 to 5.3, p-value<0.01) in a clinical trial cohort of 161 patients enrolled in chemo(immuno-)therapy-based treatments (205). Similarly, CK, defined as ≥3 aberrations excluding del17p, was prognostically significant in a cohort of relapsed/refractory CLL that were given FCR. CK was significant in both the PFS (HR: 2.6, 95% CI: 1.5 to 4.4, p-value<0.001) and OS (HR: 1.9, 95%CI: 1.1 to 3.2, p-value<0.05) multivariate models and predicted an inferior survival independently of many variables including, age, del17p events and number of prior treatments (319). Additional definitions of GC have been found to be clinically important, for example, using a cohort of 321 untreated CLL patients both CK (≥3 aberrations) and high CK (≥5 aberrations), detected using CBA, were reported to have significantly shorter TTFT in a univariate analysis (223). This definition of high CK was also used in a large retrospective study of 5290 CLL patients, with the majority being untreated. However, this research found that it was only cases with high CK, detected using CBA, that exhibited a poor clinical outcome, independently of *TP53* aberration, *IGHV* mutation status or clinical stage (HR: 2.23, 95% CI: 1.6 to 3.09, p-value<0.001) (238). And instead, CK patients were only found to have a dismal survival in the presence of *TP53* aberrations. This supports MVA results in this chapter, as only high GC had an independent detrimental impact on survival. A further large multicentre study of 2293 patients with genomic array data found that high GC (≥5 aberrations, with a ≥5Mb size cut off) was an independent predictor of a shorter TTFT (HR: 2.15, 95% CI: 1.36 to 3.41, p-value<0.01) and OS (HR: 2.54, 95% CI: 1.54 to 4.17, p-value<0.001) in MVA models including gender, age, Binet stage, *IGHV* mutation status, *TP53* aberration and del11q (103). They also reported that reducing the size cut off to ≥1Mb did not significantly improve risk assessment. Within a sub cohort of 122 patients with both genomic array and CBA data, a direct comparison of the technologies found that although genomic arrays reported more chromosomal abnormalities, the high GC variable from each technologies had a similar risk stratification significance (103). This evidence supports the use of genomic arrays and the high GC definition in the prognostication of CLL patients, both of which have been employed in this chapter.

GC has been found to be important outside of CLL, with various other haematological malignancies reporting its use as a prognostic biomarker. For example, in acute myeloid leukaemia the presence of CK (≥5 abnormalities) is associated with a poor prognosis (320). Similarly, a study including 632 Philadelphia-negative acute lymphoblastic leukaemia patients found at CK (≥5 abnormalities) was prognostic for relapse after allogeneic hematopoietic stem cell transplantation (HR: 1.69, 95% CI: 1.06 to 2.69) (321).

The main aims of this chapter were to assess the biological composition and describe the genomic profile of three GC groups: low, intermediate and high. The statistical analysis using the data-rich molecularly characterised clinical trial cohort of 495 patients found that the high GC had a unique genomic profile associated with many poor risk biomarkers. The other aim of this project was to investigate the survival impact of GC in the context of many established CLL biomarkers. As mentioned above, the clinical utility of GC could not be empirically tested. Still, this work evaluated the clinical significance of GC in a CIT clinical trial cohort with long follow-up and in the context of many established biomarkers, many for the first time, thus adding to the wealth of literature that suggests GC is a prognostically important biomarker in CLL.

A post hoc power analysis was completed to assess whether the sample size used in the survival analysis was suitable for capturing survival trends. This analysis concluded that the cohort was a sufficient size to assess a difference in PFS and OS between low GC and high or intermediate GC, as both the discovery and validation cohorts were considerably larger than the required size, see **Table 11** and **Table 12**. Whilst the usefulness of these post hoc power calculations has been disputed and even been suggested that the reporting of them can be misleading (322). In the case of this chapter a power calculation was unable to be completed at the start of the project, before the generation of data. Typically, power calculations in the clinical trial setting are used to decide the number of patients enrolled in each treatment arm, to ensure the results will be powered. The reason the power analysis was unable to be complete before, was that it was unknown what GC group each patient would be in until data generation was completed, as CNA data generated was used to define the three GC subgroups; low, intermediate and high. Therefore, the approach for this chapter was to expand the cohort to the greatest possible size, given restrictions in sample availability, money and time for the generation of new data, allowing more patients to meet inclusion criteria for the study. By constructing the largest possible cohort size, it was hoped that there would be sufficient cases in each GC group. However, the power analysis comparing the intermediate and high GC groups, highlighted that the current cohorts used were not powered enough to reported on survival difference between these subgroups. Therefore, future work expanding these clinical trial cohorts further will allow the investigation of survival trends between the intermediate and high GC patients.

In conclusion, the biological profiles created of the three GC groups examined in this chapter frequently reflected previously reported associations. However, for the first time a significant enrichment between intermediate GC and the i-CLL epitype was identified. As this association was not found between high GC patients, it suggests a unique mechanism may be at play whereby genomic instability occurs but not to the severity of the disruption reported in high GC, *TP53* aberrant or U-CLL patients. This research, as supported by published data, suggests that the

intermediate GC should not be used in risk stratification as its biological profile was highly heterogenous, had only a borderline impact on survival, and potentially is confound by the enrichment of i-CLL, and therefore influenced by IGLV3-21^{R110} mutation. Conversely, this chapter has been able to identify that high GC, defined by the presence of ≥5 numerical and/or structural chromosomal abnormalities, predicts dismal survival independently of many high risk CLL biomarkers, in two CIT based clinical trial cohorts. This finding has been extensively reported in CLL literature but also in other cancers. Also, high GC has been reported as clinically important in numerous studies that have used CBA and/or genomic arrays to detect GC. Taken all together, this chapter supports the consensus conclusion that GC is an important clinical biomarker and thus a contender to become part of the regular screening services offered to newly diagnosed patients for risk stratification. This would allow the high-risk patients that are not currently captured by clinically employed biomarkers, to be identified and given a suitable treatment plan for a greater survival outcome.

Chapter 7 General Discussion

In general, CLL presents with a relatively stable genome, with most patients only having 0-2 CNAs. No single acquired genetic defect has been identified to be adequate to trigger CLL development and the mutational landscape of this disease is strikingly heterogenous, with only a handful of mutations recurring at a frequency greater than 5% in newly diagnosed patients (323). Given the considerable heterogeneity in the biological and clinical presentation of the disease, the need for prognostic and predictive markers to be used to risk stratify patients is substantial. Additionally, as the CLL tumour, unlike other human cancers, is characterised by a low genomic burden with very few recurrent genomic mutations being reported, the use of GC observed in CLL cells, has been explored as a novel CLL biomarker in many clinical trial and institutional cohorts.

Within the CLL community, GC has been extensively reported to have prognostic significance, both in CIT based clinical trials and patients treated with targeted agents (103,198,204,232–234,238). As highlighted in Chapter 2, numerous different GC metrics have been employed as well as various technologies used to detect it. Recently, ERIC recommended that further consideration around the methodology being used in research assessing the GC biomarker is needed. This statement is supported by the biomarker validation roadmaps developed by Cancer Research UK. The roadmap depicted that the development of an accurate and reproducible assay or technology to measure the biomarker is needed before the biomarker can become validated and used in the clinical setting. An issue with validating GC as a clinically important biomarker using currently available evidence is that numerous different technologies have been employed. These different technologies have disparate resolutions, accuracies, and detection abilities. For example, the two most used techniques for GC detection identified in the systematic review, CBA and SNP array, have many technical differences in their ability to detect GC. The technical resolution of the CBA is around 4Mb and is dictated by the resolution of the light microscope whereas SNP array can detect CNAs to a resolution of around 5-50 kb, depending on probe density. Therefore, using these two techniques to explore GC can introduce technical biases, as CBA is not able to detect small CNAs that SNP array can. A previous study using a cohort of 506 CLL patients reported that a CK (≥3 abnormalities) detected by CBA was found in around 20% of patients (324). Within the cohort of 495 clinical trial patients employed in this thesis, the presence of ≥3 aberrations detected by a genomic techniques was reported in 38% of patients. This disparity between the number of detected CNA between the techniques has led to the suggestion of including a size cut off into the GC metric, therefore removing the smaller CNA that are only able to be detected by higher resolution techniques (325). Recent published work assessing the clinical significance of CK has used a conservative ≥5 Mb size cut off of CNAs (excluding recurrent CLL CNA) detected using

various genomic array (103). This size cut off was based on the FISH karyotype resolution and was hoped to improve the prognostic ability of GC by excluding smaller non tumour-associated aberrations (103). The researcher also included a lower size cutoff of ≥1 Mb, however found no significant difference in the risk assessment of GC compared to when the ≥5 Mb size cut off was used. Therefore, as it stands, no definitive answer as to the most appropriate size cutoff for GC detection can be stated. It seems to be a play-off between including small, novel and potentially clinically relevant CNAs and impacting the sensitivity of the assay by including non-pathogenic somatic or germline variations. Research comparing the CBA and genomic microarray methods for GC risk stratification in CLL found that they were significantly similar as a predictor of TTFT and OS (228). Additionally, this research reported that high GC, detected either by CBA (HR: 3.23, p-value<0.001) or genomic microarrays (HR: 2.74, p-value<0.001) were significant in MVA for TTFT. This published data supports the methodology used in this thesis as genomic array techniques (SNP 6.0, Human Omni and 450k array) and a size cut off of ~1 Mb was employed to detect CNAs.

A further difference is that certain techniques, such as SNP 6.0 array and WGS, can detected cnLOH events, whilst others; CBA, aCGH and sWGS, cannot. Within many human malignancies including CLL, LOH and cnLOH events are common and have been linked to the tumorigenesis process (326,327). LOH events occur when a segmental or numerical chromosomal deletion occurs and these events have been linked to the tumour suppressor gene inactivation theory of malignant transformation. Whereas cnLOH events occur when a duplication of one chromosome or one chromosomal region and a simultaneous loss of the other allele happen and result in a LOH that is not detected by traditional cytogenetics due to there being no change in copy number (328). Within CLL, LOH typically associates with a copy number loss whereas cnLOH occurs less frequently but typically impact 13q, 17p and 11q chromosomal regions. Additionally, cnLOH have been reported to significantly impact clinical outcome in CLL patients, for example cnLOH-17p which are typically associated with homozygous *TP53* mutations (329). Within this research, cnLOH and LOH events were excluded from GC definition as certain techniques used did not detect them. Exclusion of these events removed 59 CNAs, some of which were recurrent clinically CNA for example del17p (n=3), del11q (n=9) and del13q (n=18). 13q14 cnLOH have been suggested to lead to dysregulation of micro RNAs miR15a/16-1 as well as other genes, typically occur with a biallelic deletion within the cnLOH region and are associated with a progressive disease (144,330). This brings into question whether cnLOH and LOH events should be included within the GC metric and whether a technical bias, introduced as sWGS and 450k array techniques were not able to detect such events, has impacted the reported clinical significance of GC. Whilst previous work has shown a comparable risk stratification of GC detected using CBA and genomic arrays, this work did not include cnLOH events in the CK metric (228). Therefore, further work is

required to fully assess the inclusion criteria of the GC metric and investigate the potential impact of cnLOH and LOH events on its prognostic ability.

Within this thesis, numerous technologies have been used to detect GC; sWGS, SNP 6.0 arrary, HumanOmni array and 450k array. Whilst the inclusion of these four techniques meant a great number of clinical trial patients met the inclusion criteria of having CNA data available it did potentially introduce a technical bias into the assessment of GC. A significant difference in the CNA called by 450k array technique compared to the three other techniques was found and could not be explained by patient characteristics of the 450k array cohort. Due to this finding, this cohort was either removed from the ARC/ADM survival cohort or, if available, CNA data generated from HumanOmni array was used instead. Research comparing the 450k array technique to SNP array reported that 76% of CNA identified in the cohort were common between both technologies. Of the CNAs that had discrepancies between the two technologies, the majority (75%) were solely detected by the 450k array technology and were suggested to be candidate false positives (287). Likewise in my data, the 450k array on average called significantly more CNAs (mean: 6.1 CNAs) than any other technology used, suggesting that many of these could be false positives. Further research assessing the reliability of three popular methods of calling CNA from methylation data compared to SNP genotype data, found that all methods had a relatively low reliability (331). They found that the Conumee method, which is employed in this thesis, called the fewest CNAs within the 450k array. Overall, they found that all three of the methylation calling methods reported more CNA but also detected much larger CNAs compared to SNP array CNA calling. This highlights the need for further optimization of the 450k array data analysis pipeline by altering the default parameters to adjust for the effect of the array design. Additionally, an in-depth and systematic manual curation of this data is imperative for the removal of potential false positives reported by the 450k array technique. By completing this pipeline optimization, the number of patients in the ARC/ADM survival analysis cohort can be increased, allowing for greater statistical power in the validation cohort employed in this thesis. As it currently stands, from comparing the advantages and disadvantages of the four technologies employed in the research I would recommend SNP arrays for the generation of GC data. This is based on the fact this technique was found to be highly comparable to the gold standard FISH technique and is able to detect CNAs at a high resolution as well as cnLOH events that have a potential important but unknown role in GC CLL biology (228).

Within the cohort of 495 clinical trial patients employed in Chapter 6, a significant association between mutation count and GC was found, specifically between the high GC and mutation count of two. Furthermore, the covariate mutation count remained significant in the multivariate PFS and OS using the validation survival cohort, however only a ≥3 mutation count retained

independence in the model. This finding was also supported in the literature as a study found a significant association between CK and higher mutational burden (p-value<0.009). Survival analysis reported that mutation burden, defined a ≥2 distinct mutation genes, *TP53* aberration and CK independently predicted a poorer TTFT (332). Inclusion of mutation data into complexity metrics has been debated within the CLL community and has been shown to have clinical significance. Chauzeix et al developed an eight gene estimator to test the clinical significance of TMB. The presence of ≥2 mutations included in the estimator were found to predict TFS (HR: 3.4), however this finding was reported using a cohort of only Binet A patients (230). Conversely, Nadeu attempted to assess the clinical impact of mutational complexity, defined by combining the number of mutations and CNA (121). They found that increased mutational complexity predicted a shortened TTFT and this impact on survival was independent of clonal architecture, *IGHV* mutation status and Binet stage. This work was able to detect mutational complexity in tumour subclones and reported that the prognostic impact of a different genes was linked to the size of the mutated clone. Additionally, they reported that unlike mutations, CNA typically remained stable and were an early event in the evolution of the disease. Conversely subclone analysis found that mutation could be acquired at any time during CLL evolution and frequently later than CNAs. This strongly suggests that CNAs are the main initial events in CLL and thus employing a GC metric that includes CNAs, rather than mutation data, is backed by biological evidence. Overall, my data, as well as published data, suggests that involving CNAs rather than genetic mutations within the GC metric improves the risk stratification ability of the biomarker.

Survival analysis completed in both Chapter 4 and Chapter 6 were conducted using a discovery and validation study design, as two separate clinical trial CLL4 and ARC/ADM cohorts were analysed. Whilst it was not possible to combine these cohorts together due to the CLL4 clinical trial recording follow up data for much longer than either the ARCTIC or ADMIRE clinical trials. Using these clinical trials in a discovery and validation study design has its limitations as the trials have used considerably different therapies, for example chemotherapy-based treatments and chemoimmunotherapy regimes. Biomarker discovery and validation are important steps in biomarker development, the latter aims to establish an association between the biomarker and an endpoint, i.e. survival endpoint. This clinical validation can be completed in retrospect using clinical trial data but given the impact on survival treatment can have, including such different regimes may influence this step (333). Thus, using two trials cohorts with different treatment regimes in a discovery and validation study design may limit the usefulness of the validation step due to the confounding effect on survival treatment may have. However, to control for this confounding impact, in both univariate and multivariate survival analysis completed in this thesis, treatment arm was included as a covariate. Whilst this work has been able to investigate the

clinical impact of various novel biomarkers in both chemotherapy and chemoimmunotherapy based trials, using these cohorts in a discovery and validation study design is potentially not suitable and this data rich clinical trial cohorts could be evaluated using a different study design.

One important finding of this research was that GC, specifically high GC, predicted a dismal OS and was associated with many other biomarkers of an aggressive disease such as *TP53* aberration, *ATM* disruption and TL-S. Three main hypotheses have been proposed to explain the association between GC and aggressive disease presentation; 1) defects in elements of the DNA damage repair and apoptotic cellular pathway leads to impaired response to genotoxic therapies, 2) ongoing clonal evolution drives progression and therapeutic resistance, 3) telomere attrition leads to genomic instability.

Defects in the DNA repair and apoptotic cellular pathways have long been reported in human cancers, including CLL. Research has also found the elevated levels of GC is typically associated with disruptions in the genes (*TP53* and *ATM*) involved in DNA damage repair, this relationship was reported in my data (103,238,310). As previously discussed, the cellular environment in tumours with *TP53* aberration promote obtaining additional genomic alterations, including CNAs. Given the usual role of protein produced by *TP53,* p53, in halting cell cycle progression, orchestrating DNA repair and triggering apoptosis in response to a variety of stresses, including DNA damage. In the case where the *TP53* gene has impaired function, either due to a mutation or a loss at the chromosomal loci, its tumour suppressor functions do not occur, and thus genomic stability is lost (305). Whilst most *TP53* aberration CLL cases occur with increased GC, not all cases with increased GC are reported with *TP53* aberration. Thus, other elements of the DNA damage repair pathway that ensure genetic stability have been suggested to contribute to GC, one such element is the *ATM* gene. Previous work has found that a deletion of this gene (del11q) and a mutation have been associated with GC. However, it has been reported del11q events are associated with a greater risk of GC (OR: 2.8, 95% CI: 1.6 to 5, p-value<0.001) but a sole *ATM* mutation was not. Neither did the presence of a mutation increase the risk of GC in del11q patients (334). In my data only a significance co-occurrence between high GC and biallelic *ATM*, patients with del11q and *ATM* mutation, was identified. Potentially the reason no significance enrichment between sole del11q and GC was found is that a different GC definition was used and if a combined intermediate and high GC group was used, a similar result to the literature would be found. This evidence taken together suggests that greater GC is not driven solely by the ATM locus and potentially a combination of defect in the DNA repair mechanisms is required to cause GC in a *TP53* independent fashion. A potential candidate for future investigation is the *H2AFX* gene which encodes the protein H2AX. *H2AFX* is lost along with *ATM* in ~25% of del11q cases (334). During DNA damage, activation of ATM kinase at sites of DSBs leads to the phosphorylation of H2AX

resulting in γ-H2AX. These γ-H2AX molecules form nuclear foci covering many megabases of chromatin which is crucial for efficient DNA damage response and thus the maintenance of genomic stability (335). Work in this area has identified an increased γ-H2AX in in *SF3B1* mutated CLL cells and, as expected, a decrease of γH2AX in *ATM* mutated cells compared to γ-H2AX levels in wild type CLL samples (336). Therefore, it would be interesting to investigate if certain DNA damage markers impact GC in CLL patients independently of ATM dysfunction, to further evaluate the role of the DNA repair machinery within the biology of GC (336). At the microscopic level, the recruitment of two DNA damage markers, γ-H2AX and 53BP1 results in the formation of nuclear foci at the site of the DSBs that can be detected and quantified using a fluorescent microscopy technique developed by the Stankovic research group at the University of Birmingham (337,338). This technique has been successfully applied to a small cohort of 6 patients from the GC clinical trial cohort (data not included), but further work is needed to expand this to a statistically powerful cohort.

GC has also been reported to be linked with clinical evolution. Clonal evolution is the Darwinian selection process by which cancer cells can acquire genomic alterations that present with an advantageous phenotype, allowing the CLL disease to further progress and become resistant to therapeutic interventions. The clonal evolutionary process is fuelled by intratumoural heterogeneity as the fittest tumour subclone is selected under certain selection pressures within the tumour microenvironment and expanded. Recently, research has used a longitudinal perspective to study the clonal evolution of CLL and the molecular mechanisms that contribute to RS. They found evidence to suggest that clonal expansion of a singular cell present many years before the clinical presentation of RS occurs (339). As a greater risk of developing RS is found in patients with CK, it suggests a mechanism whereby GC promotes clonal expansion of this singular cell resulting in RS. Furthermore, WGS of longitudinal CLL and RS samples identified a continuous increase in GC from CLL diagnosis to relapse and RS (340). This work found that the majority of increased GC reported in RS is caused by a chromothripsis event targeting certain genes including; *CDKN2A/B, MGA* and *SPEN.* They concluded that structural variants, including chromothripsis, are likely to be acquired early in RS. However, the true involvement of GC in the clonal evolution of the disease is not currently fully known and is beyond the scope of this research. Molecular methodologies employed in this thesis, sWGS and microarray analysis, are unable to identify the different subclones and therefore cannot provide information on the intraclonal cytogenetic heterogeneity. Despite that, the published evidence outlined above does indicate that GC could be useful in predicting patients destined to progress to RS, however to validate this theory a longitudinal study using single-cell DNA sequencing or SNP array data to detect tumour subclonal GC is needed.

The final hypothesis proposed to explain the relationship between GC and aggressive disease presentation theorises that greater telomere erosion leads to increased genomic instability, allowing for the accumulation of aberrations and thus GC. As the progressive shortening of telomeres corresponds to the number of cell divisions, TL reflects the proliferative history of a CLL cell. It has been suggested that the genomic instability associated with short TL promotes the selection of clones that can maintain the minimal TL by activity of telomerase or have defects in DNA damage checkpoint and repair (**Figure 65**). Thereby the critical erosion length is not reached, and the presence of telomere dysfunction induced foci does not trigger a DNA damage response, and thus the clone overcomes senescence and survives (341). Research has not only reported a correlation between TL shortening and genomic instability but also an inverse relationship between TL and telomerase activity (342). Results from this thesis were able to corroborate the relationship between TL-S and GC previously reported in the literature (185), but also found that TL-S and GC independently predicted dismal OS in the discovery cohort. Whilst GC was also significant in the final OS multivariate model using the validation cohort, the covariate TL was not. Conversely within the multivariate models described in Chapter 4, which did not include the GC covariate, TL-S was found to predict poor PFS and OS across both survival cohorts, which matches published research (185,189). Therefore, this suggests that the clinical significance of TL may be confounded by the presence of GC and other DNA damage repair defaults, such as *TP53* aberration which remained significant in multivariate work. And perhaps TL-S alone is not significant enough to result in an aggressive disease with poor survival.

Similarly, evidence has shown BCR or Pi3K microenvironment-mediated signalling contributes to telomerase activation suggesting a role of BCR signalling capabilities of the cell in a mechanism that links epitype, TL, GC and CLL disease presentation together (277). This thesis was able to, for the first time, investigate together the clinical significance of TL and DME. A strong correlation between TL and DME groups was found in my data with both variables also being associated with GC. Additionally, my results highlighted the potentially utility of the i-CLL, risk stratified further by TL, in identifying M-CLL patients destined to respond poorly to CIT. Furthermore, the i-CLL epitype remained significant in all multivariate models constructed in Chapter 6 and in most cases predicted a worse survival than n-CLL patients. As previously mentioned, CLL is charactered by stereotyped BCR usage with the i-CLL epitype being comprised mainly of subset #2 stereotype. The BCR of subset #2 is composed of heavy and light chains encoded by *IGHV*3-21 and *IGLV*3-21, respectively. A BCR-BCR homotypic interaction is dependent on the *IGLV*3-21 light chains as clonotypic rearrangement of the *IGLV*3-21 genes (IGLV3-21^{R110}) can occur and result in a cell autonomous signalling. This BCR autonomous signalling results in pro-survival signals being triggered as well as increased proliferation due to upregulated *WNT5A* expression (131,274,315).

Using previously reported evidence coupled with finding from this thesis, a narrative is suggested whereby the BCR stereotypes, which are associated with specific DME subtypes, have differing signalling capabilities and thus differing levels of proliferation (343). Increased levels of proliferation due to autonomous signalling of the BCR is reflected in TL shortening. This critical shortening of TL is a selection pressure on the CLL cell to acquire dysfunction at DNA damage checkpoint and repair genes, adding to the heterogeneity of the disease. Additionally, pro survival signals are triggered from the continuous BCR activation. Overall, this results in cells that have a greater genomic instability, clonal evolution and GC and thus present with an aggressive CLL disease and poor patient outcome, see **Figure 65**. However further work is required to fully examine the biological mechanisms of GC, in the context of TL and DME, to confirm this proposed theory.

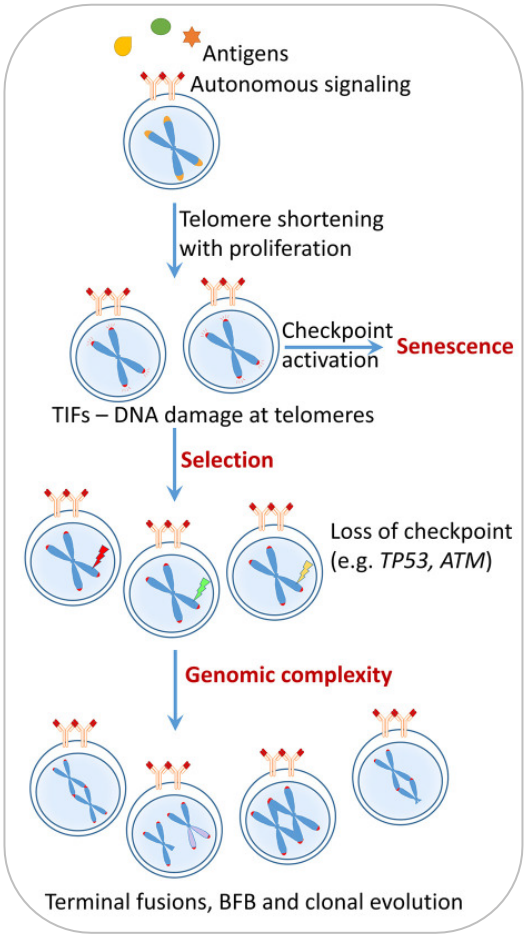

Figure 65- Schematic representing the proposed theory behind the relationship between epitype, TL and GC in CLL. Abbreviations: telomere dysfunction induced foci- TIF, breakage-fusion-bridge- BFB. Adapted from (163).

It can be concluded from the results reported in this work that patients with high GC have a significantly worse outcome than patients with low GC. This analysis was based on clinical trial patient enrolled in CIT regimes and did not include patients that have been given targeted agents,

which are becoming a preferred treatment option for many CLL patients. Thus, to further this work a cohort of patients enrolled in targeted agent clinical trials is needed. Various publicized research has investigated the use of GC as a prognostic and predictive biomarker in various targeted agent treatment regimes. For example, GC, defined as CK, was found to predict a dismal OS (HR: 5.9, 95%CI: 1.6 to 22.2, p-value<0.01) in R/R patients that were then treated with ibrutinib, a BTK inhibitor (206). Further research looking into clonal evolution found that CK evolution at progression of the disease, after ibrutinib, predicts inferior survival in a cohort of untreated and R/R CLL patients (232). Conversely, results from the CLL14 clinical trial using previously untreated patients enrolled into venetoclax plus Obinutuzumab treatment regimes did not find a significant difference in PFS, OS or minimal residual disease response in patients with CK compared to patients without (344). Similarly, no difference between CK and no CK patients were found even within 5 year follow up data. Conversely, data from the MURANO study of R/R patients that were given venetoclax found that GC was associated with a poorer PFS (HR:2.9, 95%CI: 1.4 to 6.3, p-value<0.01) and a lower undetectable minimal residual disease rate at end of treatment was lower for patients with GC compared to patients without (p-value<0.05) (233). Additionally a studying including 220 R/R CLL patients that were given idelalisib in combination with rituximab compared to a treatment of just rituximab found a difference in outcome in CK patients between the treatment arms. Specifically, CK patients responded better with a longer OS reported when given the idealalisib and rituximab treatment compared to CK patients in the rituximab only treatment arm. This suggests the combination of targeted agents increases the efficacy of treatment, even in high-risk cases such a CK patients. (232)

The relevance of GC in the target agent treatment era is not conclusive within the current published evidence, however I accept this will change as the clinical trials mature and cohort size become larger. A limitation of published work is that the majority of studies are focused on R/R CLL patient whereas targeted agents are fast becoming the primary frontline treatment. Similarly, a limitation of this work was lack of representation in the cohort used as no R/R patients or cases which had progressed to RS were included. Further inspection of the GC biomarker within these specific CLL populations would allow the complete clinical value of GC to be defined, strengthening its need to be validated and applied to guide therapeutic decisions.

In conclusion this work has investigated the biological characteristics and clinical significance of three novel CLL biomarkers; TL, DME and GC. Whilst the long-disputed question around which platform is most appropriate for GC data generation cannot be definitively answered, the evaluation of the techniques employed in this work found that SNP array was overall better than the other techniques. For the first time, TL and DME were assessed together within a clinical trial cohort. Not only was a strong association found between the two biomarkers, as previous

reported, but both biomarkers were found to independently predict poor PFS and OS in CIT treated patients. Furthermore, my data suggests that a combination of the two biomarkers leads to a greater ability in patient risk stratification, specifically in further stratifying the M-CLL cases. Similarly, it was found that high GC was an independent marker of dismal survival in patients given frontline CIT treatment and was associated with a unique genomic profile. The analysis completed within this project adds to the growing evidence that GC is a useful prognostic and predictive biomarker in CLL and therefore a great contender for further validation before implementation with the clinical setting. Due to the strong association found between the three biomarkers and all being found to correlate with poor survival, a theory was proposed. This theory outlines a biological mechanism whereby the three biomarkers all contribute to an aggressive CLL disease with dismal patient outcomes. Further investigation into this theory as well as the prognostic utility of the three biomarkers within the wider CLL population (i.e. targeted agent treated, R/R and RS patients) is needed before they can be fully validated and deployed within the clinical setting.

Supplementary Tables

Supplementary Table 1- Overview of the 25 studies that meet the eligibility requirements and therefore will be used within downstream analysis.

First Author	Year	Patient Description	GC Metric	Detection Method	Survival Data
L. Kujawski	2008	139 untreated and 39 treated CLL patients.	Copy number losses, gains and loss-of-heterozygosity added for total genomic complexity scores. A further GC score was calculated by only counting losses	50kXbaI SNP array	HRs, CIs, p-values, means TTFT and TTST
N. Kay	2011	48 untreated CLL patients.	Total number of CNAs and the sum of genomic lengths of all detected gains and losses	aCGH	CIs, median, p-value PFS, time to first response and DOR
P. Ouillette	2011	196 untreated and 59 relapsed patients.	Total sub chromosomal losses and gains: 0, >1, >2, >3 and >4. Dosage, total length of all sub chromosomal genomic lesions in Mb as a continuous variable and as a log-2 transformed variable	SNP 6.0 array with matched germline samples	HRs, CIs, p-value TTFT and OS
M. Mian	2013	329 CLL patients with normal FISH. Treatment naive.	The presence of a large genetic lesion >5 Mb which are not detected by FISH	SNP 6.0 array	HRs, CIs, p-value TTFT and OS
C. Schweighofer	2013	168 untreated CLL patients.	Number of CNAs as a continuous and categorical variable (1, 2 and 3 CNV)	SNP array	HRs, CIs, p-value and mean TTT and OS

P.Baliakas	2014	1001 untreated CLL patients	Complex karyotype; ≥3 abnormalities.	CBA	Median, p-value, HRs and CIs TTFT
J. Delgado	2014	55 CLL patients with *TP53* disruption. 20 treated and 35 untreated.	CNA count	SNP 6.0 and a custom 8x60K array	HRs, CIs, p-value TTFT and OS
I. Salaverria	2015	47 untreated and 133 treated CLL patients.	Number of CNAs (0->6)	aCGH using two different probe series	HRs, CIs, mean, p-value TTT and OS
G. Blanco	2016	101 CLL patients with *TP53* aberrations. 81 treated and 20 untreated.	Complex Karyotype; ≥3 abnormalities	Chromosome banding analysis	HRs, CIs, p-value and median OS
R. Collado	2017	60 CLL patients with chromosomal abnormalities in 17p. 47 treated and 13 untreated.	Complex karyotype; ≥3 abnormalities	FISH and aCGH	p-value and mean PFS and OS
A. Puiggros	2017	1045 patients with or without high-risk FISH deletions. Untreated MBL/CLL patients.	Complex karyotype; ≥3 abnormalities	Chromosome banding analysis	HRs, CIs, median, p-value TTFT and OS
L. Yu	2017	69 with del17p events and 208 without del17p events. Both 203 untreated and 74 treated patients.	Complex karyotype; ≥3 abnormalities. CNA low <4 and CNA high ≥4. Low and high mutation defined as <21 and ≥21 mutations respectively. Total length of CNA was also investigated	176 cases had somatic mutation profiles by WES and 200 had CNAs detected by SNP 6.0 arrays	HR, CIs, p-value OS

F Nadeu	2018	406 untreated CLL patients including 44 sequential samples.	Mutational complexity, sum of mutations and CNAs	CNA detected using SNP 6.0 array. 28 driver genes examined using deep-targeted NGS	HR, CIs and p-values. TTFT and OS
P. Baliakas	2019	5095 used in survival analysis. Majority of patients are untreated 4446 and only 461 were treated.	Complex karyotype; ≥3 abnormalities, high cytogenetic complexity ≥5 CNAs	Chromosome-banding analysis	HRs, CIs, mean and p-values OS
N. Heerema	2020	329 untreated CLL patients.	Cytogenetic complexity; ≥3 abnormalities. A cut-off of ≥5 abnormalities also used	Chromosome banding analysis	HRs, CIs, P-value TTFT and OS
A.Kater	2020	194 Ventoclax treated and 195 chemotherapy treated CLL patients.	Array-based GC was defined as follows: noncomplex: 0-2 aberrations, low: 3-4 aberrations and high: 5 or more aberrations	aCGH	HRs, CIs, median, and P-value PFS and OS.
J. Chauzeix	2020	150 CLL untreated patients	Mutational count (≥1 eight gene estimator) and tumor mutational burden	High-throughput sequencing using a custom panel of 65 targets	HR and p-value Treatment free survival
A. Leeksma	2020	2293 CLL patients, 942 treated and 1351 untreated CLL patients.	High genomic complexity ≥5 CNAs. Included a size cut off	Various genomic arrays and whole genome	HRs, CIs, P-value TTFT and OS
A. Kittai	2021	456 CLL patients treated with ibrutinib	Complex karyotype, ≥3 or ≥5 cytogenetic abnormalities and as a continuous variable	Conventional cytogenetics	HRs and CIs, p-value PFS and OS

H. Cherng	2022	130 CLL patients with TP53 alterations who received first-like BTKi-based treatment	Karyotypic complexity defined as a continuous variable and as ≥3 or ≥5 abnormalities.	CBA	HR, CIs, p-value PFS
A.Puiggros	2022	42 CLL patients, 2 treated and 40 untreated	Complex , ≥10 alterations	Optical genome mapping	Median, p-value, CIs TTFT
S.Ramos-Campy	2022(a)	340 untreated CLL patients	Copy number abnormalities; 0-2, 3-4, ≥5	Chromosome banding analysis and genomic microarrays	HR and p-value TTFT and OS
S.Ramos-Campy	2022(b)	162 untreated CLL patients with genomic complexity, of those 33 also had chromothripsis	Complex karyotype (3-4 and ≥5 abnormalities)	Various genomic microarrays	HR and p-value TTFT
P.Robbe	2022	485 untreated CLL patients	Copy number gains only, copy number losses only and both gains and losses	WGS TruSeq	HRs, CIs, p-value PFS and OS
G. Rigolin	2023	119 untreated CLL patients with isolated del13q or no lesions	Complex karyotype defined as ≥3 abnormalities, gains and losses of ≥5 Mb in length were considered	Genomic microarrays	HR, CIs and p-value TTFT and OS

Footnote: Patient description includes sample size, if they are selected based on a specific feature i.e. TP53 aberrations, patient CLL natural history status (untreated, treated, relapsed, progressed). GC metric is given, if numerous metrics were employed within a study, they are all included. Detection methods is given, if numerous techniques were employed within a study, they are all included. Survival data column explains the reported survival analysis included in each publication, such as the recorded values (HR, CI's, median survival or p-value) and the type of survival endpoint used in either univariant or multivariant analysis. Mb-megabase, SNP- single nucleotide polymorphism array, aCGH-array comparative genomic hybridization, NGS-next generation sequencing, WES-whole exome sequencing, WGS-whole genome sequencing, DOR-duration of response, TTFT-time to first treatment, TTT-time to treatment, TTST-time to subsequent treatment, PFS-progression free survival, and OS-overall survival.

Supplementary Table 2- The 72 probe targets that were designed as part of the SureSelect XT HS2 DNA target enrichment system for the identification of variants within these panel of genes. Of the 72 targets, 62 were included in a previous probe design for variant detection experiment and 10 (shown in **bold**) were added during the design of the probes, as were recently reported in the CLL literature. The three cases were adjustments to the probe design was required to improve coverage are shown by an asterisk (*).

Target ID	Interval	Size	Coverage
ARID1A	chr1:26696394-26780766	7362	100
ATM	chr11:108227615-108365518	10430	100
BCL2	chr18:63128615-63318676	793	100
BCOR	chrx:40049906-40077939	5707	100
BIRC3	chr11:102324500-102337112	2118	100
BRAF_EX15	chr7:140753275-140753393	119	100
BTK	chrx:101349875-101390559	2462	100
CARD11	chr7:2906628-2958516	3945	100
CCND3	chr6:41935841-41941659	1151	100
CD79A	chr19:41877295-41880990	1006	100
CD79B	chr17:63929216-63932271	813	100
CDH23	chr10:71397179-71815288	12544	100
CHD2	chr15:92901228-93024715	6666	100
CREBBP	chr16:3727708-3879926	7988	100
CXCR4	chr2:136114859-136118070	1359	100
DDX3X	chrx:41334243-41364352	3178	94.3
EGR2	chr10:62813197-62816039	1471	100
EZH2EX12	chr7:148816684-148816778	95	100
EZH2EX16	chr7:148811625-148811720	96	100
EZH2EX18	chr7:148809310-148809390	81	100
FBXW7	chr4:152322871-152411813	2898	100
FLNC	chr7:128830628-128858533	9138	100
ID3	chr1:23558950-23559436	400	100
IDH2EX4	chr15:90088587-90088747	161	100
JAK3	chr19:17826733-17844427	3913	100
KDM2B	chr12:121430106-121580921	4856	100
KLF2	chr19:16324914-16327041	1128	100
KLHL6	chr3:183491917-183555663	2006	100
KMT2D*	chr12:49032813-49032962	150	100
KRAS	chr12:25209785-25245394	828	100
LRP1B	chr2:140233176-142130739	15754	100
LTB	chr6:31580699-31582427	815	100
MAP2K1	chr15:66387338-66490625	1462	100
MAP3K14	chr17:45264626-45290755	3144	100
MDM2	chr12:68808468-68839859	1956	100
MED12	chrx:71118745-71142228	7477	100
MYD88	chr3:38138652-38141296	1054	100
NFKBIE	chr6:44259209-44265773	1623	100
NOTCH1EX26	chr9:136504673-136505104	432	100

NOTCH1EX27	chr9:136503182-136503330	149	100
NOTCH1EX28	chr9:136502272-136502488	217	100
NOTCH1EX34_3'UTR	chr9:136494444-136497558	3115	100
NOTCH2	chr1:119915296-120069416	8480	100
NOTCH2EX34+UTR	chr1:119911553-119916694	5142	100
NRAS	chr1:114708525-114716170	650	100
P53	chr17:7676521-7687538	264	100
PAX5NONCODING	chr9:37368943-37373596	4654	100
PLCG2	chr16:81785980-81958008	4492	100
PLS3	chrx:115610241-115649571	2502	97.0
POT1	chr7:124822518-124897183	2444	100
PRKDC	chr8:47774163-47960136	14107	100
PTPRD	chr9:8317864-8733853	6712	100
RHOA	chr3:49360199-49375599	944	100
RPS15*	chr19:1438797-1438853	57	100
SAMHD1	chr20:36892922-36951653	2249	100
SETD2	chr3:47017083-47163934	8216	100
SF3B1EX14	chr2:197402556-197402826	271	100
SF3B1EX15	chr2:197401985-197402130	146	100
SF3B1EX16	chr2:197401742-197401888	147	100
SF3B1EX18	chr2:197400715-197400936	222	100
SPEN	chr1:15848058-15939437	11596	100
STAT3EX21	chr17:42322282-42322494	213	100
TCF3	chr19:1611697-1650258	2813	100
TET2	chr4:105190460-105276529	6365	100
TNFAIP3	chr6:137871218-137881329	2533	100
TNFRSF14	chr1:2556655-2563283	1063	100
TP53*	chr17:7661929-7662024	96	100
TRAF3	chr14:102870192-102905794	1987	100
UBR5	chr8:102254292-102412244	9580	100
USP34	chr2:61188092-61470702	12245	100
XPO1EX15	chr2:61492325-61492481	157	100
XPO1EX16	chr2:61492035-61492198	164	100

Supplementary Table 3- Basic clinico-biological features of the ARCTIC and ADMIRE cohort used within this study compared to the total clinical trial cohort.

Variable	**Study cohort N (%)**	**Total cohort N (%)**	**Concordance P-value**
Total number of patients	215	414	
Age, median years (range)	62 (36-80)	63 (33-80)	0.127
Gender			
Male	167 (77.7)	298 (72)	0.123

Female	48 (22.3)	116 (28)	
Binet Stage			
A	34 (15.8)	60 (14.5)	0.876
B	107 (49.8)	205 (49.5)	
C	74 (34.4)	149 (36)	
IGHV Mutational Status			
IGHV-U	116/196 (59.2)	205/356 (57.6)	0.716
IGHV-M	80/196 (40.8)	151/356 (42.4)	
ATM Dysfunction			
Absent	120/156 (76.9)	162/209 (77.5)	0.988
Del11q	25/156 (16.0)	33/209 (15.8)	
Biallelic inactivation	11/156 (7.1)	14/209 (6.7)	
TP53 Dysfunction			
Absent	151/176 (85.8)	202/231 (87.4)	0.627
Present	25/176 (14.2)	29/231 (12.6)	
SF3B1 Mutation			
Absent	138/180 (76.7)	196/250 (78.4)	0.67
Present	42/180 (23.3)	54/250 (21.6)	
NOTCH1 Mutation			
Absent	154/180 (85.6)	217/250 (86.8)	0.711
Present	26/180 (14.4)	33/250 (13.2)	
Epigenetic Subgroup			
n-CLL	102 (47.4)	113/246 (45.9)	0.928
i-CLL	61 (28.4)	70/246 (28.5)	
m-CLL	52 (24.2)	63/246 (25.6)	
Telomere Length Group			
Short	48 (22.3)	50/252 (19.8)	0.762
Intermediate	59 (27.4)	68/252 (27)	
Long	108 (50.2)	134/252 (53.2)	

Footnote: Assessment of a variety of clinco-biological features were completed to examine the patient composition of the cohort using in this research compared to the complete clinical trial cohort. The number screened for each feature varied as the total cohort did not have complete data for all variables. Percentages were calculated using the frequency of that variable and the number of patients, in the specific cohort, that were screened for it, for example 33 patients had a NOTCH1 mutation out of the 250 clinical trial patients that were screened for it. For continuous variables, such as Age, the median and range were reported. Comparisons across the two cohorts were completed using a Wilcoxon rank sum and chi squared test for continuous and catagorical variables, respectively. A p-value<0.01 indicated that there was a signficant difference within the variable across the two cohorts.

Supplementary Tables

Supplementary Table 4- Basic clinico-biological features of the CLL4 cohort used within this study compared to the total clinical trial cohort.

Variable	**Study cohort N (%)**	**Total cohort N (%)**	**Concordance P-value**
Total number of patients	304	777	
Age, median years (range)	65 (42-86)	64 (35-86)	0.73
Gender			
Male	229 (75.3)	573 (73.7)	0.593
Female	75 (24.7)	204 (26.3)	
Binet Stage			
A	81 (26.7)	191 (24.6)	0.664
B	129 (42.4)	352 (45.3)	
C	94 (30.9)	234 (30.1)	
IGHV Mutational Status			
IGHV-U	163/267 (61)	327/533 (61.4)	0.934
IGHV-M	104 /267(39)	206/533 (38.6)	
ATM Dysfunction			
Absent	184/234 (78.6)	342/438 (78.1)	0.955
Del11q	43/234 (18.4)	84/438 (19.2)	
Biallelic inactivation	7/234 (3.0)	12/438 (2.7)	
TP53 Dysfunction			
Absent	223/250 (89.2)	407/456 (89.3)	0.982
Present	27/250 (10.8)	49/456 (10.7)	
SF3B1 Mutation			
Absent	200/264 (75.8)	352/462 (76.2)	0.895
Present	64/264 (24.2)	110/462 (23.8)	
NOTCH1 Mutation			
Absent	226/265 (85.3)	396/462 (85.7)	0.874
Present	39/265 (14.7)	66/462 (14.3)	
Epigenetic Subgroup			
n-CLL	159 (52.3)	186/359 (51.8)	0.987
i-CLL	104 (34.2)	125/359 (34.8)	
m-CLL	41 (13.5)	48/359 (13.4)	
Telomere Length Group			
Short	158 (52)	239/453 (52.8)	0.912

Intermediate	80 (26.3)	113/453 (24.9)	
Long	66 (21.7)	101/453 (22.3)	

Footnote: Assessment of a variety of clinco-biological features were completed to examine the patient composition of the cohort using in this research compared to the complete clinical trial cohort. The number screened for each feature varied as the total cohort did not have complete data for all variables. Percentages were calculated using the frequency of that variable and the number of patients, in the specific cohort, that were screened for it, for example 396 patients had a NOTCH1 mutation out of the 462 clinical trial patients that were screened for it. For continuous variables, such as Age, the median and range were reported. Comparisons across the two cohorts were completed using a Wilcoxon rank sum and chi squared test for continuous and catagorical variables, respectively. A p-value<0.01 indicated that there was a signficant difference within the variable across the two cohorts.

Supplementary Table 5- Univariate survival analysis of the CLL4 cohort examining progression free survival (PFS).

Variable	Status	Total	Events	Median (Years)	Lower Range (Years)	Upper Range (Years)	HR	Lower CI	Upper CI	P-value
Telomere Length^	Short	158	153	1.95	0.1	8.2	2.36	1.7	3.29	<0.001
	Intermediate	80	75	2.35	0	9	1.81	1.26	2.6	0.001
	Long	66	50	3.85	0.1	10.1	-	-	-	-
Epitype^	n-CLL	159	157	2	0.1	8.4	1.96	1.32	2.9	<0.001
	i-CLL	104	92	3	0	10.1	1.28	0.85	1.93	0.24
	m-CLL	41	30	2.8	0.1	8.6	-	-	-	-
TP53 dysfunction”	Yes	27	27	0.3	0.1	6.3	3.61	2.39	5.44	<0.001
	No	223	198	2.5	0	10.1	-	-	-	-
ATM Dysfunction$^{\$}$	Biallelic	7	7	1.47	0.8	3	2.42	1.12	5.2	0.024
	Del11q	43	41	2.17	0.1	8.8	1.53	1.09	2.17	0.015
	Wild Type	184	162	3.02	0	10.1	-	-	-	-
NOTCH1$^{£}$	Mutated	39	38	2.2	0.1	7.7	1.28	0.9	1.81	0.17
	Unmutated	226	202	2.5	0	10.1	-	-	-	-
SF3B1^{+}	Mutated	64	62	2.2	0.2	8.4	1.32	0.98	1.76	0.06
	Unmutated	200	177	2.5	0	10.1	-	-	-	-
Age^	-	-	-	-	-	-	1	1	1	0.094
Sex^	Female	75	67	2.9	0	9	-	-	-	-
	Male	229	211	2.2	0	10.1	1.2	0.94	1.6	0.13
Binet Stage^	C	94	86	1.9	0.1	9.5	0.98	0.69	1.4	0.91
	B	129	119	2.5	0.1	10.1	0.83	0.59	1.15	0.25

	A	81	73	2.2	0	8.8	-	-	-	-
IGHV mutation status~	Unmutated	163	159	1.9	0.1	8.3	2	1.5	2.6	<0.001
	Mutated	104	85	3.4	0.04	10.1	-	-	-	-
Treatment Arm^	FDR	71	68	2.36	0.1	8.4	-	-	-	-
	FC	120	104	3.84	0.1	10.1	0.54	0.4	0.73	<0.001
	Chl	113	106	2.07	0	9	1.13	0.83	1.53	0.43
Fusogenic median^	Below	224	214	2.55	0	9	1.77	1.33	2.36	<0.001
	Above	80	64	3.65	0.04	10.1	-	-	-	-
Fusogenic mean^	Below	26	25	1.83	0.1	6.2	1.72	1.13	2.59	0.011
	Above	278	253	2.93	0	10.1	-	-	-	-

Footnote: CI- confidenence interval, HR-hazard ratio. Wald chi squared test, p-value<0.05 is considered significant. Within each variable with multiple statuses a reference is needed to be assigned for the univariant analysis, these are shown as do not have a calculated HR or CIs, for example in the Telomere length variable the Long status is the reference. ^ Based on 304 patients and events. ”Based on 250 patients and events. $ Based on 247 patients and 222 events. £ Based on 265 patients and events. + Based on 264 patients and 220 events. ~ Based on 267 patients and 243 events.

Supplementary Table 6- Univariate survival analysis of the CLL4 cohort examining overall survival (OS).

Variable	**Status**	**Total**	**Events**	**Median (Years)**	**Lower Range (Years)**	**Upper Range (Years)**	**HR**	**Lower CI**	**Upper CI**	**P-value**
Telomere Length^	Short	158	146	4.95	0.1	15.9	2.66	1.87	3.76	<0.001
	Intermediate	80	68	6	0.1	16	2.11	1.43	3.12	<0.001
	Long	66	42	9.65	0.1	17.4	-	-	-	-
Epitype^	n-CLL	159	144	5.6	0.1	16	2.8	1.81	4.34	<0.001
	i-CLL	104	88	5.8	0.1	16.6	2.2	1.4	3.45	<0.001
	m-CLL	41	24	9.8	0.1	17.4	-	-	-	-
TP53 dysfunction”	Yes	27	26	1.5	0.2	15.6	3.66	2.4	5.57	<0.001
	No	223	183	6.3	0.1	16.6	-	-	-	-
ATM Dysfunction$	Biallelic	7	7	4.93	1	10.2	1.93	0.9	4.13	0.091
	Del11q	43	41	5.3	0.1	13	1.65	1.16	2.34	0.0051
	Wild Type	184	146	7.04	0.1	16.6	-	-	-	-

NOTCH1[£]	Mutated	39	35	5.9	0.1	16	1.36	0.94	1.95	0.099
	Unmutated	226	186	6.3	0.1	17.4	-	-	-	-
SF3B1[+]	Mutated	64	61	4.6	0.2	15.5	1.77	1.31	2.38	<0.001
	Unmutated	200	159	6.95	0.1	17.4	-	-	-	-
Age^	-	-	-	-	-	-	1.05	1.04	1.07	<0.001
Sex^	Female	75	58	6.3	0.1	17.4	-	-	-	-
	Male	229	198	6	0.1	16.6	1.27	0.95	1.7	0.11
Binet Stage^	C	94	83	4.3	0.1	16.4	1.38	0.95	2	0.089
	B	129	109	7	0.3	17.4	1.14	0.81	1.61	0.45
	A	81	64	6.7	0.2	16.5	-	-	-	-
IGHV mutation status[~]	Unmutated	163	153	4.9	0.1	16	2.3	1.73	3.06	<0.001
	Mutated	104	74	8.7	0.1	17.4	-	-	-	-
Treatment Arm^	FDR	71	59	6.31	0.1	17.4	-	-	-	-
	FC	120	98	6.86	0.2	16.6	0.89	0.64	1.23	0.47
	Chl	113	99	6.78	0.1	16.5	0.97	0.7	1.34	0.84
Fusogenic median^	Below	224	202	5.92	0.1	16	2.17	1.6	2.94	<0.001
	Above	80	54	8.9	0.1	17.4	-	-	-	-
Fusogenic mean^	Below	26	25	4.37	0.2	12.6	1.96	1.3	2.98	0.0015
	Above	278	231	6.92	0.1	17.4	-	-	-	-

Footnote: CI- confidenence interval, HR-hazard ratio. Wald chi squared test, p-value<0.05 is considered significant. Within each variable with multiple statuses a reference is needed to be assigned for the univariant analysis, these are shown as do not have a calculated HR or CIs, for example in the Telomere length variable the Long status is the reference. ^ Based on 304 patients and 256 events. ”Based on 250 patients and 209 events. $ Based on 247 patients and 206 events. £ Based on 265 patients and 221 events. + Based on 264 patients and 220 events. ~ Based on 267 patients and 227 events.

Supplementary Table 7- Univariate survival analysis of the ARCTIC/ADMIRE cohort examining progression free survival (PFS)

Variable	**Status**	**Total**	**Events**	**Median (Years)**	**Lower Range (Years)**	**Upper Range (Years)**	**HR**	**Lower CI**	**Upper CI**	**P-value**
Telomere Length^	Short	48	36	3.84	0.04	8.19	2.87	1.85	4.46	<0.001
	Intermediate	59	44	4.05	0.11	8.98	2.45	1.62	3.71	<0.001
	Long	108	47	6.06	0.02	9	-	-	-	-
Epitype^	n-CLL	102	78	3.87	0.02	8.98	4.47	2.56	7.82	0.005

	i-CLL	61	34	5.45	0.11	9	2.4	1.3	4.41	<0.001
	m-CLL	52	15	6.93	0.16	8.68	-	-	-	-
TP53 dysfunction”	Yes	25	21	2.09	0.04	8.98	4.39	2.69	7.17	<0.001
	No	151	86	5.45	0.02	8.86	-	-	-	-
ATM Dysfunction$	Biallelic	11	11	3.36	1.25	6.43	3.37	1.76	6.47	<0.001
	Del11q	25	22	3.82	0.16	6.99	2.49	1.51	4.1	<0.001
	Wild Type	120	29	4.98	0.019	8.98	-	-	-	-
NOTCH1£	Mutated	26	14	5.6	0.33	8.86	0.82	0.47	1.44	0.49
	Unmutated	154	95	4.58	0.02	9	-	-	-	-
SF3B1£	Mutated	42	27	4.48	0.02	8.98	1.23	0.8	1.91	0.35
	Unmutated	138	82	5.27	0.04	9	-	-	-	-
Age^	-	-	-	-	-	-	1.01	0.986	0.992	0.22
Sex^	Female	48	24	5.57	0.33	8.19	-	-	-	-
	Male	167	103	4.57	0.02	9	1.44	0.92	2.24	0.109
Binet Stage^	C	74	39	5.16	0.02	9	0.68	0.4	1.13	0.14
	B	107	65	4.8	0.11	8.86	0.82	0.51	1.33	0.42
	A	34	23	4.52	0.04	8.03	-	-	-	-
IGHV mutation status~	Unmutated	116	86	4.09	0.04	8.98	2.76	1.81	4.21	<0.001
	Mutated	80	30	6.76	0.02	9	-	-	-	-
Treatment Arm^	FCR	94	52	5.07	0.16	9	-	-	-	-
	FCMR	54	30	4.92	0.28	8.86	1.05	0.67	1.64	0.84
	FCMminiR	39	27	4.65	0.37	8.16	1.41	0.88	2.24	0.15
	FCMminiR/FCR	12	7	4.15	2.03	6.07	1.38	0.62	3.05	0.43
Fusogenic median^	Below	70	54	3.6	0.04	8.19	2.49	1.74	3.57	<0.001
	Above	145	73	5.29	0.02	9	-	-	-	-
Fusogenic mean^	Below	19	15	4.31	1.15	8.19	1.56	0.91	2.69	0.12
	Above	196	112	4.78	0.02	9	-	-	-	-

Footnote: CI- confidenence interval, HR-hazard ratio. Wald chi squared test, p-value<0.05 is considered significant. Within each variable with multiple statuses a reference is needed to be assigned for the univariant analysis, these are shown as do not have a calculated HR or CIs, for example in the Telomere length variable the Long status is the reference. ^ Based on 215 patients and 127 events. ”Based on 176 patients and 107 events. $ Based on 156 patients and 97 events. £ Based on 180 patients and 109 events. ~ Based on 196 patients and 116 events. * Based on 86 patients and 25 events.

Supplementary Table 8- Univariate survival analysis of the ARCTIC/ADMIRE cohort examining overall survival (OS)

Variable	Status	Total	Events	Median (Years)	Lower Range (Years)	Upper Range (Years)	HR	Lower CI	Upper CI	P-value
Telomere Length^	Short	48	18	5.8	0.04	8.19	2.56	1.37	4.79	0.0033
	Intermediate	59	18	6.28	0.11	8.99	1.6	0.86	2.96	0.14
	Long	108	23	6.99	0.02	9.1	-	-	-	-
Epitype^	n-CLL	102	38	6	0.02	9.1	3.95	1.66	9.35	0.0018
	i-CLL	61	15	6.74	0.11	9	2.22	0.86	5.73	0.1
	m-CLL	52	6	7.03	0.16	8.68	-	-	-	-
TP53 dysfunction”	Yes	25	12	3.62	0.04	8.98	3.77	1.94	7.33	<0.001
	No	151	33	6.83	0.02	9.1	-	-	-	-
ATM Dysfunction$	Biallelic	11	4	5.25	1.66	8.02	1.47	0.52	4.17	0.47
	Del11q	25	5	5.88	0.16	9.1	0.73	0.29	1.88	0.52
	Wild Type	120	16	5.78	0.019	8.98	-	-	-	-
NOTCH1£	Mutated	26	8	6.69	0.47	8.86	1.36	0.63	2.91	0.44
	Unmutated	154	38	6.73	0.02	9.1	-	-	-	-
SF3B1£	Mutated	42	9	6.91	0.02	8.99	0.78	0.38	1.61	0.5
	Unmutated	138	37	6.67	0.04	9.1	-	-	-	-
Age^	-	-	-	-	-	-	1.04	1.01	1.07	0.021
Sex^	Female	48	11	6.61	1.03	9.1	-	-	-	-
	Male	167	48	6.46	0.02	9	1.34	0.69	2.58	0.38
Binet Stage^	C	74	18	6.56	0.02	9	0.53	0.26	1.08	0.079
	B	107	27	6.75	0.11	8.99	0.56	0.29	1.08	0.082
	A	34	14	5.99	0.04	9.1	-	-	-	-
IGHV mutation status˜	Unmutated	116	38	6.05	0.04	9.1	1.81	1.01	3.26	0.047
	Mutated	80	16	6.99	0.02	9	-	-	-	-
Treatment Arm^	FCR	94	28	5.86	0.16	9.1	-	-	-	-
	FCMR	54	15	6.1	0.28	8.86	0.91	0.48	1.71	0.77
	FCMminiR	39	11	6.17	0.75	8.99	0.9	0.45	1.81	0.76
	FCMminiR/ FCR	12	2	5.15	2.05	6.92	0.71	0.17	2.99	0.64
Fusogenic median^	Below	70	29	4.93	0.04	8.19	2.87	1.71	4.88	<0.001
	Above	145	30	6.26	0.02	9.1	-	-	-	-

Fusogenic mean^	Below	19	7	5.34	1.38	8.19	1.63	0.74	3.61	0.23
	Above	196	52	5.88	0.02	9.1	-	-	-	-

Footnote: CI- confidenence interval, HR-hazard ratio. Wald chi squared test, p-value<0.05 is considered significant. Within each variable with multiple statuses a reference is needed to be assigned for the univariant analysis, these are shown as do not have a calculated HR or CIs, for example in the Telomere length variable the Long status is the reference. ^ Based on 215 patients and 59 events. ”Based on 176 patients and 45 events. $ Based on 156 patients and 42 events. £ Based on 180 patients and 46 events. ~ Based on 196 patients and 54 events. * Based on 86 patients and 16 events.

Supplementary Table 9- CLL4 multivariate PFS final model after backward elimination after starting with 8 covariates (Telomere length, Epitype, *TP53* aberration, *ATM* dysfunction, *IGHV* mutation status, Age, *SF3B1* mutation, Treatment arm).

Variable	**HR**	**Lower CI**	**Upper CI**	**P-value**
*TP53*abs	3.38	2.13	5.37	<0.001
n-CLL	2.35	1.37	4.05	0.002
TL-S	2.14	1.39	3.3	<0.001
i-CLL	1.9	1.12	3.22	0.017
SF3B1	1.55	1.13	2.13	0.006
TL-I	1.42	0.9	2.25	0.13
Chl	1.21	0.84	1.74	0.3
FC	0.47	0.33	0.68	<0.001

Footnote: Abbreviations; CI, confidence interval; HR, hazard ratio; TL-S, short telomere length; TL-I, intermediate telomere length; TL-L, long telomere length. Candidate variables were entered in the iterative backward selection method were factors with P-values $\leqslant 0.05$ in the univariable analysis. Age was entered as a continuous variable for the multivariable analysis. The final CLL4 models were based on 246 subjects and 221 events for PFS.

Supplementary Table 10- CLL4 multivariate OS final model after backward elimination after starting with 8 covariates (Telomere length, Epitype, *TP53* aberration, *ATM* dysfunction, *IGHV* mutation status, Age, *SF3B1* mutation, Treatment arm).

Variable	**HR**	**Lower CI**	**Upper CI**	**P-value**
*TP53*abs	2.77	1.74	4.4	<0.001
TL-S	2.4	1.51	3.81	<0.001
n-CLL	2.07	1.15	3.73	0.015
SF3B1	1.96	1.42	2.71	<0.001
i-CLL	1.78	1	3.18	0.049
TL-I	1.76	1.08	2.86	0.023
Age	1.06	1.04	1.08	<0.001

Chl	0.72	0.5	1.05	0.091
FC	0.66	0.45	0.96	0.03

Footnote: Abbreviations; CI, confidence interval; HR, hazard ratio; TL-S, short telomere length; TL-I, intermediate telomere length; TL-L, long telomere length. Candidate variables were entered in the iterative backward selection method were factors with P-values ⩽ 0.05 in the univariable analysis. Age was entered as a continuous variable for the multivariable analysis. The final CLL4 models were based on 246 subjects and 205 events for OS.

Supplementary Table 11- ARCTIC and ADMIRE multivariate PFS final model after backward elimination after starting with 8 covariates (Telomere length, Epitype, *TP53* aberration, *ATM* dysfunction, *IGHV* mutation status, Age, *SF3B1* mutation, Treatment arm).

Variate	**HR**	**Lower CI**	**Upper CI**	**P-value**
*TP53*abs	4.94	2.58	9.48	<0.001
bi*ATM*	2.70	1.27	5.76	0.01
IGHV-U	2.20	1.23	3.95	0.01
TL-S	2.18	1.17	4.05	0.01
del11q	1.88	1.05	3.37	0.03
TL-I	0.92	0.51	1.66	0.78

Footnote: Abbreviations; CI, confidence interval; HR, hazard ratio; TL-S, short telomere length; TL-I, intermediate telomere length; TL-L, long telomere length. Candidate variables were entered in the iterative backward selection method were factors with P-values ⩽ 0.05 in the univariable analysis. Age was entered as a continuous variable for the multivariable analysis. The final ARC/ADM models were based on 138 subjects and 86 events for PFS.

Supplementary Tables

Supplementary Table 12- ARCTIC and ADMIRE multivariate OS final model after backward elimination after starting with 8 covariates (Telomere length, Epitype, *TP53* aberration, *ATM* dysfunction, *IGHV* mutation status, Age, *SF3B1* mutation, Treatment arm).

Variate	**HR**	**Lower CI**	**Upper CI**	**P-value**
n-CLL	3.4	1.14	10.12	0.02
*TP53*ab	3.28	1.64	6.55	<0.001
TL-S	2.26	1.09	4.67	0.08
i-CLL	2.08	0.65	6.7	0.22
TL-I	0.96	0.45	2.04	0.91

Footnote: Abbreviations; CI, confidence interval; HR, hazard ratio; TL-S, short telomere length; TL-I, intermediate telomere length; TL-L, long telomere length. Candidate variables were entered in the iterative backward selection method were factors with P-values $\leqslant 0.05$ in the univariable analysis. Age was entered as a continuous variable for the multivariable analysis. The final ARC/ADM models were based on 176 subjects and 45 events for OS

Supplementary Table 13- Breakdown of available FISH data for the cohort of 495 clinical trial patients, divided according to clinical trial and genomic technology group (different columns) i.e. SNP array. The number of cases with one of the four recurrent CLL CNA, i.e. del17p, trisomy 12, is given out of the number of patients that were screened for it.

	CLL4		ARCTIC and ADMIRE	
	SNP (n=108)	sWGS (n=144)	HumanOmni (n= 212)	450K (n=31)
Del17p	6/101	7/130	13/205	1/31
Del11q	35/102	20/131	38/207	9/31
Trisomy 12	11/102	18/131	6/80	5/17
Del13q	57/102	77/131	55/81	8/16

Supplementary Table 14- Univariate survival analysis of the CLL4 cohort examining progression free survival (PFS) in a cohort of 251 clinical trial patients.

Variable	Status	Total	Events	Median (Years)	Lower Range (Years)	Upper Range (Years)	HR	Lower CI	Upper CI	P-value
GC ^	High	34	31	1.01	0.05	7.66	1.5	1.02	2.2	<0.05
	Intermediate	45	39	2	0	9.46	1.04	0.73	1.48	0.82
	Low	172	156	2.53	0	10.12	-	-	-	-
Telomere Length ^	Short	137	132	1.99	0	8.15	2.62	1.8	3.82	<0.001
	Intermediate	61	57	2.46	0	8.99	1.97	1.3	2.99	<0.01
	Long	53	37	4.04	0.08	10.12	-	-	-	-
Epitype "	n-CLL	115	113	2.1	0	8.07	2.8	1.67	4.69	<0.001
	i-CLL	83	72	2.99	0	10.12	1.78	1.05	3.02	<0.05
	m-CLL	28	17	3.7	0.07	8.57	-	-	-	-
TP53 dysfunction ^	Yes	24	24	0.43	0.08	6.28	3.72	2.41	5.75	<0.001
	No	227	202	2.57	0	10.12	-	-	-	-
IGHV mutation status *	Unmutated	141	138	1.87	0	7.71	2.39	1.74	3.27	<0.001
	Mutated	80	60	3.59	0.07	10.12	-	-	-	-
ATM disruption ^	Biallelic	5	5	1.63	0.84	3	2.2	0.9	5.41	0.08
	Deleted	41	41	1.51	0	5.5	1.97	1.39	2.8	<0.001
	Mutated	12	12	3.59	0.21	6.26	1.07	0.6	1.93	0.82
	No	246	221	2.41	0	10.12	-	-	-	-
BIRC3 biallelic loss ^	Yes	5	5	1.1	0.05	4.7	1.98	0.81	4.81	0.13
	No	203	178	2.54	0	10.12	-	-	-	-
Trisomy 12 ^	Yes	25	25	2.18	0.06	6.17	1.46	0.96	2.22	0.08
	No	226	201	2.41	0	10.12	-	-	-	-
Del(13q) ^	Biallelic	25	24	1.55	0	8.99	1.36	0.88	2.1	0.17
	Monoallelic	81	73	2.2	0	8.31	1.09	0.82	1.45	0.56
	No	145	129	2.5	0.06	10.12	-	-	-	-
SF3B1 ^	Yes	60	58	2.04	0.23	8.44	1.31	0.97	1.77	0.07

	No	191	168	2.5	0	10.12	-	-	-	-
NOTCH1 ^	Yes	39	38	2.1	0.06	7.71	1.36	0.96	1.93	0.08
	No	212	188	2.48	0	10.12	-	-	-	-
Mutation count ^	≥3	14	14	1.1	0.28	7.71	2.23	1.27	3.92	<0.01
	2	34	33	1.43	0.16	7.03	1.81	1.21	2.69	<0.01
	1	87	83	2.13	0.05	8.44	1.61	1.2	2.18	<0.01
	0	116	96	3.07	0	10.12	-	-	-	-
Treatment Arm ^	FC	108	92	3.69	0	10.12	0.5	0.36	0.7	<0.001
	Chl	86	79	1.38	0	8.99	1.1	0.78	1.56	0.56
	FDR	57	55	1.69	0.05	7.49	-	-	-	-
Age ^		-	-	-	-	-	1.01	1	1.03	0.12

Footnote: CI- confidenence interval, HR-hazard ratio. Wald chi squared test, p-value<0.05 is considered significant. Within each variable with multiple statuses a reference is needed to be assigned for the univariant analysis, these are shown as do not have a calculated HR or CIs, for example in the Telomere length variable the Long status is the reference. ^ Based on 251 patients and 226 events. ”Based on 226 patients and 202 events. * Based on 221 patients and 198 events.

Supplementary Table 15- Univariate survival analysis of the CLL4 cohort examining overall survival (OS) in a cohort of 251 clinical trial patients.

Variable	**Status**	**Total**	**Events**	**Median (Years)**	**Lower Range (Years)**	**Upper Range (Years)**	**HR**	**Lower CI**	**Upper CI**	**P-value**
GC ^	High	34	31	4.2	0	14.3	1.62	1.1	2.4	<0.05
	Intermediate	45	37	6	0.28	16	1	0.7	1.44	0.99
	Low	172	141	6.25	0.06	17.37	-	-	-	-
Telomere Length ^	Short	137	124	5.3	0.05	15.9	2.51	1.71	3.68	<0.001
	Intermediate	61	50	6.25	0.07	16	1.9	1.23	2.94	<0.01
	Long	53	35	10.1	0.08	17.37	-	-	-	-
Epitype “	n-CLL	115	103	5.86	0.05	16	2.9	1.68	5	<0.001
	i-CLL	83	71	5.39	0.06	16.65	2.59	1.48	4.53	<0.001
	m-CLL	28	15	10.82	0.07	17.37	-	-	-	-
TP53 dysfunction ^	Yes	24	23	1.47	0.23	15.63	3.71	2.38	5.78	<0.001

	No	227	186	6.6	0.05	17.37	-	-	-	-
IGHV mutation status *	Unmutated	141	130	5.23	0.05	16	2.31	1.67	3.19	<0.001
	Mutated	80	55	8.94	0.07	17.37	-	-	-	-
ATM disruption ^	Biallelic	5	5	3.87	1	10.17	1.9	0.78	4.65	0.16
	Deleted	41	38	5.56	0.05	12.97	1.5	1.05	2.15	<0.05
	Mutated	12	12	6.13	1.59	10.17	1.5	0.83	2.71	0.18
	No	193	154	6.25	0.06	17.37	-	-	-	-
BIRC3 biallelic loss ^	Yes	5	5	3.32	0.05	6.32	2.73	1.12	6.68	<0.05
	No	246	204	6.06	0.06	17.37	-	-	-	-
Trisomy 12 ^	Yes	25	24	4.16	0.06	15.72	1.57	1.03	2.41	<0.05
	No	226	185	6.25	0.05	17.37	-	-	-	-
Del(13q) ^	Biallelic	25	20	7.03	0.07	16.53	0.86	0.53	1.38	0.53
	Monoallelic	81	69	5.86	0.05	17.37	0.99	0.74	1.33	0.95
	No	145	120	5.95	0.06	16.65	-	-	-	-
SF3B1 ^	Yes	60	54	4.61	0.23	15.53	1.54	1.13	2.11	<0.01
	No	191	155	6.6	0.05	17.37	-	-	-	-
NOTCH1 ^	Yes	39	36	4.93	0.06	16	1.52	1.06	2.18	<0.05
	No	212	173	6.53	0.05	17.37	-	-	-	-
Mutation count ^	≥3	14	13	3.52	0.94	15.46	2.4	1.34	4.32	<0.01
	2	34	33	4.47	0.23	12.56	2.47	1.64	3.72	<0.001
	1	87	78	5.36	0.05	16.36	1.78	1.31	2.42	<0.001
	0	116	85	7.9	0.07	17.37	-	-	-	-
Treatment Arm ^	FC	108	85	6.29	0.16	16.65	0.78	0.55	1.11	0.16
	Chl	86	74	5.92	0.08	16.53	0.99	0.69	1.43	0.98
	FDR	57	50	5.59	0.05	17.37	-	-	-	-
Age ^		-	-	-	-	-	1.05	1.03	1.07	<0.001

Footnote: CI- confidenence interval, HR-hazard ratio. Wald chi squared test, p-value<0.05 is considered significant. Within each variable with multiple statuses a reference is needed to be assigned for the univariant analysis, these are shown as do not have a calculated HR or CIs, for example in the Telomere length variable the Long status is the

reference. ^ Based on 251 patients and 209 events. ”Based on 226 patients and 189 events. * Based on 221 patients and 185 events.

Supplementary Table 16- Univariate survival analysis of the ARCTIC and ADMIRE cohort examining progression free survival (PFS) in a cohort of 226 clinical trial patients.

Variable	Status	Total	Events	Median (Years)	Lower Range (Years)	Upper Range (Years)	HR	Lower CI	Upper CI	P-value
GC ^	High	34	23	2.53	0.04	8.62	2.02	1.27	3.22	<0.01
	Intermediate	52	33	4.86	0.63	8.68	1.08	0.72	1.62	0.7
	Low	104	82	5.05	0.02	9	-	-	-	-
Telomere Length ^	Short	53	40	3.7	0.04	8.19	2.57	1.7	3.88	<0.001
	Intermediate	58	43	3.93	0.11	8.86	2.21	1.48	3.31	<0.001
	Long	115	55	5.83	0.02	8.99	-	-	-	-
Epitype “	n-CLL	93	73	3.77	0.02	8.98	4.35	2.51	7.52	<0.001
	i-CLL	59	32	5.45	0.11	9	2.09	1.15	3.83	<0.05
	m-CLL	50	16	6.85	0.16	8.68	-	-	-	-
TP53 dysfunction ^	Yes	26	23	2.17	0.04	8.98	4.65	2.93	7.41	<0.001
	No	200	115	5.06	0.02	9	-	-	-	-
IGHV mutation status *	Unmutated	119	93	4.06	0.04	8.98	3.04	2	4.61	<0.001
	Mutated	81	31	6.43	0.02	9	-	-	-	-
ATM disruption ^	Biallelic	12	9	3.36	0.16	6.43	2.1	1.05	4.18	<0.05
	Deleted	28	24	4.02	0.52	6.99	2.1	1.33	3.32	<0.01
	Mutated	22	15	4.49	1.66	7.33	1.4	0.8	2.42	0.23
	No	164	90	4.99	0.02	9	-	-	-	-
BIRC3 biallelic loss ^	Yes	5	5	4.06	2.39	5.91	2.07	0.84	5.06	0.11
	No	221	113	4.76	0.02	9	-	-	-	-
Trisomy 12 ^	Yes	33	20	4.57	0.13	8.98	1.04	0.64	1.67	0.88
	No	193	118	4.76	0.02	9	-	-	-	-
Del(13q) ^	Biallelic	23	11	5.76	0.11	8.62	0.64	0.34	1.22	0.18
	Monoallelic	97	60	4.51	0.02	4.51	1	0.7	1.42	0.99
	No	106	67	4.58	0.13	8.98	-	-	-	-

SF3B1 ^	Yes	48	32	4.38	0.02	8.98	1.3	0.87	1.94	0.19
	No	178	106	4.86	0.04	9	-	-	-	-
NOTCH1 ^	Yes	32	18	5.22	0.33	8.86	0.85	0.52	1.4	0.54
	No	194	120	4.58	0.02	9	-	-	-	-
Mutation count ^	≥3	17	13	2.61	0.02	5.82	3.26	1.74	6.11	<0.001
	2	32	25	3.56	0.16	8.98	2.29	1.4	3.76	<0.001
	1	90	56	4.48	0.04	8.55	1.64	1.1	2.44	<0.05
	0	87	44	5.83	0.13	9	-	-	-	-
Treatment Arm ^	FC	51	31	4.76	0.55	8.86	1.1	0.71	1.71	0.66
	Chl	45	32	4.58	0.37	8.16	1.41	0.91	2.17	0.12
	FDR	13	8	4.29	2.03	6.07	1.38	0.65	2.9	0.4
Age ^		101	56	5.45	0.16	9	-	-	-	-

Footnote: CI- confidenence interval, HR-hazard ratio. Wald chi squared test, p-value<0.05 is considered significant. Within each variable with multiple statuses a reference is needed to be assigned for the univariant analysis, these are shown as do not have a calculated HR or CIs, for example in the Telomere length variable the Long status is the reference. ^ Based on 226 patients and 138 events. ”Based on 202 patients and 121 events. * Based on 200 patients and 124 events.

Supplementary Table 17- Univariate survival analysis of the ARCTIC and ADMIRE cohort examining overall survival (OS) in a cohort of 226 clinical trial patients.

Variable	**Status**	**Total**	**Events**	**Median (Years)**	**Lower Range (Years)**	**Upper Range (Years)**	**HR**	**Lower CI**	**Upper CI**	**P-value**
GC ^	High	34	13	4.48	0.04	8.62	2.21	1.17	4.17	<0.05
	Intermediate	52	12	6.58	1.4	8.68	0.87	0.45	1.67	0.67
	Low	104	37	6.82	0.02	9.1	-	-	-	-
Telomere Length ^	Short	53	20	5.91	0.04	8.19	2.55	1.39	4.67	<0.01
	Intermediate	58	19	5.99	0.11	8.99	1.81	0.98	3.32	0.05
	Long	115	23	6.92	0.02	9.1	-	-	-	-
Epitype “	n-CLL	93	35	6	0.02	9.1	4.69	1.83	11.99	<0.01
	i-CLL	59	13	6.74	0.11	9	2.28	0.81	6.41	0.12
	m-CLL	50	5	7	0.16	8.68	-	-	-	-
TP53 dysfunction ^	Yes	26	12	3.62	0.04	8.98	2.97	1.58	5.59	<0.001

	No	200	50	6.69	0.02	9.1	-	-	-	-
IGHV mutation status *	Unmutated	119	40	6.09	0.04	9.1	1.86	1.04	3.33	<0.05
	Mutated	81	16	6.9	0.02	9	-	-	-	-
ATM disruption ^	Biallelic	12	3	5.94	0.16	8.2	1.06	0.33	3.4	0.93
	Deleted	28	6	6.87	0.75	9.1	0.74	0.31	1.73	0.48
	Mutated	22	7	6.12	1.66	8.99	1.05	0.47	2.34	0.9
	No	164	46	6.66	0.02	9	-	-	-	-
BIRC3 biallelic loss ^	Yes	5	2	5.91	2.56	9.1	1.28	0.3	5.5	0.74
	No	221	60	6.43	0.02	9	-	-	-	-
Trisomy 12 ^	Yes	33	12	5.99	0.13	8.98	1.59	0.85	3	0.15
	No	193	50	6.72	0.02	9.1	-	-	-	-
Del(13q) ^	Biallelic	23	2	7.1	0.11	8.62	0.23	0.06	1	0.05
	Monoallelic	97	25	6.46	0.02	9	0.77	0.46	1.28	0.31
	No	106	35	6.07	0.13	9.1	-	-	-	-
SF3B1 ^	Yes	48	11	6.8	0.02	8.99	0.79	0.41	1.53	0.49
	No	178	51	6.39	0.04	9.1	-	-	-	-
NOTCH1 ^	Yes	32	11	6.46	0.47	8.86	1.43	0.74	2.75	0.28
	No	194	51	6.43	0.02	9.1	-	-	-	-
Mutation count ^	≥3	17	7	4.25	0.02	7.92	3.68	1.51	8.96	<0.01
	2	32	9	7	0.16	8.99	1.47	0.65	3.3	0.35
	1	90	29	6.04	0.04	9.1	2.02	1.11	3.69	<0.05
	0	87	17	6.97	0.13	9	-	-	-	-
Treatment Arm ^	FC	51	14	6.74	0.63	8.86	0.82	0.43	1.54	0.53
	Chl	45	12	6.98	0.75	8.99	0.8	0.41	1.56	0.51
	FDR	13	2	5.78	2.05	6.92	0.6	0.14	2.5	0.48
Age ^		101	31	6.14	0.16	9.1	-	-	-	-

Footnote: CI- confidenence interval, HR-hazard ratio. Wald chi squared test, p-value<0.05 is considered significant. Within each variable with multiple statuses a reference is needed to be assigned for the univariant analysis, these are shown as do not have a calculated HR or CIs, for example in the Telomere length variable the Long status is the

reference. ^ Based on 226 patients and 62 events. ”Based on 202 patients and 53 events. * Based on 200 patients and 56 events.

Supplementary Table 18- CLL4 multivariate PFS final model after backward elimination after starting with 13 covariates (GC, Telomere length, Epitype, *TP53* aberration, *ATM* disruption, *BIRC3* biallelic loss, Trisomy 12, *IGHV* mutation status, Age, *SF3B1* mutation, *NOTCH1* mutation, mutation count, and treatment arm).

Covariate	Subgroup	HR	Lower 95% CI	Upper 95% CI	P-value
TP53 dysfunction	Yes	3.13	1.87	5.26	<0.001
IGHV mutation status	Unmutated	2.34	1.36	4.04	<0.001
ATM disruption	Biallelic	2	0.79	5.08	0.15
	Del11q	1.62	1.07	2.49	<0.05
	Mutation	1.05	0.56	2	0.87
Epitype	n-CLL	1.84	0.87	3.90	0.11
	i-CLL	2.34	1.22	4.49	<0.05
Telomere length	TL-S	1.46	0.85	2.48	0.17
	TL-I	0.92	0.51	1.66	0.78
Treatment	FC	0.30	0.20	0.45	<0.001
	Chl	0.98	0.64	1.48	0.91

Footnote: Model included 198 cases with 176 events. Abbreviations; 95% CI, 95% confidence interval; HR, hazard ratio; TL-S, short telomere length; TL-I, intermediate telomere length. Candidate variables were entered in the iterative backward selection method were factors with P-values $\leqslant 0.05$ in the univariable analysis. Age was entered as a continuous variable for the multivariable analysis.

Supplementary Table 19- CLL4 multivariate OS final model after backward elimination after starting with 13 covariates (GC, Telomere length, Epitype, *TP53* aberration, *ATM* disruption, *BIRC3* biallelic loss, Trisomy 12, *IGHV* mutation status, Age, *SF3B1* mutation, *NOTCH1* mutation, mutation count, and treatment arm).

Covariate	Subgroup	HR	Lower 95% CI	Upper 95% CI	P-value
TP53 aberration	Yes	3.4	2.05	5.64	<0.001
Epitype	n-CLL	2.17	1.18	3.99	<0.05
	i-CLL	2.19	1.21	3.98	<0.01

TL	TL-S	1.84	1.16	2.94	<0.05
	TL-I	1.26	0.76	2.12	0.37
SF3B1	Yes	1.79	1.26	2.55	<0.01
Trisomy 12	Yes	1.74	1.08	2.83	<0.05
GC	High	1.60	1.05	2.44	<0.05
	Intermediate	0.8	0.53	1.20	0.28
Age		1.05	1.04	1.07	<0.001
Treatment arm	Chl	0.77	0.51	1.15	0.2
	FC	0.61	0.41	0.89	<0.05

Footnote: Model included 226 cases with 189 events. Abbreviations; 95% CI, 95% confidence interval; HR, hazard ratio; TL-S, short telomere length; TL-I, intermediate telomere length. Candidate variables were entered in the iterative backward selection method were factors with P-values ⩽ 0.05 in the univariable analysis. Age was entered as a continuous variable for the multivariable analysis.

Supplementary Table 20- ARCTIC and ADMIRE multivariate PFS final model after backward elimination after starting with 13 covariates (GC, Telomere length, Epitype, *TP53* aberration, *ATM* disruption, *BIRC3* biallelic loss, Trisomy 12, *IGHV* mutation status, Age, *SF3B1* mutation, *NOTCH1* mutation, mutation count, and treatment arm).

Covariate	Subgroup	HR	Lower 95% CI	Upper 95% CI	P-value
Epitype	n-CLL	3.67	2.08	6.47	<0.011
	i-CLL	2.21	1.20	4.07	<0.05
TP53 dysfunction	Yes	2.60	1.39	4.85	<0.01
Mutation count	≥3	2.59	1.24	5.38	<0.01
	2	1.24	0.67	2.32	0.49
	1	1.39	0.90	2.15	0.14
GC	High	1.94	1.15	3.27	<0.05
	Intermediate	1.27	0.82	1.95	0.29

Footnote: Model included 202 cases and 121 events. Abbreviations; 95% CI, 95% confidence interval; HR, hazard ratio. Candidate variables were entered in the iterative backward selection method were factors with P-values ⩽ 0.05 in the univariable analysis. Age was entered as a continuous variable for the multivariable analysis.

Supplementary Table 21- ARCTIC and ADMIRE multivariate OS final model after backward elimination after starting with 13 covariates (GC, Telomere length, Epitype, *TP53* aberration, *ATM* disruption, *BIRC3* biallelic loss, Trisomy 12, *IGHV* mutation status, Age, *SF3B1* mutation, *NOTCH1* mutation, mutation count, and treatment arm).

Covariate	Subgroup	HR	Lower 95% CI	Upper 95% CI	P-value
Epitype	n-CLL	3.55	1.35	9.35	<0.05
	i-CLL	3.09	1.06	9.03	<0.05
Mutation count	≥3	3.52	1.18	10.5	<0.05
	2	1.09	0.39	3.03	0.869
	1	2.03	0.99	4.11	0.050
TP53 dysfunction	Yes	2.72	1.14	6.45	<0.05
Trisomy 12	Yes	2.58	1.15	5.79	<0.05
GC	High	2.44	1.18	5.03	<0.05
	Intermediate	1.13	0.55	2.34	0.74
Age		1.05	1.01	1.08	<0.01

Footnote: Model included 202 cases and 53 events. Abbreviations; 95% CI, 95% confidence interval; HR, hazard ratio. Candidate variables were entered in the iterative backward selection method were factors with P-values ⩽ 0.05 in the univariable analysis. Age was entered as a continuous variable for the multivariable analysis.

Supplementary Figures

Supplementary Figure 1- Violin plot showing the relationship between epitype and telomere length as a continuous variable, a pairwise Wilcoxon test was used to compare the average TL across the three epitype groups in the violin plot, p-value<0.01 is indicated by **.

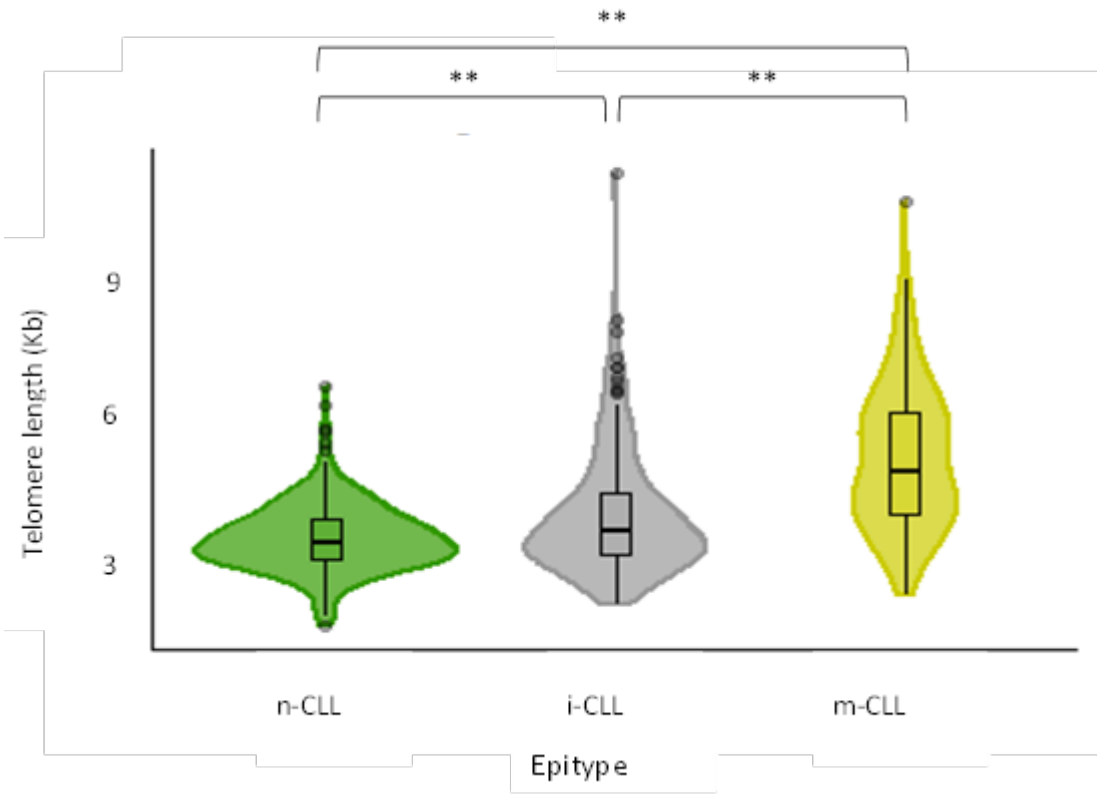

Supplementary Figure 2- Stacked bar chart displaying the distribution of the IGLV3-21^{R110} mutation across the epitype groups, a p-value<0.01 from a chi squared test is shown by two asterisks (**).

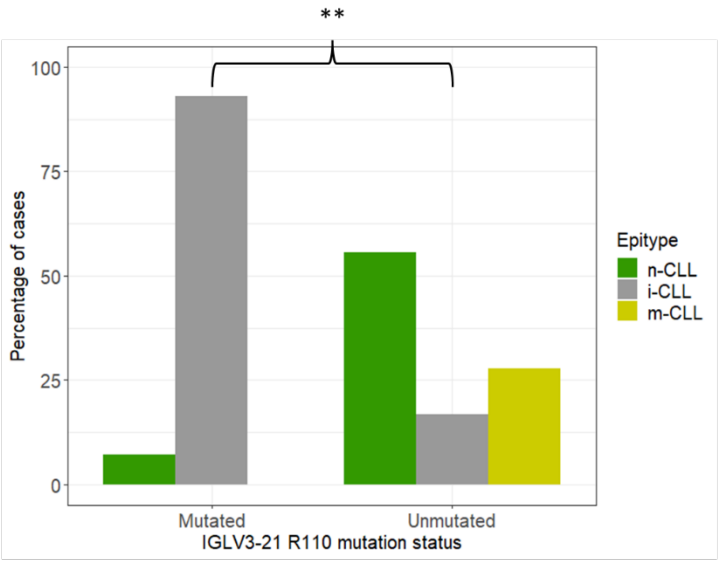

N (%)	n-CLL	i-CLL	m-CLL	Total
IGLV3-21 R110 mutation	1 (7)	13 (93)	0 (0)	14
IGLV3-21 R110 wild type	40 (55)	12 (17)	20 (28)	72
Total	41	25	20	86

Supplementary Figure 3- Stacked bar chart displaying the distribution of the IGLV3-21^{R110} mutation across the TL groups, a p-value<0.05 from a chi squared test is shown by two asterisks (*). Median TL for the IGLV3-21^{R110} mutated and wild type patient is given in the table.

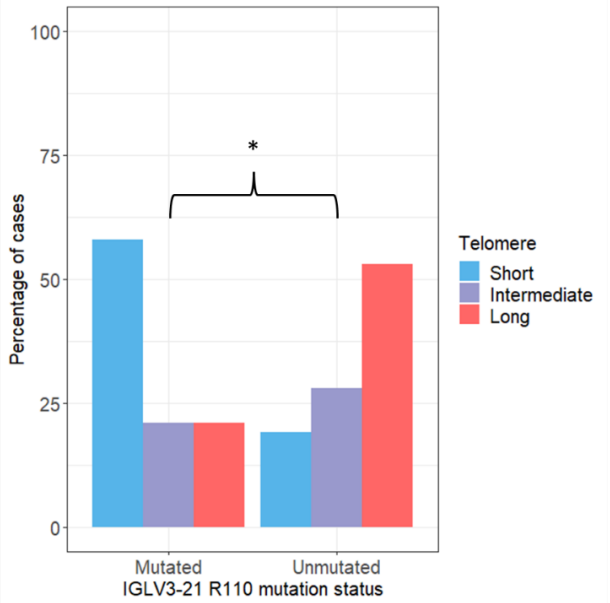

N (%)	Median TL (Kb)	Short TL	Intermediate TL	Long TL	Total
IGLV3-21 R110 mutation	2.8	8 (58)	3 (21)	3 (21)	14
IGLV3-21 R110 wild type	3.7	14 (19)	20 (28)	38 (53)	72
Total		22	23	41	86

Supplementary Figures

Supplementary Figure 4- Univariant analysis of the telomere length variable within the CLL4 cohort. A pairwise log rank test was employed to compare survival plots, p-value<0.01 is indicated by two astericks (**).

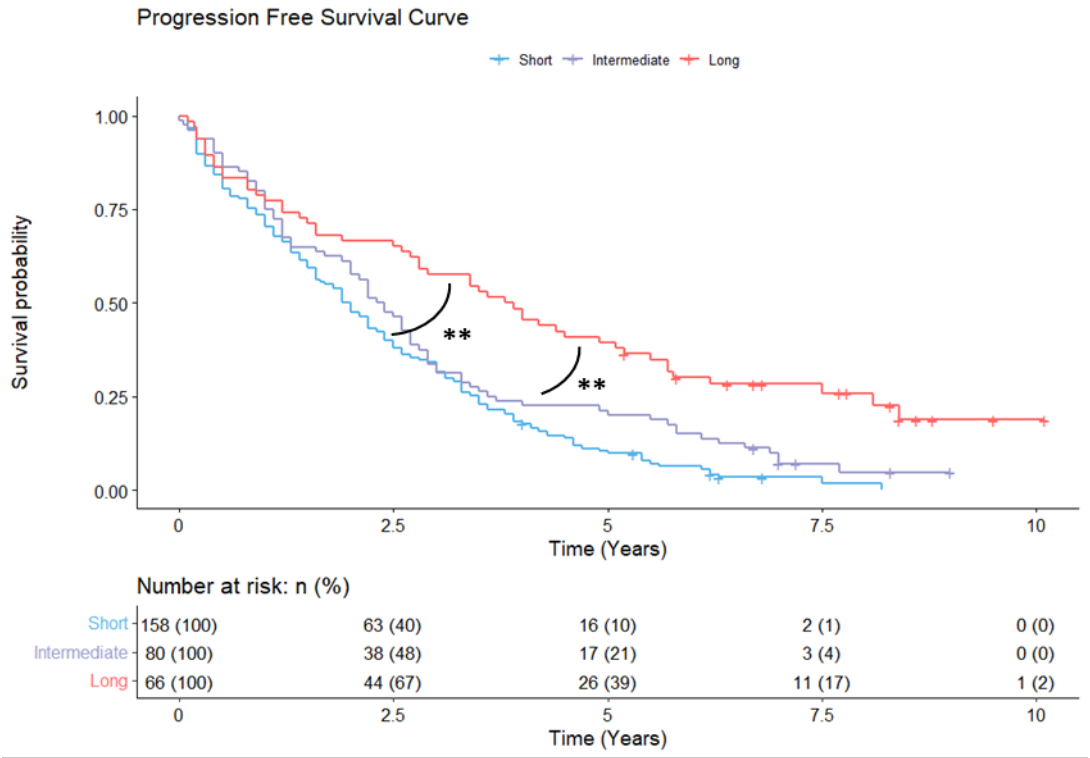

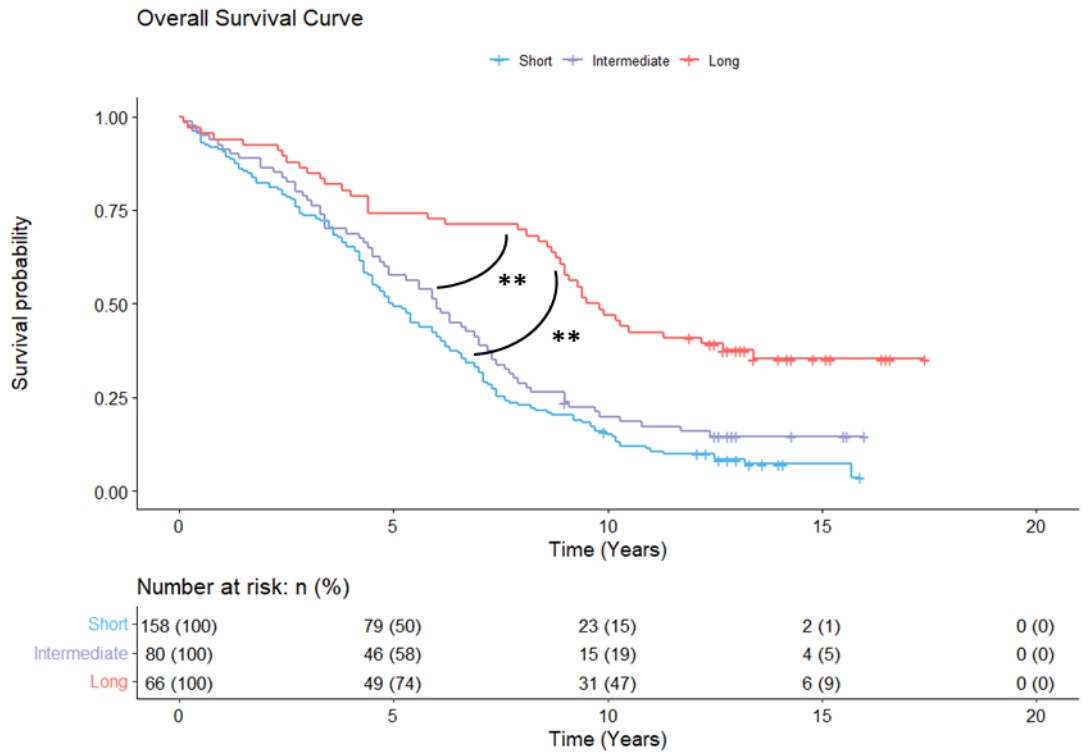

Supplementary Figure 5- Kaplan-Meier plot of the three epitype groups for PFS and OS using the cohort of 108 ARCTIC and ADMIRE patients with TL-L. A pairwise log rank test was employed to compare survival plots, p-value<0.05 is indicated by an asterick (*) and a p-value<0.01 is indicated by two astericks (**).

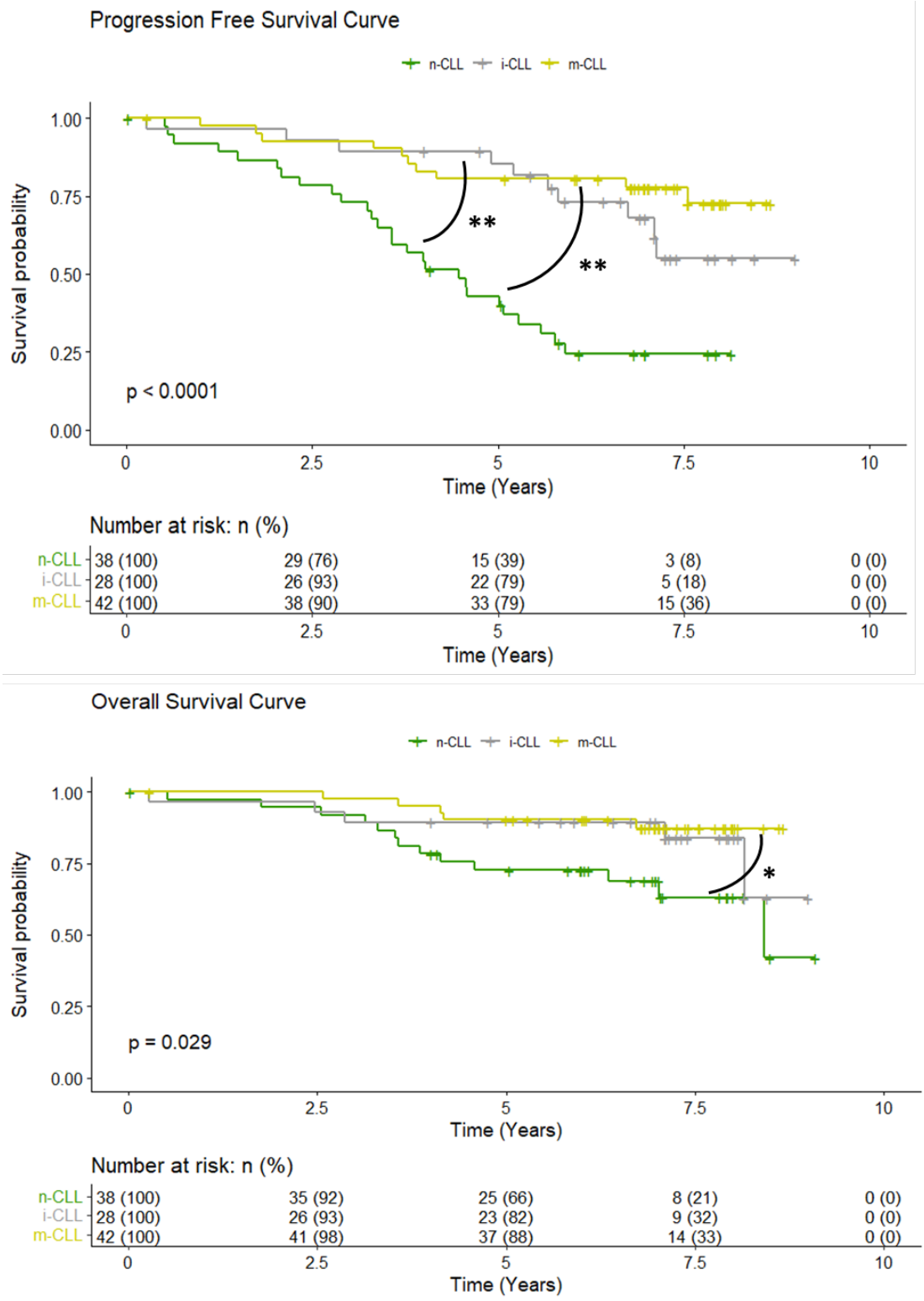

Supplementary Figure 6- Copy number called plot using a stringent bin size of 50 kb. The whole genome and chromosome 13 plots are shown for sample 555. Less CNAs are being called compared to when smaller bin sizes were used but del13q has been called.

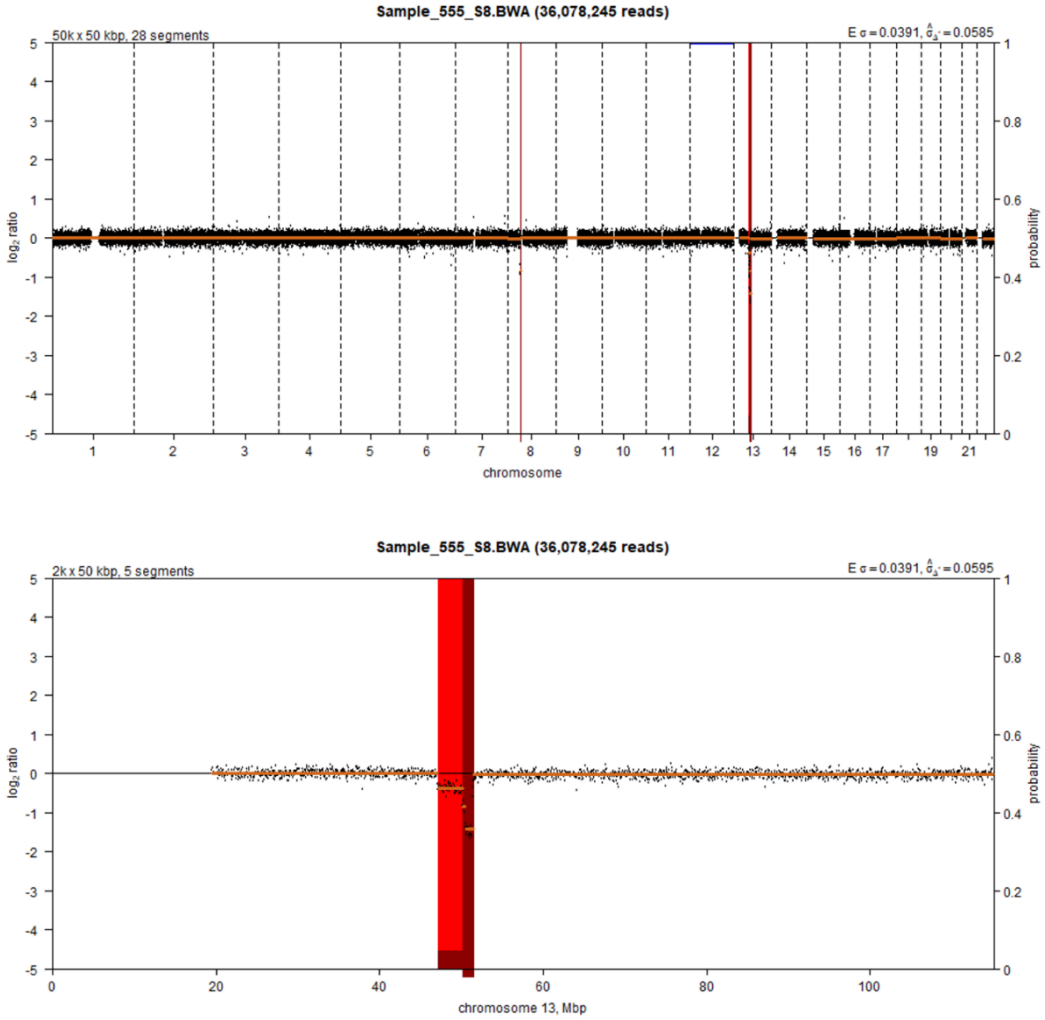

Supplementary Figure 7- Scatter plot showing the TL measurements from the two technologies, MMQPCR and STELA, employed for a sub cohort of 80 CLL4 patients. A Kendall's rank correlation test was used to compare the TL given by the two metrics for each patient.

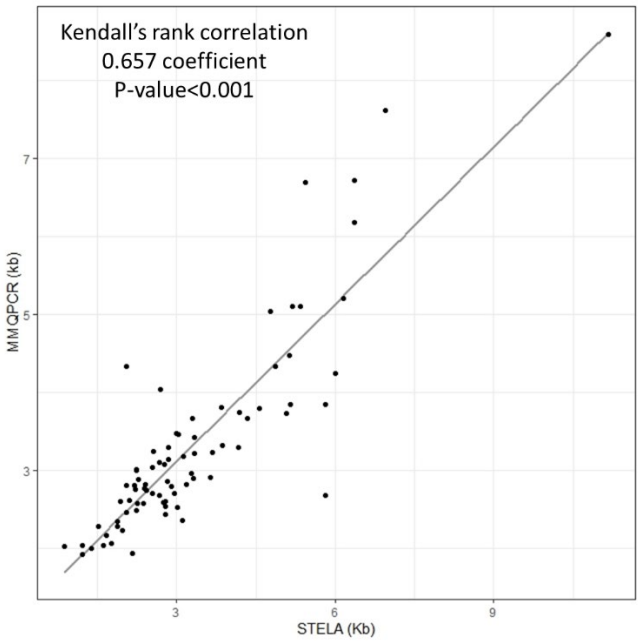

Supplementary Figure 8- Sankey diagram illustrating the association between three categorical variables; GC, TL and epitype. To the left and right of the Sankey are stacked bar charts showing the percentage of each TL group and epitype group that have low, intermediate or high GC. A chi-squared test was employed to examine the difference across the three stacked bar charts; a p-value <0.05 is indicated by a single asterisk (*) and a p-value<0.01 is indicated by two asterisk (**).

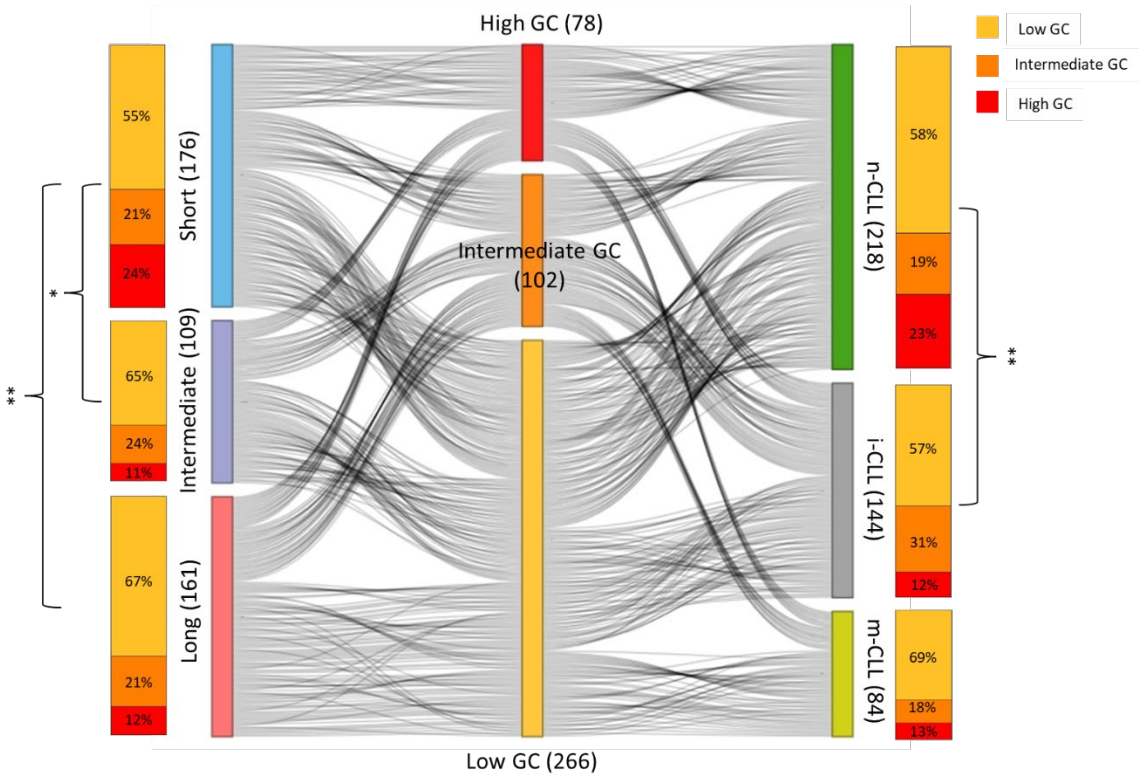

Supplementary Figure 9- Boxplot of the CNA count against mutation count. A pairwise wilcoxon test using Benjamini Hochberg adjustment found no signficant difference in CNA count as mutation count increased.

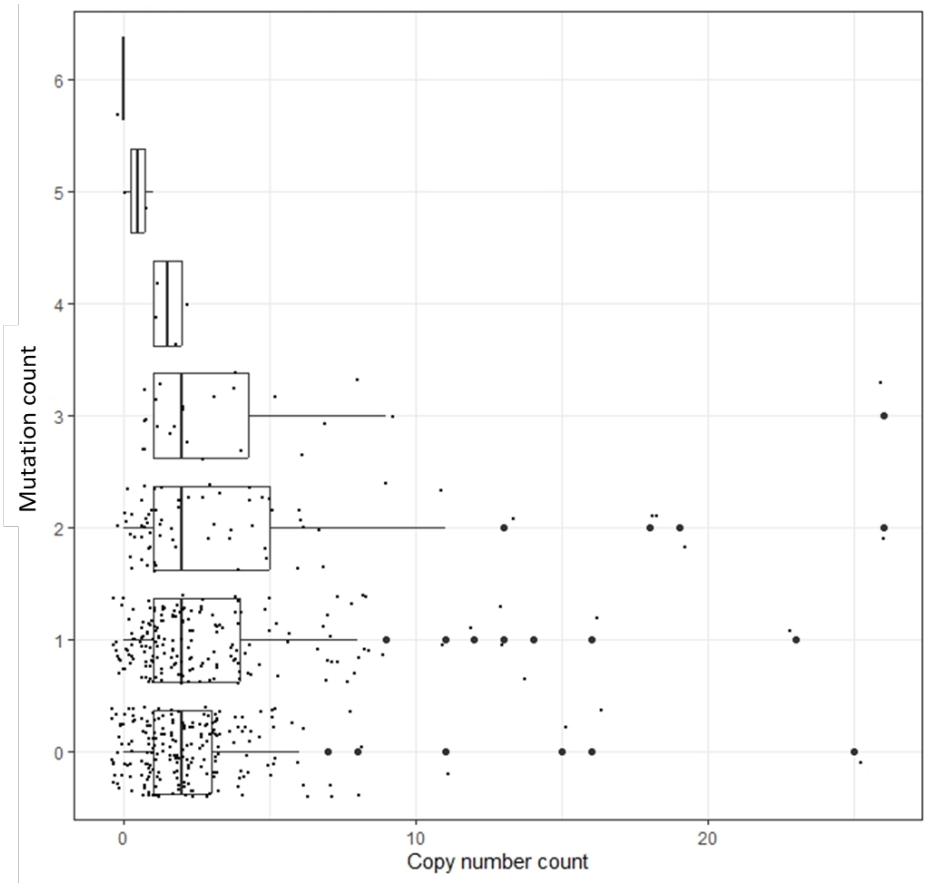

Supplementary Figure 10- Boxplot showing the CNA count across the two del13q classes (class 1 and 2) (A) and the two del13 types (type 1 and 2) (B). A pairwise wilcoxon test using Benjamini Hochberg adjustment assessed if there was a signficant difference in CNA count between the various del13q class and type events. A p-value<0.001 is indicated by three asterisk (***).

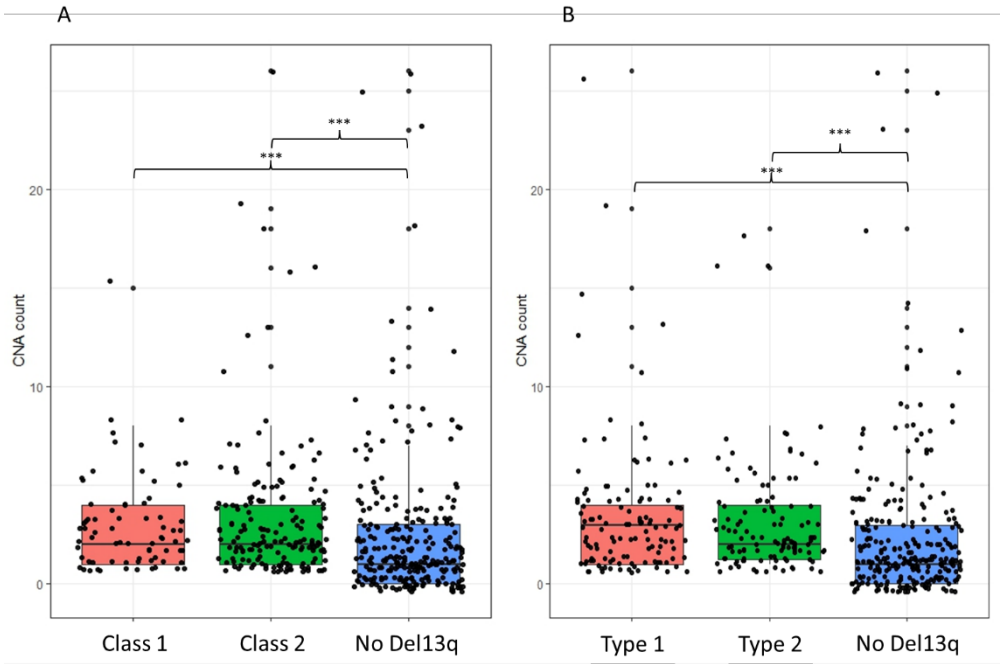

Supplementary Figure 11- Stacked bar chart of the proportion of the three GC groups in each of the four del13q subgroups; class 1 or 2 and type 1 or 2. A pairwise chi-squared test was employed to examine the difference across the four stacked bar charts, no significant difference was found.

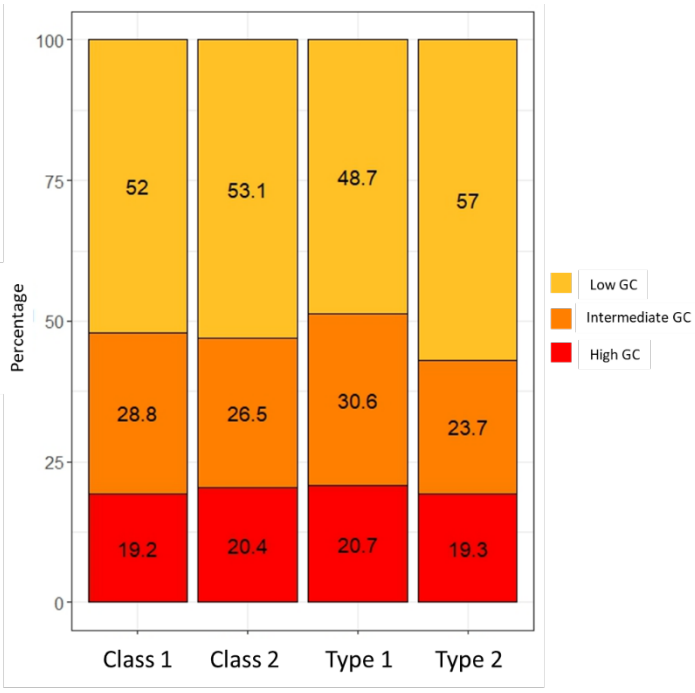

Supplementary Figures

Supplementary Figure 12- Stacked bar charting showing the distribution of the three GC groups across the different del13q subgroup. A pairwise chi squared was employed to test the significance difference in the GC prevalence across the five del13q classes, no significant difference was found.

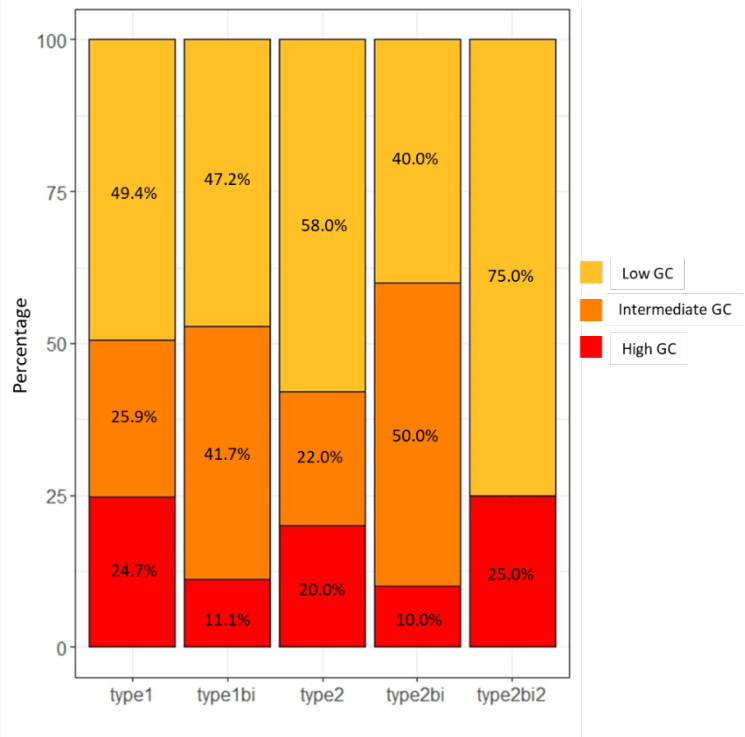

Supplementary Figure 13- Density curve of CNA count across the cohort of 244 ARCTIC and ADMIRE clinical trial patients, the three GC classification groups are coloured with the number and percentage of the cohort each group has is also given.

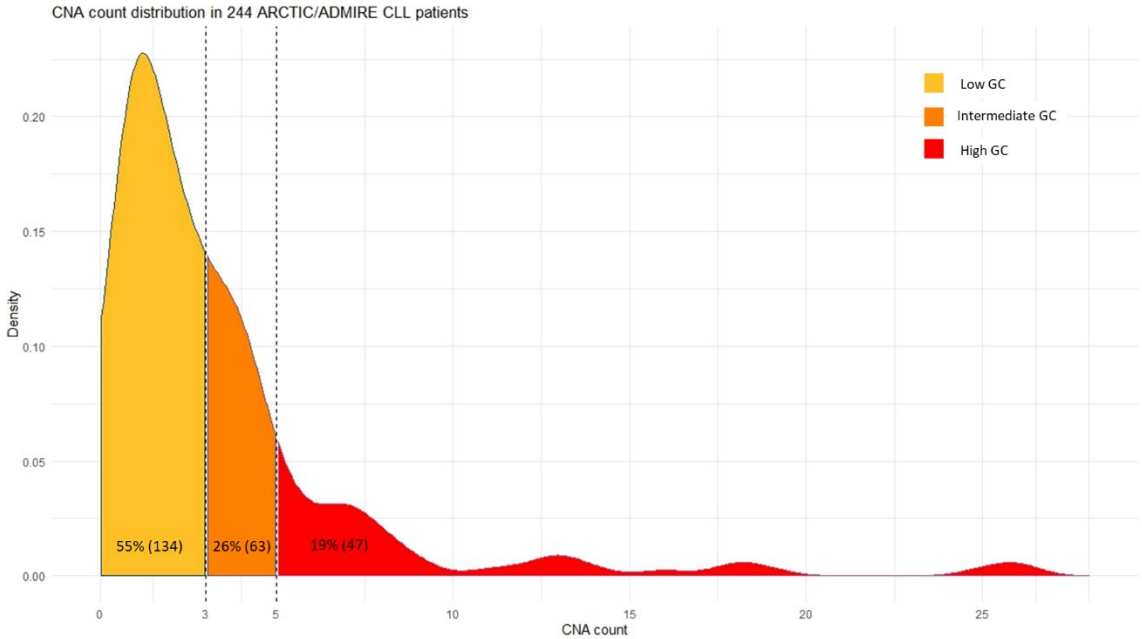

Supplementary Figure 14- Density curve of CNA count across the cohort of 251 CLL4 clinical trial patients, the three GC classification groups are coloured with the number and percentage of the cohort each group has is also given.

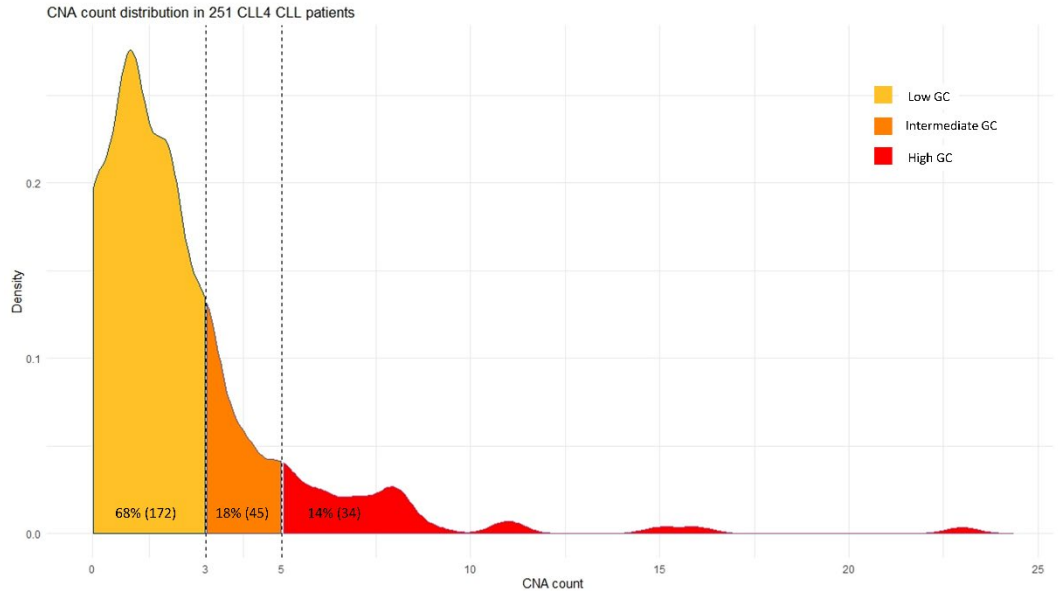

Supplementary Figure 15- Kaplan-Meier plot displaying the PFS of the three GC from the 251 CLL4 patients. A pairwise log rank test was employed to compare survival plots, no signficant difference was found.

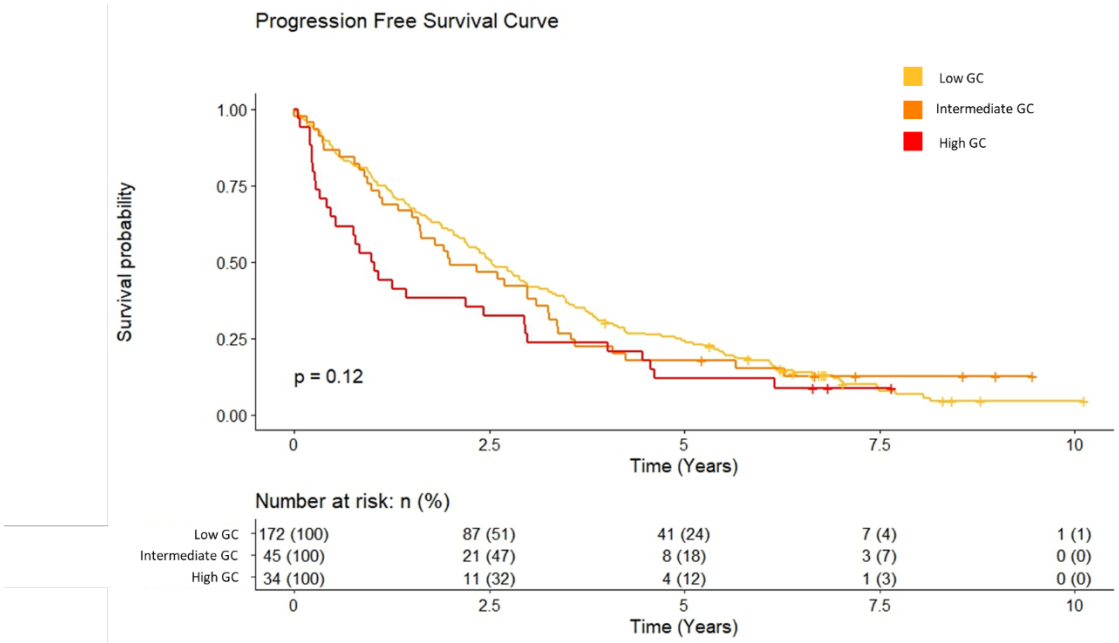

Supplementary Figure 16- Kaplan-Meier plot displaying the 52 ARCTIC and ADMIRE patients with intermediate GC stratified by the presence of *TP53* aberration. A log rank test was employed to compare survival plots and the result is annotated to the plot.

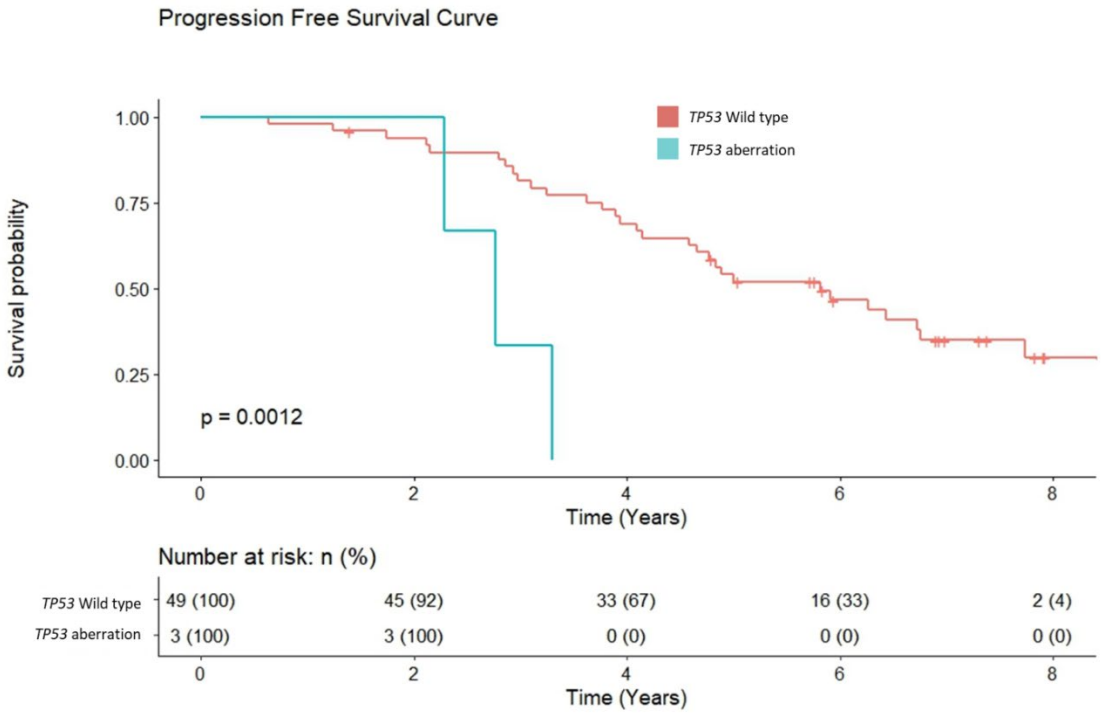

Supplementary Figure 17- Kaplan-Meier plot displaying the OS from the 172 CLL4 patients with low GC. These cases were divided into two groups depending on if patients had both a trisomy 12 and NOTCH1 mutation present (Low GC+tri12+NOTCH1) or not (Low GC without tri12+NOTCH1). Low GC without tri12+NOTCH1 included cases where a trisomy 12 or NOTCH1 mutation was present but did not include patients that had both. A log rank test was employed to compare survival plots and the result is annotated to the plot.

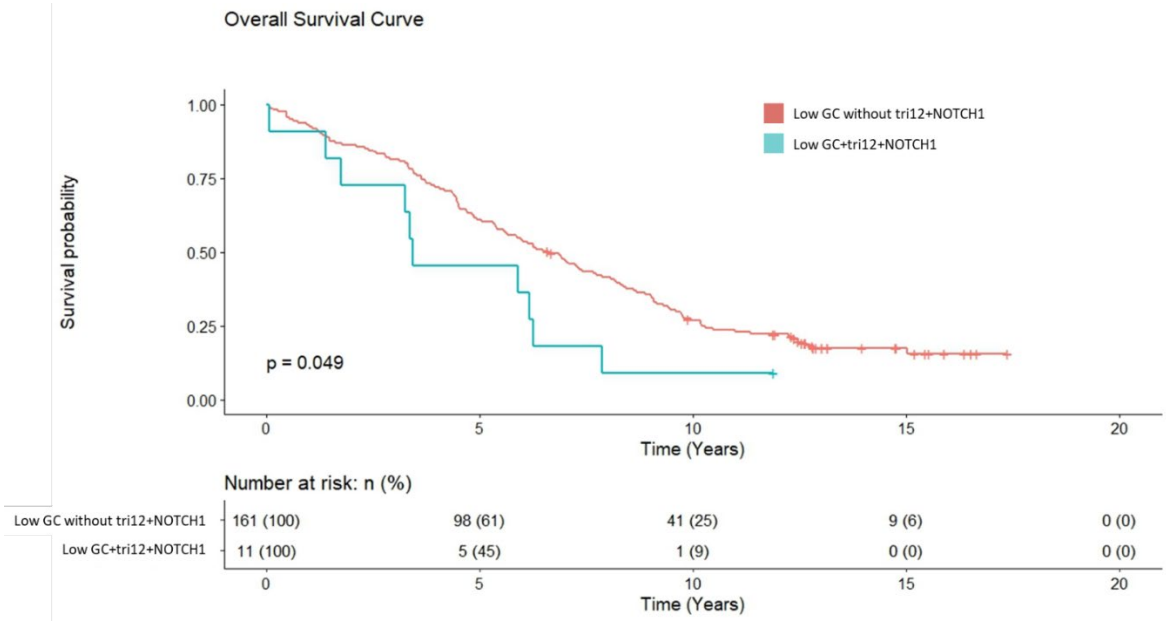

List of References

1. Hanahan D, Weinberg RA. The hallmarks of cancer. Vol. 100, Cell. 2000. p. 57–70.

2. Cancer Statistics for the UK [Internet]. [cited 2024 Apr 14]. Available from: https://master-7rqtwti-hreqyzlibi4ac.uk-1.platformsh.site/health-professional/cancer-statistics-for-the-uk

3. Cooper GM. The Development and Causes of Cancer. 2000 [cited 2023 Oct 17]; Available from: https://www.ncbi.nlm.nih.gov/books/NBK9963/

4. Matthews HK, Bertoli C, de Bruin RAM. Cell cycle control in cancer. Nature Reviews Molecular Cell Biology 2021 23:1 [Internet]. 2021 Sep 10 [cited 2023 Oct 19];23(1):74–88. Available from: https://www.nature.com/articles/s41580-021-00404-3

5. Chang HHY, Pannunzio NR, Adachi N, Lieber MR. Non-homologous DNA end joining and alternative pathways to double-strand break repair. Nature Reviews Molecular Cell Biology 2017 18:8 [Internet]. 2017 May 17 [cited 2022 May 27];18(8):495–506. Available from: https://www.nature.com/articles/nrm.2017.48

6. Molinari M. Cell cycle checkpoints and their inactivation in human cancer. Cell Prolif [Internet]. 2001 [cited 2024 Nov 15];33(5):261. Available from: https://pmc.ncbi.nlm.nih.gov/articles/PMC6496592/

7. Matthews HK, Bertoli C, de Bruin RAM. Cell cycle control in cancer. Nature Reviews Molecular Cell Biology 2021 23:1 [Internet]. 2021 Sep 10 [cited 2024 Mar 6];23(1):74–88. Available from: https://www.nature.com/articles/s41580-021-00404-3

8. Stewart ZA, Westfall MD, Pietenpol JA. Cell-cycle dysregulation and anticancer therapy. Trends Pharmacol Sci. 2003 Mar 1;24(3):139–45.

9. Sanchez-Vega F, Mina M, Armenia J, Chatila WK, Luna A, La KC, et al. Oncogenic Signaling Pathways in The Cancer Genome Atlas. Cell [Internet]. 2018 Apr 4 [cited 2024 Mar 6];173(2):321. Available from: /pmc/articles/PMC6070353/

10. Zasadil LM, Andersen KA, Yeum D, Rocque GB, Wilke LG, Tevaarwerk AJ, et al. Cytotoxicity of paclitaxel in breast cancer is due to chromosome missegregation on multipolar spindles. Sci Transl Med [Internet]. 2014 Mar 26 [cited 2024 Nov 15];6(229):229ra43. Available from: https://pmc.ncbi.nlm.nih.gov/articles/PMC4176609/

11. Bates M, Furlong F, Gallagher MF, Spillane CD, McCann A, O'Toole S, et al. Too MAD or not MAD enough: The duplicitous role of the spindle assembly checkpoint protein MAD2 in cancer. Cancer Lett [Internet]. 2020 Jan 28 [cited 2024 Mar 6];469:11–21. Available from: https://pubmed.ncbi.nlm.nih.gov/31593803/

12. Yuan B, Xu Y, Woo JH, Wang Y, Bae YK, Yoon DS, et al. Increased expression of mitotic checkpoint genes in breast cancer cells with chromosomal instability. Clin Cancer Res [Internet]. 2006 Jan 15 [cited 2024 Mar 6];12(2):405–10. Available from: https://pubmed.ncbi.nlm.nih.gov/16428479/

13. Kwok M, Davies N, Agathanggelou A, Smith E, Oldreive C, Petermann E, et al. ATR inhibition induces synthetic lethality and overcomes chemoresistance in TP53- or ATM-defective chronic lymphocytic leukemia cells. Blood [Internet]. 2016 Feb 4 [cited 2024 Nov 15];127(5):582–95. Available from: https://dx.doi.org/10.1182/blood-2015-05-644872

14. Biermann J, Parris TZ, Nemes S, Danielsson A, Engqvist H, Werner Rönnerman E, et al. Clonal relatedness in tumour pairs of breast cancer patients. Breast Cancer Research [Internet]. 2018 Aug 9 [cited 2023 Oct 17];20(1):1–16. Available from: https://breast-cancer-research.biomedcentral.com/articles/10.1186/s13058-018-1022-y

15. Wang M, Zhao J, Zhang L, Wei F, Lian Y, Wu Y, et al. Role of tumor microenvironment in tumorigenesis. J Cancer [Internet]. 2017 [cited 2023 Oct 19];8(5):761. Available from: /pmc/articles/PMC5381164/

16. Ashley DJB. The two "hit" and multiple "hit" theories of carcinogenesis. Br J Cancer [Internet]. 1969 [cited 2023 Oct 19];23(2):313. Available from: https://www.ncbi.nlm.nih.gov/pmc/articles/PMC2008269/

17. Nowell PC. The clonal evolution of tumor cell populations. Science [Internet]. 1976 [cited 2023 Oct 17];194(4260):23–8. Available from: https://pubmed.ncbi.nlm.nih.gov/959840/

18. Liu J, Adhav R, Xu X. Current progresses of single cell DNA sequencing in breast cancer research. Int J Biol Sci. 2017;13(8):949–60.

19. Garnis C, Buys TPH, Lam WL. Genetic alteration and gene expression modulation during cancer progression. Mol Cancer [Internet]. 2004 Mar 22 [cited 2023 Oct 17];3. Available from: https://pubmed.ncbi.nlm.nih.gov/15035667/

20. Hanahan D, Weinberg RA. Hallmarks of cancer: The next generation. Vol. 144, Cell. 2011. p. 646–74.

21. Hanahan D. Hallmarks of Cancer: New Dimensions. Cancer Discov [Internet]. 2022 Jan 1 [cited 2023 Oct 20];12(1):31–46. Available from: https://dx.doi.org/10.1158/2159-8290.CD-21-1059

22. Cheng N, Chytil A, Shyr Y, Joly A, Moses HL. Transforming growth factor-beta signaling-deficient fibroblasts enhance hepatocyte growth factor signaling in mammary carcinoma cells to promote scattering and invasion. Mol Cancer Res [Internet]. 2008 Oct 1 [cited 2023 Oct 23];6(10):1521–33. Available from: https://pubmed.ncbi.nlm.nih.gov/18922968/

23. Berghoff AS, Magerle M, Ilhan-Mutlu A, Dinhof C, Widhalm G, Dieckman K, et al. Frequent overexpression of ErbB--receptor family members in brain metastases of non-small cell lung cancer patients. APMIS [Internet]. 2013 Dec [cited 2024 Dec 6];121(12):1144–52. Available from: https://pubmed.ncbi.nlm.nih.gov/23756255/

24. Ménard S, Casalini P, Campiglio M, Pupa S, Agresti R, Tagliabue E. HER2 overexpression in various tumor types, focussing on its relationship to the development of invasive breast cancer. Ann Oncol [Internet]. 2001 [cited 2024 Dec 6];12 Suppl 1(SUPPL. 1). Available from: https://pubmed.ncbi.nlm.nih.gov/11521715/

25. Levine AJ. p53, the cellular gatekeeper for growth and division. Cell [Internet]. 1997 Feb 7 [cited 2024 Dec 6];88(3):323–31. Available from: http://www.cell.com/article/S0092867400818711/fulltext

26. Cavallaro U, Christofori G. Cell adhesion and signalling by cadherins and Ig-CAMs in cancer. Nature Reviews Cancer 2004 4:2 [Internet]. 2004 [cited 2023 Oct 23];4(2):118–32. Available from: https://www.nature.com/articles/nrc1276

27. Kim NW, Piatyszek MA, Prowse KR, Harley CB, West MD, Ho PLC, et al. Specific association of human telomerase activity with immortal cells and cancer. Science [Internet]. 1994 [cited 2024 Dec 6];266(5193):2011–5. Available from: https://pubmed.ncbi.nlm.nih.gov/7605428/

28. Raica M, Cimpean AM, Ribatti D. Angiogenesis in pre-malignant conditions. Eur J Cancer. 2009 Jul 1;45(11):1924–34.

29. Hanahan D, Folkman J. Patterns and Emerging Mechanisms of the Angiogenic Switch during Tumorigenesis. Cell. 1996 Aug 9;86(3):353–64.

30. Ozaki T, Nakagawara A. Role of p53 in Cell Death and Human Cancers. Cancers (Basel) [Internet]. 2011 Mar [cited 2024 Dec 6];3(1):994. Available from: https://pmc.ncbi.nlm.nih.gov/articles/PMC3756401/

31. Watanabe A, Yasuhira S, Inoue T, Kasai S, Shibazaki M, Takahashi K, et al. BCL2 and BCLxL are key determinants of resistance to antitubulin chemotherapeutics in melanoma cells. Exp Dermatol [Internet]. 2013 Aug 1 [cited 2024 Jun 24];22(8):518–23. Available from: https://onlinelibrary.wiley.com/doi/full/10.1111/exd.12185

32. Dunn GP, Bruce AT, Ikeda H, Old LJ, Schreiber RD. Cancer immunoediting: from immunosurveillance to tumor escape. Nature Immunology 2002 3:11 [Internet]. 2002 [cited 2024 Dec 6];3(11):991–8. Available from: https://www.nature.com/articles/ni1102-991

33. Smyth MJ, Crowe NY, Godfrey DI. NK cells and NKT cells collaborate in host protection from methylcholanthrene-induced fibrosarcoma. Int Immunol [Internet]. 2001 [cited 2024 Dec 6];13(4):459–63. Available from: https://pubmed.ncbi.nlm.nih.gov/11282985/

34. Kim R, Emi M, Tanabe K. Cancer immunoediting from immune surveillance to immune escape. Immunology [Internet]. 2007 May [cited 2023 Oct 23];121(1):1. Available from: /pmc/articles/PMC2265921/

35. Warburg O. The Metabolism of Carcinoma Cells. J Cancer Res [Internet]. 1925 Mar 1 [cited 2024 Dec 6];9(1):148–63. Available from: /jcancerres/article/9/1/148/450038/The-Metabolism-of-Carcinoma-Cells1

36. Heiden MGV, Cantley LC, Thompson CB. Understanding the Warburg effect: the metabolic requirements of cell proliferation. Science [Internet]. 2009 May 22 [cited 2023 Oct 23];324(5930):1029–33. Available from: https://pubmed.ncbi.nlm.nih.gov/19460998/

37. Flier JS, Underhill LH, Dvorak HF. Tumors: wounds that do not heal. Similarities between tumor stroma generation and wound healing. N Engl J Med [Internet]. 1986 Dec 25 [cited 2024 Dec 6];315(26):1650–9. Available from: https://pubmed.ncbi.nlm.nih.gov/3537791/

38. Pagès F, Galon J, Dieu-Nosjean MC, Tartour E, Sautès-Fridman C, Fridman WH. Immune infiltration in human tumors: a prognostic factor that should not be ignored. Oncogene [Internet]. 2010 Feb [cited 2024 Dec 6];29(8):1093–102. Available from: https://pubmed.ncbi.nlm.nih.gov/19946335/

39. Mantovani A, Allavena P, Sica A, Balkwill F. Cancer-related inflammation. Nature [Internet]. 2008 Jul 24 [cited 2024 Dec 6];454(7203):436–44. Available from: https://pubmed.ncbi.nlm.nih.gov/18650914/

40. Liubomirski Y, Lerrer S, Meshel T, Rubinstein-Achiasaf L, Morein D, Wiemann S, et al. Tumor-Stroma-Inflammation Networks Promote Pro-metastatic Chemokines and Aggressiveness Characteristics in Triple-Negative Breast Cancer. Front Immunol [Internet]. 2019 [cited 2024 Dec 6];10(APR). Available from: https://pubmed.ncbi.nlm.nih.gov/31031757/

41. Jaiswal M, LaRusso NF, Burgart LJ, Gores GJ. Inflammatory cytokines induce DNA damage and inhibit DNA repair in cholangiocarcinoma cells by a nitric oxide-dependent mechanism. Volume 60, Issue 1, Pages 184 - 190. 2000 Jan 1;60(1):184–90.

42. Maréchal A, Zou L. DNA damage sensing by the ATM and ATR kinases. Cold Spring Harb Perspect Biol [Internet]. 2013 Sep [cited 2024 Dec 6];5(9). Available from: https://pubmed.ncbi.nlm.nih.gov/24003211/

43. Zhao Y, Epstein RJ. Unexpected functional similarities between gatekeeper tumour suppressor genes and proto-oncogenes revealed by systems biology. Journal of Human Genetics 2011 56:5 [Internet]. 2011 Mar 3 [cited 2024 Dec 6];56(5):369–76. Available from: https://www.nature.com/articles/jhg201121

44. Zhang S, Xiao X, Yi Y, Wang X, Zhu L, Shen Y, et al. Tumor initiation and early tumorigenesis: molecular mechanisms and interventional targets. Signal Transduction and Targeted Therapy 2024 9:1 [Internet]. 2024 Jun 19 [cited 2024 Dec 6];9(1):1–36. Available from: https://www.nature.com/articles/s41392-024-01848-7

45. Ku CS, Loy EY, Salim A, Pawitan Y, Chia KS. The discovery of human genetic variations and their use as disease markers: past, present and future. Journal of Human Genetics 2010 55:7 [Internet]. 2010 May 20 [cited 2024 Nov 15];55(7):403–15. Available from: https://www.nature.com/articles/jhg201055

46. Tao Z, Wang S, Wu C, Wu T, Zhao X, Ning W, et al. The repertoire of copy number alteration signatures in human cancer. Brief Bioinform [Internet]. 2023 Mar 1 [cited 2024 Jun 24];24(2):1–15. Available from: /pmc/articles/PMC10025440/

47. Carvalho CMB, Lupski JR. Mechanisms underlying structural variant formation in genomic disorders. Nat Rev Genet [Internet]. 2016 Apr 1 [cited 2024 Jun 24];17(4):224–38. Available from: https://pubmed.ncbi.nlm.nih.gov/26924765/

48. Brookes AJ. The essence of SNPs. Gene. 1999 Jul 8;234(2):177–86.

49. Stephens PJ, Greenman CD, Fu B, Yang F, Bignell GR, Mudie LJ, et al. Massive genomic rearrangement acquired in a single catastrophic event during cancer development. Cell [Internet]. 2011 Jan 7 [cited 2024 Jun 24];144(1):27–40. Available from: https://pubmed.ncbi.nlm.nih.gov/21215367/

50. Cortés-Ciriano I, Lee JJK, Xi R, Jain D, Jung YL, Yang L, et al. Comprehensive analysis of chromothripsis in 2,658 human cancers using whole-genome sequencing. Nature Genetics 2020 52:3 [Internet]. 2020 Feb 5 [cited 2024 Dec 7];52(3):331–41. Available from: https://www.nature.com/articles/s41588-019-0576-7

51. Maciejowski J, Li Y, Bosco N, Campbell PJ, De Lange T. Chromothripsis and kataegis induced by telomere crisis. Cell [Internet]. 2015 Dec 12 [cited 2024 Jun 24];163(7):1641. Available from: /pmc/articles/PMC4687025/

52. Pohlreich P, Zikan M, Stribrna J, Kleibl Z, Janatova M, Kotlas J, et al. High proportion of recurrent germline mutations in the BRCA1 gene in breast and ovarian cancer patients from the Prague area. Breast Cancer Res [Internet]. 2005 Jul 19 [cited 2024 Jun 24];7(5). Available from: https://pubmed.ncbi.nlm.nih.gov/16168118/

53. Moynahan ME, Chiu JW, Koller BH, Jasint M. Brca1 controls homology-directed DNA repair. Mol Cell [Internet]. 1999 [cited 2024 Jun 24];4(4):511–8. Available from: https://pubmed.ncbi.nlm.nih.gov/10549283/

54. Kuchenbaecker KB, Hopper JL, Barnes DR, Phillips KA, Mooij TM, Roos-Blom MJ, et al. Risks of Breast, Ovarian, and Contralateral Breast Cancer for BRCA1 and BRCA2 Mutation Carriers. JAMA [Internet]. 2017 Jun 20 [cited 2024 Jun 24];317(23):2402–16. Available from: https://pubmed.ncbi.nlm.nih.gov/28632866/

55. Foulkes WD, Metcalfe K, Sun P, Hanna WM, Lynch HT, Ghadirian P, et al. Estrogen receptor status in BRCA1- and BRCA2-related breast cancer: the influence of age, grade, and histological type. Clin Cancer Res [Internet]. 2004 Mar 15 [cited 2024 Jun 24];10(6):2029–34. Available from: https://pubmed.ncbi.nlm.nih.gov/15041722/

56. Tomasetti C, Li L, Vogelstein B. Stem cell divisions, somatic mutations, cancer etiology, and cancer prevention. Science [Internet]. 2017 Mar 24 [cited 2024 Dec 7];355(6331):1330. Available from: https://pmc.ncbi.nlm.nih.gov/articles/PMC5852673/

57. Wu S, Zhu W, Thompson P, Hannun YA. Evaluating intrinsic and non-intrinsic cancer risk factors. Nat Commun [Internet]. 2018 Dec 1 [cited 2023 Oct 25];9(1). Available from: /pmc/articles/PMC6113228/

58. Alexandrov LB, Nik-Zainal S, Wedge DC, Aparicio SAJR, Behjati S, Biankin A V., et al. Signatures of mutational processes in human cancer. Nature [Internet]. 2013 [cited 2020 Oct 27];500(7463):415–21. Available from: https://pubmed.ncbi.nlm.nih.gov/23945592/

59. Wu S, Powers S, Zhu W, Hannun YA. Substantial contribution of extrinsic risk factors to cancer development. Nature [Internet]. 2016 Jan 7 [cited 2023 Oct 25];529(7584):43–7. Available from: https://pubmed.ncbi.nlm.nih.gov/26675728/

60. Tomasetti C, Vogelstein B. Cancer etiology. Variation in cancer risk among tissues can be explained by the number of stem cell divisions. Science [Internet]. 2015 Jan 2 [cited 2023 Oct 25];347(6217):78–81. Available from: https://pubmed.ncbi.nlm.nih.gov/25554788/

61. Hyun SY, Jang YJ. p53 activates G1 checkpoint following DNA damage by doxorubicin during transient mitotic arrest. Oncotarget [Internet]. 2014 [cited 2024 Dec 7];6(7):4804. Available from: https://pmc.ncbi.nlm.nih.gov/articles/PMC4467116/

62. Finlay CA, Hinds PW, Levine AJ. The p53 proto-oncogene can act as a suppressor of transformation. Cell [Internet]. 1989 Jun 30 [cited 2023 Oct 26];57(7):1083–93. Available from: https://pubmed.ncbi.nlm.nih.gov/2525423/

63. Kuchenbaecker KB, Hopper JL, Barnes DR, Phillips KA, Mooij TM, Roos-Blom MJ, et al. Risks of Breast, Ovarian, and Contralateral Breast Cancer for BRCA1 and BRCA2 Mutation Carriers. JAMA [Internet]. 2017 Jun 20 [cited 2024 Dec 7];317(23):2402–16. Available from: https://jamanetwork.com/journals/jama/fullarticle/2632503

64. Kontomanolis EN, Koutras A, Syllaios A, Schizas D, Mastoraki A, Garmpis N, et al. Role of Oncogenes and Tumor-suppressor Genes in Carcinogenesis: A Review. Anticancer Res [Internet]. 2020 Nov 1 [cited 2023 Oct 25];40(11):6009–15. Available from: https://ar.iiarjournals.org/content/40/11/6009

65. Prior IA, Lewis PD, Mattos C. A comprehensive survey of Ras mutations in cancer. Cancer Res [Internet]. 2012 May 5 [cited 2023 Oct 26];72(10):2457. Available from: /pmc/articles/PMC3354961/

66. Yam-Puc JC, Toellner KM, Zhang L, Zhang Y. Role of B-cell receptors for B-cell development and antigen-induced differentiation. F1000Res [Internet]. 2018 [cited 2022 Mar 7];7. Available from: /pmc/articles/PMC5893946/

67. ten Hacken E, Gounari M, Ghia P, Burger JA. The importance of B cell receptor isotypes and stereotypes in Chronic Lymphocytic Leukemia. Leukemia [Internet]. 2019 Feb 1 [cited 2024 Mar 8];33(2):287. Available from: /pmc/articles/PMC7182338/

68. De Silva NS, Klein U. Dynamics of B cells in germinal centres. Nat Rev Immunol [Internet]. 2015 Mar 27 [cited 2024 Dec 7];15(3):137. Available from: https://pmc.ncbi.nlm.nih.gov/articles/PMC4399774/

69. Stebegg M, Kumar SD, Silva-Cayetano A, Fonseca VR, Linterman MA, Graca L. Regulation of the germinal center response. Front Immunol. 2018 Oct 25;9(OCT):2469.

70. Muramatsu M, Sankaranand VS, Anant S, Sugai M, Kinoshita K, Davidson NO, et al. Specific Expression of Activation-induced Cytidine Deaminase (AID), a Novel Member of the RNA-editing Deaminase Family in Germinal Center B Cells. Journal of Biological Chemistry. 1999 Jun 25;274(26):18470–6.

71. Pilzecker B, Jacobs H. Mutating for good: DNA damage responses during somatic hypermutation. Front Immunol. 2019;10(MAR):438.

72. Victora GD, Schwickert TA, Fooksman DR, Kamphorst AO, Meyer-Hermann M, Dustin ML, et al. Germinal Center Dynamics Revealed by Multiphoton Microscopy Using a Photoactivatable Fluorescent Reporter. Cell [Internet]. 2010 Nov 12 [cited 2024 Dec 7];143(4):592. Available from: https://pmc.ncbi.nlm.nih.gov/articles/PMC3035939/

73. García-Muñoz R, Galiacho VR, Llorente L. Immunological aspects in chronic lymphocytic leukemia (CLL) development. Ann Hematol [Internet]. 2012 Jul [cited 2022 Mar 28];91(7):981. Available from: /pmc/articles/PMC3368117/

74. Mesin L, Ersching J, Victora GD. GERMINAL CENTER B CELL DYNAMICS. Immunity [Internet]. 2016 Sep 20 [cited 2022 Mar 28];45(3):471. Available from: /pmc/articles/PMC5123673/

75. Kraus M, Alimzhanov MB, Rajewsky N, Rajewsky K. Survival of resting mature B lymphocytes depends on BCR signaling via the Igalpha/beta heterodimer. Cell [Internet]. 2004 Jun 11 [cited 2022 Mar 28];117(6):787–800. Available from: https://pubmed.ncbi.nlm.nih.gov/15186779/

76. Yang J, Reth M. Receptor Dissociation and B-Cell Activation. Curr Top Microbiol Immunol [Internet]. 2016 Oct 2 [cited 2024 Mar 6];393:27–43. Available from: https://pubmed.ncbi.nlm.nih.gov/26428245/

77. Schamel WWA, Reth M. Monomeric and Oligomeric Complexes of the B Cell Antigen Receptor. Immunity. 2000 Jul 1;13(1):5–14.

78. Hombach J, Lottspeich F, Reth M. Identification of the genes encoding the IgM-α and Ig-β components of the IgM antigen receptor complex by amino-terminal sequencing. Eur J Immunol [Internet]. 1990 Dec 1 [cited 2024 Mar 6];20(12):2795–9. Available from: https://onlinelibrary.wiley.com/doi/full/10.1002/eji.1830201239

79. Volkmann C, Brings N, Becker M, Hobeika E, Yang J, Reth M. Molecular requirements of the B-cell antigen receptor for sensing monovalent antigens. EMBO J [Internet]. 2016 Nov 2 [cited 2024 Nov 15];35(21):2371. Available from: https://pmc.ncbi.nlm.nih.gov/articles/PMC5090217/

80. Tolar P, Hanna J, Krueger PD, Pierce SK. The Constant Region of the Membrane Immunoglobulin Mediates B Cell-Receptor Clustering and Signaling in Response to Membrane Antigens. Immunity. 30:44–55.

81. Ackermann JA, Nys J, Schweighoffer E, McCleary S, Smithers N, Tybulewicz VLJ. Syk Tyrosine Kinase Is Critical for B Cell Antibody Responses and Memory B Cell Survival. The Journal of Immunology [Internet]. 2015 May 15 [cited 2024 Mar 6];194(10):4650–6. Available from: /pmc/articles/PMC4416743/

82. Al Zaouk S, Matar T, Ali MA, Kassem A, Hamawy L. Classification of Leukemia and Lymphoma using Faster R-CNN. 2022 International Conference on Microelectronics, ICM 2022. 2022;25–9.

83. Küppers R, Rajewsky K, Zhao M, Simons G, Laumann R, Fischer R, et al. Hodgkin disease: Hodgkin and Reed-Sternberg cells picked from histological sections show clonal immunoglobulin gene rearrangements and appear to be derived from B cells at various stages of development. Proc Natl Acad Sci U S A [Internet]. 1994 Nov 11 [cited 2024 Mar 7];91(23):10962. Available from: /pmc/articles/PMC45146/?report=abstract

84. Hallek M, Cheson BD, Catovsky D, Caligaris-Cappio F, Dighiero G, Döhner H, et al. iwCLL guidelines for diagnosis, indications for treatment, response assessment, and supportive management of CLL. Blood [Internet]. 2018 Jun 21 [cited 2023 Apr 24];131(25):2745–60. Available from: https://pubmed.ncbi.nlm.nih.gov/29540348/

85. Mafra A, Laversanne M, Gospodarowicz M, Klinger P, De Paula Silva N, Piñeros M, et al. Global patterns of non-Hodgkin lymphoma in 2020. Int J Cancer [Internet]. 2022 Nov 1 [cited 2024 Mar 8];151(9):1474–81. Available from: https://onlinelibrary.wiley.com/doi/full/10.1002/ijc.34163

86. Efremov DG, Turkalj S, Laurenti L. Mechanisms of B Cell Receptor Activation and Responses to B Cell Receptor Inhibitors in B Cell Malignancies. Cancers (Basel) [Internet]. 2020 Jun 1 [cited 2024 Mar 7];12(6). Available from: https://pubmed.ncbi.nlm.nih.gov/32481736/

87. Hallek M. Chronic lymphocytic leukemia: 2020 update on diagnosis, risk stratification and treatment. Am J Hematol. 2019 Nov 1;94(11):1266–87.

88. Messmer BT, Messmer D, Allen SL, Kolitz JE, Kudalkar P, Cesar D, et al. In vivo measurements document the dynamic cellular kinetics of chronic lymphocytic leukemia B cells. J Clin Invest [Internet]. 2005 [cited 2021 Jul 30];115(3):755–64. Available from: https://pubmed.ncbi.nlm.nih.gov/15711642/

89. Damle RN, Wasil T, Fais F, Ghiotto F, Valetto A, Allen SL, et al. Ig V gene mutation status and CD38 expression as novel prognostic indicators in chronic lymphocytic leukemia. Blood. 1999 Sep 15;94(6):1840–7.

90. Strati P, Shanafelt TD. Monoclonal B-cell lymphocytosis and early-stage chronic lymphocytic leukemia: diagnosis, natural history, and risk stratification. Blood. 2015 Jul 23;126(4):454.

91. Parikh SA, Kay NE, Shanafelt TD. How we treat Richter syndrome. Blood. 2014 Mar 13;123(11):1647.

92. Dreger P, Schetelig J, Andersen N, Corradini P, Van Gelder M, Gribben J, et al. Managing high-risk CLL during transition to a new treatment era: Stem cell transplantation or novel agents? Vol. 124, Blood. American Society of Hematology; 2014. p. 3841–9.

93. Pettitt AR. Mechanism of action of purine analogues in chronic lymphocytic leukaemia. Br J Haematol [Internet]. 2003 Jun 1 [cited 2023 Oct 30];121(5):692–702. Available from: https://onlinelibrary.wiley.com/doi/full/10.1046/j.1365-2141.2003.04336.x

94. Osawa T, Davies D, Hartley JA. Mechanism of cell death resulting from DNA interstrand cross-linking in mammalian cells. Cell Death & Disease 2011 2:8 [Internet]. 2011 Aug 4 [cited 2024 Dec 7];2(8):e187–e187. Available from: https://www.nature.com/articles/cddis201170

95. Catovsky D, Richards S, Matutes E, Oscier D, Dyer M, Bezares R, et al. Assessment of fludarabine plus cyclophosphamide for patients with chronic lymphocytic leukaemia (the LRF CLL4 Trial): a randomised controlled trial. Lancet [Internet]. 2007 Jul 21 [cited 2022 Jul 11];370(9583):230–9. Available from: https://pubmed.ncbi.nlm.nih.gov/17658394/

96. Tam CS, O'Brien S, Wierda W, Kantarjian H, Wen S, Do KA, et al. Long-term results of the fludarabine, cyclophosphamide, and rituximab regimen as initial therapy of chronic lymphocytic leukemia. Blood [Internet]. 2008 Aug 15 [cited 2023 Oct 30];112(4):975–80. Available from: https://pubmed.ncbi.nlm.nih.gov/18411418/

97. Maloney DG, Grillo-López AJ, White CA, Bodkin D, Schilder RJ, Neidhart JA, et al. IDEC-C2B8 (Rituximab) Anti-CD20 Monoclonal Antibody Therapy in Patients With Relapsed Low-Grade Non-Hodgkin's Lymphoma. Blood [Internet]. 1997 Sep 15 [cited 2024 Dec 7];90(6):2188–95. Available from: https://ashpublications.org/blood/article/90/6/2188/174699/IDECC2B8-Rituximab-AntiCD20-Monoclonal-Antibody

98. Bonavida B. Rituximab-induced inhibition of antiapoptotic cell survival pathways: implications in chemo/immunoresistance, rituximab unresponsiveness, prognostic and novel therapeutic interventions. Oncogene [Internet]. 2007 May 28 [cited 2023 Oct 30];26(25):3629–36. Available from: https://pubmed.ncbi.nlm.nih.gov/17530016/

99. Jones J, Mato A, Coutre S, Byrd JC, Furman RR, Hillmen P, et al. Evaluation of 230 patients with relapsed/refractory deletion 17p chronic lymphocytic leukaemia treated with ibrutinib from 3 clinical trials. Br J Haematol [Internet]. 2018 Aug 1 [cited 2024 Dec 7];182(4):504–12. Available from: https://pubmed.ncbi.nlm.nih.gov/29873072/

100. Hallek M, Fischer K, Fingerle-Rowson G, Fink AM, Busch R, Mayer J, et al. Addition of rituximab to fludarabine and cyclophosphamide in patients with chronic lymphocytic leukaemia: a randomised, open-label, phase 3 trial. The Lancet. 2010 Oct 2;376(9747):1164–74.

101. Eichhorst B, Fink AM, Busch R, Lange E, Köppler H, Kiehl M, et al. Chemoimmunotherapy With Fludarabine (F), Cyclophosphamide (C), and Rituximab (R) (FCR) Versus Bendamustine and Rituximab (BR) In Previously Untreated and Physically Fit Patients (pts) With Advanced Chronic Lymphocytic Leukemia (CLL): Results Of a Planned Interim Analysis Of The CLL10 Trial, An International, Randomized Study Of The German CLL Study Group (GCLLSG). Blood [Internet]. 2013 Nov 15 [cited 2023 Nov 1];122(21):526–526. Available from: https://dx.doi.org/10.1182/blood.V122.21.526.526

102. Hampel PJ, Parikh SA. Chronic lymphocytic leukemia treatment algorithm 2022. Blood Cancer Journal 2022 12:11 [Internet]. 2022 Nov 29 [cited 2023 Oct 30];12(11):1–10. Available from: https://www.nature.com/articles/s41408-022-00756-9

103. Leeksma A, Baliakas P, Moysiadis T, Mellink C, Puiggros A, Plevova K, et al. Genomic arrays identify high-risk chronic lymphocytic leukemia with genomic complexity: a multi-center study. Haematologica. 2020 Jun;3:513.

104. Goede V, Fischer K, Busch R, Engelke A, Eichhorst B, Wendtner CM, et al. Obinutuzumab plus Chlorambucil in Patients with CLL and Coexisting Conditions. New England Journal of Medicine [Internet]. 2014 Mar 20 [cited 2023 Oct 31];370(12):1101–10. Available from: https://www.nejm.org/doi/10.1056/NEJMoa1313984

105. Hus I, Puła B, Robak T. PI3K Inhibitors for the Treatment of Chronic Lymphocytic Leukemia: Current Status and Future Perspectives. Cancers (Basel) [Internet]. 2022 Mar 1 [cited 2023 Nov 1];14(6). Available from: /pmc/articles/PMC8945984/

106. Flinn IW, Hillmen P, Montillo M, Nagy Z, Illés Á, Etienne G, et al. The phase 3 DUO trial: duvelisib vs ofatumumab in relapsed and refractory CLL/SLL. Blood [Internet]. 2018 Dec 6 [cited 2023 Nov 1];132(23):2446–55. Available from: https://dx.doi.org/10.1182/blood-2018-05-850461

107. Lima BHF, Marques PE, Gomides LF, Mattos MS, Kraemer L, Queiroz-Junior CM, et al. Converging TLR9 and PI3Kgamma signaling induces sterile inflammation and organ damage. Scientific Reports 2019 9:1 [Internet]. 2019 Dec 13 [cited 2024 Jan 2];9(1):1–15. Available from: https://www.nature.com/articles/s41598-019-55504-0

108. Shanafelt TD, Wang XV, Hanson CA, Paietta EM, O'Brien S, Barrientos J, et al. Long-term outcomes for ibrutinib-rituximab and chemoimmunotherapy in CLL: updated results of the E1912 trial. Blood [Internet]. 2022 Jul 14 [cited 2023 Nov 1];140(2):112–20. Available from: https://pubmed.ncbi.nlm.nih.gov/35427411/

109. Byrd JC, Brown JR, O'Brien S, Barrientos JC, Kay NE, Reddy NM, et al. Ibrutinib versus Ofatumumab in Previously Treated Chronic Lymphoid Leukemia. N Engl J Med [Internet]. 2014 Jul 7 [cited 2023 Nov 3];371(3):213. Available from: /pmc/articles/PMC4134521/

110. Pontoriero M, Fiume G, Vecchio E, de Laurentiis A, Albano F, Iaccino E, et al. Activation of NF-κB in B cell receptor signaling through Bruton's tyrosine kinase-dependent phosphorylation of IκB-α. J Mol Med (Berl) [Internet]. 2019 May 1 [cited 2023 Nov 1];97(5):675–90. Available from: https://pubmed.ncbi.nlm.nih.gov/30887112/

111. Certo M, Moore VDG, Nishino M, Wei G, Korsmeyer S, Armstrong SA, et al. Mitochondria primed by death signals determine cellular addiction to antiapoptotic BCL-2 family members. Cancer Cell. 2006 May 1;9(5):351–65.

112. Roberts AW, Ma S, Kipps TJ, Coutre SE, Davids MS, Eichhorst B, et al. Efficacy of venetoclax in relapsed chronic lymphocytic leukemia is influenced by disease and response variables. Blood [Internet]. 2019 Jul 11 [cited 2023 Nov 1];134(2):111–22. Available from: https://dx.doi.org/10.1182/blood.2018882555

113. Fischer K, Al-Sawaf O, Bahlo J, Fink AM, Tandon M, Dixon M, et al. Venetoclax and Obinutuzumab in Patients with CLL and Coexisting Conditions. New England Journal of Medicine [Internet]. 2019 Jun 6 [cited 2023 Nov 3];380(23):2225–36. Available from: https://www.nejm.org/doi/full/10.1056/nejmoa1815281

114. Stilgenbauer S, Eichhorst B, Schetelig J, Hillmen P, Seymour JF, Coutre S, et al. Venetoclax for patients with chronic lymphocytic leukemia with 17p deletion: Results from the full population of a phase ii pivotal trial. Journal of Clinical Oncology. 2018 Jul 1;36(19):1973–80.

115. Mato AR, Barrientos JC, Ghosh N, Pagel JM, Brander DM, Gutierrez M, et al. Prognostic Testing and Treatment Patterns in Chronic Lymphocytic Leukemia in the Era of Novel Targeted Therapies: Results From the informCLL Registry. Clin Lymphoma Myeloma Leuk. 2020 Mar 1;20(3):174-183.e3.

116. Cohen JA, Bomben R, Pozzo F, Tissino E, Härzschel A, Hartmann TN, et al. An Updated Perspective on Current Prognostic and Predictive Biomarkers in Chronic Lymphocytic Leukemia in the Context of Chemoimmunotherapy and Novel Targeted Therapy. Cancers (Basel) [Internet]. 2020 Apr 1 [cited 2021 Aug 10];12(4). Available from: /pmc/articles/PMC7226446/

117. Stilgenbauer S, Eichhorst B, Schetelig J, Coutre S, Seymour JF, Munir T, et al. Venetoclax in relapsed or refractory chronic lymphocytic leukaemia with 17p deletion: a multicentre, open-label, phase 2 study. Lancet Oncol [Internet]. 2016 Jun 1 [cited 2023 Nov 3];17(6):768–78. Available from: https://pubmed.ncbi.nlm.nih.gov/27178240/

118. Stilgenbauer S, Schnaiter A, Paschka P, Zenz T, Rossi M, Döhner K, et al. Gene mutations and treatment outcome in chronic lymphocytic leukemia: results from the CLL8 trial. Blood [Internet]. 2014 May 22 [cited 2023 Nov 3];123(21):3247–54. Available from: https://pubmed.ncbi.nlm.nih.gov/24652989/

119. González-Gascón-y-Marín I, Muñoz-Novas C, Rodríguez-Vicente AE, Quijada-Álamo M, Hernández-Sánchez M, Pérez-Carretero C, et al. From Biomarkers to Models in the Changing Landscape of Chronic Lymphocytic Leukemia: Evolve or Become Extinct. Cancers 2021, Vol 13, Page 1782. 2021 Apr 8;13(8):1782.

120. Guièze R, Wu CJ. Genomic and epigenomic heterogeneity in chronic lymphocytic leukemia. Vol. 126, Blood. American Society of Hematology; 2015. p. 445–53.

121. Nadeu F, Clot G, Delgado J, Martín-García D, Baumann T, Salaverria I, et al. Clinical impact of the subclonal architecture and mutational complexity in chronic lymphocytic leukemia. Leukemia. 2018 Mar 1;32(3):645–53.

122. Crombie J, Davids MS. IGHV mutational status testing in chronic lymphocytic leukemia. Am J Hematol. 2017 Dec 1;92(12):1393–7.

123. Hamblin TJ, Davis Z, Gardiner A, Oscier DG, Stevenson FK. Unmutated Ig V(H) genes are associated with a more aggressive form of chronic lymphocytic leukemia. Blood. 1999 Sep 15;94(6):1848–54.

124. Mockridge CI, Potter KN, Wheatley I, Neville LA, Packham G, Stevenson FK. Reversible anergy of sIgM-mediated signaling in the two subsets of CLL defined by VH-gene mutational status. Blood [Internet]. 2007 May 15 [cited 2024 Aug 8];109(10):4424–31. Available from: https://dx.doi.org/10.1182/blood-2006-11-056648

125. Thompson PA, Tam CS, O'Brien SM, Wierda WG, Stingo F, Plunkett W, et al. Fludarabine, cyclophosphamide, and rituximab treatment achieves long-term disease-free survival in IGHV-mutated chronic lymphocytic leukemia. Blood [Internet]. 2016 Jan 21 [cited 2022 Mar 7];127(3):303–9. Available from: https://pubmed.ncbi.nlm.nih.gov/26492934/

126. Byrd JC, Furman RR, Coutre SE, Burger JA, Blum KA, Coleman M, et al. Three-year follow-up of treatment-naïve and previously treated patients with CLL and SLL receiving single-agent ibrutinib. Blood [Internet]. 2015 Apr 16 [cited 2022 Mar 7];125(16):2497–506. Available from: https://pubmed.ncbi.nlm.nih.gov/25700432/

127. O'brien SM, Furman RR, Coutre SE, Flinn IW, Burger J, Blum K, et al. Five-Year Experience with Single-Agent Ibrutinib in Patients with Previously Untreated and Relapsed/Refractory Chronic Lymphocytic Leukemia/Small Lymphocytic Leukemia. 2016; Available from: http://doi.org/10.1182/blood.V128.22.233.233

128. Agathangelidis A, Darzentas N, Hadzidimitriou A, Brochet X, Murray F, Yan XJ, et al. Stereotyped B-cell receptors in one-third of chronic lymphocytic leukemia: a molecular classification with implications for targeted therapies. Blood [Internet]. 2012 May 10 [cited 2022 Mar 28];119(19):4467. Available from: /pmc/articles/PMC3392073/

129. Stamatopoulos K, Belessi C, Moreno C, Boudjograh M, Guida G, Smilevska T, et al. Over 20% of patients with chronic lymphocytic leukemia carry stereotyped receptors: Pathogenetic implications and clinical correlations. Blood [Internet]. 2007 Jan 1 [cited 2022 Mar 28];109(1):259–70. Available from: https://pubmed.ncbi.nlm.nih.gov/16985177/

130. Matthews C, Catherwood MA, Morris TCMC, Alexander HD. V(H)3-48 and V(H)3-53, as well as V(H)3-21, gene rearrangements define unique subgroups in CLL and are associated with biased lambda light chain restriction, homologous LCDR3 sequences and poor prognosis. Leuk Res [Internet]. 2007 Feb [cited 2024 Mar 9];31(2):231–4. Available from: https://pubmed.ncbi.nlm.nih.gov/16714060/

131. Nadeu F, Royo R, Clot G, Duran-Ferrer M, Navarro A, Martín S, et al. IGLV3-21R110 identifies an aggressive biological subtype of chronic lymphocytic leukemia with intermediate epigenetics. Blood [Internet]. 2021 May 27 [cited 2023 Aug 5];137(21):2935–46. Available from: https://dx.doi.org/10.1182/blood.2020008311

132. Forconi F, Potter KN, Wheatley I, Darzentas N, Sozzi E, Stamatopoulos K, et al. The normal IGHV1-69–derived B-cell repertoire contains stereotypic patterns characteristic of unmutated CLL. Blood [Internet]. 2010 Jan 7 [cited 2024 Mar 9];115(1):71–7. Available from: https://dx.doi.org/10.1182/blood-2009-06-225813

133. Myhrinder AL, Hellqvist E, Sidorova E, Söderberg A, Baxendale H, Dahle C, et al. A new perspective: molecular motifs on oxidized LDL, apoptotic cells, and bacteria are targets for chronic lymphocytic leukemia antibodies. Blood [Internet]. 2008 Apr 1 [cited 2024 Mar 9];111(7):3838–48. Available from: https://dx.doi.org/10.1182/blood-2007-11-125450

134. Pinkel D, Straume T, Gray JW. Cytogenetic analysis using quantitative, high-sensitivity, fluorescence hybridization. Proc Natl Acad Sci U S A [Internet]. 1986 [cited 2024 Mar 11];83(9):2934. Available from: /pmc/articles/PMC323421/?report=abstract

135. Döhner H, Stilgenbauer S, Benner A, Leupolt E, Kröber A, Bullinger L, et al. Genomic aberrations and survival in chronic lymphocytic leukemia. New England Journal of Medicine. 2000 Dec 28;343(26 I):1910–6.

136. Campo E, Cymbalista F, Ghia P, Jäger U, Pospisilova S, Rosenquist R, et al. TP53 aberrations in chronic lymphocytic leukemia: An overview of the clinical implications of improved diagnostics. Vol. 103, Haematologica. Ferrata Storti Foundation; 2018. p. 1956–68.

137. Puiggros A, Blanco G, Espinet B. Genetic Abnormalities in Chronic Lymphocytic Leukemia: Where We Are and Where We Go. Biomed Res Int. 2014;2014.

138. Te Raa GD, Moerland PD, Leeksma AC, Derks IA, Yigittop H, Laddach N, et al. Assessment of p53 and ATM functionality in chronic lymphocytic leukemia by multiplex ligation-dependent probe amplification. Cell Death Dis. 2015 Aug 6;6(8):e1852.

139. Zilfou JT, Lowe SW. Tumor suppressive functions of p53. Vol. 1, Cold Spring Harbor perspectives in biology. Cold Spring Harbor Laboratory Press; 2009.

140. Riley T, Sontag E, Chen P, Levine A. Transcriptional control of human p53-regulated genes. Nat Rev Mol Cell Biol. 2008 May;9(5):402–12.

141. Rose-Zerilli MJJ, Forster J, Parker H, Parker A, Rodri AÉ, Chaplin T, et al. ATM mutation rather than BIRC3 deletion and/or mutation predicts reduced survival in 11q-deleted chronic lymphocytic leukemia: Data from the UK LRF CLL4 trial. Haematologica. 2014;99(4):736–42.

142. Abruzzo L V., Herling CD, Calin GA, Oakes C, Barron LL, Banks HE, et al. Trisomy 12 chronic lymphocytic leukemia expresses a unique set of activated and targetable pathways. Haematologica [Internet]. 2018 Nov 30 [cited 2024 Aug 9];103(12):2069. Available from: /pmc/articles/PMC6269288/

143. Grygalewicz B, Woroniecka R, Rygier J, Borkowska K, Rzepecka I, Łukasik M, et al. Monoallelic and biallelic deletions of 13q14 in a group of CLL/SLL patients investigated by CGH Haematological Cancer and SNP array (8x60K). Mol Cytogenet [Internet]. 2016 Jan 6 [cited 2022 May 27];9(1):1–17. Available from: https://molecularcytogenetics.biomedcentral.com/articles/10.1186/s13039-015-0212-x

144. Parker H, Rose-Zerilli MJJ, Parker A, Chaplin T, Wade R, Gardiner A, et al. 13q deletion anatomy and disease progression in patients with chronic lymphocytic leukemia. Leukemia. 2011;25(3):489–97.

145. Khalid K, Padda J, Syam M, Moosa A, Kakani V, Sanka S, et al. 13q14 Deletion and Its Effect on Prognosis of Chronic Lymphocytic Leukemia. Cureus [Internet]. 2021 Aug 3 [cited 2022 May 27];13(8). Available from: /pmc/articles/PMC8424995/

146. Agathaggelou A, Murina O, Jackson AP, Moss P, Paneesha S, Stewart GS, et al. Targeting an RNaseH2 Defect in Chronic Lymphocytic Leukaemia with PARP Inhibitors. Blood. 2018 Nov 29;132(Supplement 1):1835.

147. Parker H, Strefford JC. The mutational signature of chronic lymphocytic Leukemia [Internet]. Vol. 473, Biochemical Journal. Portland Press Ltd; 2016 [cited 2020 Oct 28]. p. 3725–40. Available from: http://portlandpress.com/biochemj/article-pdf/473/21/3725/689734/bcj-2016-0256c.pdf

148. Landau DA, Carter SL, Stojanov P, McKenna A, Stevenson K, Lawrence MS, et al. Evolution and impact of subclonal mutations in chronic lymphocytic leukemia. Cell. 2013 Feb 14;152(4):714–26.

149. Skowronska A, Parker A, Ahmed G, Oldreive C, Davis Z, Richards S, et al. Biallelic ATM inactivation significantly reduces survival in patients treated on the United Kingdom leukemia research fund chronic lymphocytic leukemia 4 trial. Journal of Clinical Oncology. 2012 Dec 20;30(36):4524–32.

150. Bednarski JJ, Sleckman BP. Integrated signaling in developing lymphocytes: The role of DNA damage responses. Vol. 11, Cell Cycle. Taylor and Francis Inc.; 2012. p. 4129–34.

151. Choi M, Kipps T, Kurzrock R. ATM mutations in cancer: Therapeutic implications. Vol. 15, Molecular Cancer Therapeutics. American Association for Cancer Research Inc.; 2016. p. 1781–91.

152. Blasius M, Bartek J. ATM targets hnRNPK to control p53. Vol. 12, Cell cycle (Georgetown, Tex.). Taylor & Francis; 2013. p. 1162.

153. Savic V, Yin B, Maas NL, Bredemeyer AL, Carpenter AC, Helmink BA, et al. Formation of dynamic gamma-H2AX domains along broken DNA strands is distinctly regulated by ATM and MDC1 and dependent upon H2AX densities in chromatin. Mol Cell [Internet]. 2009 May 15 [cited 2022 May 27];34(3):298–310. Available from: https://pubmed.ncbi.nlm.nih.gov/19450528/

154. Kleiner RE, Verma P, Molloy KR, Chait BT, Kapoor TM. Chemical proteomics reveals a γH2AX-53BP1 interaction in the DNA damage response. Nat Chem Biol [Internet]. 2015 [cited 2022 May 27]; Available from: www.nature.com/naturechemicalbiology

155. Mah LJ, El-Osta A, Karagiannis TC. γH2AX: a sensitive molecular marker of DNA damage and repair. Leukemia 2010 24:4 [Internet]. 2010 Feb 4 [cited 2022 May 27];24(4):679–86. Available from: https://www.nature.com/articles/leu20106

156. Zha S, Sekiguchi JA, Brush JW, Bassing CH, Alt FW. Complementary functions of ATM and H2AX in development and suppression of genomic instability. Proc Natl Acad Sci U S A [Internet]. 2008 Jul 8 [cited 2022 May 27];105(27):9302–6. Available from: www.pnas.orgcgidoi10.1073pnas.0803520105

157. Landau DA, Tausch E, Taylor-Weiner AN, Stewart C, Reiter JG, Bahlo J, et al. Mutations driving CLL and their evolution in progression and relapse. Nature. 2015 Oct 22;526(7574):525–30.

158. Puente XS, Beà S, Valdés-Mas R, Villamor N, Gutiérrez-Abril J, Martín-Subero JI, et al. Non-coding recurrent mutations in chronic lymphocytic leukaemia. Nature. 2015 Oct 22;526(7574):519–24.

159. Blakemore SJ, Clifford R, Parker H, Antoniou P, Stec-Dziedzic E, Larrayoz M, et al. Clinical significance of TP53, BIRC3, ATM and MAPK-ERK genes in chronic lymphocytic leukaemia: data from the randomised UK LRF CLL4 trial. Leukemia [Internet]. 2020 Jul 1 [cited 2022 May 27];34(7):1760. Available from: /pmc/articles/PMC7326706/

160. Capper R, Britt-Compton B, Tankimanova M, Rowson J, Letsolo B, Man S, et al. The nature of telomere fusion and a definition of the critical telomere length in human cells. Genes Dev. 2007;21(19):2495–508.

161. Rossi D, Bodoni CL, Genuardi E, Monitillo L, Drandi D, Cerri M, et al. Telomere length is an independent predictor of survival, treatment requirement and Richter's syndrome transformation in chronic lymphocytic leukemia. Leukemia. 2009;23(6):1062–72.

162. Mansouri L, Grabowski P, Degerman S, Svenson U, Gunnarsson R, Cahill N, et al. Short telomere length is associated with NOTCH1/SF3B1/TP53 aberrations and poor outcome in newly diagnosed chronic lymphocytic leukemia patients. Am J Hematol. 2013;88(8):647–51.

163. Jebaraj BMC, Stilgenbauer S. Telomere Dysfunction in Chronic Lymphocytic Leukemia. Front Oncol. 2021 Jan 15;10:3062.

164. Harley CB. Telomere loss: mitotic clock or genetic time bomb? Mutat Res [Internet]. 1991 [cited 2022 Mar 7];256(2–6):271–82. Available from: https://pubmed.ncbi.nlm.nih.gov/1722017/

165. Griffith JD, Comeau L, Rosenfield S, Stansel RM, Bianchi A, Moss H, et al. Mammalian Telomeres End in a Large Duplex Loop. Cell. 1999 May 14;97(4):503–14.

166. Sellmann L, De Beer D, Bartels M, Opalka B, Nückel H, Dührsen U, et al. Telomeres and prognosis in patients with chronic lymphocytic leukaemia. Int J Hematol. 2011;93(1):74–82.

167. Poncet D, Belleville A, De Roodenbeke CTK, De Climens AR, Simon E Ben, Merle-Beral H, et al. Changes in the expression of telomere maintenance genes suggest global telomere dysfunction in B-chronic lymphocytic leukemia. Blood. 2008;111(4):2388–91.

168. Weng NP, Palmer L, Levine B, Lane HC, June C, Hodes R. Tales of tails: regulation of telomere length and telomerase activity during lymphocyte development, differentiation, activation, and aging.

169. Poncet D, Belleville A, De Roodenbeke CTK, De Climens AR, Simon E Ben, Merle-Beral H, et al. Changes in the expression of telomere maintenance genes suggest global telomere dysfunction in B-chronic lymphocytic leukemia. Blood. 2008;111(4):2388–91.

170. Jebaraj BMC, Tausch E, Landau DA, Bahlo J, Robrecht S, Taylor-Weiner AN, et al. Short telomeres are associated with inferior outcome, genomic complexity, and clonal evolution in chronic lymphocytic leukemia. Leukemia. 2019 Sep 1;33(9):2183–94.

171. Hastie ND, Dempster M, Dunlop MG, Thompson AM, Green DK, Allshire RC. Telomere reduction in human colorectal carcinoma and with ageing. 1990;346(August):866–8.

172. Lin TT, Letsolo BT, Jones RE, Rowson J, Pratt G, Fegan C, et al. Telomere dysfunction and fusion during the progression of a human malignancy. Blood. 2010;44(0):1899–908.

173. Jones CH, Pepper C, Baird DM. Telomere dysfunction and its role in haematological cancer. Br J Haematol. 2012;156(5):573–87.

174. Lin TT, Norris K, Heppel NH, Pratt G, Allan JM, Allsup DJ, et al. Telomere dysfunction accurately predicts clinical outcome in chronic lymphocytic leukaemia, even in patients with early stage disease. Br J Haematol. 2014;167(2):214–23.

175. Cleal K, Baird DM. Catastrophic Endgames: Emerging Mechanisms of Telomere-Driven Genomic Instability. Trends in Genetics. 2020;36(5):347–59.

176. Thomay K, Fedder C, Hofmann W, Kreipe H, Stadler M, Titgemeyer J, et al. Telomere shortening, TP53 mutations and deletions in chronic lymphocytic leukemia result in increased chromosomal instability and breakpoint clustering in heterochromatic regions. Ann Hematol. 2017;96(9):1493–500.

177. Lin TT, Letsolo BT, Jones RE, Rowson J, Pratt G, Fegan C, et al. Telomere dysfunction and fusion during the progression of a human malignancy. Blood. 2010;44(0):1899–908.

178. Bechter O. Telomere length and telomerase activity precict survival in patients with b cell chronic lymphocytic leukemia (b-cll). Exp Hematol. 1998;26(8):788.

179. Trentin L, Ballon G, Ometto L, Perin A, Basso U, Chieco-Bianchi L, et al. Telomerase activity in chronic lymphoproliferative disorders of B-cell lineage. Br J Haematol. 1999;106:662–8.

180. Palma M, Parker A, Hojjat-Farsangi M, Forster J, Kokhaei P, Hansson L, et al. Telomere length and expression of human telomerase reverse transcriptase splice variants in chronic lymphocytic leukemia. Exp Hematol. 2013;41(7):615–26.

181. Rossi D, Bodoni CL, Genuardi E, Monitillo L, Drandi D, Cerri M, et al. Telomere length is an independent predictor of survival, treatment requirement and Richter's syndrome transformation in chronic lymphocytic leukemia. Leukemia. 2009;23(6):1062–72.

182. Ballon G, Trentin L, De Rossi A, Semenzato G. Telomerase activity and clinical progression in chronic lymphoproliferative disorders of B-cell lineage. Leuk Lymphoma. 2001;41(1–2):35–45.

183. Damle RN, Batliwalla FM, Ghiotto F, Valetto A, Albesiano E, Sison C, et al. Telomere length and telomerase activity delineate distinctive replicative features of the B-CLL subgroups defined by immunoglobulin V gene mutations. Blood. 2004;103(2):375–82.

184. Guièze R, Pages M, Véronèse L, Combes P, Lemal R, Gay-bellile M, et al. Telomere status in chronic lymphocytic leukemia with TP53 disruption. Oncotarget. 2016;7(35):56976–85.

185. Strefford JC, Kadalayil L, Forster J, Rose-Zerilli MJJ, Parker A, Lin TT, et al. Telomere length predicts progression and overall survival in chronic lymphocytic leukemia: Data from the UK LRF CLL4 trial [Internet]. Vol. 29, Leukemia. Nature Publishing Group; 2015 [cited 2020 Aug 6]. p. 2411–4. Available from: https://www.ncbi.nlm.nih.gov/pmc/articles/PMC4676082/

186. Roos G, Kröber A, Grabowski P, Kienle D, Bühler A, Döhner H, et al. Short telomeres are associated with genetic complexity, high-risk genomic aberrations, and short survival in chronic lymphocytic leukemia. Blood. 2008;111(4):2246–52.

187. Maciejowski J, De Lange T. Telomeres in cancer: Tumour suppression and genome instability. Vol. 18, Nature Reviews Molecular Cell Biology. Nature Publishing Group; 2017. p. 175–86.

188. Lin TT, Norris K, Heppel NH, Pratt G, Allan JM, Allsup DJ, et al. Telomere dysfunction accurately predicts clinical outcome in chronic lymphocytic leukaemia, even in patients with early stage disease. Br J Haematol. 2014;167(2):214–23.

189. Norris K, Hillmen P, Rawstron A, Hills R, Baird DM, Fegan CD, et al. Telomere length predicts for outcome to FCR chemotherapy in CLL. Leukemia 2019 33:8 [Internet]. 2019 Jan 30 [cited 2021 Aug 10];33(8):1953–63. Available from: https://www.nature.com/articles/s41375-019-0389-9

190. Locke WJ, Guanzon D, Ma C, Liew YJ, Duesing KR, Fung KYC, et al. DNA Methylation Cancer Biomarkers: Translation to the Clinic. Front Genet. 2019 Nov 14;10:1150.

191. Jin B, Li Y, Robertson KD. DNA Methylation: Superior or Subordinate in the Epigenetic Hierarchy? Genes Cancer [Internet]. 2011 Jun [cited 2022 May 14];2(6):607. Available from: /pmc/articles/PMC3174260/

192. Kulis M, Esteller M. DNA Methylation and Cancer. Adv Genet. 2010 Jan 1;70(C):27–56.

193. Bird A. DNA methylation patterns and epigenetic memory. Genes Dev [Internet]. 2002 Jan 1 [cited 2022 May 14];16(1):6–21. Available from: http://genesdev.cshlp.org/content/16/1/6.full

194. Queirós AC, Villamor N, Clot G, Martinez-Trillos A, Kulis M, Navarro A, et al. A B-cell epigenetic signature defines three biologic subgroups of chronic lymphocytic leukemia with clinical impact. Leukemia 2015 29:3 [Internet]. 2014 Aug 25 [cited 2022 May 14];29(3):598–605. Available from: https://www.nature.com/articles/leu2014252

195. Wojdacz TK, Amarasinghe HE, Kadalayil L, Beattie A, Forster J, Blakemore SJ, et al. Clinical significance of DNA methylation in chronic lymphocytic leukemia patients: Results from 3 UK clinical trials. Blood Adv. 2019 Aug 27;3(16):2474–81.

196. González-Gascón-y-Marín I, Muñoz-Novas C, Rodríguez-Vicente AE, Quijada-Álamo M, Hernández-Sánchez M, Pérez-Carretero C, et al. From Biomarkers to Models in the

Changing Landscape of Chronic Lymphocytic Leukemia: Evolve or Become Extinct. Cancers 2021, Vol 13, Page 1782. 2021 Apr 8;13(8):1782.

197. Yu L, Kim HT, Kasar SN, Benien P, Du W, Hoang K, et al. Cancer Therapy: Clinical Survival of Del17p CLL Depends on Genomic Complexity and Somatic Mutation. 2017;

198. Kujawski L, Ouillette P, Erba H, Saddler C, Jakubowiak A, Kaminski M, et al. Genomic complexity identifies patients with aggressive chronic lymphocytic leukemia. Blood. 2008 Sep 1;112(5):1993–2003.

199. Sharma S, Rai KR. Chronic lymphocytic leukemia (CLL) treatment: So many choices, such great options. Cancer. 2019 May 26;125(9):1432–40.

200. Harkins RA, Patel SP, Flowers CR. Cost-Effectiveness of New Targeted Agents in the Treatment of Chronic Lymphocytic Leukemia. Cancer J. 2019 Nov 1;25(6):418.

201. T H, JA B, JF L. Economic Impact of Oral Therapies for Chronic Lymphocytic Leukemia-the Burden of Novelty. Curr Hematol Malig Rep. 2018 Aug 1;13(4):237–43.

202. M H, K F, G FR, AM F, R B, J M, et al. Addition of rituximab to fludarabine and cyclophosphamide in patients with chronic lymphocytic leukaemia: a randomised, open-label, phase 3 trial. Lancet [Internet]. 2010 Oct 2 [cited 2021 Aug 18];376(9747):1164–74. Available from: https://pubmed.ncbi.nlm.nih.gov/20888994/

203. Blanco G, Puiggros A, Baliakas P, Athanasiadou A, García-Malo MD, Collado R, et al. Karyotypic complexity rather than chromosome 8 abnormalities aggravates the outcome of chronic lymphocytic leukemia patients with TP53 aberrations. Oncotarget. 2016;7(49):80916–24.

204. Delgado J, Salaverria I, Baumann T, Martínez-Trillos A, Lee E, Jiménez L, et al. Genomic complexity and IGHV mutational status are key predictors of outcome of chronic lymphocytic leukemia patients with TP53 disruption. Vol. 99, Haematologica. Ferrata Storti Foundation; 2014. p. e231–4.

205. Herling CD, Klaumünzer M, Rocha CK, Altmüller J, Thiele H, Bahlo J, et al. Complex karyotypes and KRAS and POT1 mutations impact outcome in CLL after chlorambucil-based chemotherapy or chemoimmunotherapy. Blood. 2016 Jul 21;128(3):395–404.

206. Thompson PA, O'Brien SM, Wierda WG, Ferrajoli A, Stingo F, Smith SC, et al. Complex karyotype is a stronger predictor than del(17p) for an inferior outcome in relapsed or

refractory chronic lymphocytic leukemia patients treated with ibrutinib-based regimens. Cancer. 2015 Oct 1;121(20):3612–21.

207. Anderson MA, Tam C, Lew TE, Juneja S, Juneja M, Westerman D, et al. Clinicopathological features and outcomes of progression of CLL on the BCL2 inhibitor venetoclax. Blood. 2017 Jun 22;129(25):3362–70.

208. Mato AR, Hill BT, Lamanna N, Barr P, Ujjani CS, Brander DM, et al. Optimal Sequencing of Ibrutinib, Idelalisib, and Venetoclax in CLL: Results from a Large Multi-Center Study of 683 US-Patients. Blood. 2016 Dec 2;128(22):4400–4400.

209. Mcneil N, Ried T. Novel molecular cytogenetic techniques for identifying complex chromosomal rearrangements: technology and applications in molecular medicine. Expert Rev Mol Med [Internet]. 2000 Sep 14 [cited 2024 Mar 11];2000(7):1–14. Available from: https://pubmed.ncbi.nlm.nih.gov/14585138/

210. Rack KA, van den Berg E, Haferlach C, Beverloo HB, Costa D, Espinet B, et al. European recommendations and quality assurance for cytogenomic analysis of haematological neoplasms. Vol. 33, Leukemia. Nature Publishing Group; 2019. p. 1851–67.

211. Sanger F, Nicklen S, Coulson AR. DNA sequencing with chain-terminating inhibitors. Proc Natl Acad Sci U S A [Internet]. 1977 [cited 2024 Mar 13];74(12):5463. Available from: /pmc/articles/PMC431765/?report=abstract

212. Shin HT, Choi Y La, Yun JW, Kim NKD, Kim SY, Jeon HJ, et al. Prevalence and detection of low-allele-fraction variants in clinical cancer samples. Nat Commun [Internet]. 2017 Dec 1 [cited 2024 Apr 16];8(1). Available from: /pmc/articles/PMC5680209/

213. Scheinin I, Sie D, Bengtsson H, Van De Wiel MA, Olshen AB, Van Thuijl HF, et al. DNA copy number analysis of fresh and formalin-fixed specimens by shallow whole-genome sequencing with identification and exclusion of problematic regions in the genome assembly. Genome Res [Internet]. 2014 Dec 1 [cited 2022 May 21];24(12):2022. Available from: /pmc/articles/PMC4248318/

214. Lioumi M, Newell D. CR-UK biomarker roadmaps. Clinical Cancer Research [Internet]. 2010 Oct 1 [cited 2024 Mar 11];16(19_Supplement):B33–B33. Available from: /clincancerres/article/16/19_Supplement/B33/196630/CR-UK-biomarker-roadmaps

215. Gopalakrishnan S, Ganeshkumar P. Systematic Reviews and Meta-analysis: Understanding the Best Evidence in Primary Healthcare. J Family Med Prim Care [Internet]. 2013 [cited 2024 Jan 9];2(1):9. Available from: /pmc/articles/PMC3894019/

216. Liberati A, Altman DG, Tetzlaff J, Mulrow C, Gøtzsche PC, Ioannidis JPA, et al. The PRISMA Statement for Reporting Systematic Reviews and Meta-Analyses of Studies That Evaluate Health Care Interventions: Explanation and Elaboration. PLoS Med. 2009 Jul 21;6(7):e1000100.

217. Ben-Dali Y, Hleuhel MH, Andersen MA, Brieghel C, Clasen-Linde E, Da Cunha-Bang C, et al. Risk Factors Associated with Richter's Transformation in Patients with Chronic Lymphocytic Leukemia. Blood. 2018 Nov 29;132(Supplement 1):1697.

218. Kirchhoff M, Rose H, Lundsteen C. High resolution comparative genomic hybridisation in clinical cytogenetics. J Med Genet [Internet]. 2001 [cited 2023 Dec 4];38(11):740–4. Available from: https://pubmed.ncbi.nlm.nih.gov/11694545/

219. Zhang Z, Chen S, Chen S, Chen G, Zhang R, Li J, et al. SF3B1 mutation is a prognostic factor in chronic lymphocytic leukemia: A meta-analysis. Oncotarget. 2017 Jul 23;8(41):69916–23.

220. Schweighofer CD, Coombes KR, Majewski T, Barron LL, Lerner S, Sargent RL, et al. Genomic variation by whole-genome SNP mapping arrays predicts time-to-event outcome in patients with chronic lymphocytic Leukemia: A comparison of CLL and HapMap genotypes. Journal of Molecular Diagnostics. 2013 Mar;15(2):196–209.

221. Mian M, Rinaldi A, Mensah AA, Rossi D, Ladetto M, Forconi F, et al. Large genomic aberrations detected by SNP array are independent prognosticators of a shorter time to first treatment in chronic lymphocytic leukemia patients with normal FISH. Annals of Oncology. 2013 May;24(5):1378–84.

222. Puiggros A, Collado R, Calasanz MJ, Ortega M, Ruiz-Xivillé N, Rivas-Delgado A, et al. Patients with chronic lymphocytic leukemia and complex karyotype show an adverse outcome even in absence of TP53/ATM FISH deletions. Oncotarget. 2017;8(33):54297–303.

223. Heerema NA, Muthusamy N, Zhao Q, Ruppert AS, Breidenbach H, Andritsos LA, et al. Prognostic significance of translocations in the presence of mutated IGHV and of cytogenetic complexity at diagnosis of chronic lymphocytic leukemia. Haematologica. 2020;105.

224. Kay NE, Eckel-Passow JE, Braggio E, VanWier S, Shanafelt TD, Van Dyke DL, et al. Progressive but previously untreated CLL patients with greater array CGH complexity exhibit a less durable response to chemoimmunotherapy. Cancer Genet Cytogenet. 2010 Dec;203(2):161–8.

225. Baliakas P, Iskas M, Gardiner A, Davis Z, Plevova K, Nguyen-Khac F, et al. Chromosomal translocations and karyotype complexity in chronic lymphocytic leukemia: A systematic reappraisal of classic cytogenetic data. Am J Hematol [Internet]. 2014 Mar [cited 2020 Dec 15];89(3):249–55. Available from: https://pubmed.ncbi.nlm.nih.gov/24166834/

226. Robbe P, Ridout KE, Vavoulis D V., Dréau H, Kinnersley B, Denny N, et al. Whole-genome sequencing of chronic lymphocytic leukemia identifies subgroups with distinct biological and clinical features. Nat Genet [Internet]. 2022 Nov 1 [cited 2023 Sep 23];54(11):1675–89. Available from: https://pubmed.ncbi.nlm.nih.gov/36333502/

227. Rigolin GM, Traversa A, Caputo V, Del Giudice I, Bardi A, Saccenti E, et al. Additional lesions identified by genomic microarrays are associated with an inferior outcome in low-risk chronic lymphocytic leukaemia patients. Br J Haematol [Internet]. 2023 Sep 1 [cited 2023 Sep 22];202(5). Available from: https://pubmed.ncbi.nlm.nih.gov/37357817/

228. Ramos-Campoy S, Puiggros A, Beà S, Bougeon S, Larráyoz MJ, Costa D, et al. Chromosome banding analysis and genomic microarrays are both useful but not equivalent methods for genomic complexity risk stratification in chronic lymphocytic leukemia patients. Haematologica [Internet]. 2022 Mar 1 [cited 2023 Sep 22];107(3):593–603. Available from: https://pubmed.ncbi.nlm.nih.gov/33691382/

229. Ramos-Campoy S, Puiggros A, Kamaso J, Beà S, Bougeon S, Larráyoz MJ, et al. TP53 Abnormalities Are Underlying the Poor Outcome Associated with Chromothripsis in Chronic Lymphocytic Leukemia Patients with Complex Karyotype. Cancers (Basel) [Internet]. 2022 Aug 1 [cited 2023 Sep 22];14(15). Available from: https://pubmed.ncbi.nlm.nih.gov/35954380/

230. Chauzeix J, Pastoret C, Donaty L, Gachard N, Fest T, Feuillard J, et al. A reduced panel of eight genes (ATM, SF3B1, NOTCH1, BIRC3, XPO1, MYD88, TNFAIP3, and TP53) as an estimator of the tumor mutational burden in chronic lymphocytic leukemia. Int J Lab Hematol [Internet]. 2021 Aug 1 [cited 2023 Sep 23];43(4):683–92. Available from: https://pubmed.ncbi.nlm.nih.gov/33325634/

231. Cherng HJJ, Khwaja R, Kanagal-Shamanna R, Tang G, Burger J, Thompson P, et al. TP53-altered chronic lymphocytic leukemia treated with firstline Bruton's tyrosine kinase inhibitor-based therapy: A retrospective analysis. Am J Hematol [Internet]. 2022 Aug 1 [cited 2023 Sep 22];97(8):1005–12. Available from: https://pubmed.ncbi.nlm.nih.gov/35567779/

232. Kittai AS, Miller C, Goldstein D, Huang Y, Abruzzo L V., Beckwith K, et al. The impact of increasing karyotypic complexity and evolution on survival in patients with CLL treated with ibrutinib. Blood [Internet]. 2021 Dec 9 [cited 2023 Sep 22];138(23):2372–82. Available from: https://pubmed.ncbi.nlm.nih.gov/34314481/

233. Kater AP, Wu JQ, Kipps T, Eichhorst B, Hillmen P, D'Rozario J, et al. Venetoclax Plus Rituximab in Relapsed Chronic Lymphocytic Leukemia: 4-Year Results and Evaluation of Impact of Genomic Complexity and Gene Mutations From the MURANO Phase III Study. Journal of Clinical Oncology [Internet]. 2020 Dec 1 [cited 2022 Apr 11];38(34):4042. Available from: /pmc/articles/PMC7768340/

234. Collado R, Puiggros A, López-Guerrero JA, Calasanz MJ, Larráyoz MJ, Ivars D, et al. Chronic lymphocytic leukemia with isochromosome 17q: An aggressive subgroup associated with TP53 mutations and complex karyotypes. Cancer Lett. 2017 Nov 28;409:42–8.

235. Salaverria I, Martín-Garcia D, López C, Clot G, García-Aragonés M, Navarro A, et al. Detection of chromothripsis-like patterns with a custom array platform for chronic lymphocytic leukemia. Genes Chromosomes Cancer. 2015 Nov 1;54(11):668–80.

236. Yu L, Kim HT, Kasar SN, Benien P, Du W, Hoang K, et al. Survival of Del17p CLL depends on genomic complexity and somatic mutation. Clinical Cancer Research. 2017 Feb 1;23(3):735–45.

237. Puiggros A, Ramos-Campoy S, Kamaso J, de la Rosa M, Salido M, Melero C, et al. Optical Genome Mapping: A Promising New Tool to Assess Genomic Complexity in Chronic Lymphocytic Leukemia (CLL). Cancers (Basel) [Internet]. 2022 Jul 1 [cited 2023 Sep 23];14(14). Available from: https://pubmed.ncbi.nlm.nih.gov/35884436/

238. Baliakas P, Jeromin S, Iskas M, Puiggros A, Plevova K, Nguyen-Khac F, et al. Cytogenetic complexity in chronic lymphocytic leukemia: Definitions, associations, and clinical impact. Blood. 2019;133(11):1205–16.

239. Ouillette P, Collins R, Shakhan S, Li J, Peres E, Kujawski L, et al. Acquired genomic copy number aberrations and survival in chronic lymphocytic leukemia. Blood. 2011 Sep 15;118(11):3051–61.

240. Oder B, Chatzidimitriou A, Langerak AW, Rosenquist R, Österholm C. Recent revelations and future directions using single-cell technologies in chronic lymphocytic leukemia. Front Oncol. 2023 Apr 6;13:1143811.

241. Yuan Y, Zhu H, Wu J, Xia Y, Liang J, Wu W, et al. The percentage of cells with 17p deletion and the size of 17p deletion subclones show prognostic significance in chronic lymphocytic leukemia. Genes Chromosomes Cancer. 2019 Jan 29;58(1):43–51.

242. Hallek M, Cheson BD, Catovsky D, Caligaris-Cappio F, Dighiero G, Döhner H, et al. Guidelines for the diagnosis and treatment of chronic lymphocytic leukemia: a report from the International Workshop on Chronic Lymphocytic Leukemia updating the National Cancer Institute-Working Group 1996 guidelines. Blood [Internet]. 2008 Jun 15 [cited 2024 Jan 10];111(12):5446–56. Available from: https://pubmed.ncbi.nlm.nih.gov/18216293/

243. Suresh K, Chandrashekara S. Sample size estimation and power analysis for clinical research studies. J Hum Reprod Sci. 2012 Jan;5(1):7.

244. Joober R, Schmitz N, Annable L, Boksa P. Publication bias: What are the challenges and can they be overcome? Vol. 37, Journal of Psychiatry and Neuroscience. Canadian Medical Association; 2012. p. 149–52.

245. Misra DP, Agarwal V. Systematic Reviews: Challenges for Their Justification, Related Comprehensive Searches, and Implications. J Korean Med Sci. 2018 Mar 19;33(12):92.

246. Bernardini L, Alesi V, Loddo S, Novelli A, Bottillo I, Battaglia A, et al. High-resolution SNP arrays in mental retardation diagnostics: How much do we gain. European Journal of Human Genetics. 2010 Feb;18(2):178–85.

247. Wang X, Li X, Cheng Y, Sun X, Sun X, Self S, et al. Copy number alterations detected by whole-exome and whole-genome sequencing of esophageal adenocarcinoma. Hum Genomics. 2015 Dec 15;9(1):22.

248. Chen Q, Jain N, Ayer T, Wierda WG, Flowers CR, O'Brien SM, et al. Economic Burden of Chronic Lymphocytic Leukemia in the Era of Oral Targeted Therapies in the United States. Journal of Clinical Oncology [Internet]. 2017 Jan 1 [cited 2024 Jan 10];35(2):166. Available from: /pmc/articles/PMC5559889/

249. Clifford RM, Robbe P, Weller S, Timbs AT, Titsias M, Burns A, et al. Towards Response Prediction Using Integrated Genomics in Chronic Lymphocytic Leukaemia: Results on 250 First-Line FCR Treated Patients from UK Clinical Trials. Blood. 2014 Dec 6;124(21):1942–1942.

250. Fisher Scientific T. Qubit ® 3.0 Fluorometer Catalog Number Q33216.

251. Lucena-Aguilar G, Sánchez-López AM, Barberán-Aceituno C, Carrillo-Ávila JA, López-Guerrero JA, Aguilar-Quesada R. DNA Source Selection for Downstream Applications Based on DNA Quality Indicators Analysis. Biopreserv Biobank [Internet]. 2016 Aug 8 [cited 2024 Apr 22];14(4):264. Available from: /pmc/articles/PMC4991598/

252. García-Alegría AM, Anduro-Corona I, Pérez-Martínez CJ, Corella-Madueño MAG, Rascón-Durán ML, Astiazaran-Garcia H. Quantification of DNA through the NanoDrop Spectrophotometer: Methodological Validation Using Standard Reference Material and Sprague Dawley Rat and Human DNA. Int J Anal Chem [Internet]. 2020 [cited 2024 Apr 22];2020. Available from: /pmc/articles/PMC7719535/

253. Technologies A. 5200, 5300, and 5400 Fragment Analyzer System Manual.

254. ProSize Data Analysis Software for RNA and DNA quality control | Agilent [Internet]. [cited 2022 Apr 13]. Available from: https://www.agilent.com/en/product/automated-electrophoresis/fragment-analyzer-systems/fragment-analyzer-systems-software/fragment-analyzer-software-1149185

255. Agilent Technologies SureSelect XT HS2 DNA System DNA Library Preparation and Target Enrichment for the Illumina Platform Protocol SureSelect platform manufactured with Agilent SurePrint Technology For Research Use Only. Not for use in diagnostic procedures. 2006 [cited 2022 Apr 19]; Available from: www.agilent.com/en/contact-us/page.

256. Adaptive Focused Acoustics (AFA) Technology | Covaris [Internet]. [cited 2022 Apr 19]. Available from: https://www.covaris.com/technology/afa-technology

257. Protocols | Covaris [Internet]. [cited 2022 Apr 28]. Available from: https://www.covaris.com/protocols

258. Cawthon RM. Telomere length measurement by a novel monochrome multiplex quantitative PCR method. Nucleic Acids Res [Internet]. 2009 [cited 2020 Aug 5];37(3):21. Available from: https://academic.oup.com/nar/article-abstract/37/3/e21/1074965

259. Tavtigian S V., Oefner PJ, Babikyan D, Hartmann A, Healey S, Le Calvez-Kelm F, et al. Rare, evolutionarily unlikely missense substitutions in ATM confer increased risk of breast cancer. Am J Hum Genet [Internet]. 2009 Oct 9 [cited 2024 May 4];85(4):427–46. Available from: https://pubmed.ncbi.nlm.nih.gov/19781682/

260. Skowronska A, Parker A, Ahmed G, Oldreive C, Davis Z, Richards S, et al. Biallelic ATM inactivation significantly reduces survival in patients treated on the United Kingdom Leukemia Research Fund Chronic Lymphocytic Leukemia 4 trial. J Clin Oncol [Internet]. 2012 Dec 20 [cited 2024 May 4];30(36):4524–32. Available from: https://pubmed.ncbi.nlm.nih.gov/23091097/

261. Barnell EK, Ronning P, Campbell KM, Krysiak K, Ainscough BJ, Sheta LM, et al. Standard operating procedure for somatic variant refinement of sequencing data with paired tumor and normal samples. Genetics in Medicine. 2019 Apr 1;21(4):972–81.

262. The conumee vignette [Internet]. [cited 2020 Mar 18]. Available from: https://bioconductor.org/packages/devel/bioc/vignettes/conumee/inst/doc/conumee.html

263. Hansen D, Aryee M, Timp W, Kasper M. Package “minfiData” Title Example data for the Illumina Methylation 450k array Description Data from 6 samples across 2 groups from 450k methylation arrays. 2020.

264. Marzouka N al dain, Nordlung J, Backlin C, Lonnerholm G, Syvanen AC, Almlof JC. CopyNumber450kCancer: baseline correction for accurate copy number calling from the 450k methylation array. Bioinformatics. 2016;1080–2.

265. Agilent Technologies SureSelect QXT Whole Genome Library Prep for Illumina Multiplexed Sequencing Featuring Transposase-Based Library Prep Technology Protocol SureSelect platform manufactured with Agilent SurePrint Technology For Research Use Only. Not for use in diagnostic procedures. 2018.

266. Parker H, Carr L, Syeda S, Bryant D, Strefford JC. Characterization of Somatically-Acquired Copy Number Alterations in Chronic Lymphocytic Leukaemia Using Shallow Whole Genome Sequencing. Methods Mol Biol [Internet]. 2019 [cited 2020 Mar 18];1881:327–53. Available from: http://www.ncbi.nlm.nih.gov/pubmed/30350215

267. van de Wie MA, Kim KI, Vosse SJ, van Wieringen WN, Wilting SM, Ylstra B. CGHcall: calling aberrations for array CGH tumor profiles. Bioinformatics [Internet]. 2007 Apr 1 [cited 2022

May 29];23(7):892–4. Available from: https://academic.oup.com/bioinformatics/article/23/7/892/217759

268. Buder A, Heitzer E, Waldispühl-Geigl J, Weber S, Moser T, Hochmair MJ, et al. Somatic copy-number alterations in plasma circulating tumor dna from advanced egfr-mutated lung adenocarcinoma patients. Biomolecules [Internet]. 2021 May 1 [cited 2022 May 21];11(5). Available from: /pmc/articles/PMC8143372/

269. Xi R, Hadjipanayis AG, Luquette LJ, Kim TM, Lee E, Zhang J, et al. Copy number variation detection in whole-genome sequencing data using the Bayesian information criterion. Proc Natl Acad Sci U S A [Internet]. 2011 Nov 15 [cited 2022 May 21];108(46):E1128. Available from: /pmc/articles/PMC3219132/

270. Xi R, Lee S, Xia Y, Kim TM, Park PJ. Copy number analysis of whole-genome data using BIC-seq2 and its application to detection of cancer susceptibility variants. Nucleic Acids Res [Internet]. 2016 Jul 27 [cited 2022 May 21];44(13):6274–86. Available from: https://academic.oup.com/nar/article/44/13/6274/2457607

271. Walewska R, Parry-Jones N, Eyre TA, Follows G, Martinez-Calle N, McCarthy H, et al. Guideline for the treatment of chronic lymphocytic leukaemia. Br J Haematol [Internet]. 2022 Jun 1 [cited 2023 Apr 24];197(5):544–57. Available from: https://pubmed.ncbi.nlm.nih.gov/35313007/

272. Clifford R, Louis T, Robbe P, Ackroyd S, Burns A, Timbs AT, et al. SAMHD1 is mutated recurrently in chronic lymphocytic leukemia and is involved in response to DNA damage. Blood [Internet]. 2014 Feb 13 [cited 2020 Nov 3];123(7):1021–31. Available from: /pmc/articles/PMC3924925/?report=abstract

273. Kulis M, Heath S, Bibikova M, Queirós AC, Navarro A, Clot G, et al. Epigenomic analysis detects widespread gene-body DNA hypomethylation in chronic lymphocytic leukemia. Nature Genetics 2012 44:11 [Internet]. 2012 Oct 14 [cited 2023 Jun 6];44(11):1236–42. Available from: https://www.nature.com/articles/ng.2443

274. Stamatopoulos B, Smith T, Crompot E, Pieters K, Clifford R, Mraz M, et al. The light chain IgLV3-21 defines a new poor prognostic subgroup in chronic lymphocytic leukemia: Results of a multicenter study. Clinical Cancer Research [Internet]. 2018 Oct 15 [cited 2023 Aug 5];24(20):5048–57. Available from: https://dx.doi.org/10.1158/1078-0432.CCR-18-0133

275. Duran-Ferrer M, Mansouri L, Nadeu F, Clot G, Bhoi S, Ann Sutton L, et al. A Comprehensive DNA Methylome Analysis of Stereotyped and Non-Stereotyped CLL Reveals an Epigenetic

Signature with Strong Clinical Impact Encompassing IGHV Status, Stereotypes and IGLV3-21R110. Blood. 2022 Nov 15;140(Supplement 1):1800–2.

276. Damle RN, Batliwalla FM, Ghiotto F, Valetto A, Albesiano E, Sison C, et al. Telomere length and telomerase activity delineate distinctive replicative features of the B-CLL subgroups defined by immunoglobulin V gene mutations. Blood [Internet]. 2004 Jan 15 [cited 2024 Apr 10];103(2):375–82. Available from: https://dx.doi.org/10.1182/blood-2003-04-1345

277. Damle RN, Temburni S, Banapour T, Paul S, Mongini PKA, Allen SL, et al. T-cell independent, B-cell receptor-mediated induction of telomerase activity differs among IGHV mutation-based subgroups of chronic lymphocytic leukemia patients. Blood [Internet]. 2012 Sep 20 [cited 2024 Aug 25];120(12):2438–49. Available from: https://pubmed.ncbi.nlm.nih.gov/22875913/

278. Britt-Compton B, Lin TT, Ahmed G, Weston V, Jones RE, Fegan C, et al. Extreme telomere erosion in ATM-mutated and 11q-deleted CLL patients is independent of disease stage. Leukemia [Internet]. 2012 [cited 2024 Apr 9];26(4):826–30. Available from: https://pubmed.ncbi.nlm.nih.gov/21986843/

279. Navrkalova V, Young E, Baliakas P, Radova L, Sutton LA, Plevova K, et al. ATM mutations in major stereotyped subsets of chronic lymphocytic leukemia: enrichment in subset #2 is associated with markedly short telomeres. Haematologica [Internet]. 2016 Sep 1 [cited 2024 Apr 9];101(9):e369–73. Available from: https://haematologica.org/article/view/7831

280. Duran-Ferrer M, Mansouri L, Nadeu F, Clot G, Bhoi S, Ann Sutton L, et al. A Comprehensive DNA Methylome Analysis of Stereotyped and Non-Stereotyped CLL Reveals an Epigenetic Signature with Strong Clinical Impact Encompassing IGHV Status, Stereotypes and IGLV3-21R110. Blood [Internet]. 2022 Nov 15 [cited 2024 Apr 9];140(Supplement 1):1800–2. Available from: https://dx.doi.org/10.1182/blood-2022-165181

281. Sutton LA, Young E, Baliakas P, Hadzidimitriou A, Moysiadis T, Plevova K, et al. Different spectra of recurrent gene mutations in subsets of chronic lymphocytic leukemia harboring stereotyped B-cell receptors. Haematologica [Internet]. 2016 Jul 31 [cited 2024 Apr 9];101(8):959–67. Available from: https://pubmed.ncbi.nlm.nih.gov/27198719/

282. Minici C, Gounari M, Übelhart R, Scarfò L, Dühren-von Minden M, Schneider D, et al. Distinct homotypic B-cell receptor interactions shape the outcome of chronic lymphocytic leukaemia. Nat Commun [Internet]. 2017 Aug 30 [cited 2024 Dec 29];8(1). Available from: https://pubmed.ncbi.nlm.nih.gov/28598442/

283. Janovska P, Poppova L, Plevova K, Plesingerova H, Behal M, Kaucka M, et al. Autocrine signaling by Wnt-5a deregulates chemotaxis of leukemic cells and predicts clinical outcome in chronic lymphocytic leukemia. Clin Cancer Res [Internet]. 2016 Jan 1 [cited 2024 Apr 10];22(2):459. Available from: /pmc/articles/PMC4716000/

284. Rossi D, Terzi-Di-Bergamo L, De Paoli L, Cerri M, Ghilardi G, Chiarenza A, et al. Molecular prediction of durable remission after first-line fludarabine-cyclophosphamide-rituximab in chronic lymphocytic leukemia. Blood [Internet]. 2015 Oct 15 [cited 2022 May 31];126(16):1921–4. Available from: https://pubmed.ncbi.nlm.nih.gov/26276669/

285. Chelliah Jebaraj BM, Busch R, Zenz T, Bühler A, Winkler D, Schnaiter A, et al. Telomere Length and Treatment Outcome In Chronic Lymphocytic Leukemia: Results From The CLL8 Trial. Blood. 2013 Nov 15;122(21):671.

286. Lin J, Smith DL, Esteves K, Drury S. Telomere length measurement by qPCR – Summary of critical factors and recommendations for assay design. Psychoneuroendocrinology [Internet]. 2019 Jan 1 [cited 2023 Jan 16];99:271. Available from: /pmc/articles/PMC6363640/

287. Feber A, Guilhamon P, Lechner M, Fenton T, Wilson GA, Thirlwell C, et al. Using high-density DNA methylation arrays to profile copy number alterations. Genome Biol [Internet]. 2014 Feb 3 [cited 2020 Mar 24];15(2):R30. Available from: http://genomebiology.biomedcentral.com/articles/10.1186/gb-2014-15-2-r30

288. Shaffer LG, Bejjani BA, Torchia B, Kirkpatrick S, Coppinger J, Ballif BC. The identification of microdeletion syndromes and other chromosome abnormalities: Cytogenetic methods of the past, new technologies for the future. Am J Med Genet C Semin Med Genet [Internet]. 2007 Nov 15 [cited 2024 Mar 12];145C(4):335–45. Available from: https://onlinelibrary.wiley.com/doi/full/10.1002/ajmg.c.30152

289. Solinas-Toldo S, Lampel S, Stilgenbauer S, Nickolenko J, Benner A, Dö H, et al. Matrix-Based Comparative Genomic Hybridization: Biochips to Screen for Genomic Imbalances. Genes Chromosomes Cancer [Internet]. 1997 [cited 2024 Mar 12];20:399–407. Available from: https://onlinelibrary.wiley.com/doi/10.1002/

290. Bignell GR, Huang J, Greshock J, Watt S, Butler A, West S, et al. High-Resolution Analysis of DNA Copy Number Using Oligonucleotide Microarrays. Genome Res [Internet]. 2004 Feb [cited 2024 Mar 12];14(2):287. Available from: /pmc/articles/PMC327104/

291. Bewicke-Copley F, Arjun Kumar E, Palladino G, Korfi K, Wang J. Applications and analysis of targeted genomic sequencing in cancer studies. Comput Struct Biotechnol J [Internet]. 2019 Jan 1 [cited 2024 Apr 16];17:1348. Available from: /pmc/articles/PMC6861594/

292. Schenk D, Song G, Ke Y, Wang Z. Amplification of overlapping DNA amplicons in a single-tube multiplex PCR for targeted next-generation sequencing of BRCA1 and BRCA2. PLoS One [Internet]. 2017 Jul 1 [cited 2024 Apr 16];12(7). Available from: /pmc/articles/PMC5507532/

293. Cawthon RM. Telomere measurement by quantitative PCR. Nucleic Acids Res [Internet]. 2002 [cited 2022 Mar 25];30(10). Available from: https://pubmed.ncbi.nlm.nih.gov/12000852/

294. Baird DM, Rowson J, Wynford-Thomas D, Kipling D. Extensive allelic variation and ultrashort telomeres in senescent human cells. Nature Genetics 2003 33:2 [Internet]. 2003 Jan 21 [cited 2024 Aug 12];33(2):203–7. Available from: https://www.nature.com/articles/ng1084z

295. Zhao S, Fernald RD. Comprehensive Algorithm for Quantitative Real-Time Polymerase Chain Reaction. https://home.liebertpub.com/cmb [Internet]. 2005 Oct 21 [cited 2022 May 6];12(8):1047–64. Available from: https://www.liebertpub.com/doi/abs/10.1089/cmb.2005.12.1047

296. Evaluation validation of a qPCR curve analysis method and conventional approaches. [cited 2022 May 6]; Available from: https://doi.org/10.1101/2020.06.18.158873

297. Bustin SA, Benes V, Garson JA, Hellemans J, Huggett J, Kubista M, et al. The MIQE Guidelines: Minimum Information for Publication of Quantitative Real-Time PCR Experiments. 2009 [cited 2022 May 7]; Available from: http://www.mibbi.org

298. Per Sequence Quality Scores [Internet]. [cited 2024 May 2]. Available from: https://www.bioinformatics.babraham.ac.uk/projects/fastqc/Help/3%20Analysis%20Modules/3%20Per%20Sequence%20Quality%20Scores.html

299. Raman L, Dheedene A, de Smet M, van Dorpe J, Menten B. WisecondorX: improved copy number detection for routine shallow whole-genome sequencing. Nucleic Acids Res [Internet]. 2019 Feb 2 [cited 2022 May 21];47(4):1605. Available from: /pmc/articles/PMC6393301/

300. Raman L, van der Linden M, van der Eecken K, Vermaelen K, Demedts I, Surmont V, et al. Shallow whole-genome sequencing of plasma cell-free DNA accurately differentiates small from non-small cell lung carcinoma. Genome Med [Internet]. 2020 Apr 21 [cited 2022 May 21];12(1):1–12. Available from: https://genomemedicine.biomedcentral.com/articles/10.1186/s13073-020-00735-4

301. Kucharík M, Budiš J, Hýblová M, Minárik G, Szemes T. Copy number variant detection with low-coverage whole-genome sequencing represents a viable alternative to the conventional array-cgh. Diagnostics [Internet]. 2021 Apr 1 [cited 2022 May 21];11(4). Available from: /pmc/articles/PMC8071346/

302. Schoenfeld DA. Sample-Size Formula for the Proportional-Hazards Regression Model. Biometrics. 1983 Jun;39(2):499.

303. Wan Y, Wu CJ. SF3B1 mutations in chronic lymphocytic leukemia. Blood [Internet]. 2013 Jun 6 [cited 2024 Jul 24];121(23):4627–34. Available from: https://dx.doi.org/10.1182/blood-2013-02-427641

304. Ouillette P, Erba H, Kujawski L, Kaminski M, Shedden K, Malek SN. Integrated genomic profiling of chronic lymphocytic leukemia identifies subtypes of deletion 13q14. Cancer Res [Internet]. 2008 Feb 15 [cited 2024 Dec 29];68(4):1012–21. Available from: https://pubmed.ncbi.nlm.nih.gov/18281475/

305. Ouillette P, Fossum S, Parkin B, Ding L, Bockenstedt P, Al-Zoubi A, et al. Aggressive chronic lymphocytic leukemia with elevated genomic complexity is associated with multiple gene defects in the response to DNA double-strand breaks. Clinical Cancer Research [Internet]. 2010 Feb 1 [cited 2020 Nov 16];16(3):835–47. Available from: /pmc/articles/PMC2818663/?report=abstract

306. Baliakas P, Espinet B, Mellink C, Jarosova M, Athanasiadou A, Ghia P, et al. Cytogenetics in Chronic Lymphocytic Leukemia: ERIC Perspectives and Recommendations. Hemasphere [Internet]. 2022 Apr 25 [cited 2024 Aug 6];6(4):E707. Available from: /pmc/articles/PMC8984316/

307. Rücker FG, Schlenk RF, Bullinger L, Kayser S, Teleanu V, Kett H, et al. TP53 alterations in acute myeloid leukemia with complex karyotype correlate with specific copy number alterations, monosomal karyotype, and dismal outcome. Blood [Internet]. 2012 Mar 1 [cited 2024 Aug 7];119(9):2114–21. Available from: https://dx.doi.org/10.1182/blood-2011-08-375758

308. Bowen D, Groves MJ, Burnett AK, Patel Y, Allen C, Green C, et al. TP53 gene mutation is frequent in patients with acute myeloid leukemia and complex karyotype, and is associated with very poor prognosis. Leukemia 2009 23:1 [Internet]. 2008 Jul 3 [cited 2024 Aug 7];23(1):203–6. Available from: https://www.nature.com/articles/leu2008173

309. Lazaryan A, Dolan M, Zhang MJ, Wang HL, Kharfan-Dabaja MA, Marks DI, et al. Impact of cytogenetic abnormalities on outcomes of adult Philadelphia-negative acute lymphoblastic leukemia after allogeneic hematopoietic stem cell transplantation: a study by the Acute Leukemia Working Committee of the Center for International Blood and Marrow Transplant Research. Haematologica [Internet]. 2020 May 1 [cited 2024 Aug 7];105(5):1329. Available from: /pmc/articles/PMC7193485/

310. Le Bris Y, Struski S, Guièze R, Rouvellat C, Prade N, Troussard X, et al. Major prognostic value of complex karyotype in addition to TP53 and IGHV mutational status in first-line chronic lymphocytic leukemia. Hematol Oncol [Internet]. 2017 Dec 1 [cited 2024 Aug 10];35(4):664–70. Available from: https://onlinelibrary.wiley.com/doi/full/10.1002/hon.2349

311. Visentin A, Bonaldi L, Rigolin GM, Mauro FR, Martines A, Frezzato F, et al. The combination of complex karyotype subtypes and IGHV mutational status identifies new prognostic and predictive groups in chronic lymphocytic leukaemia. Br J Cancer [Internet]. 2019 Jul 7 [cited 2024 Aug 7];121(2):150. Available from: /pmc/articles/PMC6738078/

312. Rigolin GM, Saccenti E, Guardalben E, Cavallari M, Formigaro L, Zagatti B, et al. In chronic lymphocytic leukaemia with complex karyotype, major structural abnormalities identify a subset of patients with inferior outcome and distinct biological characteristics. Br J Haematol [Internet]. 2018 Apr 1 [cited 2024 Aug 7];181(2):229–33. Available from: https://pubmed.ncbi.nlm.nih.gov/29611195/

313. Chiorazzi N, Stevenson FK. Celebrating 20 Years of IGHV Mutation Analysis in CLL. Hemasphere [Internet]. 2020 [cited 2024 Aug 8];4(1):1. Available from: /pmc/articles/PMC7000474/

314. Stevenson FK, Forconi F, Kipps TJ. Exploring the pathways to chronic lymphocytic leukemia. Blood [Internet]. 2021 Sep 9 [cited 2024 Aug 8];138(10):827. Available from: /pmc/articles/PMC8432043/

315. Syrykh C, Pons-Brun B, Russiñol N, Playa-Albinyana H, Baumann T, Duran-Ferrer M, et al. IGLV3-21R110 mutation has prognostic value in patients with treatment-naive chronic

lymphocytic leukemia. Blood Adv [Internet]. 2023 Dec 12 [cited 2024 Aug 9];7(23):7384–91. Available from: https://dx.doi.org/10.1182/bloodadvances.2023010132

316. Yu J, Chen L, Cui B, Widhopf GF, Shen Z, Wu R, et al. Wnt5a induces ROR1/ROR2 heterooligomerization to enhance leukemia chemotaxis and proliferation. J Clin Invest [Internet]. 2016 Feb 1 [cited 2024 Aug 9];126(2):585–98. Available from: https://pubmed.ncbi.nlm.nih.gov/26690702/

317. Helbig DR, Zeinah GFA, Bhavsar EB, Allan JN. Outcomes in chronic lymphocytic leukemia (CLL) patients with NOTCH1 signaling pathway mutations. https://doi.org/101200/JCO20193715_suppl7524 [Internet]. 2019 May 26 [cited 2024 Aug 9];37(15_suppl):7524–7524. Available from: https://ascopubs.org/doi/10.1200/JCO.2019.37.15_suppl.7524

318. Balatti V, Bottoni A, Palamarchuk A, Alder H, Rassenti LZ, Kipps TJ, et al. NOTCH1 mutations in CLL associated with trisomy 12. Blood [Internet]. 2012 Jan 1 [cited 2024 Aug 9];119(2):329. Available from: /pmc/articles/PMC3257004/

319. Badoux XC, Keating MJ, Wang X, O'Brien SM, Ferrajoli A, Faderl S, et al. Fludarabine, cyclophosphamide, and rituximab chemoimmunotherapy is highly effective treatment for relapsed patients with CLL. Blood [Internet]. 2011 Mar 3 [cited 2024 Aug 10];117(11):3016. Available from: /pmc/articles/PMC4123386/

320. Lazaryan A, Dolan M, Zhang MJ, Wang HL, Kharfan-Dabaja MA, Marks DI, et al. Impact of cytogenetic abnormalities on outcomes of adult Philadelphia-negative acute lymphoblastic leukemia after allogeneic hematopoietic stem cell transplantation: a study by the Acute Leukemia Working Committee of the Center for International Blood and Marrow Transplant Research. Haematologica [Internet]. 2020 May 1 [cited 2024 Aug 10];105(5):1329. Available from: /pmc/articles/PMC7193485/

321. Bowen D, Groves MJ, Burnett AK, Patel Y, Allen C, Green C, et al. TP53 gene mutation is frequent in patients with acute myeloid leukemia and complex karyotype, and is associated with very poor prognosis. Leukemia 2009 23:1 [Internet]. 2008 Jul 3 [cited 2024 Aug 10];23(1):203–6. Available from: https://www.nature.com/articles/leu2008173

322. Dziak JJ, Dierker LC, Abar B. The Interpretation of Statistical Power after the Data have been Gathered. Curr Psychol [Internet]. 2020 Jun 1 [cited 2024 Aug 5];39(3):870. Available from: /pmc/articles/PMC7286546/

323. Knisbacher BA, Lin Z, Hahn CK, Nadeu F, Duran-Ferrer M, Stevenson KE, et al. Molecular map of chronic lymphocytic leukemia and its impact on outcome. Nat Genet [Internet]. 2022 Nov 1 [cited 2024 Aug 21];54(11):1664. Available from: /pmc/articles/PMC10084830/

324. Haferlach C, Dicker F, Schnittger S, Kern W, Haferlach T. Comprehensive genetic characterization of CLL: a study on 506 cases analysed with chromosome banding analysis, interphase FISH, IgVH status and immunophenotyping. Leukemia 2007 21:12 [Internet]. 2007 Sep 6 [cited 2024 Aug 20];21(12):2442–51. Available from: https://www.nature.com/articles/2404935

325. Schoumans J, Suela J, Hastings R, Muehlematter D, Rack K, van den Berg E, et al. Guidelines for genomic array analysis in acquired haematological neoplastic disorders. Genes Chromosomes Cancer [Internet]. 2016 May 1 [cited 2025 Jan 11];55(5):480–91. Available from: https://onlinelibrary.wiley.com/doi/full/10.1002/gcc.22350

326. Melcher R, Hartmann E, Zopf W, Herterich S, Wilke P, Müller L, et al. LOH and copy neutral LOH (cnLOH) act as alternative mechanism in sporadic colorectal cancers with chromosomal and microsatellite instability. Carcinogenesis [Internet]. 2011 Apr 1 [cited 2025 Jan 11];32(4):636–42. Available from: https://dx.doi.org/10.1093/carcin/bgr011

327. O'Keefe C, McDevitt MA, Maciejewski JP. Copy neutral loss of heterozygosity: a novel chromosomal lesion in myeloid malignancies. Blood [Internet]. 2010 Apr 8 [cited 2025 Jan 11];115(14):2731–9. Available from: https://dx.doi.org/10.1182/blood-2009-10-201848

328. Lee GT, Chung YJ. Comparison of the copy-neutral loss of heterozygosity identified from whole-exome sequencing data using three different tools. Genomics Inform [Internet]. 2022 Mar 1 [cited 2024 Aug 20];20(1). Available from: /pmc/articles/PMC9001996/

329. Saddler C, Ouillette P, Kujawski L, Shangary S, Talpaz M, Kaminski M, et al. Comprehensive biomarker and genomic analysis identifies p53 status as the major determinant of response to MDM2 inhibitors in chronic lymphocytic leukemia. Blood. 2008 Feb 1;111(3):1584–93.

330. Gunnarsson R, Mansouri L, Isaksson A, Göransson H, Cahill N, Jansson M, et al. Array-based genomic screening at diagnosis and during follow-up in chronic lymphocytic leukemia. Haematologica [Internet]. 2011 Aug [cited 2024 Aug 20];96(8):1161. Available from: /pmc/articles/PMC3148910/

331. Kilaru V, Knight AK, Katrinli S, Cobb D, Lori A, Gillespie CF, et al. Critical evaluation of copy number variant calling methods using DNA methylation. Genet Epidemiol [Internet]. 2020

Mar 18 [cited 2020 Apr 26];44(2):148–58. Available from: https://onlinelibrary.wiley.com/doi/abs/10.1002/gepi.22269

332. Mikhaleva M, Tyekucheva S, Mashima K, Fernandes SM, Davids MS, Brown JR. Higher Mutational Burden Is an Independent Predictor of Shorter Time to First Treatment in Untreated Chronic Lymphocytic Leukemia Patients. Blood [Internet]. 2023 Nov 2 [cited 2024 Aug 21];142(Supplement 1):3270–3270. Available from: https://dx.doi.org/10.1182/blood-2023-173738

333. Ou FS, Michiels S, Shyr Y, Adjei AA, Oberg AL. Biomarker Discovery and Validation: Statistical Considerations. J Thorac Oncol [Internet]. 2021 Apr 1 [cited 2025 Jan 28];16(4):537. Available from: https://pmc.ncbi.nlm.nih.gov/articles/PMC8012218/

334. Rose-Zerilli MJJ, Parker H, Parker A, Rodriguez A, Chaplin T, Gardiner A, et al. 1.9 The Significance of Deletion Architecture, ATM Mutational Status and Genomic Complexity in 11q Deleted CLL. Clin Lymphoma Myeloma Leuk [Internet]. 2011 Oct 1 [cited 2024 Aug 23];11:S146–7. Available from: http://www.clinical-lymphoma-myeloma-leukemia.com/article/S2152265011002801/fulltext

335. Bonner WM, Redon CE, Dickey JS, Nakamura AJ, Sedelnikova OA, Solier S, et al. γH2AX and cancer. Nat Rev Cancer [Internet]. 2008 Dec [cited 2025 Jan 11];8(12):957. Available from: https://pmc.ncbi.nlm.nih.gov/articles/PMC3094856/

336. Te Raa GD, Derks IAM, Navrkalova V, Skowronska A, Moerland PD, Van Laar J, et al. The impact of SF3B1 mutations in CLL on the DNA-damage response. Leukemia. 2015 May 11;29(5):1133–42.

337. Stewart GS, Stankovic T, Byrd PJ, Wechsler T, Miller ES, Huissoon A, et al. RIDDLE immunodeficiency syndrome is linked to defects in 53BP1-mediated DNA damage signaling. Proc Natl Acad Sci U S A [Internet]. 2007 Oct 23 [cited 2025 Jan 11];104(43):16910. Available from: https://pmc.ncbi.nlm.nih.gov/articles/PMC2040433/

338. Marston E, Weston V, Jesson J, Maina E, McConville C, Agathanggelou A, et al. Stratification of pediatric ALL by in vitro cellular responses to DNA double-strand breaks provides insight into the molecular mechanisms underlying clinical response. Blood [Internet]. 2009 Jan 1 [cited 2025 Jan 11];113(1):117–26. Available from: https://dx.doi.org/10.1182/blood-2008-03-142950

339. The clonal evolution of Richter transformation cells uncovers therapeutic vulnerabilities. Nature Medicine 2022 28:8 [Internet]. 2022 Aug 11 [cited 2024 Aug 21];28(8):1546–7. Available from: https://www.nature.com/articles/s41591-022-01928-7

340. Nadeu F, Royo R, Massoni-Badosa R, Playa-Albinyana H, Garcia-Torre B, Duran-Ferrer M, et al. Detection of early seeding of Richter transformation in chronic lymphocytic leukemia. Nat Med [Internet]. 2022 Aug 1 [cited 2024 Aug 21];28(8):1662. Available from: /pmc/articles/PMC9388377/

341. Hemann MT, Strong MA, Hao LY, Greider CW. The Shortest Telomere, Not Average Telomere Length, Is Critical for Cell Viability and Chromosome Stability. Cell. 2001 Oct 5;107(1):67–77.

342. Damle RN, Batliwalla FM, Ghiotto F, Valetto A, Albesiano E, Sison C, et al. Telomere length and telomerase activity delineate distinctive replicative features of the B-CLL subgroups defined by immunoglobulin V gene mutations. Blood [Internet]. 2004 Jan 15 [cited 2024 Aug 25];103(2):375–82. Available from: https://dx.doi.org/10.1182/blood-2003-04-1345

343. Ghia P, Stamatopoulos K. In CLL, epigenetics also points to the BCR. Blood [Internet]. 2021 May 27 [cited 2024 Aug 25];137(21):2863–5. Available from: https://dx.doi.org/10.1182/blood.2020010036

344. Al-Sawaf O, Lilienweiss E, Bahlo J, Robrecht S, Fink AM, Patz M, et al. High efficacy of venetoclax plus obinutuzumab in patients with complex karyotype and chronic lymphocytic leukemia. Blood [Internet]. 2020 Mar 12 [cited 2024 Aug 23];135(11):866–70. Available from: https://pubmed.ncbi.nlm.nih.gov/31990291/